VOLCANIC   ROCKS   FROM   SOUTHEASTERN   PAPUA

The evolution of volcanism at a plate boundary

by

Ian   Ernest   Masterman   Smith

A thesis submitted for the degree of

Doctor of Philosophy

Australian National University

April, 1976

Analyses, interpretations and arguements presented

in this thesis are my own unless otherwise acknowledged.

....

Ian E. M. Smith

ABSTRACT

The east Papuan peninsula, extending southeastward from New Guinea, straddles a minor plate boundary separating the Indian-Australian and Solomon Sea crustal plates. Cenozoic volcanic rocks at the southeastern tip of the peninsular record a complex series of volcano-tectonic events which reflect interaction between crustal plates. This thesis documents the geochemical evolution of volcanism on the plate boundary and is based on the analysis for major and trace elements in one hundred and ninety six volcanic rock specimens.

The oldest volcanic rocks in southeast Papua are Upper Cretaceous and Eocene submarine basalts which form the main ranges at the eastern tip of the Papuan peninsula. The chemical compositions of these rocks are closely comparable to those of tholeiitic basalts from the mid-Ocean ridges and they are thought to have originated in a similar manner during volcanic activity associated with sea floor spreading in the Coral Sea.

A major episode of volcanic activity in southeast Papua began during the Miocene and has continued through to the present day. The distribution of volcanic rocks erupted during this period define a southern volcanic belt which is characterised by high-K basaltic rocks, and a northern volcanic belt which contains rocks ranging from basalts to rhyolites with andesites predominating. The andesitic rocks in the northern volcanic belt are generally comparable to high-potassium calc-alkaline suites in some island arc settings and they are assumed to have originated by petrogenetic processes similar to those which operate in island arcs. The proposed model involves an early episode of subduction during which the upper mantle was modified by a silica- and incompatible element-rich liquid derived by melting of subducted oceanic crust, followed by partial melting of this modified mantle at a much later time. Although slightly different, the rocks of the southern volcanic belt have chemical compositions which overlap with those of rocks in the northern volcanic belt. For this reason, and because the two belts are closely associated in space and time the rocks in the southern volcanic belt are thought to have originated by the same general process as those in the north. Differences between rock types in the two belts are thought to be due to variations in the upper mantle source which can be related to the initial subduction -related modification process.

Two episodes of Quaternary volcanism are quite distinct from that which formed the northern and southern volcanic belts. Eruption of high-potassium trachytes in the Lusancay Islands during the Pleistocene does not appear to be related to any recognisable tectonic event. The trace element contents of the trachytes indicate an origin by partial melting of eclogite with a composition similar to that which gave rise to the andesites in the northern volcanic belt. The generation of magmas at the depths required by the eclogite melting model suggest a relatively high heat flow in the area which is supported by the limited heat flow data. The second episode of Quaternary volcanism gave rise to peralkaline rhyolites which together with minor associated basaltic and intermediate rocks define a transitional basalt - comendite association typical of those found in association with major rift structures in other parts of the world. The eruption of peralkaline rocks in southeast Papua is anomalous in terms of the tectonic environment which produced the Miocene to Recent andesitic rocks but is consistent with geophysical evidence for sea floor spreading at the present time in the area immediately to the east.

Because southeastern Papua straddles a circum-Pacific plate boundary the geology of the area has in the past been interpreted in terms of island arc type tectonism and volcanism. This study shows that the evolution of southeastern Papua can not be interpreted in terms of simplistic models of island arc development, the area is a complex one in which episodes of extension (sea floor spreading) and compression (subduction) are reflected in a series of distinctive volcanic episodes.

TABLE OF CONTENTS

TABLES OF CHEMICAL ANALYSES

CHAPTER 1

INTRODUCTION

Eastern Papua has been in an area of interaction between major crustal plates since the late Mesozoic, and changes in tectonic environment from extension (sea floor spreading, rifting) to compression (subduction) and back again are reflected in a series of volcanic rock associations. Detailed study of these volcanic rocks has provided a key to unravelling the complex tectonic history of the area and on a broader perspective provides further insight into the origin of magmas at active plate margins. This thesis is primarily a regional petro-chemical study in space and time of volcanic rocks in southeastern Papua but is also a study of individual volcanic rock suites and some of the conclusions reached have global implications.

The study has its origins in regional mapping at 1;250,000 scale of southeastern Papua, and in detailed investigation of the occurrence of volcanic rocks in the islands to the north and northeast of the Papuan mainland. Both of these projects formed part of the geological program of the Australian Bureau of Mineral Resources, Geology and Geophysics (BMR) in Papua New Guinea during the period 1968 to 1970. Material collected by the author while employed by BMR on these projects has provided the basis for a geochemical study subsequently carried out at the Australian National University (ANU). Some rock samples collected by other geologists involved in the regional mapping, and rock samples donated by other persons, have also been used; credit for collection of material is given, with a petrographic outline and locality details, in appendix II.

The results of regional mapping in southeast Papua have appeared as BMR map series publications (Davies, 1973; Davies and Smith, 1974; Smith and Davies, 1973a, 1973b) and a general summary of the geology of the Papuan peninsula and the offshore islands has been presented by Davies and Smith (1971). Published geochemical work on the volcanoes of the Papuan peninsula comprises that of Jakes and Smith (1970) on the Cape Nelson complex and Ruxton (1966) in the Managlase Plateau area to the west. A brief description of the volcanics in the D'Entrecasteaux Islands appears in an account of the geology of the islands by Davies and Ives (1965), and in explanatory notes for the
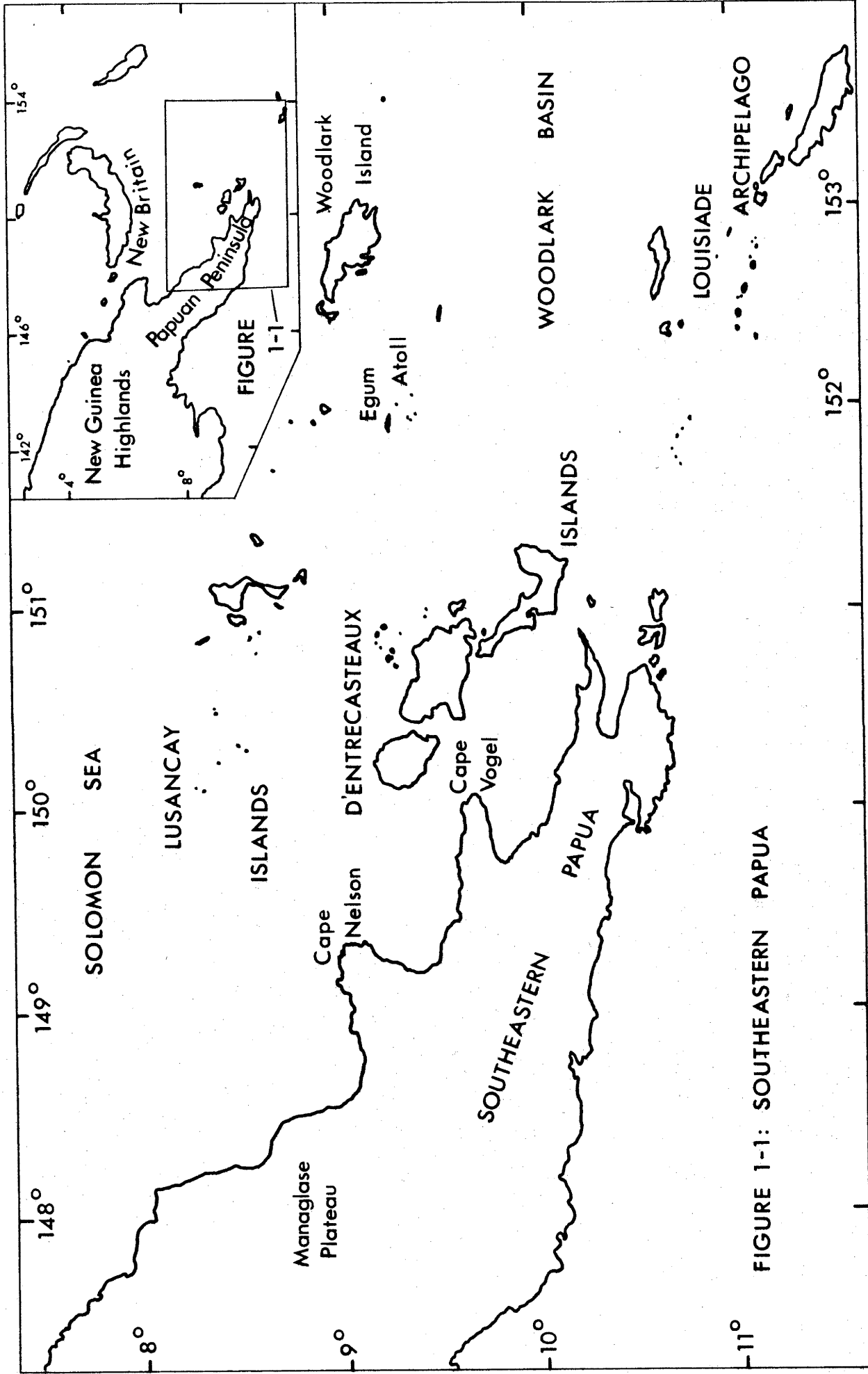
FIGURE 1-1: SOUTHEASTERN PAPUA

1:250 000 map of the area (Davies, 1973). An unpublished BMR record
on the occurrence of volcanic rocks in the offshore islands was
prepared by the writer as a preliminary to writing this thesis
(Smith, 1973a).

1-1 Thesis Scope and Organisation

The area covered in this thesis is the southeast Papuan
mainland east of 149°E longitude, and the islands to the east and
northeast, namely the D'Entrecasteaux, Lusancay, and Louisiade island
groups, Egum Atoll and Woodlark Island (Figure 1-1). Volcanic rocks
within this area range in age from Upper Cretaceous to Recent. The
Cape Nelson volcanic complex, which lies in the northwest of the
area, was the subject of earlier work (Jakes and Smith, 1970) and no
new work on this complex was undertaken during the present study,
although some use of these published results and of results published
from volcanoes immediately west of 149°E has been made in discussion.

Volcanic evolution in southeastern Papua has progressed in
a number of distinct episodes each characterised by a particular
volcanic rock association. Because of the separate identity of each
of these associations they have been treated independently in the
following chapters and this has resulted in some fragmentation of the
central theme of this thesis which is documentation of volcanic
evolution at a circum-Pacific plate boundary. The individual
associations have been treated in some detail because unless each
volcanic rock type can be understood in relation to others of the
same suite and to comparable suites in other geological settings
elsewhere, the evolutionary sequence in southeastern Papua becomes
meaningless.

Chapter 2 gives an outline of the geological setting of
southeast Papua in terms of currently accepted tectonic models for
Papua New Guinea. This is followed in chapter 3 by an account of
the late Mesozoic and Eocene submarine basalts which were erupted
during the earliest period of activity in southeastern Papua.
Volcanic activity extending from mid-Miocene to Recent times
produced a variety of rock suites which are described in chapters 4
to 6 and interpreted in chapter 7. Quaternary volcanic activity has
given rise to an unusual suite of high-K trachytes described and
discussed in chapter 8 to a peralkaline rhyolite association which
is the subject of chapter 9. The concluding chapter is a synthesis
of the volcanic evolution of southeastern Papua.

Presentation of data.

The bulk of the geochemical data on which this thesis is
based are whole rock major and trace element analyses carried out
by X-ray fluorescence spectrometry. These analyses are supplemented
by spark-source spectrometric analysis for additional trace elements,
strontium isotope measurements, and electron microprobe analysis of
minerals in selected specimens. Analytical techniques are detailed
in appendix I. In addition some use has been made of previously
published major element analyses. Major and trace element analyses
are tabulated through the text in association with appropriate
descriptive passages; CIPW norms calculated from these analyses are
tabulated in appendix III. The mass spectrometric trace element
determinations are tabulated separately but adjacent to appropriate
passages of text. Strontium isotopic measurements formed part of a
joint project carried out with Dr. W. Compston (Research School of
Earth Sciences, ANU) and these results are presented in appendix IV.
Details of analysed specimens are given in appendix II.

1-2 Rock Classification

Rock classification is a recurring problem in the study of
volcanic rocks despite recent attempts to clarify the position. At
the root of the problem is the characteristically fine grained nature
of volcanic rocks which defies modal analysis and hence classificatory
schemes based on mineral assemblage. For these reasons volcanic rock
nomenclature has come to rely heavily on the chemical composition of
rocks using either derivative calculations (e.g. the C.I.P.W. norm)
or chemical data unmodified. Traditionally alkali and SiO_2 content
have played a major role in grouping rocks together and in subdividing
individual groups. However, as more geochemical data becomes available
it is increasingly obvious that the spectrum of volcanic rock compos-
itions is continuous and that subdivision of this spectrum is
necessarily arbitary.

The concept of rock associations underlies the approach to
rock classification in this thesis. A rock association was defined
by Bowen (1928) . . . 'to designate a group of rocks associated in
the field and the same age'. If the concept of an association is to
have any real use then the rocks which make up an association must be
related in the sense that they originated by essentially similar
processes. Ideally an association should not be too restricted in

space and time. for example, in a broad sense it is possible to
recognise an association of rocks found at active converging plate
margins (island arcs, active continental margins) which has global
distribution but it is equally valid to recognise an association of
rocks which is severely restricted in time and space, for example
the Hawaiian tholeiite association.

The volcanic rock associations identified in southeastern
Papua have spatial and temporal significance in the volcanic
evolution of southeastern Papua and are comparable with associations
identified in similar tectonic settings in other parts of the world.
Each association has tectonic significance and is recognised by
characteristic petrographic and geochemical features and by distrib-
ution of rock types.   Subdivision of associations into rock types is
mainly on the basis of arbitrary but well established values of SiO_2.
and to a lesser extent on normative criteria. A summary of the
classification used in this thesis is given in Figure 1-2.

FIGURE 1-2: ROCK TERMS USED IN THIS THESIS.

(The use of these terms is discussed in more detail in respective chapters.)

ANDESITIC ROCKS

	BASALT	BASALTIC ANDESITE	ANDESITE	DACITE	RHYOLITE
SiO₂ wt.% (arbitary)	52		56	63	67
	TRACHYBASALT (Ne-normative)			ALKALI-DACITE >7% alkalies	

SiO_2 wt.% (arbitary)

TRACHYBASALT (Ne-normative)

ALKALI-DACITE
>7% alkalies

52   56   63   67

TRANSITIONAL BASALT - COMENDITE ASSOCIATION

	TRANSITIONAL BASALT	HAWAIITE	MUGEARITE	TRACHYTE	COMENDITE
normative feldspar	labradorite	andesine	oligoclase		>68% SiO_2 >10% Al_2O_3 <5% total Fe

undersaturated to slightly oversaturated

THOLEIITIC BASEMENT

	BASALT	FERROGABBRO
	<52% SiO_2	<52% SiO_2 >14% total Fe >2% TiO_2

QUATERNARY HIGH-K TRACHYTES (Lusancay Islands)

TRACHYTE
>8% total alkalies
$K_2O/Na_2O > 1$

CHAPTER 2

GEOLOGICAL SETTING OF SOUTHEAST PAPUA

2.1 Plate Tectonics of West Melanesia

Papua New Guinea straddles the zone of interaction between the Indian-Australian plate and the Pacific plate. Current interpretations of the geology of the area involve processes which relate directly to the differential movements of these two major plates.

Studies of earthquake distribution, linear magnetic anomalies, and heat flow (Denham, 1969; Johnson and Molnar, 1972; MacDonald and others, 1973; Curtis, 1973) have outlined the present day plate boundaries in the New Guinea area. A belt of strong seismic activity, running through the Solomon Island chain, New Britain and along the north coast of New Guinea, defines the principal locus of relative motion between the major plates at the present time. This seismic belt coincides with an almost continuous zone of Quaternary volcanoes which, in the New Guinea area, is known as the Bismarck volcanic arc (Johnson and others, 1973).

Belts of mainly shallow earthquake foci define relatively inactive, minor, plate boundaries in west Melanesia. The seismic data require the existence of three smaller plates separating the Indian - Australian and Pacific plates in this area (Johnson and Molnar, 1972; Curtis, 1973); these are the Solomon Sea plate, the south Bismarck plate, and the north Bismarck plate (terminology of Johnson and Molnar, 1972) (Figure 2-1). As well as these, Johnson (1975) has postulated another small plate-like feature in the northwestern corner of the Solomon Sea to account for the distribution pattern of volcanoes in the Bismarck volcanic arc. A belt of shallow seismicity (Figure 2-1) which runs down the east Papuan peninsula and eastward through the Woodlark Rise, is interpreted as a minor plate boundary (Denham, 1969; Johnson and Molnar, 1972).

The Tertiary plate-tectonic story in eastern Papua is extremely complex. The Coral Sea Basin to the south of the Papuan peninsula, was apparently formed by an episode of sea-floor spreading during the Eocene (Gardner, 1970; Mutter, 1975). Following this there is some evidence for an episode of compression (subduction) during which the Papuan ultramafic belt was emplaced (Davies 1971).

FIGURE 2-1
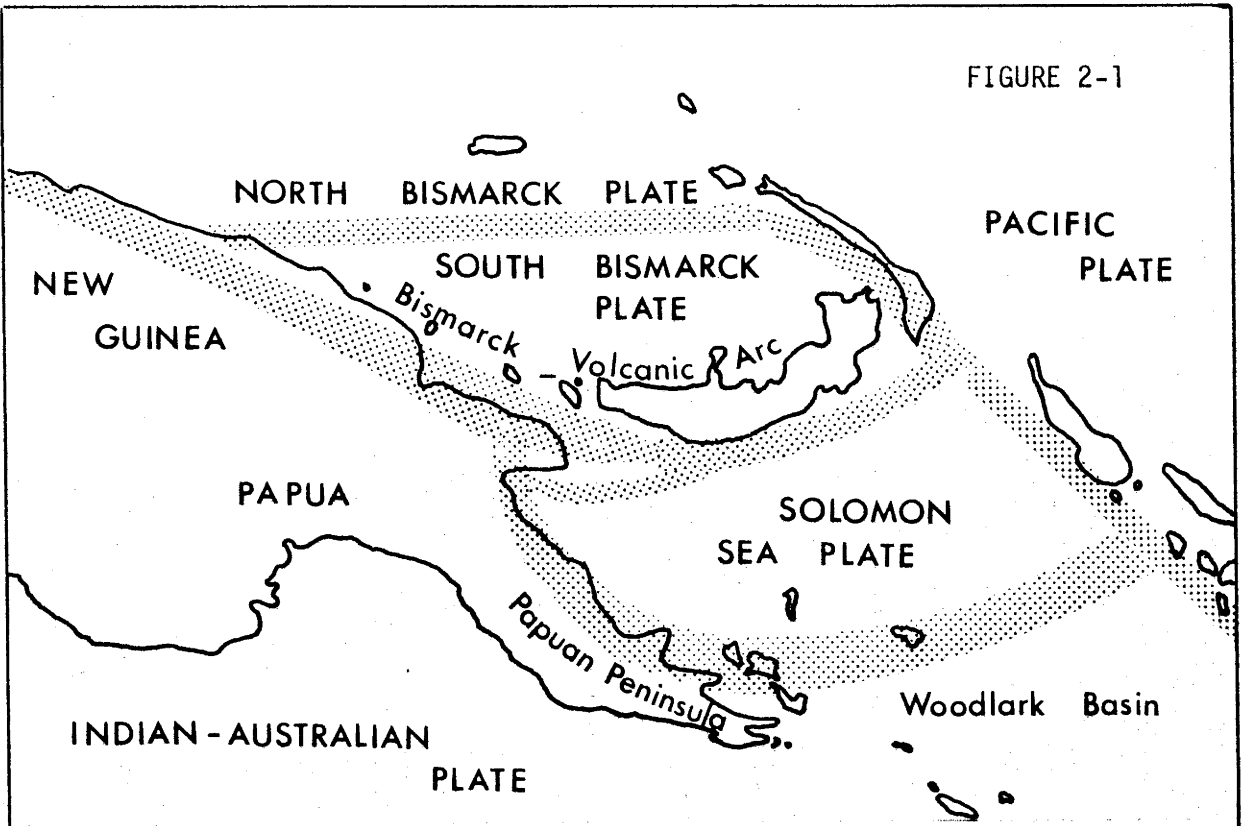
PLATE BOUNDARIES IN PAPUA NEW GUINEA.

Boundaries (shown stippled) are after Johnson and Molnar (1972), and Johnson (1975).
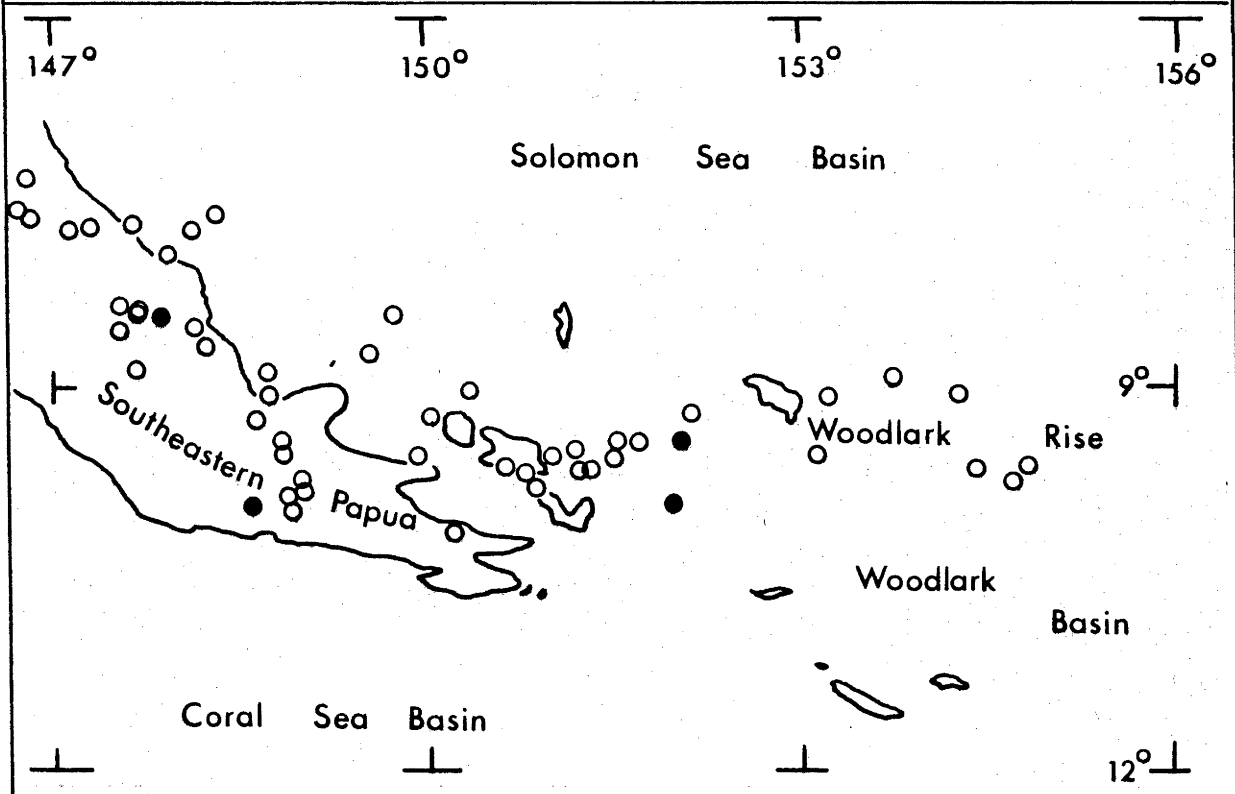
SEISMICITY IN EASTERN PAPUA.

Seismicity after Curtis (1973),
Open circles - depth <125 km.,
closed circles - 250>depth>125 km.

Late Tertiary and Quaternary tectonics are at least partly extensional, as evidenced by rifting in the Woodlark Basin, east of the peninsula (Milsom, 1970; Luyendyk and others, 1973) and by rifting and block faulting associated with uplift of the peninsula.

2-2 Geological History of Papua New Guinea

Magnetic lineations to the south of Australia indicate that the Indian - Australian plate rifted from the Antarctic plate about 40 to 50 million years ago (mid Eocene) and has drifted northward since (Weissel and Hayes, 1971). The Pacific plate has been moving relatively westward since Jurassic times (Fisher and others, 1970). Geological evidence (e.g. Dow, 1973a; 1973b) suggests that by late Eocene to early Oligocene times, northward movement of the Indian - Australian plate had brought the Australian continental block into collision with a volcanic arc which lay to the north. The collision of the Australian continental block with this volcanic arc modified the pattern of major plate interaction in western Melanesia, and it was possibly at this stage that the smaller plates buffering the two major plates came into being.

A north-south section across the central part of Papua New Guinea encounters three geological provinces (Dow, 1973a; 1973b), namely, the Australian platform, the New Guinea mobile belt, and the Melanesian oceanic province. The Australian platform is part of the stable Australian continental block, and is made up of a basement of Palaeozoic and older metamorphic rocks and Permian granites under-lying a thick Permian to Upper Tertiary sequence of shelf-type sediments, which are almost completely undeformed.

The New Guinea mobile belt is a zone of intense faulting and deformation to the north of the Australian platform. Throughout its history, the mobile belt has been an unsettled sedimentary environment, and was the repository of thick, predominantly volcanogenic, trough-type sediments. Sedimentation in the northern part of the belt was interrupted in the late Eocene or early Oligocene by a severe tectonic episode which metamorphosed to low greenschist facies most of the sediments on the outer margin of the belt, and deformed those to the south. Dow suggests that the metamorphism was caused by compression resulting from collision between the Australian continental block and oceanic plates to the north and northeast. The collision zone is now

marked by a belt of intense deformation containing fault-bounded blocks of ultramafic rock and high pressure metamorphic rocks, including glaucophane schists and eclogites.

North of the collision zone, the Melanesian oceanic province is represented by widespread lower Tertiary volcanic rocks unconformably underlying thick clastic sediments and limestone (Hutchison, pers. comm.; Jaques, in press). These volcanic rocks are variable in age from Eocene to Lower Miocene, and in some areas, more than one distinct episode of volcanism is recorded. They are described as arc-type volcanics and are generally assumed to have developed over northward-dipping subduction zones, which lay to the north of the Australian continental block during the lower Tertiary. This model provides a general explanation of the gross geological features of the province, but in detail is an oversimplification. For example, in the one area where chemical data on the volcanics is available (Finisterre and Adelbert Ranges, Jaques in press), the rocks are high-potassium types, atypical of true island arcs, and they are Oligocene to early Miocene in age, which suggests that they developed after the main collision took place.

In general terms, collision of the Australian continental block with a volcanic arc, or with the leading edge of an oceanic plate in a subduction zone, explains the main features of the geology of the western half of Papua New Guinea. Although the New Guinea mobile belt is commonly drawn as a continuous arc through the New Guinea Highlands and down the mountainous spine of the Papuan Peninsula, and although some tectonic events in the east can be correlated with events in western Papua New Guinea, a cross-section through the peninsula reveals little in common with the cross-section described in the preceding paragraphs (Figure 2-2).

The axial mountains of the Papuan peninsula are made up of metamorphosed sediments, known as the Owen Stanley Metamorphics. The original rocks were Mesozoic tuffaceous sandstone, siltstone and mudstone; metamorphic grade now ranges from low greenschist facies in the south to upper biotite zone and amphibolite facies rocks, with some development of glaucophane schist mineralogy on the north-east margin (Davies and Smith, 1971). The metamorphic rocks form a continuous belt southeastward to about $148^{\circ}30'E$; to the east there

11
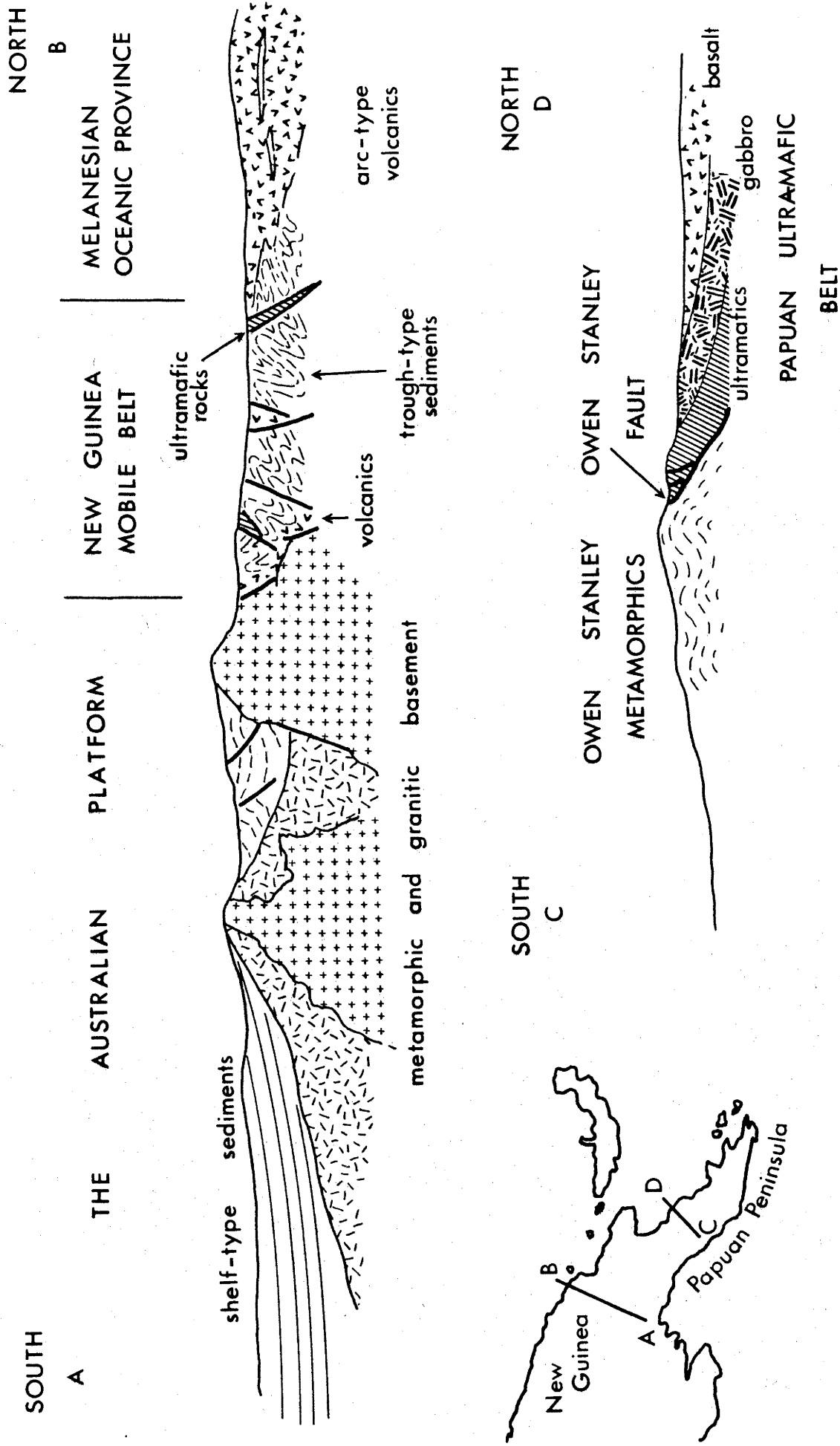
FIGURE 2-2: GENERALISED GEOLOGICAL CROSS SECTIONS THROUGH NORTHERN NEW GUINEA AND EASTERN PAPUA.

is some evidence from geophysical work (Milsom, 1973b),that metamorphic rocks occur at depth underneath the Goropu Mountains, and they reappear as fault-bounded blocks in the D'Entrecasteaux Islands where metamorphic grade is predominantly amphibolite facies (Davies and Ives, 1965), and in the Louisiade Archipelago where low greenschist facies schists predominate (De Keyser, 1961; Smith and Pieters, 1969). These meta-morphic rocks possibly formed a continuous belt which became fragmented by Tertiary tectonic events; however, the rocks have only been mildly deformed, so tectonically this metamorphic belt is not equated with the New Guinea mobile belt. The source of the original sediments is not known; the partly volcanogenic character of some of the rocks in the Owen Stanley Metamorphics suggests that at least some sediment was derived from the volcanic sources which supplied the New Guinea mobile belt. A proportion of the sediment may also have been derived from Northern Queensland, which was adjacent to the Owen Stanley belt prior to the opening of the Coral Sea Basin.

The Owen Stanley Metamorphics are separated from the Papuan ultramafic belt to the northeast by a major fault, the Owen Stanley Fault. The Papuan ultramafic belt (Davies, 1971) is a linear, layered, peridotite-gabbro-basalt complex, which extends 400 km down the north-east Papuan coast. It has been interpreted as an over-thrust slice of oceanic crust and upper mantle at the site of a former subduction zone, which became uplifted when buoyant sialic material (the Owen Stanley Metamorphics), halted subduction by entering the zone (Davies and Smith, 1971). In the sense that the rocks of the Papuan ultramafic belt were part of the plate lying to the north of a subduction zone, they can be equated with the Melanesian oceanic province to the northwest but the rock types are completely different. Whereas the volcanic rocks in the Melanesian oceanic province are island-arc type, the basalts of the Papuan ultramafic belt are true tholeiitic oceanic basalts.

The collision zone between the oceanic plate to the north and sedimentary rocks to the south, is represented by the Owen Stanley fault. This is a major structure, but compared to the collision zone in northern New Guinea, it is narrow, and there has been relatively little deformation outside the fault zone. Metamorphic grade decreases southwestward away from the fault, and as in the north, metamorphism is thought to have been produced by collision between two plates.

Timing of the collision in eastern Papua is uncertain. Davies (1971) and Davies and Smith (1971), among others, have suggested, on geological grounds, that this event took place in the early Eocene. However, this evidence is not conclusive, and new data and a reassessment of the geological development of Papua New Guinea suggest that a more likely time was late Eocene to early Oligocene. The late Eocene and early Oligocene was a time of major tectonic upheaval and metamorphism in northern New Guinea, and it is reasonable to expect that similar events in eastern Papua can be correlated. The evidence from DSDP holes on the Queensland Plateau and in the Coral Sea Basin, suggests that the Coral Sea Basin opened during the early Eocene (Mutter, 1975), and not as previously thought, in the late Eocene - Oligocene (Ewing and others, 1970; Gardner, 1970; Davies and Smith, 1971). Deformation of Eocene sediments in the Coral Sea Basin during late Eocene - Oligocene times (Mutter, 1975; Burns and others 1973) is logically associated with a compressive event.

2-3 Southeast Papua - Geology

In the southeastern tip of the Papuan peninsula (east of about 148° 30' E longitude) and in the islands to the east, the geological picture becomes complicated, due at least in part, to late Tertiary fragmentation of the area. In simple terms the area is a platform of thickened crust extending from the Kiriwina trough in the north to the Papuan shelf; geophysical data indicates crustal thicknesses of the order of 25 km (Milsom and Smith, 1975). Evidence of late Tertiary warping of the platform is provided by the presence of thick (over 4000 m) Upper Tertiary sedimentary sequences on the Trobriand platform (Stoen and Garside, 1973) and in the Cape Vogel sedimentary basin (Bickell, 1974). The late Pliocene and Quaternary history of the area has been dominated by block faulting and uplift (e.g. Smith, 1970) accompanying rifting in the Woodlark basin (Milsom, 1970; Luyendyk and others, 1973). Faulted margins and lack of sediment despite the presence of an adjacent source suggests that the basin to the east of Goodenough Bay may also be a recent extensional feature; if this is the case, it would explain the offset of the Owen Stanley metamorphics into the D'Entrecasteaux Islands, noted by Davies and Ives (1965).

FIGURE 2-3: EASTERN PAPUA - GENERALISED GEOLOGY.

(after Davies and Smith, 1971)

Owen Stanley fault

Managlase Plateau

Musa Valley

Goropu Mts.

OWEN STANLEY RANGE

Cape Vogel

Goodenough Bay

D'ENTRECASTEAUX

Dawson Strait

ISLANDS

TROBRIAND PLATFORM

KIRIWINA TROUGH

Lusancay Islands

Woodlark Island

LOUISIADE

ARCHIPELAGO

kilometers

0   50   100   150

8°
9°
10°
11°

148° 149° 150° 151° 152° 153°

Late Cenozoic intrusive rocks.

Late Cenozoic volcanic rocks.

Cretaceous and Eocene submarine volcanic rocks.

Late Mesozoic metamorphic rocks.

Papuan ultramafic belt.

Current interpretations of the geology of the area are dominated by the concept of overthrusting of the Papuan ultramafic belt (e.g. Davies and Smith, 1971) although there is scope for alternative interpretations (Rod, 1974; chapter 10). Following the overthrusting model the present distribution of ultramafic rocks suggests that basaltic and sedimentary rocks in the Goropu Mountains were completely underthrust during emplacement of the Papuan ultramafic belt. To the east of the Goropu Mountains ultramafic rocks do not crop out on the mainland but fault-bounded blocks of peridotite and gabbro are found at the margins of the high grade metamorphic rocks forming the cores of the D'Entrecasteaux Islands. It is likely that the overthrust zone continued well to the east of the present eastern limit of the Papuan ultramafic belt but that evidence for this has been obscured by late Tertiary and Quaternary tectonism.

Basement rocks

The basement rocks in southeastern Papua can be divided into 1) rocks associated with the overthrust plate, 2) metamorphosed sedimentary rocks and 3) basaltic rocks which are found mainly to the south of the overthrust zone.

Overthrust rocks

The overthrust rocks are a section of basaltic sea floor and underlying upper mantle. A representative section is found in the western part of the Papuan peninsula (the Papuan ultramafic belt, Davies, 1971); in the east, rocks belonging to the overthrust plate are represented only by ultramafic blocks in the D'Entrecasteaux Islands. Much of the area to the north of the D'Entrecasteaux Islands is presumably underlain by oceanic crust of the Solomon Sea plate but the only possible representative of this are submarine basalts (Loluai Volcanics) on Woodlark Island.

Metamorphosed sedimentary rocks

Metamorphic rocks in the Owen Stanley Ranges, the D'Entrecasteaux Islands and the Louisiade Archipelago represent sediments deposited in a trough which is thought to have extended down the present length of the Papuan peninsula roughly parallel to the Australian continental block. Emplacement of the Papuan ultramafic belt resulted in metamorphism of the sediments; the metamorphic belt so produced is more or less

continuous apart from a break in the Musa Valley - Goropu Mountains area, but geophysical measurements (Milsom, 1973b) indicate its under-lying presence in this area.

In the Owen Stanley Ranges the Papuan ultramafic belt has been thrust against, but not over, the sediments and metamorphic grades are mostly low greenschist facies (Davies and Smith, 1971). To the east in the D'Entrecasteaux Islands, metamorphic grades are mainly amphibolite and locally pyroxene granulite facies (Davies and Ives, 1965). These relatively high metamorphic grades can be explained in part by high metamorphic gradients induced by tectonic over pressure resulting from overthrusting of the Papuan ultramafic belt but there is also some evidence for a high temperature/pressure metamorphic event. Isostatic adjustment of this relatively bouyant material can explain both the marked late Tertiary and Quaternary uplift and the observed distribution of ultramafic rocks.

Basaltic rocks

There are three areas of basaltic volcanic rocks in south-eastern Papua, namely the Goropu Metabasalt in the Goropu Mountains, the Kutu Volcanics forming the main ranges at the southeastern tip of the peninsula and the Dabi Volcanics making up basement inliers on Cape Vogel Peninsula. These are described in chapter 3.

Mid-Miocene to Recent volcanism

After the major tectonic event which resulted in emplacement of the Papuan Ultramafic Belt, the character of volcanism in south-eastern Papua changed. In the earlier part of this period activity was partly submarine but during the Pliocene and Quaternary, activity was entirely terrestrial. This reflects the emergence of eastern Papua as a landmass during the latter part of the Cenozoic (Smith, 1970). Mid-Miocene to Recent volcanic rocks occur in a northern volcanic belt which extends from the Louisiade Archipelago through the D'Entrecasteaux Islands onto the north coast of the Papuan peninsula, and a southern volcanic belt which runs along the south coast and then turns northward to meet the northern belt in the Managlase Plateau area.

Quaternary volcanism

Two distinct suites of Quaternary high-Si alkali-rich rocks are recognised in the islands immediately north of the Papuan peninsula.

In the Dawson Strait area of the D'Entrecasteaux Islands there is a
well developed series of peralkaline rhyolites and in the Lusancay
Islands there are several outcrops of an unusual high-K trachyte.

The Dawson Strait peralkaline rhyolites and associated
low-Si rocks are closely comparable with the transitional basalt
association characteristic of extensional areas of the earth's crust.
The occurrence of these rocks in southeast Papua is anomalous in
terms of the tectonic setting which gave rise to the Miocene to
Recent volcanic belts but is consistent with the observation (Milsom,
1970; Luyendyk and others, 1973) that spreading has taken place in
recent times. This implies that as the earlier presumably compressional
regime which gave rise to the Miocene-Recent volcanic arcs was replaced
from the east the nature of volcanism also changed.

The potassium-rich trachytes are unique in eastern Papua and
are not clearly comparable with any previously described rock type.
Dating of these trachytes shown them to be extremely young (less than
2 m.y.) so that it is unlikely that their present tectonic setting is
significantly different from that in which the magmas were generated.
In spite of this they cannot be clearly associated with any recognised
Recent tectonic event. These trachytes provide one of the more
intriguing problems of the area.

CHAPTER 3

THOLEIITIC BASALTS IN SOUTHEAST PAPUA

3-1   Introduction

In the western part of the Papuan peninsula Upper Mesozoic
basalts overlie peridotites of the Papuan ultramafic belt (Davies,
1971). According to Davies' interpretation, these basalts represent
former oceanic crust over-thrust and uplifted by plate collision;
as such, they are irrelevant to the problems posed by the basalts to
the southeast and are not discussed further. In the Goropu Mountains,
the Goropu Metabasalt underlies the ultramafic rocks and apparently
represents Cretaceous sea floor. To the southeast the Kutu Volcanics
are partly Upper Cretaceous and partly Middle Eocene; the Cretaceous
rocks are probably part of the oceanic crust represented by the Goropu
Metabasalt but the Eocene basalts were apparently erupted during a
distinct volcanic episode, as were the Dabi Volcanics of Oligocene age
on Cape Vogel Peninsula. The Loluai Volcanics on Woodlark Island are
not directly correlated with any of the basalts on the mainland.

Pillow structures, and the presence of interbedded pelagic
calcareous sediments show the east Papuan basalts are submarine.
Recent literature (e.g. Jakes and Gill, 1970; Miyashiro, 1974) has
stressed the importance of an early stage of submarine volcanism in
the development of some island arc systems. It is important for
paleotectonic reconstruction and for hypotheses of magmatic evolution
to determine whether the basement basalts in southeastern Papua are
of an early island arc type or are of ocean floor type. Recent workers
(e.g. Cann, 1970; Kay and others, 1970; Pearce and Cann, 1971; 1973)
have suggested that the distinction between basalt types can be made on
the basis of chemical composition and this is the approach used.

3-2   Description of the basalt formations

Goropu Metabasalt

The Goropu Metabasalt (Smith and Davies, 1976) forms a
contiguous outcrop area from the Goropu Mountains east to the Kiramara
River ($9^{o}32'$ - $9^{o}38'$S; $148^{o}35'$ - $149^{o}41'$E); the total area of outcrop
is about 1600 km^2. About 80% of the formation consists of basalt,
microgabbro and gabbro which have been sheared and metamorphosed to
varying degrees. Subordinate calcareous sediments intercalated with

the basaltic rocks contain Upper Cretaceous (Maestrictian) microfossils (Belford in Smith and Davies, 1976). The present exposed thickness of the Goropu Metabasalt is about 4000 m.

Some of the metabasalts are strongly schistose and completely recrystallised, others are strongly schistose but contain relic clino-pyroxene, some are completely recrystallised but non schistose and others are moderately or weakly schistose but retain part of their original igneous texture. Almost all of the rocks are metamorphosed at least to prehnite or pumpellyite-bearing grades, and in some cases up to actinolite-bearing grades.

The most common mineral assemblage observed in basaltic rocks exposed in the western part of the outcrop area is chlorite-albite-epidote-actinolite. Relic clinopyroxene is preserved in many specimens and in some this shows marginal alteration to glaucophane or, less commonly, crossite. Other common minerals are quartz and calcite in veins, pumpellyite, white mica, stilpnomelane, and in a very few samples, lawsonite; iron-titanium oxides are accessory. To the east, in the Dayman Dome area, the basaltic rocks typically contain the assemblage albite-chlorite-epidote-actinolite with or without relic clinopyroxene. Stilpnomelane, quartz and calcite are common, glaucophane and chloritoid are less common. East of the Dayman Dome, the basaltic rocks retain much of their primary mineralogy and texture. Clinopyroxene and less commonly altered plagioclase are preserved; pumpellyite, chlorite, epidote, calcite and quartz replace up to 50% of the rocks.

A major fault, the Mai'iu fault defines the northern boundary of the Dayman Dome. This fault separates metamorphosed basalt (Goropu Metabasalt) from minor outcrops of ultramafic rock to the north and is therefore thought to be the equivalent of the major thrust zone along which the Papuan ultramafic belt was emplaced. Metamorphic grade decreases southward away from the Mai'iu fault suggesting that meta-morphism was caused by tectonic overpressures associated with emplacement of the belt.

Of the five specimens of Goropu Metabasalt analysed, four are from the Dayman Dome. Two of these (586,587) are completely recrystallised chlorite-albite-epidote schists from the northern margin of the dome where metamorphic grade is highest. The other two are from the dissected core of the dome and are less metamorphosed;

FIGURE 3-1: THOLEIITIC BASALTS IN SOUTHEAST PAPUA.
(numbers refer to analysed specimens)
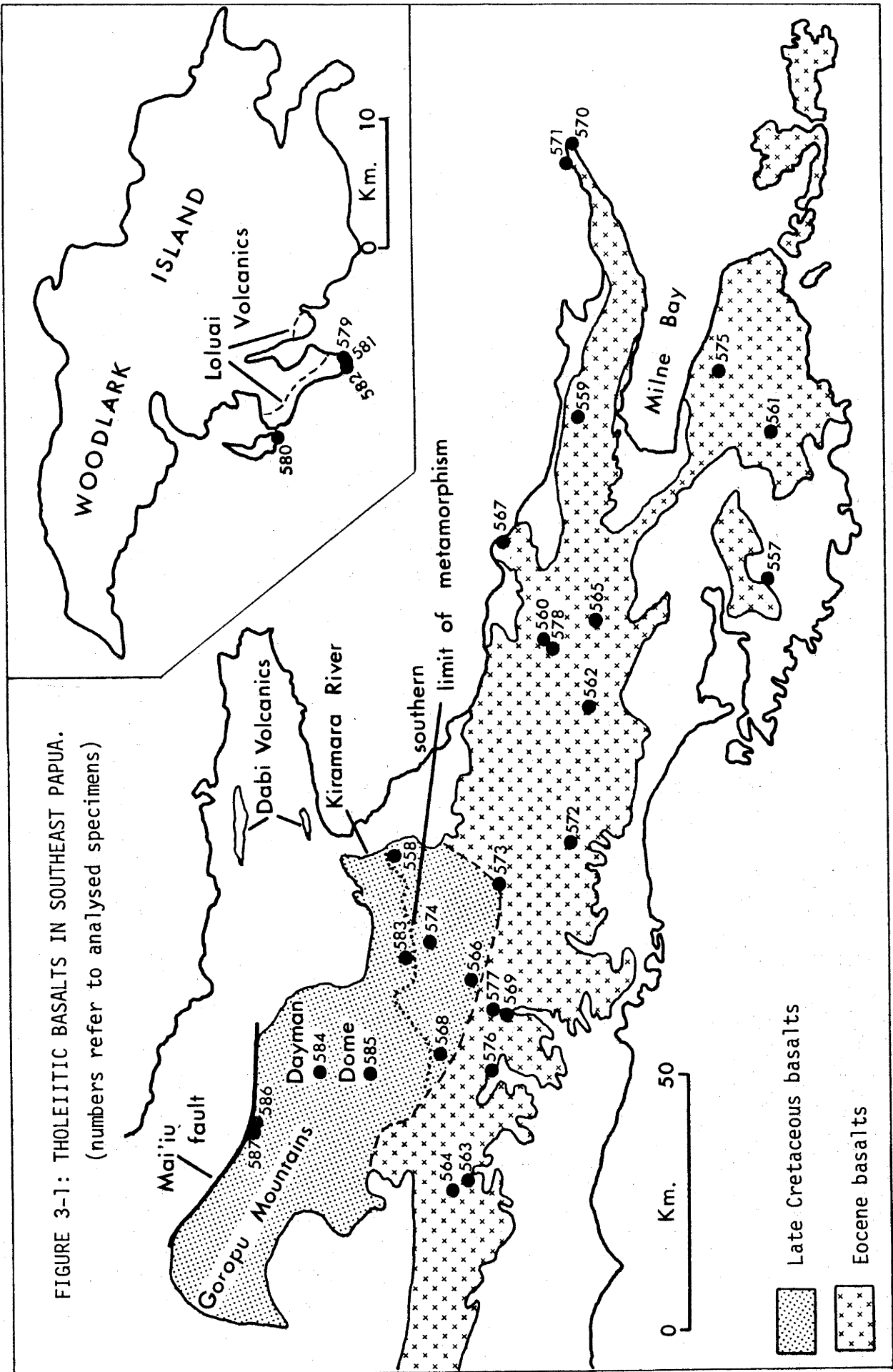
one (585), is a partly recrystallised metabasalt containing relic
pyroxene in a finer matrix of epidote, albite and chlorite, the
other (584) is a fine grained basalt containing moderate amounts
of epidote and chlorite. The fifth analysed specimen (583) is from
the area southeast of the Dayman Dome close to the contact with
unmetamorphosed Upper Cretaceous basalt; the major minerals in this
rock have undergone some retrogressive alteration but are not
recrystallised.

Kutu Volcanics

The Kutu Volcanics (Smith and Davies, 1976) outcrop over
an area of about 5000 km^2 in the main ranges of southeast Papua and
to the south of Milne Bay. Over 95% of the formation is made up of
basaltic rocks. These are for the most part massive and structureless
although bedded flows have been recognised and well developed pillow
structures are not uncommon. The rock types are basalt (average grain
size <1 mm) 70%, with subordinate microgabbro (average grainsize 1-5
mm) 25%, and minor gabbro and ferrogabbro (average grainsize >5 mm).
Minor sedimentary rocks (volcanolithic sandstone and argillite,
calcilutite and limestone) from lenses and beds intercalated with the
basalts.

Microfossil ages in the northern part of the area mapped as
Kutu Volcanics are Upper Cretaceous, those to the south and southeast
are middle Eocene. The contact between unmetamorphosed Upper
Cretaceous basalt (Kutu Volcanics) and metamorphosed Upper Cretaceous
basalt (Goropu Metabasalt) is poorly defined and is probably
transitional. Available evidence suggests that the contact between
Upper Cretaceous and Eocene basalts is a fault. The two formations
are each composed of essentially the same rock types and microfossils
in the associated sediments indicate a predominantly deep water oceanic
environment. The microfossil data indicate that there were two distinct
episodes of submarine volcanism, one late Cretaceous and the other
middle Eocene.

Basaltic rocks of the Kutu Volcanics consist of labradorite,
typically An_{50-55} (40-60%), clinopyroxene (20-30%) and iron-titanium
oxides (5%). Fresh olivine has not been observed but green-brown
pseudomorphs probably after olivine, are found as microphenocrysts in
some specimens. Fine grained interstitial material is common in many

specimens. The texture in these rocks ranges from porphyritic to equigrangular and in the coarser basalts (>0.5 mm average grainsize) and microgabbros plagioclase-pyroxene intergrowths are well developed. The groundmass in porphyritic specimens is typically microcrystalline but in a few it is glass. Phenocrysts in porphyritic specimens are labradorite and clinopyroxene.

Quartz and quartz-feldspar intergrowths occur in a few differentiated coarse-grained specimens. These minerals comprise up to 20 vol. % of the specimens and are associated with more sodic plagioclase (An_{35-45}), iron-rich clinopyroxene and abundant iron-titanium oxides. Iron staining of grain boundaries and interstitial material is common. These are the rocks referred to as ferrogabbros and they occur as discrete bodies within the basaltic pile. Two of these bodies have been mapped as the East Cape Gabbro and the Yau Gabbro (Smith and Davies, 1976).

Rocks of the Kutu Volcanics are generally fresh apart from the altered olivine. Basaltic rocks adjacent to intrusive bodies commonly show some degree of local alteration. In the northwest there is an increase in pervasive alteration and in secondary veining adjacent to the metamorphosed basalts of the Goropu Metabasalt. Sericite and chlorite are typical alteration products of plagioclase and amphibole and chlorite are alteration products of pyroxene. Prehnite, epidote, K-feldspar and calcite occur as secondary and vein minerals and are locally abundant.

Twenty two specimens of Kutu Volcanics were selected for chemical study and these are considered to be representative of the rock types which make up the formation. Four specimens (574,575,576, 577) have suffered extensive alteration and one (578) adjacent to a middle Miocene intrusive has been contact metamorphosed to a fine grained chlorite-epidote-actinolite rock.

Dabi Volcanics

The Dabi Volcanics (Smith and Davies, 1976) form small basement inliers within a thick late Tertiary sedimentary sequence on Cape Vogel peninsula. The formation is made up of pillow lavas, lava flows, and interbedded tuff which are predominantly of basaltic composition but include rocks of intermediate composition. Maximum exposed thickness of the formation is only a few hundred meters;

age based on a single whole rock K-Ar determination (Dallwitz and others, 1966) is Upper Oligocene.

Earlier studies (Dallwitz and others, 1966; Dallwitz, 1968) have concentrated on the unique clinoenstatite-bearing rocks. These rocks are not typical of the formation as a whole and do not form part of the present study. The typical rock type of the formation is fine to very fine grained although some specimens contain small (0.5 mm) rare phenocrysts. They consist of labradorite and clinopyroxene with subordinate iron-titanium oxides; olivine or more commonly quartz is present in some specimens. Interstitial glass is an important constituent in some specimens, in others it has apparently been replaced by zeolites which are also present as cavity fillings. Calcite and less commonly epidote occur as secondary minerals.

Loluai Volcanics

The Loluai Volcanics on Woodlark Island have been breifly described by Trail (1967). The formation consists of tuff, lava, pillow lava and thin-bedded agglomerate interbedded with fine siltstone, mudstone, some shale, and minor quartzite all of which unconformably underlie Lower Miocene limestone. The significance of the Loluai Volcanics is that they are the oldest rocks exposed on the Woodlark Rise and so they may provide some insight into the nature of the crust to the northeast of the Papuan mainland.

According to Trail (1967) the rocks of the Loluai Volcanics consist mainly of altered calcic andesine and pyroxene; fresh pyroxene is rare, magnetite and pyrite are abundant. The four specimens available were collected from a well exposed pillow lava sequence at Suloga Point (579, 581, 582) and from volcanic rocks unconformably underlying Miocene limestone at Kwagai Passage (580). All are fine-grained to slightly porphyritic basalts consisting of labradorite and clinopyroxene with subordinate interstitial material and accessory iron-titatium oxides. Phenocrysts where present are labradorite and clinopyroxene. Chlorite, epidote and calcite are minor secondary minerals in these specimens. These four basalts are petrographically very similar to basalts on the mainland (Kutu Volcanics).

TABLE 3-1: THOLEIITIC BASALTS AND ASSOCIATED ROCKS

Kutu Volcanics

No.	557*	558*	559*	560*	561*	562*	563	564	565*	566	567*	568	569	570*	571*
wt%															
SiO_2	48.60	49.10	48.10	48.90	48.00	48.30	48.00	48.00	47.50	47.85	48.50	45.99	48.14	47.70	49.50
TiO_2	1.44	1.16	1.29	1.18	1.29	1.39	1.47	1.29	1.57	1.34	1.41	3.81	1.97	2.60	2.90
Al_2O_3	14.80	14.10	14.50	13.20	14.50	13.00	13.29	13.49	13.90	13.73	13.40	14.83	12.77	12.40	11.40
Fe_2O_3	4.35	4.50	4.20	3.30	4.30	4.75	4.21	5.75	4.90	5.22	4.45	3.92	5.33	4.90	3.75
FeO	6.55	7.00	6.20	8.05	6.55	8.90	8.05	6.41	6.20	6.94	8.10	10.22	10.38	12.60	16.00
MnO	.17	.19	.16	.19	.18	.26	.22	.21	.23	.21	.17	.24	.25	.25	.31
MgO	12.10	12.20	8.00	8.55	7.75	9.45	8.07	7.87	6.85	7.47	7.35	5.19	5.41	5.45	2.70
CaO	6.45	7.65	11.80	11.60	11.10	6.55	11.23	12.04	11.80	11.66	11.50	9.86	9.01	9.05	6.80
Na_2O	2.55	2.10	2.75	2.20	2.10	3.50	2.58	2.22	2.30	2.46	2.25	2.47	2.99	2.50	3.15
K_2O	.13	.07	.07	.24	.14	.08	.24	.05	.15	.09	.07	.13	.16	.09	.12
P_2O_5	.13	.10	.11	.06	.07	.13	.10	.11	.13	.12	.11	.10	.19	.08	.30
S	nd	nd	nd	nd	nd	nd	.16	.02	nd	.06	nd	nd	nd	nd	nd
H_2O+	1.08	1.25	1.47	1.75	1.85	2.40	1.71	1.21	2.05	1.48	1.74	2.02	2.08	1.83	2.32
H_2O-	1.44	.63	1.47	.57	1.61	1.00	.52	1.18	2.20	.96	1.16	.23	.60	.35	.54
CO_2	.40	.03	.08	.30	.20	.20	.11	.0	.10	.19	.03	.62	.39	.05	.05
Total	100.19	100.08	100.20	100.09	99.64	99.91	99.96	99.85	99.88	99.78	100.24	99.63	99.67	99.85	99.84
Fe_2O_3/FeO	.66	.64	.68	.41	.66	.53	.52	.90	.79	.75	.55	.38	.51	.39	.23
Mg.No. $(Fe_2O_3/FeO=0.2)$	70.6	69.6	62.4	61.7	60.7	59.8	58.6	58.5	57.3	57.1	55.7	43.9	42.5	39.9	22.4
ppm Ba	0	0	0	5	5	0	0	0	7	0	0	0	0	0	0
Rb	1	1	0	2	2	1	5	1	2	1	0	1	2	1	1
Sr	176	113	125	133	180	106	128	121	192	115	101	142	148	100	115
Pb	23	8	1	9	7	9	7	8	7	8	0	8	10	10	9
Th	1	1	0	0	1	0	1	0	0	1	0	0	0	0	0
U	0	1	8	0	0	0	0	0	0	0	0	0	0	1	1
Zr	87	64	71	59	72	83	51	69	93	67	73	56	101	61	146
Nb	5	4	4	4	3	4	4	4	5	4	5	6	7	3	12
Y	24	22	23	22	20	29	21	24	25	24	27	20	36	25	53
La	5	3	3	2	3	4	1	2	4	3	4	1	6	2	7
Ce	4	4	4	6	13	8	3	5	7	3	7	2	8	2	14
Sc	28	33	37	45	26	35	49	43	44	44	39	43	44	49	33
V	307	312	283	314	239	410	458	382	372	361	360	496	417	373	71
Cr	166	139	203	269	221	36	227	131	169	156	86	0	0	0	0
Ni	62	84	77	120	116	55	95	101	62	89	74	0	35	12	0
Cu	129	143	129	149	117	199	234	167	158	162	173	31	240	277	9
Zn	79	73	75	84	72	96	101	96	93	95	77	93	99	117	137
Ga	19	14	18	15	17	16	15	17	17	16	17	20	20	17	22
K/Rb	1079.19	581.10	-	996.18	581.10	664.12	398.47	415.07	622.61	747.13	-	1079.19	664.12	747.13	996.18
Zr/Nb	17.40	16.00	17.75	14.75	24.00	20.75	12.75	17.25	18.60	16.75	14.60	9.33	14.43	20.33	12.17

nd = not determined.   Abundances < 0.5 ppm recorded as 0.   * = major element analysis by AMDL.

TABLE 3-1 (CONTINUED)

No. wt%	Kutu Volcanics — Glassy Basalts		Kutu Volcanics — Altered Basalts					Loluai Volcanics				Goropu Metabasalt				
	572*	573*	574*	575*	576	577	578*	579	580	581	582	583*	584	585	586	587
SiO$_2$	53.60	53.00	44.10	49.00	49.01	48.86	50.40	49.21	49.47	49.25	49.81	50.33	48.01	47.65	46.11	47.92
TiO$_2$	.76	.78	.99	1.49	1.80	1.79	1.28	1.34	1.34	1.37	1.37	.53	1.78	1.75	1.95	1.78
Al$_2$O$_3$	12.90	13.40	15.80	13.80	14.56	13.34	13.60	14.84	14.23	15.15	15.01	14.97	13.46	14.39	14.10	13.81
Fe$_2$O$_3$	4.05	3.45	4.05	8.50	4.11	5.15	4.40	4.54	4.55	4.30	4.21	2.19	4.32	4.61	5.09	4.97
FeO	7.20	7.45	6.15	4.10	7.08	8.62	7.40	6.27	6.34	6.69	6.83	6.45	7.25	7.04	7.06	7.06
MnO	.15	.21	.15	.20	.20	.22	.19	.18	.18	.17	.17	.17	.18	.18	.19	.20
MgO	6.40	4.05	10.50	9.35	7.09	6.11	7.85	6.27	6.30	6.28	5.85	8.38	7.02	6.86	7.33	6.71
CaO	3.25	7.90	7.70	6.90	10.64	9.13	9.65	12.78	11.33	12.92	12.57	12.25	10.21	9.82	10.76	10.17
Na$_2$O	1.93	1.62	3.30	2.95	2.46	3.52	3.20	2.44	2.71	2.52	2.64	1.66	3.69	3.81	2.45	2.87
K$_2$O	.52	.15	.90	1.37	.42	.32	.39	.07	.14	.06	.05	.11	.09	.14	.90	.77
P$_2$O$_5$	.08	.07	.15	.15	.21	.19	.06	.12	.14	.12	.14	.05	.19	.19	.20	.20
S	0.00	0.00	0.00	0.00	.12	0.00	0.00	.02	.04	.01	.10	.18	.01	0.00	.22	0.00
H$_2$O+	5.95	5.95	4.05	1.50	1.42	1.78	1.33	.26	.61	.26	.11	2.46	2.74	3.06	3.11	2.89
H$_2$O-	2.65	1.71	.44	.66	.57	.76	.09	.88	2.04	1.14	.99	.24	.28	.17	.15	.14
CO$_2$	.40	.16	1.70	.0.	.0	.13	.20	.20	.29	.25	.07	.23	.04	.06	.33	.39
Total	99.84	99.90	99.98	100.02	99.69	99.92	100.04	99.42	99.71	100.49	99.92	100.20	99.27	99.73	99.95	99.88
Fe$_2$O$_3$/FeO	.56	.46	.66	2.07	.58	.60	.59	.72	.72	.64	.62	.34	.60	.65	.72	.70
Mg.No. (Fe$_2$O$_3$/FeO=0.2)	55.0	44.3	69.0	62.3	57.7	48.9	58.9	55.7	55.6	55.2	53.3	67.4	56.7	56.0	56.6	54.7
ppm Ba	7	3	17	137	49	16	0	nd	nd	nd	nd	0	0	0	40	26
Rb	13	4	23	31	4	5	5	"	"	"	"	2	0	1	21	15
Sr	100	88	208	337	215	151	93	"	"	"	"	85	105	181	173	148
Pb	8	1	7	7	9	6	10	"	"	"	"	5	1	7	8	8
Th	0	1	0	0	1	1	0	"	"	"	"	0	0	0	0	0
U	0	0	0	0	0	0	9	"	"	"	"	0	1	1	0	2
Zr	51	51	72	87	120	89	70	"	"	"	"	28	105	99	129	110
Nb	2	2	4	5	7	6	5	"	"	"	"	3	4	6	9	6
Y	20	19	19	26	28	31	26	"	"	"	"	13	28	28	32	31
La	1	2	3	4	7	4	2	"	"	"	"	0	4	4	4	4
Ce	1	3	5	13	16	9	7	"	"	"	"	0	8	10	10	11
Sc	30	36	26	36	36	48	54	41	43	41	43	41	39	37	43	45
V	381	403	192	277	285	401	398	nd	nd	nd	nd	238	330	328	383	360
Cr	1	7	278	125	170	52	193	"	"	"	"	107	194	145	191	230
Ni	14	21	174	60	69	66	91	"	86	"	63	87	43	62	58	65
Cu	133	149	54	144	130	55	56	"	129	"	147	95	106	90	103	98
Zn	99	88	76	80	83	119	77	"	89	"	92	72	111	109	117	118
Ga	14	16	13	17	19	17	17	"	nd	"	nd	14	17	18	18	18
K/Rb	332.06	311.31	324.84	366.87	871.66	531.30	647.52	-	-	-	-	456.58	-	1162.21	355.78	426.14
Zr/Nb	25.50	25.50	18.00	17.40	17.14	14.83	14.00	-	-	-	-	9.33	26.25	16.50	14.33	18.33

TABLE 3-2: SELECTED MAJOR ELEMENT ANALYSES FROM THE DABI VOLCANICS

(analyses from Smith and Davies, 1976)

No.	33	35	37	38	39	40	42	44	62	63	64	65	66	67	68	69	70
SiO_2	46.66	48.60	49.80	50.00	50.10	50.80	52.20	52.50	57.64	59.40	60.10	62.22	64.60	66.30	66.60	66.60	67.10
TiO_2	1.18	.59	.65	.66	1.08	.75	.76	.28	1.25	.81	.65	.69	.82	.86	.85	.86	.88
Al_2O_3	11.81	14.90	15.30	14.70	14.20	14.90	10.43	15.80	12.41	15.50	14.50	15.01	13.30	12.80	12.60	12.80	12.80
Fe_2O_3	5.23	1.53	5.05	5.45	7.85	4.05	5.24	2.05	6.83	5.10	3.60	5.94	3.95	3.10	2.80	3.05	2.85
FeO	7.73	5.85	4.65	4.80	6.05	5.70	8.19	5.00	3.53	3.70	4.05	1.69	3.45	3.95	4.10	4.10	4.10
MnO	.17	.13	.11	.11	.14	.15	.18	.13	.07	.13	.10	.08	.09	.10	.10	.09	.09
MgO	7.88	10.90	7.40	7.35	5.40	7.10	7.31	6.90	5.51	2.50	3.85	1.79	2.50	2.15	2.05	2.05	1.92
CaO	11.00	13.10	9.70	9.30	7.75	8.40	9.48	10.20	7.91	7.50	8.90	6.89	7.30	6.65	6.55	6.75	6.50
Na_2O	2.14	1.57	1.81	1.78	2.30	4.20	2.02	1.83	2.09	2.55	1.87	1.97	2.20	2.20	2.15	2.30	2.35
K_2O	.34	.14	.04	.04	.16	.07	.29	.34	.08	.55	.13	.71	.26	.34	.17	.21	.22
P_2O_5	.15	.04	.06	.05	.06	.05	.14	.03	.15	.09	.07	.10	.08	.09	.09	.09	.75
S	.00	.00	.00	.00	.00	.00	.00	.00	.00	.00	.00	.00	.00	.00	.00	.00	.00
H_2O+	4.73	2.05	1.39	1.43	1.37	2.27	2.86	3.70	1.93	.88	.83	2.38	.85	.73	.65	.69	.75
H_2O-	.98	.49	3.85	3.95	3.45	1.57	.39	1.17	2.35	.91	1.11	1.36	.82	.58	1.13	.66	.49
CO_2	.00	.05	.02	.29	.13	.06	.00	.05	.00	.02	.06	.00	.09	.06	.05	.09	.08
Total	100.00	99.94	99.83	99.91	100.04	100.07	99.49	99.98	101.80	99.64	99.82	100.83	100.31	99.91	99.89	100.34	100.88

3-3   CHEMICAL COMPOSITION

Thirty one major and trace element analyses of specimens collected from the basement formations of eastern Papua are presented in Table 3-1, five of the analysed specimens are from the Goropu Metabasalt, twenty two from the Kutu Volcanics and four from the Loluai Volcanics.   In addition seventeen representative published major element analyses of Dabi Volcanics (Smith and Davies, 1976) are tabulated in Table 3-2.

The chemical data on the Dabi Volcanics differs from that on the other three basement formations in two important respects. Firstly, because of the occurrence of clino-enstatite bearing rocks in the formation they have been intensively studied and the major element chemical data available is out of all proportion to their extent on a regional scale.   Secondly, although broadly similar in major element composition to the other basement formations, the Dabi Volcanics do show significant differences.   Consequently, in the following descriptions and discussion the Dabi Volcanics are generally treated as a special case.

Major elements

The analysed specimens from the Goropu Metabasalt, Kutu Volcanics and Loluai Volcanics are typically basaltic (i.e. <52% SiO_2) and most silica values fall within the range 47.5 to 49% SiO_2.   In view of the wide geographic spread of sample localities this uniformity in SiO_2 content is an important chemical feature of the rocks.

As a group, the analyses show variations in composition that can be explained by processes of secondary alteration, metamorphism and fractionation discussed in detail in the following sections. General characteristics of the group are relatively low Al_2O_3 (typically 13-14%), low K_2O (less than 0.2% in unaltered specimens) and high water contents (typically 2-3% in apparently unaltered specimens).   The rocks are all partly oxidised with Fe_2O_3/FeO ratios ranging from 0.3 to 0.9. TiO_2 contents range from normal basaltic values (1-2%) to relatively high values (2.5 - 3%).

In contrast to the other formations the Dabi Volcanics (Table 3-2) show a wider range of SiO_2 content and are generally

TABLE 3-3: KUTU VOLCANICS AND GOROPU METABASALT - CORRELATION MATRIX

	SiO₂	TiO₂	Al₂O₃	Fe₂O₃	FeO	MnO	MgO	CaO	Na₂O	K₂O	P₂O₅	Rb	Ba	Sr	La	Ce	Y	Th	U	Zr	Nb	Zn	Cu	Ni	V	Cr	Ga	Pb
SiO₂	100	-42	-41						-51																	-41		
TiO₂		100			66	64	-49				46						51			43	61	55		-56		53	74	
Al₂O₃			100		-68	-66	56										-62					-62		56				
Fe₂O₃				100							52	50	69	64		44					50							
FeO					100	77	-64							-41			64				51	62		-56		-58	51	
MnO						100	-51										64					59		-53		-55	54	
MgO							100										-46					-62		62		56	-50	
CaO								100																		46		
Na₂O									100		58				48	45	50			53	43							
K₂O										100		98	83	70														
P₂O₅											100				82	49	84			92	83	65					61	
Rb												100	78	65														
Ba													100	83														
Sr														100														
La															100	48	48			88	70						64	
Ce																100	57			58	47							
Y																	100			85	86	70		-40			71	
Th																		100										
U																			100									
Zr																				100	84	57					68	
Nb																					100	55	-41				75	
Zn																						100					44	
Cu																							100		40			
Ni																								100		80		
V																									100			
Cr																										100	-53	
Ga																											100	
Pb																												100

Correlations less than 40 are omitted

higher in Al_2O_3 and water, and lower in TiO_2. They also show a higher degree of oxidation and there is more variability in elements, such as K_2O. Some of these differences can be related to alteration and fractionation; however, the limited data indicate that the basalts of the Dabi Volcanics are different from the basalts on the mainland.

Trace elements

A feature of the trace element composition of specimens from the Goropu Metabasalt, Kutu Volcanics and Loluai Volcanics is the extremely low abundance of incompatible elements (Rb, Ba, La, Ce, U, Th, Pb). Abundances of these elements greater than 'normal' can be correlated with alteration or metamorphism. The transition elements Zn, Cu, Ni, V, Cr display variations of the order of 100 ppm, these can be related to fractionation but alteration may be a contributing factor. Sr in the basalts typically lies within the range 100-200 ppm; values significantly outside this range can be related to secondary alteration. A correlation matrix for all of the analysed specimens from the Goropu Metabasalt and Kutu Volcanics is presented in Table 3-3. There is a good correlation between K_2O, Rb, Ba and Sr, between P_2O_5, La, Y, Nb and Zr, and between MgO, Ni and Cr, there is a poor correlation of all elements with SiO_2. A general trend within the data is an increase in total iron (as FeO) and TiO_2 both of which are correlated with a decrease in MgO, Ni and Cr.

Rare earth elements

Rare earth element (REE) measurements on three specimens of basalt from the Kutu Volcanics have been published (Jakes and Gill, 1970; Table 3). This data has been reprocessed using a new technique of data reduction (appendix I) and is presented with new data on a ferrogabbro in Table 3-4. These four specimens display flat chondrite normalised REE patterns and the ferrogabbro shows a greater degree of enrichment than the basalts (Figure 3-2). Because Y provides an approximate measure of the abundance of the heavy REE (Taylor, 1966) the La/Y ratio can give an indication of the degree of fractionation of the light REE (La to Eu) over the heavy REE (Gd to Yb). Low La/Y ratios (based on the data presented in Table 3-1 in the range 0.05 to
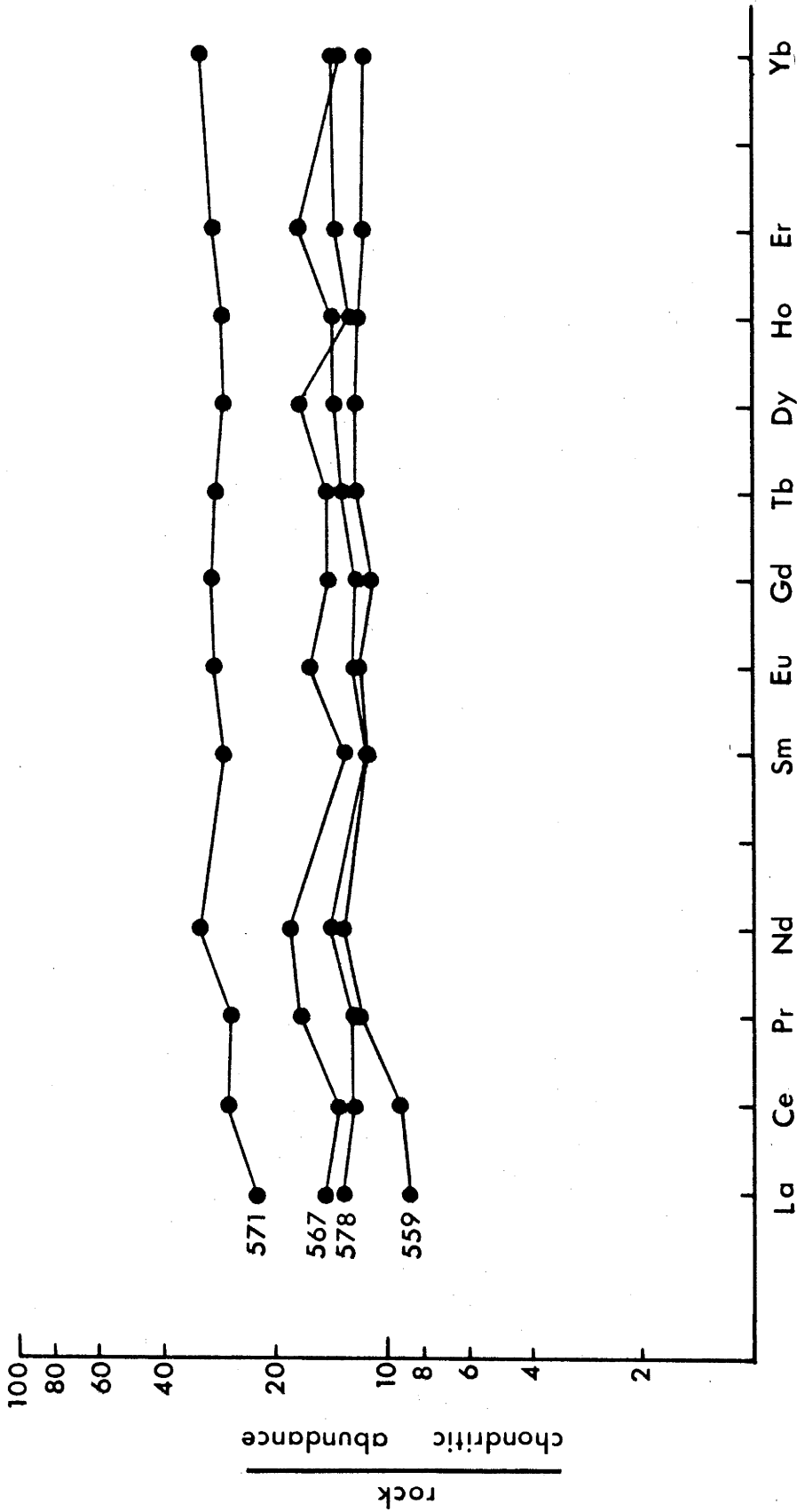
FIGURE 3-2: Chondrite normalised rare earth element patterns in three basalts and a ferrogabbro from the Kutu Volcanics. Numbers refer to analyses in Table 3-4.

TABLE 3-4: RARE EARTH ELEMENT AND OTHER SELECTED
TRACE ELEMENT ABUNDANCES FROM FOUR THOLEIITIC SAMPLES

	No.	559	567	578	571
ppm					
	La	2.6	4.4	3.9	6.8
	Ce	7.8	11.2	10.4	23.0
	Pr	1.4	2.1	1.5	3.2
	Nd	7.7	10.7	8.3	18.9
	Sm	2.5	3.3	2.4	6.0
	Eu	.90	1.2	.92	2.2
	Gd	2.9	3.9	3.1	7.9
	Tb	.60	.72	.65	1.5
	Dy	3.8	5.4	4.4	9.1
	Ho	.89	.92	1.04	2.2
	Er	2.5	2.9	3.7	6.3
	Tm[1]	.39	.47	.45	1.09
	Yb	2.3	2.8	2.7	6.6
	Lu[1]	.36	.44	.42	1.02
	La/Yb	1.13	1.57	1.44	1.03
	Eu/Eu	1.05	1.06	1.06	1.01
	Cs	.41	.26	.60	.12
	Th	.30	.33	.44	1.07
	U	7.3	.71	9.0	.46
	Th/V	.04	.46	.05	2.3
	Hf	1.9	2.1	2.4	4.7
	Zr/Hf	37.4	34.8	29.2	31.1

analyses by spark source mass spectrometry.   [1] estimated abundance

0.25 (but generally < 0.16) typify all of the analysed specimens indicating that the flat chondrite normalised REE patterns measured on the four specimens (figure 3-2) are typical of the formation as a whole. Overall, REE abundances are 10 to 40 times chondritic.

Strontium Isotopes

The major and trace element compositions of the basement tholeiitic basalts in southeast Papua indicate that the rocks are comparable to oceanic basalts. Fresh ocean-ridge tholeiites from the Atlantic, Pacific and Indian Oceans have a mean $^{87}Sr/^{86}Sr$ ratio of .7025 and a range of .7020 - .7030 (Hedge and Peterman, 1970; Hart, 1971). In contrast, ocean and island basalts have ratios of .703 - .706. Limited measurements of the east Papuan tholeiites (Appendix IV) are higher than the ocean ridge basalt range but close to the lower end of the ocean island basalt range.

3-4   Nomenclature and classification

Because the modal mineralogy of the basement basalts in southeast Papua approximate to the mineral end members of the normative iron free basalt tetrahedron (Yoder and Tilley, 1962) they can be plotted within this tetrahedron. In Figure 3-3a the analyses plot from the quartz-tholeiite field into the field of olivine tholeiite. In spite of the alteration only two analyses from the Goropu Metabasalt plot in the region of the critical plane of silica undersaturation separating tholeiitic basalts from alkaline basalts.

Analyses of altered and obviously fractionated rocks have been removed and the normative compositions of the remaining analyses recalculated using an arbitary value of the ratio Fe_2O_3/FeO (0.2, Figure 3-3b). This arbitary value differs from the value 0.1 used by Cann (1971) and from the ratio derived using an Fe_2O_3 value of 1.5 (Coombs, 1963; Kay and others, 1970) or an Fe_2O_3 value as determined by Irvine and Barager (1971) (Fe_2O_3 = 1.5 + TiO_2). An arbitary value of 0.1 appears to be unrealistically low, the other methods of recalculating Fe_2O_3 would produce distortions in the data from eastern Papua because of highly variable total iron and TiO_2 contents. The recalculated analyses plot mainly within the olivine tholeiite field and substantially overlap the fields of oceanic basalts from
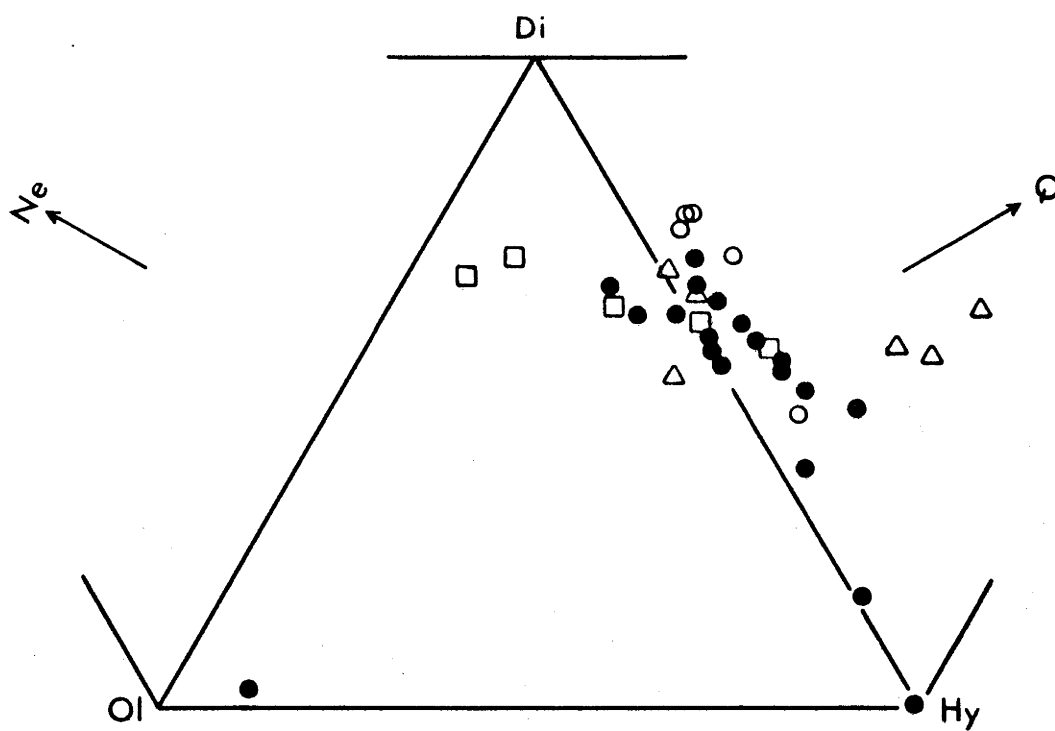
(a) Normative mineralogy calculated using Fe_2O_3/FeO as measured.
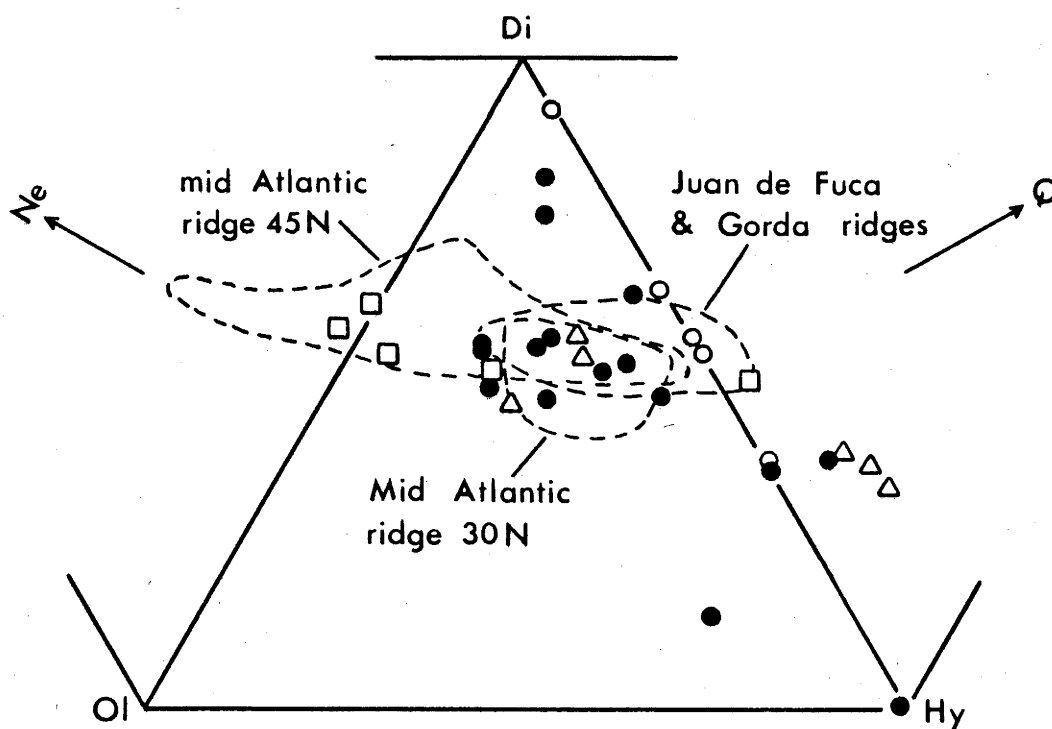
(b) Normative mineralogy calculated with $Fe_2O_3/FeO=0.2$, altered and fractionated samples omitted.

FIGURE 3-3: Expanded normative iron-free basalt tetrahedron.

Open squares - Goropu Metavolcanics, solid circles - Kutu Volcanics, open circles - Loluai Volcanics, open triangles - Dabi Volcanics.

several different localities presented by Kay and others (1970).

On an alkali/silica plot (Figure 3-4a) the analyses all lie on the tholeiitic side of the line dividing Hawaiian tholeiite from Hawaiian alkali basalt (MacDonald and Katsura, 1964). On a FMA diagram the analyses show a trend of extreme iron enrichment (Figure 3-4b).

The basaltic basement rocks in southeastern Papua are tholeiitic in character according to these classic criteria. The low Al_2O_3 and incompatible element content, and high Na_2O/K_2O (generally >10) and K/Rb (300-1100) ratios are most comparable to oceanic basalts as described by Engel and others (1965) and Kay and others (1970).

A similar conclusion is reached using the trace element approach developed by Pearce and Cann (1971, 1973). On a Ti-Zr-Sr diagram (Figure 3-5) the Papuan basalts lie mainly within the field of 'ocean floor' basalts. Overlap into the field of low potassium tholeiites is considered to result from alteration and the trend toward the Ti apex is thought to reflect fractionation. On a plot of Ti-Zr-Y (Figure 3-5) the Papuan basalts plot mainly in the field of ocean floor basalts but overlap into the field of low potassium tholeiites and extend toward the Ti apex.

In conclusion, the chemical and petrographic data show that the basaltic basement in southeastern Papua and on Woodlark Island is made up of tholeiitic basalt of the type characteristically found in the ocean basins.

3-5   VARIATIONS IN CHEMICAL COMPOSITION

Secondary alteration

Volatile content and particularly the content of H_2O- is often taken as an indicator of the degree of alteration of a rock. Despite the fact that many of the east Papuan basaltic rocks appear fresh in thin section, water contents are relatively high. Typical values lie within the range 1 to 2% H_2O+ with a few values as high as 2 to 4% H_2O+ and 0.5 to 1% H_2O- with several values greater than this and some as high as 2% H_2O-. On the other hand CO_2 values are typically low. By comparison, measurements of the water content of oceanic basalt from Juan de Fuca Ridge (Moore, 1970) have shown typical H_2O+
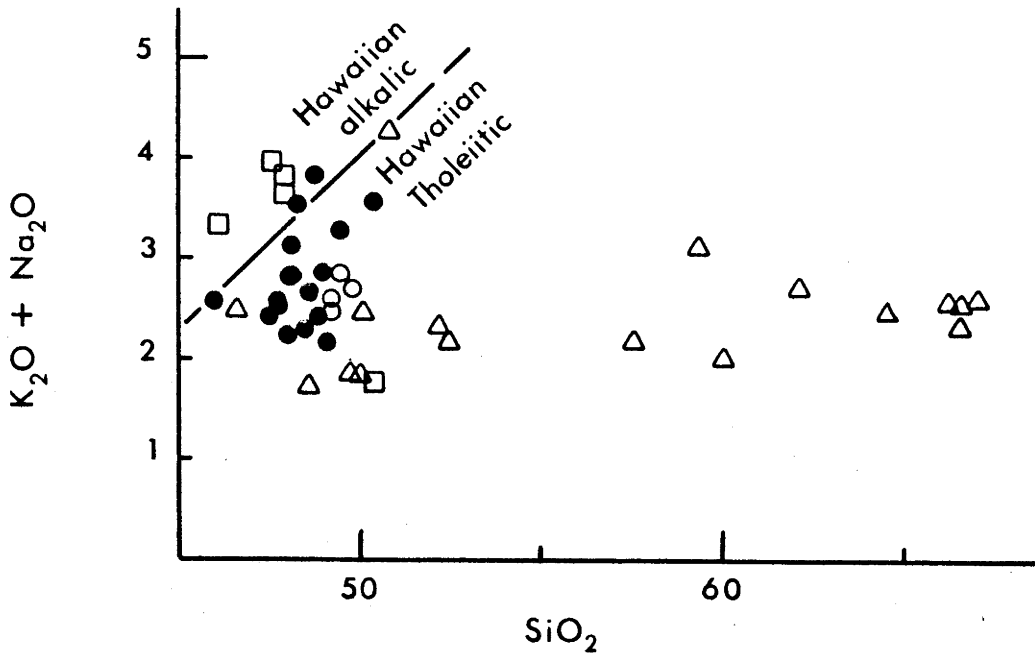
FIGURE 3-4a: Total alkalies (wt.%) against SiO_2.

The line dividing Hawaiian alkalic from Hawaiian tholeiitic rocks is taken from Macdonald and Katsura (1964).
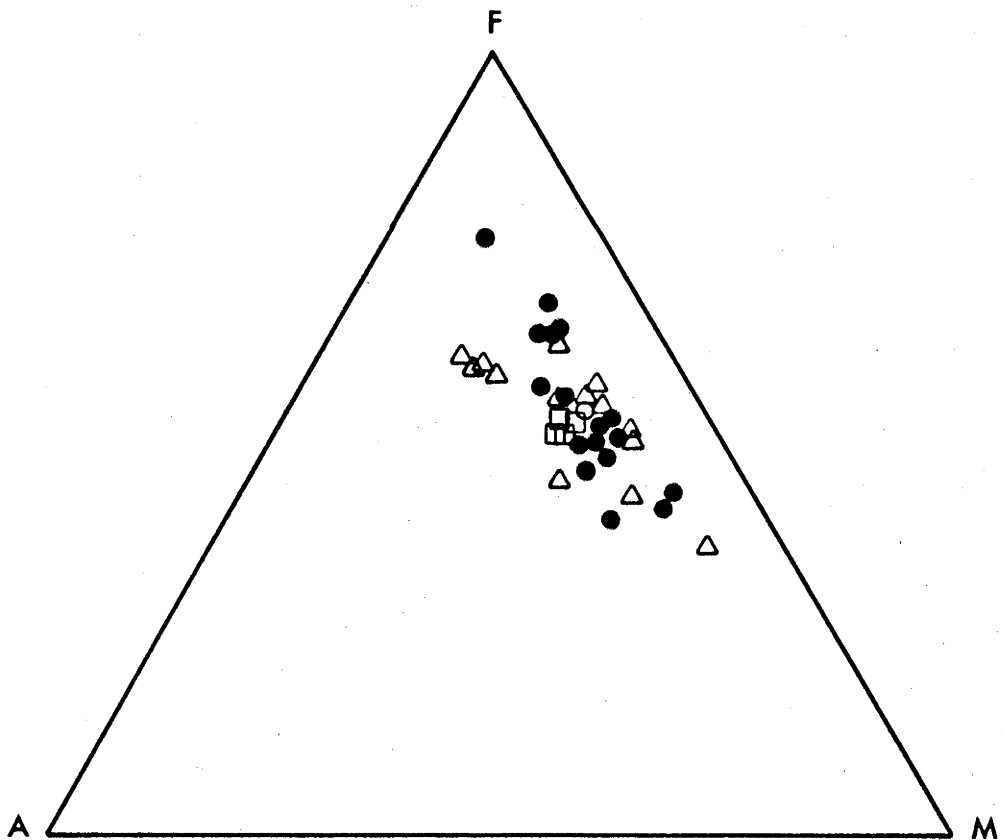
FIGURE 3-4b: Ternary diagram F(total iron as FeO), M(MgO), A(Na_2O+K_2O).

Open squares - Goropu Metabasalt, solid circles - Kutu Volcanics, open circles - Loluai Volcanics, open triangles - Dabi Volcanics.
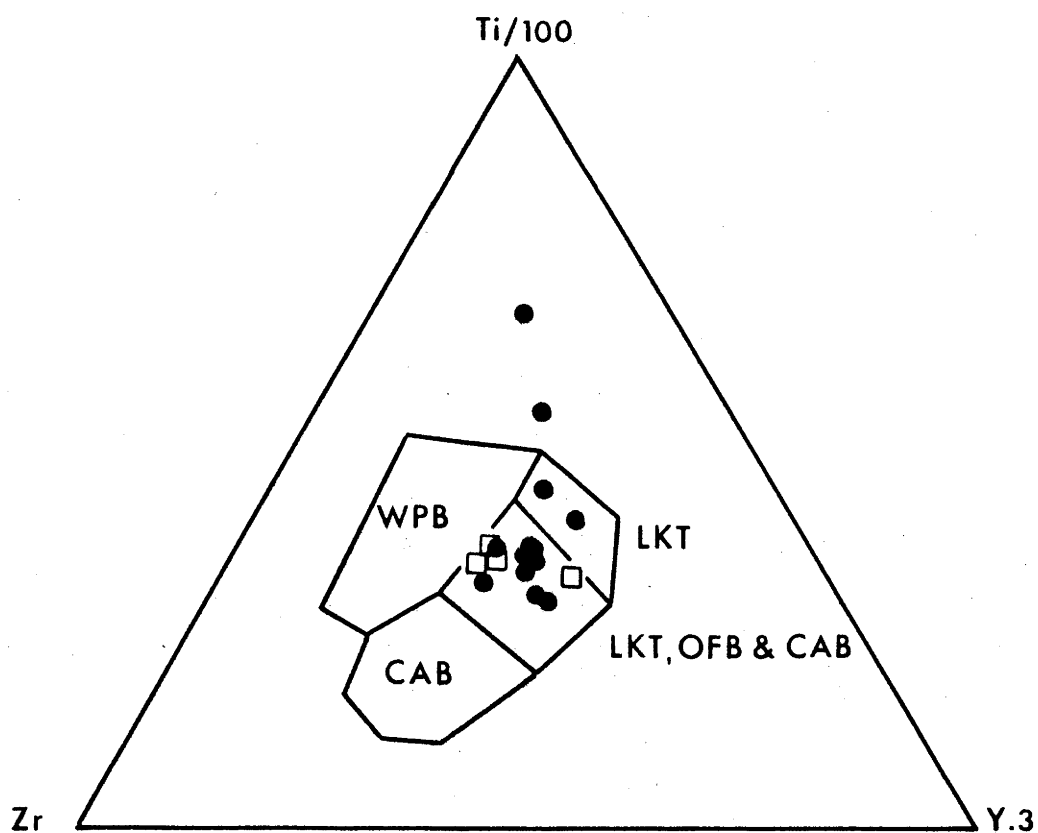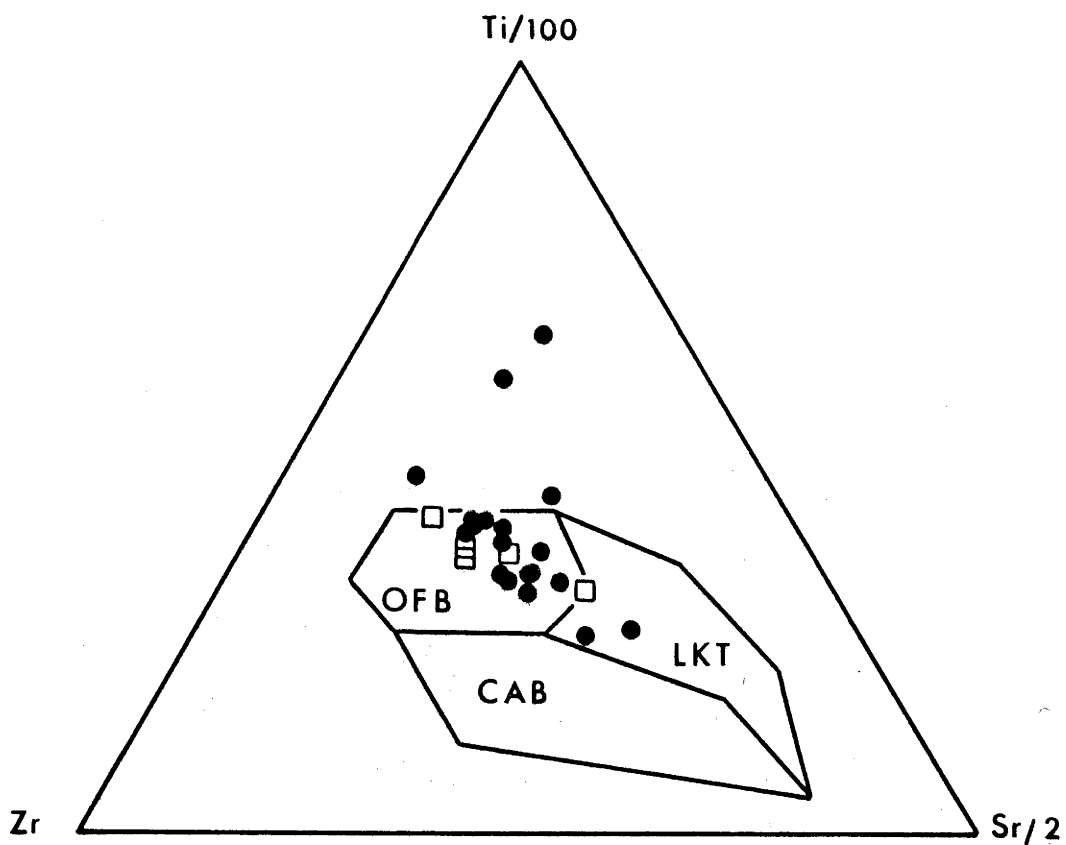
FIGURE 3-5: Ternary plots Ti-Zr-Sr and Ti-Zr-Y, after Pearce and Cann
(1971;1973)

OFB - ocean floor basalts, LKT - low-potassium tholeiites,
CAB - calc-alkali basalts, WPB - within plate basalts.
Open squares - Goropu Metabasalt, solid circles - Kutu
Volcanics.

contents of 0.42 to 0.6%, and H_2O-contents of 0.02 to 0.23%; Moore has suggested that the original total water content of potassium-poor oceanic tholeiites is 0.25%.

Low temperature reaction of sea water with submarine basalt has been discussed by Hart (1971) and Hekinian (1971) who have presented data to show that a continuous reaction can take place so that the older submarine basalts are likely to have higher water contents. This process probably accounts for the relatively high H_2O-contents of some of the Papuan basalts.

Two of the analysed samples from the Kutu Volcanics (572, 573) have significantly higher water contents than the other analyses (H_2O+ 5.95%, H_2O- 1.71 and 2.65%). These samples are composed mainly of glass and the high water contents are due to hydration of this glass. As H_2O+ is affected it would appear that at least some of the water absorbed during hydration of glass, enters mineral structures. These specimens also have significantly lower Na_2O than other basalts - indicating reaction with sea water.

Oxidation of iron as indicated by high Fe_2O_3/FeO ratios is also commonly taken as a measure of the degree of alteration of a rock. The trend of enrichment in total iron and titanium resulting from fractionation of the Papuan basalts suggests that iron-titanium oxides were not early phases indicating that conditions of low oxygen fugacity prevailed in the magma during at least the early stages of crystallisation. The high Fe_2O_3/FeO ratios which typify the rocks are therefore thought to be caused by subsolidus low temperature processes.

A limitation on the efficiency of hydration to alter the bulk composition of these basalts is suggested by their very low incompatible element contents. These elements are typically thought to be more abundant in altered rocks.

Although this conclusion is a general one, the Dabi Volcanics are a special case. Many of the lavas are glassy so the high water contents can be related to hydration of glass. However, K_2O contents are significantly higher than in the other basalts and it seems likely that this is due at least in part to secondary alteration.

A few specimens from Kutu Volcanics show chemical evidence for secondary alteration (analyses 574 to 578 in Table 3-1). These are all specimens which display some degree of alteration of feldspar

and pyroxene. The main effects of secondary alteration are significantly higher K_2O, Rb, Ba and total water and markedly variable Sr contents. In one specimen (578) this alteration is due to an adjacent intrusion; in the others these chemical changes appear to result from normal processes of secondary alteration.

Metamorphism

Five specimens from the Goropu Metabasalt were analysed with the view to gaining insight into chemical changes of the east Papuan basalts during metamorphism. The composition of sample 583 (Table 3-1) is unlike either the unmetamorphosed basalts or the metamorphosed basalts and so is not useful in this comparison. However, the other four analyses represent a trend of increasing metamorphism of a basaltic composition. The composition of the two partly recrystallised basalts (584, 585) is not notably different from that of unaltered basalt with the exception that although total water content is comparable, the H_2O+/H_2O- ratio is very much higher. Presumably this reflects redistribution of available water into the growing metamorphic minerals. The completely recrystallised specimens show increase in K_2O, Rb, Ba, P_2O_5 and CO_2; the H_2O+/H_2O- ratio is again high. The other elements appear to be little affected and in particular La, Ce and Y are little changed; this supports the observation of Frey and others (1968) that REE abundances in basalts are not significantly changed by metamorphism.

The data from analysed specimens of Goropu Metabasalt suggest that the chemical composition of oceanic basalts suffers only minor changes even in moderately altered specimens but, that with complete recrystallisation to greenschist facies mineral assemblages signif-icant changes in some more mobile elements occur.

Crystal fractionation

The east Papuan basalts show a negative correlation between total iron and TiO_2, and MgO, Ni and Cr which can be explained by a process of fractional crystallisation. The SiO_2 content of the Papuan basalts is remarkably uniform and apparently bears no relation to the degree of fractionation a rock has undergone. As Miyashiro (1973) has pointed out, some parameter involving the ratio FeO/MgO is probably the best index of fractionation in tholeiitic basaltic rocks; the

parameter used here is the magnesium number (atomic $100 \times Mg/Mg + Fe^{2+}$; $Fe_2O_3/FeO = 0.2$).

Mg number decreases from 71 (sample 557) to 23 (sample 571); correlated with this is an increase in total iron, TiO_2, MnO, Ni and Cr. As Thompson and others (1972) point out depletion in Ni and Cr reflect precipitation of olivine. Petrographic observations show that olivine was the first phase to crystallise and that olivine was always followed by plagioclase and then by pyroxene co-precipitating with iron-titanium oxides.

Petrographic observations that the main mineral components of oceanic basalt crystallise either in the order olivine, plagioclase, pyroxene or in the order plagioclase, olivine, pyroxene have led Miyashiro and others (1970) and Shido and others (1971) to divide oceanic basalts into OL or PL tholeiites respectively depending on which mineral crystallises first. Essentially the same separation occurs when normative constituents of these basalts are plotted on the normative ternary pyroxene-plagioclase-olivine diagram. Shido and others (1971) suggest that the line separating PL from OL tholeiites is in fact a cotectic. Thus crystallisation of either olivine or plagioclase will drive derivative liquids on to this cotectic at which stage both minerals will crystallise together and further fractionation will result in a mixed trend. The east Papuan basalts plot in the OL tholeiite field of the normative ternary diagram (Figure 3-6) but close to the olivine-plagioclase cotectic; this is consistent with the petrographic observation that olivine is a minor phase.

Mg-numbers of almost all of the east Papuan basalts are lower than that to be expected of magmas which originated by partial melting in equilibrium with residual olivine in the upper mantle according to the model of Green (1971). This, and the scarcity of olivine in the basalts indicates that they have already undergone some fractionation of olivine which explains their proximity to the olivine-plagioclase cotectic. Further fractionation of olivine would drive the compositions of derivative liquids onto the cotectic. It could be expected that subsequent fractionation of plagioclase would show up in the relative abundances of, for example, CaO and Sr but this has not been observed either in the east Papuan basalts or in the
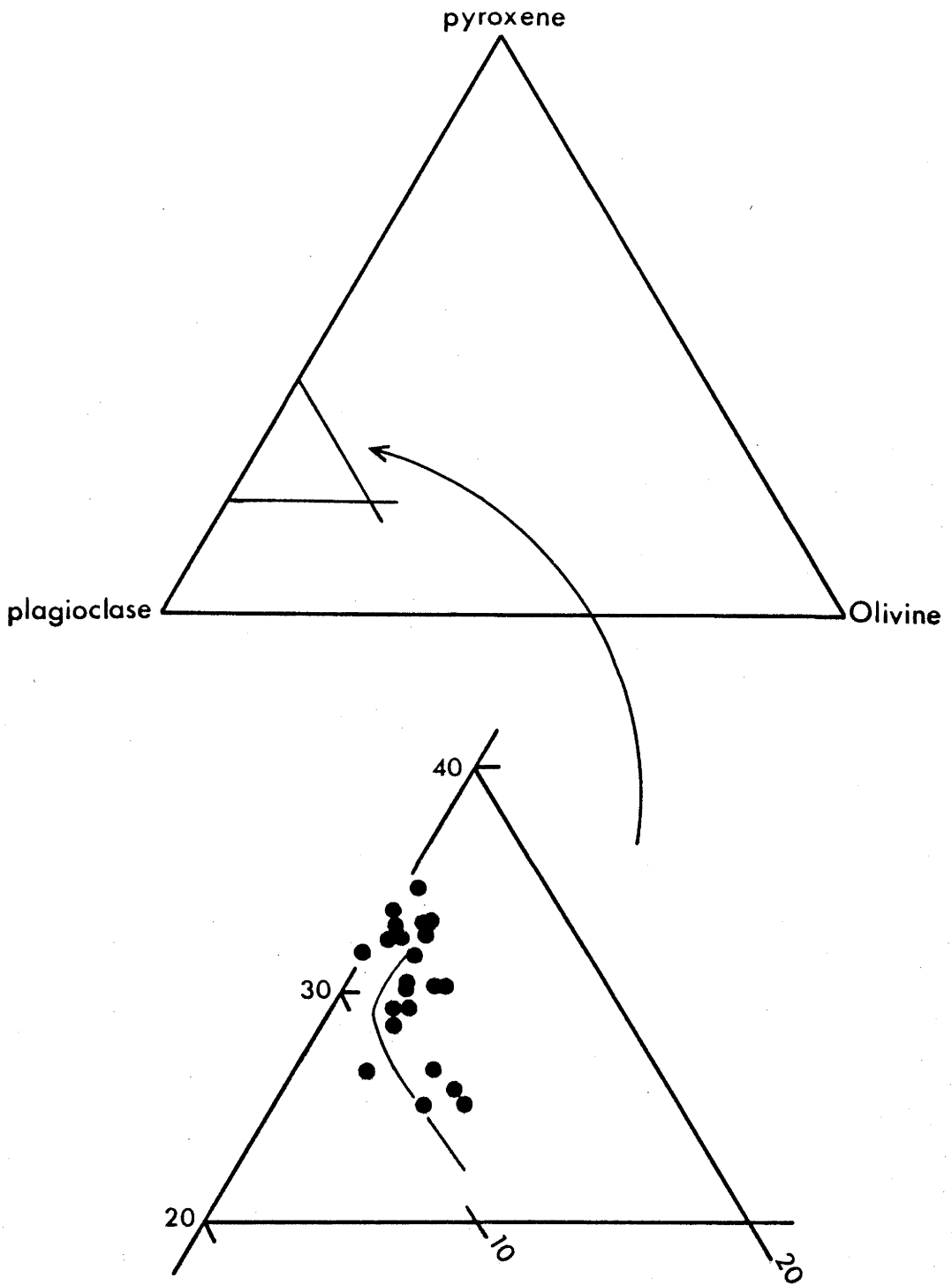
FIGURE 3-6: Normative olivine-plagioclase-pyroxene diagram for the Kutu Volcanics (solid circles).

The curved line within the triangle in the lower part of the diagram is the suggested cotectic separating presumptive OL- and PL- tholeiites (from Shido and others, 1971).

oceanic basalts studied by Thompson and others (1972). The absence
of an Eu anomaly in the most fractionated rock (571) also indicates that
feldspar has not been a fractionating phase. Thompson and others make
the point that although OL-tholeiites show a clearly definable differ-
entiation trend the PL-tholeiites do not. The explanation for this
may be that once crystallisation of plagioclase is initiated, solid-
ification of the whole magma follows rapidly and there is no opportunity
for crystal settling.

Fractionation in the east Papuan tholeiites appears to have
been controlled entirely by removal of olivine and has followed the
classic tholeiitic differentiation trend characterised by enrichment in
iron and TiO_2 relative to MgO with silica and the alkalis remaining
relatively constant. Similar trends are documented for continental
tholeiites, e.g., the Skaergaard complex (Wager 1960) for ocean ridge
basalts (e.g. Shido and others, 1971) and for oceanic islands, e.g.
the Uwekahuna Lacclith, Hawaii (Murata and Richter, 1961). This
uniquely tholeiitic differentiation pattern is not so much a pattern
of iron enrichment as one of inhibition of the trend of silica
enrichment observed in other rock series. Typical oceanic basalts
contain 49-50% SiO_2 (Cann, 1971), typical east Papuan basalts contain
slightly less. Simple calculations show that separation of magnesian
olivine crystals (about 40 wt.% SiO_2) will enrich derivative liquids in
SiO_2, but only after about 20-25% of olivine has been removed will the
silica content of derivitive liquids exceed 53 wt.%, on the other hand
removal of this amount of olivine will drastically modify the FeO/MgO
ratio. Only in the late stages of tholeiitic fractionation when iron-
rich silica-poor olivine becomes a liquids phase will a trend of
silica enrichment become established.

The critical factors leading to a tholeiitic differentiation
trend characterised by enrichment of iron relative to SiO_2 are a
basaltic parental magma (<50% SiO_2) and limited fractionation of olivine
at low oxygen fugacities which will inhibit the development of iron-
titanium oxides on the liquidus. Petrogenetic models for tholeiitic
basalts (Green, 1971) suggest that this will be a relatively low
pressure fractionation trend. If a trend of iron enrichment is
characteristic of olivine-bearing basaltic rocks fractionating at
relatively low pressures it is interesting to speculate that the trend

to intermediate and high-Si compositions observed in many alkali-
basalt associations is initiated at relatively high pressures. This
is embodied in the suggestion of Green and others (1974) that
intermediate alkaline rocks may originate at depth within the mantle.

Differentiated rocks in the Papuan ultramafic belt

Davies (1971) has described basic tonalite, tonalite and
diorite associated with basalts of the Papuan ultramafic belt in the
northwest of the Papuan peninsula. Compared with the differentiated
ferrogabbros in southeastern Papua these tonalitic rocks are high in
SiO_2 (54-65%) and low in TiO_2 but for their SiO_2 content are high in
iron and CaO and low in K_2O (.08 to 1%).

They are comparable to the oceanic plagiogranite described by
Coleman and Peterman (1975) and interpreted as differentiates of
oceanic basalt. It follows that they are not island arc type rocks
related to early Tertiary subduction as has been suggested by Davies
and Smith (1971).

3-6   CONCLUSION

The chemical compositions of the basaltic rocks of the
southeast Papuan ranges (Goropu Metabasalt, Kutu Volcanics) and of
Woodlark Island (Loluai Volcanics) show clearly that these are
tholeiitic rocks comparable to the basalts making up the floor of
the ocean basins. They are not island arc tholeiites forming the
basement of a late Cenozoic island arc volcanic association.

The Goropu Metabasalt and the Upper Cretaceous part of the
Kutu Volcanics could represent former oceanic crust on the leading
edge of the Indian-Australian plate to the north of the Australian
continental block, but that they are contemporaneous or younger than
the metamorphosed sediments (Cretaceous, possibly older) in the area
conflicts with this. Alternatively they may be basalts which were
erupted at an early stage in the spreading of the Coral Sea basin.

The Coral Sea basin is thought to have opened during early
Eocene times. The middle Eocene basalts in southeast Papua (Kutu
Volcanics in part) can only be directly related to this spreading
episode if they spreading was asymetric about a center on the
northern side of the basin so that the youngest 'new ocean floor'
is found on the northern edge of the basin. A second possibility is

that the middle Eocene basalts were erupted during a short lived event on the northern side of the basin after the main spreading episode.

Submarine basalts forming the basement on Woodlark Island should, in a tectonically consistent model, be part of the plate to the north of the lower Tertiary plate boundary and are therefore equivalent to basaltic rocks forming the upper layer of the Papuan ultramafic belt.

The Dabi Volcanics form a basement ridge underlying the thick mid-Miocene to Recent sedimentary sequence on Cape Vogel peninsula immediately north of the main ranges in southeast Papua. Although altered, some of the basalts in the formation are recognisable as tholeiitic; others are unique clino-enstatite bearing basalts (Dallwitz and others, 1966). Dallwitz (1968) has suggested that these clino-enstatite bearing basalts may have originated by partial melting of refractory material consisting mainly of aluminous orthopyroxene formed by fractional crystallisation of basaltic magma at depths of about 60 km. A multistage model of this type would explain the low TiO_2 contents and possibly the lack of iron enrichment which are the main differences between these basalts and those to the south. One of the main problems posed by the Dabi Volcanics from a regional point of view is their young age (28 m.y., Dallwitz and others, 1966). This age is a minimum whole rock K-Ar determination. If correct it indicates that the basalts were erupted immediately after the Papuan ultramafic belt was emplaced and subduction in southeast Papua ceased; this could be one explanation for their lack of metamorphism.

CHAPTER 4

MIDDLE MIOCENE VOLCANISM

The major tectonic event which led to emplacement of the Papuan ultramafic belt in the western part of the Papuan peninsula was followed in the southeast, by extrusion and intrusion of potassium-rich magmas. The earliest record of this activity is the presence of tuffaceous material in Miocene sediments which outcrop in the extreme southeast of the peninsula (Smith and Davies, 1976). These sediments contain a distinctive pale green clinopyroxene which is characteristic of nearby middle Miocene volcanism. A similar record is found in the cuttings of two exploration drill holes put down in sediments to the north of the D'Entrecasteaux Islands (Stoen and Garside, 1973).

Extrusive rocks outcrop in two main areas along the southeast coast of the Papuan peninsula. The Fife Bay Volcanics outcrop to the southwest of Milne Bay and the Cloudy Bay Volcanics outcrop to the west in the vicinity of Cloudy Bay (Figure 4-1). Rock types are agglomerate and lava of predominantly basaltic composition; pillow lavas in some coastal outcrops indicate that at least some of the extrusive activity was submarine. A major part of the Fife Bay Volcanics is made up of a thick (about 300 m) sheet of 'welded' agglomerate which has been interpreted as an autobrecciated lava flow or series of flows (Smith and Davies, 1976).

Small plutons intruding the Eocene tholeiitic basalts to the north and northwest of the Fife Bay Volcanics (Smith, 1972) are comparable in chemical composition to the extrusive rocks and are apparently intrusive equivalents.

Whole rock K-Ar dating of a feeder dyke to the Fife Bay Volcanics (Smith and Davies, 1973a) and of the associated intrusive rocks (Smith, 1972) gives ages of 12 to 16 m.y. These data shows the magmatic event to be Middle Miocene, extending back into the upper part of the Lower Miocene.

4-1 Petrography

Typical specimens of Fife Bay and Cloudy Bay Volcanics are strongly porphyritic rocks of basaltic composition containing well formed phenocrysts in a fine grained groundmass. Phenocrysts are pale green clinopyroxene (4 mm, 10-20 vol. %) typically accompanied by smaller (up to 2 mm across) phenocrysts of olivine (up to 15 vol. %) or plagioclase (up to 30 vol. %) or both. Small (less than 0.5 mm)

FIGURE 4-1: THE SOUTHERN VOLCANIC BELT
(numbers refer to analysed specimens.)
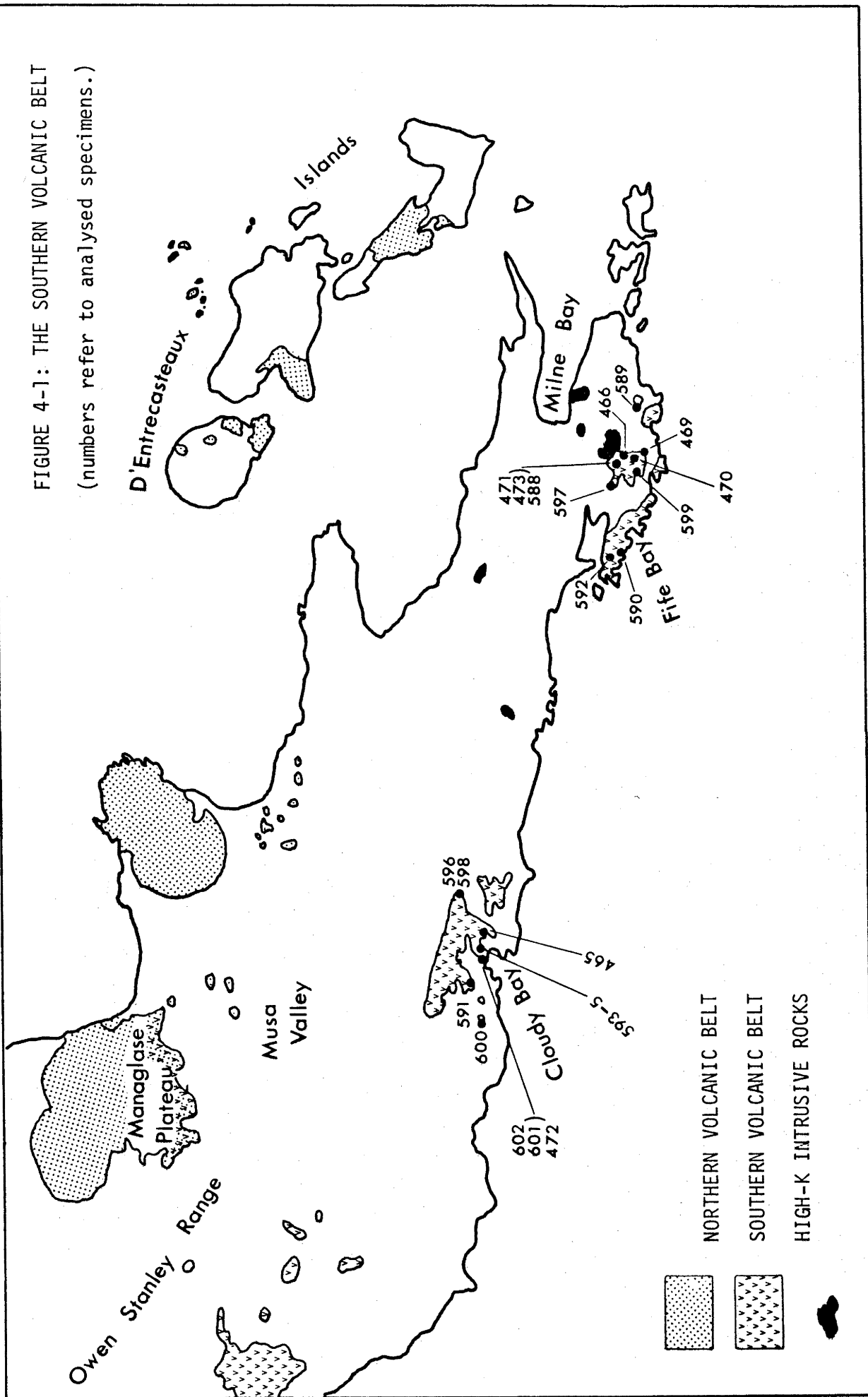
TABLE 4-1: CLINOPYROXENE AND OLIVINE ANALYSES FROM TWO TRACHYBASALTS FROM THE FIFE BAY VOLCANICS.

CLINOPYROXENES

Rock No.	590											592	
Phenocryst	2	2	2	3	3		4	4	4	4	4	1	1
	core	rim	rim	core	rim	core	core	core	rim	rim	rim	core	rim
SiO_2	47.87	49.07	48.54	47.93	47.36	48.28	46.91	47.28	47.67	47.43	47.76	48.48	48.22
TiO_2	.44	.28	.46	.66	.81	.61	.96	.98	.85	.93	.90	.51	.72
Al_2O_3	4.52	3.31	3.03	4.98	5.28	4.12	6.32	6.16	5.46	6.21	5.96	5.52	5.34
FeO	7.54	7.46	7.85	7.19	8.68	8.81	9.33	9.45	9.09	9.18	9.32	5.95	8.88
MgO	13.44	13.88	13.77	13.58	12.81	13.33	12.51	12.29	12.94	12.63	12.30	14.18	13.10
CaO	21.45	21.56	21.16	21.90	21.47	21.75	22.18	22.22	22.27	22.37	22.15	22.72	21.95
Na_2O	.47	.17	.23	.20	.41	.55	.58	.55	.58	.57	.62	.45	.51
Cr_2O_3	.44	.12	.14	.19	.21	.12	.0	.0	.0	.0	.0	.73	.26

number of ions on the basis of 6 oxygens.

	core	rim	rim	core	rim	core	core	core	rim	rim	rim	core	rim
Si^{4+}	1.90	1.96	1.96	1.88	1.88	1.92	1.84	1.85	1.87	1.84	1.87	1.85	1.88
Al^{3+}	.07	.04	.04	.08	.08	.06	.10	.09	.08	.09	.09	.08	.08
Al^{3+}	-	.01	.01	-	-	-	-	-	-	-	-	-	-
Ti	.01	.01	.01	.02	.02	.02	.03	.03	.03	.03	.03	.01	.02
Fe^{2+}	.32	.23	.22	.35	.37	.29	.44	.43	.38	.43	.41	.37	.37
Mg	.80	.82	.83	.80	.76	.79	.73	.72	.76	.73	.72	.80	.76
Ca	.91	.92	.92	.92	.91	.93	.93	.93	.93	.93	.93	.93	.92
Na	.04	.01	.02	.02	.03	.04	.04	.04	.04	.04	.05	.03	.04
Cr	.01	-	-	.01	.01	-	-	-	-	-	-	.02	.01
X+Y+Z	4.06	4.00	4.01	4.08	4.06	4.05	4.11	4.09	4.09	4.09	4.10	4.09	4.08
mol.% Ca	44.8	46.7	46.7	44.4	44.6	46.3	44.3	44.7	44.9	44.5	45.1	44.3	44.9
mol.% Mg	39.4	41.6	42.1	38.6	37.3	39.3	34.8	34.6	36.7	34.9	35.0	38.1	37.1
mol.% Fe	15.8	11.7	11.2	16.9	18.1	14.4	21.0	20.1	18.4	20.6	19.9	17.6	18.0

OLIVINES

Rock No.	'sieved' phenocrysts			inclusions			'fresh' phenocrysts					inclusions	'sieved' phenocrysts		'fresh' phenocryst
	1-1	1-2	2	3	4	5	6	7	8	9-1	9-2	10	11-1	11-2	12
	core	rim	core				core	core	core	core	rim		core	rim	core
SiO_2	38.5	38.2	38.0	38.4	37.7	37.7	37.9	37.9	37.4	38.3	38.3	38.2	37.5	37.9	37.7
FeO	22.1	24.1	24.0	23.7	25.7	25.9	26.0	26.1	26.8	22.8	22.6	23.6	26.0	25.7	26.2
MnO	.4	.4	.3	.3	.5	.4	.5	.5	.5	.3	.3	.4	.3	.3	.4
MgO	38.5	36.7	37.0	37.0	35.3	35.1	35.0	35.0	34.9	38.0	38.3	37.1	35.6	35.7	35.2
CaO	.6	.6	.7	.8	.8	.8	.6	.6	.5	.6	.5	.8	.5	.5	.5

number of ions on the basis of 4 oxygens.

	core	rim	core				core	core	core	core	rim		core	rim	core
Si	1.00	1.00	1.00	1.01	1.00	1.00	1.01	1.00	1.00	1.00	1.00	1.00	1.00	1.00	1.00
Fe^{2+}	.48	.53	.53	.52	.57	.57	.58	.58	.60	.50	.49	.52	.58	.57	.58
Mn	.01	.01	.01	.01	.01	.01	.01	.01	.01	.01	.01	.01	.01	.01	.01
Mg	1.49	1.44	1.45	1.45	1.40	1.39	1.38	1.38	1.39	1.48	1.49	1.45	1.41	1.41	1.39
Ca	.02	.02	.02	.02	.02	.02	.02	.02	.01	.02	.01	.02	.02	.01	.01
mol.% Fo	75.65	73.03	73.35	73.60	71.00	70.78	70.61	70.47	69.88	74.84	75.10	73.73	70.99	71.26	70.55

analyses by electron microprobe. Fe measured as FeO.

phenocrysts of iron-titanium oxides are also present in many specimens.

Clinopyroxene phenocrysts typically show well defined zones differing in shades of pale green. Despite this clear optical evidence of zoning, microprobe analyses of pyroxene phenocrysts in two specimens (Table 4-1) show only minor compositional variation between zones. In general there is enrichment of Fe in the outer zones relative to the core in any particular phenocryst, however in one analysed phenocryst (Table 4-1, phenocryst 2) this trend is reversed, and in another (Table 4-1, phenocryst 4) the compositional zoning is oscillatory (Figure 4-2). The analysed pyroxene phenocrysts are rich in CaO and MgO relative to FeO and plot in the salite field of the pyroxene tetrahedron; Joplin and others (1972) have suggested that clinopyroxene of this composition is characteristic of high-potassium rocks over a wide range of whole rock compositions.

In at least two specimens, olivine occurs as small, well formed, unaltered phenocrysts, as sieved corroded and partly altered phenocrysts and as small rounded and typically partly altered inclusions within large clinopyroxene phenocrysts. Analysis of these olivines (Table 4-1) shows that the sieved corroded phenocrysts and the inclusions are significantly more magnesian than the cores of well formed unaltered phenocrysts (Figure 4-3).

Plagioclase phenocrysts are labradorite (An_{55-70}) or less commonly bytownite (An_{70-80}); normal and oscillatory zoning over a narrow compositional range is common. In some apparently fractionated specimens plagioclase is the main phenocrystic phase.

Analcime (identification confirmed by X-ray diffraction) makes up 5 to 15 vol. % of three specimens from the Cloudy Bay Volcanics (593, 594, 595) all of which were collected from the same rock unit. The analcime forms small (0.2 to 0.5 mm) rounded and hexagonal shaped crystals occurring singly or in aggregates; textural relationships indicate that the analcime crystallised before solidification of the groundmass. Analcime is thought to be a primary constituent of some basaltic rocks but its occurrence in a suite of typically potassium-rich rocks seems anomalous. It is possible that the analcime is secondary after leucite or pseudoleucite.

The groundmass in these basaltic rocks consists of labradorite microlites with interstitial K-feldspar, iron-titanium oxides, minor clinopyroxene and olivine, and accessory apatite. Small crystals of
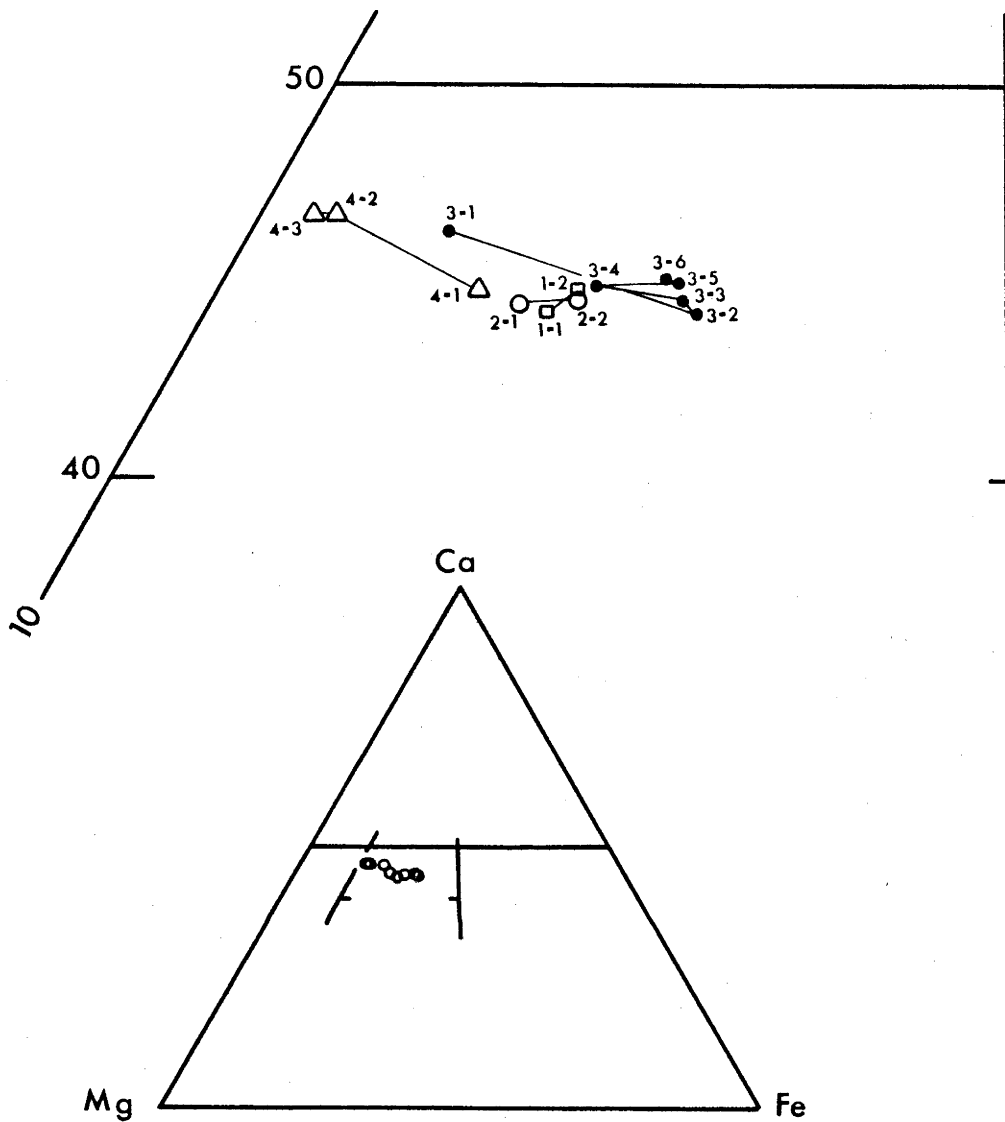
FIGURE 4-2: Compositions of clinopyroxene phenocrysts in two
trachybasalts from the Fife Bay Volcanics.
(numbers refer to data in Table 4-1, eg. 3-1 is
the core of phenocryst 3, 3-6 is the rim of
phenocryst 3.)
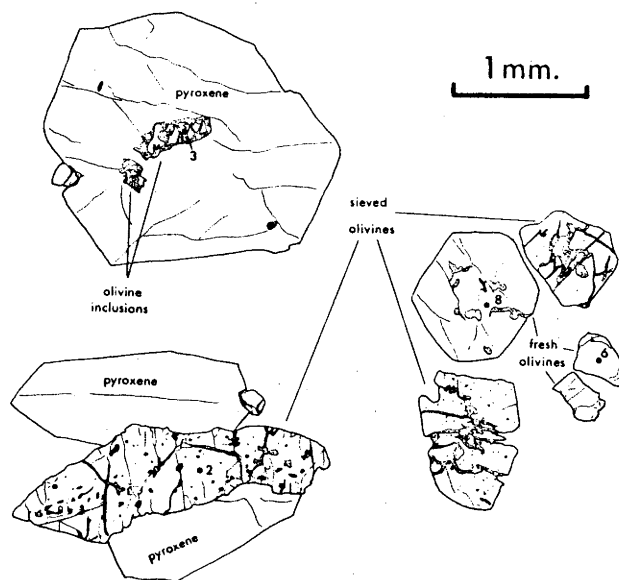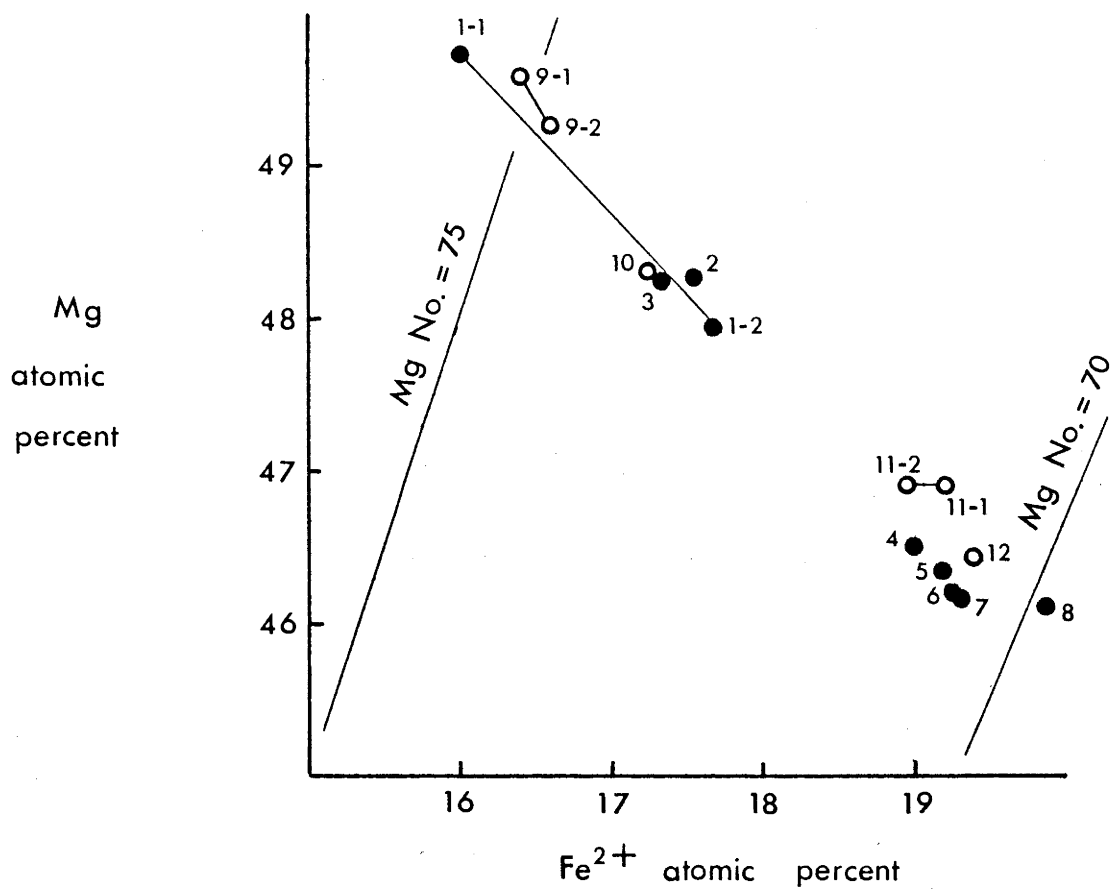
FIGURE 4-3: Compositions of olivine phenocrysts in two trachybasalts
from the Fife Bay Volcanics expressed in terms of MgO
and FeO. (numbers refer to data in Table 4-1)
The lower part of the diagram illustrates the typical
mode of occurence of olivine inclusions, sieved olivines.
and 'fresh' olivines.

biotite are common in the groundmass of some specimens; in other specimens a medium to dark brown glass is an important constituent. Chlorite, calcite and, in some specimens minor prehnite and epidote are secondary minerals, typically occurring as vesicle infillings.

The 'welded' agglomerate of the Fife Bay Volcanics is made of clasts which are the same as the basaltic lavas described above. These clasts are set in an igneous matrix. The matrix is fine grained or glassy and has essentially the same mineralogy as the clasts which it encloses with the exception that secondary minerals are more common.

Intermediate rock types are a minor part of both the Fife Bay Volcanics and the Cloudy Bay Volcanics. These are typically porphyritic and contain phenocrysts of andesine with or without pheno-crysts of biotite, hornblende, clinopyroxene, iron-titanium oxides, and rarely, olivine. The fine grained groundmass is composed of andesine, K-feldspar, clinopyroxene, iron-titanium oxides, sphene, apatite, and secondary chlorite, calcite and zeolites.

4-2   Chemical Composition

Twenty-two analyses of specimens from the Fife Bay Volcanics and the Cloudy Bay Volcanics are presented in Table 4-2; with one exception (597), the major element compositions were determined by Australian Mineral Development Laboratories and have been published (Smith and Davies, 1976). Trace element abundances were determined on the same material during this study. The analysed specimens are from lava flows, agglomerate clasts and 'welded' agglomerate and were selected as being representative of the exposed rock types in the two formations.

The analysed rocks are predominantly basaltic (less than 52 % SiO_2). TiO_2, typically less than 1 % is unusually low for rocks of basaltic composition. Al_2O_3 is also generally low (less than 15 %) but variable, and a few specimens contain up to 19 % Al_2O_3 . CaO and P_2O_5 contents are high, MgO contents are variable and with the exception of the three analcime bearing samples K_2O/Na_2O ratios are generally greater than one.

Water contents in these rocks are variable and typically high especially in specimens of the 'welded' agglomerate. In some specimens, high H_2O contents are correlated with the presence of minor secondary phases (predominantly calcite and zeolites). However, in many there is no evidence of secondary crystallisation and water is probably held in

TABLE 4-2: MIDDLE MIOCENE VOLCANIC ROCKS

No.	588*	471*	469*	589*	590*	466*	465*	591*	592*	473*	593*	594*	595*	596*	597	598*	472*	599*	470*	600	601	602
wt%																						
SiO_2	48.30	49.00	48.20	47.90	49.30	47.30	47.20	46.20	48.50	51.50	48.70	48.10	49.10	50.20	46.83	50.90	50.30	53.60	48.60	59.00	57.10	57.00
TiO_2	.60	.54	.75	.62	.61	.78	1.01	.97	.80	.65	1.03	1.06	1.08	.97	.73	.97	1.17	.72	.88	.55	.80	.76
Al_2O_3	13.40	15.90	17.20	10.20	14.60	11.30	13.20	13.40	15.40	16.00	13.70	14.10	13.70	19.10	15.55	19.90	17.80	17.30	17.40	17.80	19.60	19.50
Fe_2O_3	2.85	3.15	7.15	5.85	3.00	7.05	4.60	3.95	3.35	4.10	7.00	7.85	7.10	4.20	5.78	3.90	7.95	4.60	5.80	4.15	5.90	3.85
FeO	6.15	4.30	1.81	4.55	5.45	5.90	4.65	5.40	6.00	4.50	2.90	2.10	2.85	2.85	4.55	2.30	1.33	3.05	4.10	.90	.20	1.85
MnO	.14	.14	.17	.16	.14	.20	.16	.15	.15	.16	.13	.15	.11	.13	.18	.13	.15	.15	.18	.06	.55	.11
MgO	13.10	8.95	9.35	10.60	8.65	11.80	8.15	8.20	7.15	5.55	6.00	5.90	5.90	3.95	5.76	2.55	3.70	3.10	3.80	1.90	1.70	1.60
CaO	9.35	6.46	3.95	12.50	11.20	8.00	10.10	10.00	11.10	7.45	9.90	9.75	9.95	7.20	9.75	6.20	8.35	7.30	9.35	4.30	3.00	5.15
Na_2O	1.30	3.05	2.45	1.40	2.05	1.50	2.10	1.50	2.10	4.05	3.75	4.25	3.45	2.85	2.40	4.20	3.65	2.85	3.05	4.15	4.05	4.15
K_2O	2.50	3.05	2.60	2.25	2.60	4.05	3.85	3.75	3.00	3.15	1.35	1.29	1.70	3.75	3.58	4.00	2.70	3.10	2.55	4.10	3.10	3.40
P_2O_5	.39	.40	.49	.46	.40	.68	.82	.88	.46	.52	.87	.95	.87	.69	.56	.55	.60	.56	.32	.38	.50	.46
H_2O+	1.51	1.91	4.05	2.10	1.27	1.05	2.75	4.25	1.34	2.00	3.40	2.70	2.55	1.45	2.86	2.50	.95	1.82	2.30	1.07	2.00	.89
H_2O-	.29	2.90	1.71	1.09	.65	.25	1.13	.94	.40	.28	1.05	1.40	1.21	1.59	.25	1.07	.97	1.52	.73	1.17	1.15	.35
CO_2	.08	.40	.40	.47	.12	.05	.11	.11	.07	.20	.03	.10	.08	.69	.69	.52	.13	.08	1.20	1.11	.05	.53
Total	99.96	100.15	100.28	100.15	100.04	100.01	99.83	99.70	99.82	100.11	99.81	99.70	99.65	99.62	99.47	99.69	99.75	99.75	100.26	100.64	99.70	99.60
Mg.No.	78.9	78.5	90.1	80.4	73.6	77.9	75.5	72.7	67.7	68.4	78.4	83.2	78.4	70.9	69.0	66.1	83.0	64.1	62.0	78.8	93.7	60.3
FeO as measured $(Fe_2O_3/FeO=0.2)$	75.7	72.2	70.2	69.1	68.8	66.7	65.8	65.5	62.2	58.4	57.5	57.2	57.0	55.3	55.1	47.7	47.5	47.2	45.8	46.0	39.0	38.4
ppm Ba	353	341	651	482	320	775	568	546	312	642	599	621	560	1223	774	1783	801	1076	552	705	1451	834
Rb	76	102	69	37	99	105	229	200	127	71	47	33	38	85	81	96	86	83	74	142	70	83
Sr	474	447	1822	616	540	1270	857	729	606	687	908	934	898	2051	846	2242	1560	1170	983	935	2279	1648
Pb	13	21	13	9	13	15	38	19	17	15	18	20	18	56	20	58	25	37	18	32	49	27
Th	1	0	2	3	3	1	6	6	2	2	6	7	7	21	2	24	11	10	5	9	15	16
U	0	1	1	0	0	1	0	1	1	1	3	3	2	4	4	5	4	2	1	2	2	3
Zr	44	49	62	35	42	57	127	71	51	65	130	139	129	200	42	201	238	186	61	153	303	296
Nb	1	2	2	2	2	2	4	3	2	2	3	3	4	8	3	8	5	6	3	5	7	6
Y	10	12	15	12	10	14	10	12	14	15	12	14	12	16	12	19	20	20	15	15	19	20
La	5	6	9	8	5	9	14	6	8	8	15	14	13	39	8	43	29	19	10	27	33	36
Ce	10	10	20	12	11	15	32	19	18	20	38	33	34	82	16	87	65	43	21	42	81	83
Sc	24	21	14	50	31	38	22	21	28	20	22	23	22	12	27	8	18	18	26	9	6	6
V	171	176	163	280	189	346	246	217	223	198	291	284	288	209	327	196	269	194	300	103	137	135
Cr	611	85	3	398	255	90	272	181	123	126	220	253	217	36	108	0	30	1	19	33	0	0
Ni	337	43	8	98	85	48	62	60	49	33	69	57	71	26	30	7	10	4	13	27	5	3
Cu	78	69	118	115	91	124	102	97	91	107	76	119	100	187	181	149	29	32	108	28	9	153
Zn	63	66	71	70	71	95	74	65	67	84	79	88	80	76	81	66	66	85	84	56	79	69
Ga	12	16	17	11	13	12	16	12	15	16	17	16	17	19	15	22	22	17	17	12	20	21
K/Rb	273.08	248.23	312.81	504.82	218.02	320.20	139.57	155.65	196.10	368.31	238.45	324.51	371.38	366.24	366.91	345.90	260.63	310.06	286.06	239.69	367.64	340.06
Ba/Sr	.74	.76	.36	.78	.59	.61	.66	.75	.51	.93	.66	.66	.62	.60	.91	.80	.51	.92	.56	.75	.64	.51
Zr/Nb	44.00	24.50	31.00	17.50	21.00	28.50	31.75	23.67	25.50	32.50	43.33	46.33	32.25	25.00	14.00	25.13	47.60	31.00	20.33	30.60	43.29	49.33

Abundances < 0.5 ppm recorded as O. * major element analysis by AMDL.

hydrous groundmass phases (mainly biotite) and in interstitial material. Although the variations in H_2O and CO_2 content may reflect a degree of secondary alteration the generally high H_2O contents of all of these rocks is probably a primary magmatic feature. High water contents appear to be a feature of alkali rich rocks especially those rich in K_2O.

Ferric/ferrous ratio

The ratio Fe^{3+}/Fe^{2+} (atomic %) in the analysed rocks is generally high (> 0.4) and variable (up to 4.0 with one extreme value of 26 (601)). The factors which may affect the ferric/ferrous ratio in magmas are crystal-liquid equilibria, temperature, oxygen fugacity and alkali content (Carmichael & Nicholls, 1967). Increase in alkali content is correlated with an increase in the observed ferric/ferrous ratio (the alkali-ferric iron effect (AFE) of Carmichael & Nicholls) and Paul & Douglas (1965) have shown that this effect is emphasised by high potassium contents. It follows that relatively high ferric/ferrous ratios are to be expected in alkali rocks generally, and in potassium-rich rocks in particular provided that the AFE is not overshadowed by one of the other factors. Interpretation of measured ferric/ferrous ratios is a recurring problem in the study of volcanic rocks because it affects calculation of normative mineralogy and of parameters such as Mg-number. One commonly used approach to the problem is to select an arbitary value for the ratio Fe_2O_3/FeO (wt. %) and recalculate relative abundances of the iron oxides accordingly. Typical ratios which have been used are 0.1 (Fe^{3+}/Fe^{2+} = 0.09) for tholeiitic rocks (e.g. Cann, 1971) and 0.25 (Fe^{3+}/Fe^{2+} = 0.22) for alkali basalts (Kesson, 1973).

If the ferric/ferrous ratio of a cooling magma is relatively high then a spinel phase will be one of the first phases to appear on the crystallisation surface (Carmichael & Nicholls, 1967). The common occurrence of iron-titanium oxides as phenocrysts in basaltic specimens from both the Fife Bay and Cloudy Bay Volcanics is thus indicative of a relatively high degree of oxidation in the magma of an early stage in the crystallisation history. However, when $Fe^{3+}/(Fe^{2+} + Fe^{3+})$ is compared with total alkalies (Figure 4-4a) the ferric/ferrous ratios of these rocks are by no means anomalously high (cf. Nicholls and Carmichael, 1967). It is suggested that a moderate amount of oxidation is a primary magmatic feature of these east Papuan volcanics and perhaps also of potassium rich rocks generally. A value of Fe^{3+}/Fe^{2+} = 0.5 (Fe_2O_3/FeO = 0.56)
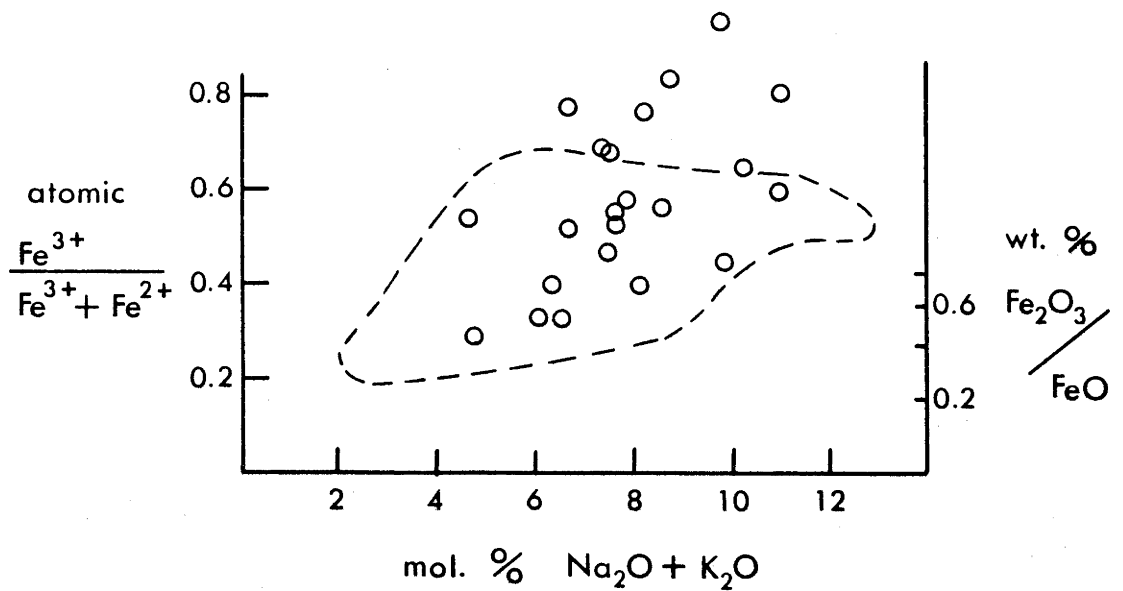
FIGURE 4-4a: Middle Miocene volcanic rocks plotted in terms of their $Fe^{3+}/(Fe^{3+}+ Fe^{2+})$ ratios (atomic) and their molecular proportions of $Na_2O + K_2O$. The dashed line outlines the field of average rock analyses as plotted by Carmichael and Nicholls (1967).
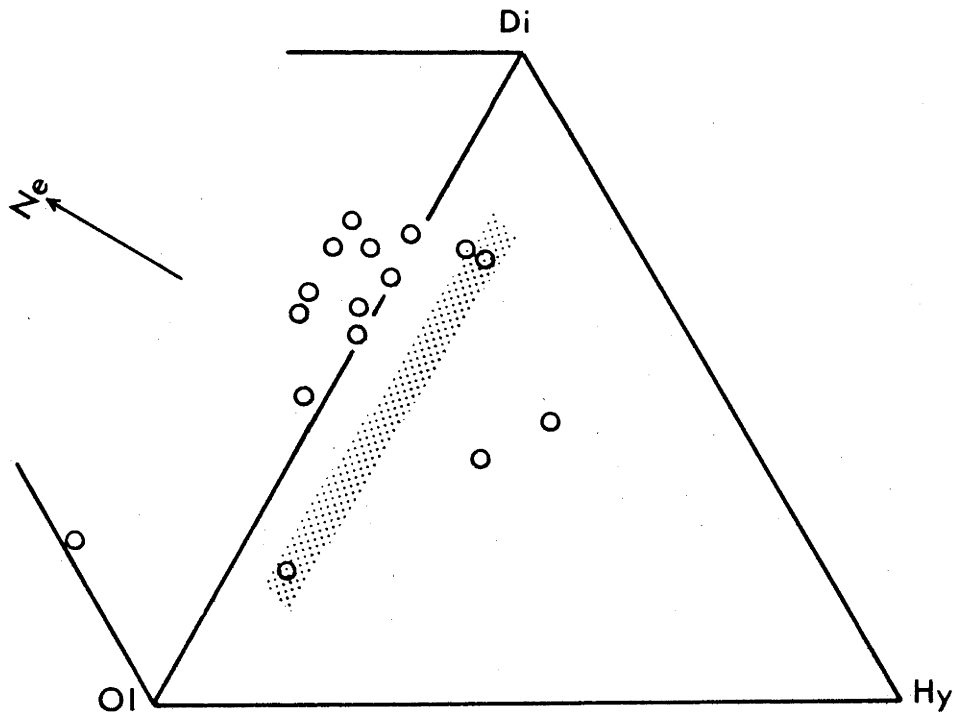
FIGURE 4-4b: Middle Miocene volcanic rocks plotted in the normative iron free basalt tetrahedron. The position of the low temperature thermal divide is shown stippled.

which is close to the lower end of the range of measured ratios has been used in some of the normative and other calculations.

Normative mineralogy

Most of the analysed rocks are undersaturated; a few are critically undersaturated and contain small amounts of normative nepheline (less than 5%). This trend is emphasised when the normative mineralogy is recalculated with Fe^{3+}/Fe^{2+} = 0.5 (Figure 4-4b) and the analyses plot mainly on the undersaturated side of the low pressure thermal divide in the simplified basalt tetrahedron. The normative mineralogy of these rocks thus emphasises their essentially alkaline character.

The high Al_2O_3 and alkali contents of some of the analyses is reflected in high normative feldspar contents and especially high Or contents. In some specimens normative feldspar is well in excess of normative pyroxene plus olivine and their analyses plot anomalously in the projection of the normative basalt tetrahedron used in Figure 4-4b.

Trace elements

For basaltic compositions the Rb and particularly the Ba and Sr contents of the analysed rocks are notably high. K/Rb ratios are variable but characteristically low, Ba/Sr ratios are high. Th/U ratios can be high but absolute and relative abundances of these elements are variable. Zr and Nb abundances are low but Zr/Nb ratios are high (14-50); this is in contrast to typical alkaline rocks which are high in Zr and Nb but have low Zr/Nb ratios (generally <5). V and Cr content is generally high, Ni is typically low although higher than in typical island arc type basalts. Anomalously high Ni and Cr is correlated with accumulation of early crystallising olivine and clinopyroxene.

Rare earth elements

Relative La, Ce and Y abundances indicate REE patterns showing enrichment relative to chondrites and enrichment of the light REE (20-200 times chondritic abundances) relative to the heavy REE (5-10 times chondritic abundances). Increase in total REE and to some extent in light/heavy fractionation is correlated with an increase in SiO_2 and a decrease in Mg-number. In detail the REE patterns of three specimens (Table 4-3, Figure 4-5) confirm these trends. The REE patterns are comparable to patterns obtained for andesites and basalts associated with andesites (e.g. Jakes and Gill, 1970; chapter 5). The apparently
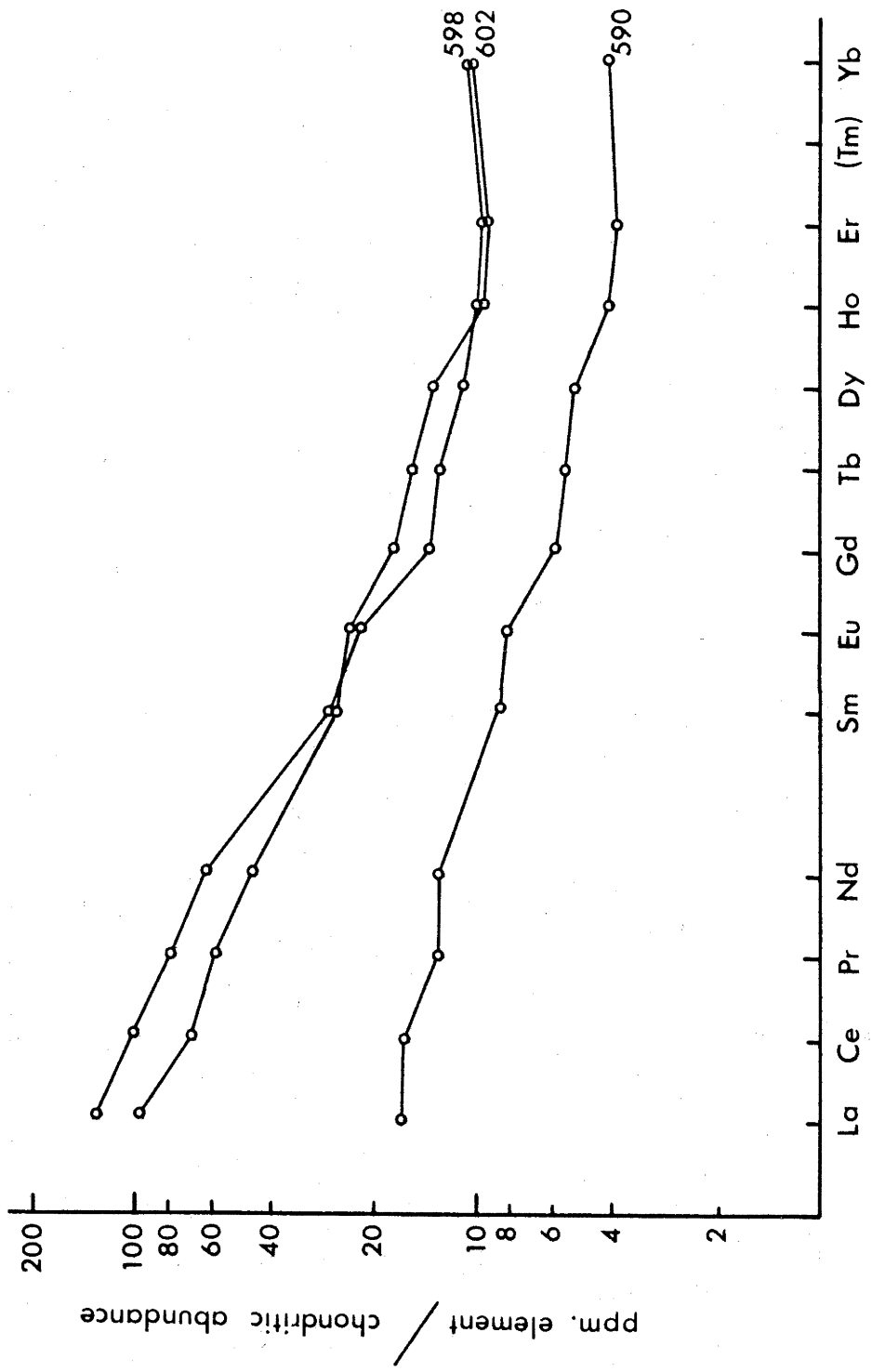
FIGURE 4-5: Chondrite normalised rare earth element patterns in specimens of the Fife Bay and Cloudy Bay Volcanics. Numbers refer to analyses in Table 4-3.

TABLE 4-3: RARE EARTH ELEMENTS AND SOME OTHER TRACE ELEMENTS IN
THREE SPECIMENS FROM THE MIDDLE MIOCENE VOLCANICS.

No.	590	598	602
ppm			
La	5.0	36*	43*
Ce	11*	87*	83*
Pr	1.6	7.0	9.6
Nd	7.5	26.6	36.2
Sm	1.8	5.4	5.7
Eu	.61	1.8	1.6
Gd	1.5	4.6	3.6
Tb	.27	.77	.63
Dy	1.6	4.1	3.4
Ho	.30	.70	.73
Er	.82	2.0	2.0
Yb	.84	2.1	2.1
La/Yb	5.9	15.1	18.5
Eu/Eu*	1.1	1.1	1.1
Cs	2.7	10.4	1.7
Pb	9.8	63.4	24.0
Th	1.8	16.1	12.9
U	.7	4.6	3.0
Hf	.9	4.8	7.6
Th/U	2.6	3.5	4.3
Zr/Hf	46.7	41.9	38.9

*analysis by XRF.

unfractionated basaltic specimen (590) shows less light/heavy fraction-
ation and markedly lower total REE content than basaltic alkaline rocks
(e.g. Price and Taylor, 1973).

Strontium isotope ratios

Four specimens from the middle Miocene volcanic rocks in south-
eastern Papua show a range in initial $^{87/86}$ratio from .7036 to .7049
(Appendix IV) which is within the range of initial ratios measured for
Quaternary volcanic rocks from Papua New Guinea by Page and Johnson
(1974). There is no clear relationship between initial ratio and either
Sr or SiO_2 content although the lowest ratio is found in specimen 602
which has the highest Ba and SiO_2 content and is apparently fractionated.
Powell (1969) suggested that a negative initial ratio/SiO_2 correlation
could, in some circumstances, be taken as an indication of crustal
contamination. One explanation of this is that initial $^{87/86}$Sr ratios
in rocks with lower Sr contents are more easily changed by contamination
(Faure and Powell, 1972) but this unlikely to be an explanation in this
case because Sr content is universally high.

The observed range in initial $^{87/86}$Sr ratios is high for a group
of rocks which are assumed to be closely related. As there is no evidence
for contamination or even for the underlying presence of crustal material
which could include evolved Sr, this range of values is assumed to be a
primary feature of the rocks and by implication of the source.

Chemical variations

A feature of both the major and trace element abundances is
their marked variability; despite this, there are some consistent
geochemical trends within the analysed rocks which point to a genetic
relationship. There is an inverse correlation between a group of
elements comprising TiO_2, Al_2O_3, alkalies, Ba, Sr, Pb, Th, U, Zr, Nb, Y,
La, Ce, and Ga) and a group comprising FeO, MgO, CaO, Cr and Ni (Table
4-4) which is indicative of a fractionation process controlled by
olivine and pyroxene. Petrographic observations show clinopyroxene and
olivine to be the most abundant early crystallising phases, followed by
iron-titanium oxides with or without plagioclase. Lack of a marked
trend toward silica enrichment precludes extensive removal of olivine
and points to clinopyroxene as the major fractionating phase. Anomalous
contents of MgO, CaO, Cr and Ni in a few of the analysed samples are
thought to be due to accumulation or removal of olivine or clinopyroxene
or both.

TABLE 4-4: MIDDLE MIOCENE VOLCANIC ROCKS — CORRELATION MATRIX

	SiO_2	TiO_2	Al_2O_3	Fe_2O_3	FeO	MnO	MgO	CaO	Na_2O	K_2O	P_2O_5	Rb	Ba	Sr	La	Ce	Y	Th	U	Zr	Nb	Zn	Cu	Ni	V	Cr	Ga	Pb
SiO_2	100		57		-62		-55	-70	72		-43		41	50	46	42	46	50	47	54	41				-69	-42		
TiO_2		100									64				44	50				42	47						56	44
Al_2O_3			100		-77		-85	-72	85				64	70	76	78	75	72	70	73	75			-52	-52	-72	82	66
Fe_2O_3				100										40								40			50			
FeO					100		75	79	-78				-63	-74	-76	-75	-75	-65	-56	-80	-71			55	49	64	-66	-57
MnO						100																						
MgO							100	52	-86				-64	-57	-77	-77	-78	-73	-68	-77	-80			67		74	-69	-65
CaO								100					-56	-67	-57	-57	-61	-45		-61	-51				62	62	-50	-47
Na_2O									100		57		57	53	71	69	73	60	59	69	64			-58	-48	-68	71	54
K_2O										100	55	57	45		41			40	42		46							54
P_2O_5											100	62																
Rb												100																
Ba													100	87	83	83	71	86	74	72	88			-45		-54	66	85
Sr														100	83	85	75	80	67	76	80			-49		-62	76	72
La															100	98	76	96	77	90	95			-42		-53	75	85
Ce																100	79	96	75	94	95			-43		-54	81	84
Y																	100	70	67	82	73			-59		-73	78	53
Th																		100	74	83	96					-47	72	88
U																			100	61	75			-48		-60	71	64
Zr																				100	87			-42		-52	77	74
Nb																					100			-49		-57	72	93
Zn																						100			56			
Cu																							100					
Ni																								100		92	-53	-45
V																									100			
Cr																										100	-63	
Ga																											100	63
Pb																												100

Correlations less than 40 are omitted

Although these samples were collected from widely separate localities and are clearly not a single fractionation series the inter-element correlations suggest that they may represent such a series. A parent magma from which such a series of rocks could have been produced is thought to be comparable to specimen 465 (Table 4-2). The main features of this composition are low TiO_2, Al_2O_3, Zr, Nb, Ni and relatively high MgO, CaO, K_2O/Na_2O, P_2O_5, Ba and Sr.

Al_2O_3 in the analysed rocks is highly variable within the range 10 to 20 %. Al_2O_3-rich rocks characteristically contain abundant plagioclase phenocrysts and one obvious explanation is that high Al_2O_3 contents are due to plagioclase accumulation. The favoured alternative however, is that these rocks are highly fractionated derivatives of low-Al_2O_3 rocks (such as 465) in a series controlled by Al_2O_3-poor phases such as olivine and clinopyroxene. Some support for this hypothesis comes from the high Al_2O_3 contents of interstitial glass in a basaltic rock from the Fife Bay Volcanics reported by Joplin and others (1972) and from low Mg-numbers in the Al_2O_3-rich specimens. There is good correlation (70+) between Al_2O_3 and elements such as Na, Ba, Sr, Th, U, Zr, Nb, Y, La, Ce and Ga which could be expected to become enriched during fractionation (Table 4-4) although the inclusion of Na, Ba and Sr in this group precludes fractionation of feldspar.

Magnesium numbers

The magnesium numbers (100 Mg/Mg + Fe^{2+}) of the analysed rocks are variable to high and this is due in part to relatively high ferric/ferrous ratios. For Fe^{3+}/Fe^{2+} ratios recalculated to 0.5 magnesium numbers of apparently non accumulative specimens range from 77 to 45, even if an extreme value of Fe^{3+}/Fe^{2+} = 0.2 is assumed magnesium numbers range from 72 to 38. The importance of high Mg number is that provided it can be shown to be a primary feature of the magma from which the rocks was derived (i.e. not due to accumulation of magnesian phases) it can be used as an indicator of an origin within the upper mantle.

Roeder & Emslie (1970) have shown that the distribution of Mg and Fe between liquid and coexisting olivine crystals is effectively independent of temperature and can be represented by the equilibrium distribution coefficient (K_D) = (Mg/Fe) liquid / (Mg/Fe) olivine. According to these authors K_D = 0.3. This expression can be rearranged (Irving, 1971) to give Xoliv = $[100X_{liq}/(X_{liq}+K_D(100-X_{liq}))]$ where X = magnesium number; the curve generated by this expression relates the

Fo content of olivine crystals to the Mg-number of the coexisting liquid.
It follows because the composition of upper mantle olivines has been
estimated to fall in the range Fo_{87} to about Fo_{92} that magmas in
equilibrium with olivine in upper mantle source regions must have Mg
numbers in the range 68 to 77 (cf. Green, 1970; 1971).

Notwithstanding the problem of estimating ferric/ferrous
ratios the Mg-numbers of the potassium-rich volcanics in southeastern
Papua do not preclude an origin by partial melting in equilibrium with
olivine in an upper mantle source region. In this context it is
relevant to examine the Mg/Fe ratios of the two specimens in which early
forming olivines have been analysed. These rocks contain olivine
phenocrysts with compositions in the range Fo_{70-75}; applying the
crystal/liquid distribution expression, the Mg/Fe ratios (expressed as
Mg-number) of the total rocks should lie in the range 48 to 41. In
fact, even assuming unrealistically low ferric/ferrous ratios the Mg
numbers of these two rocks is significantly higher than this. It can
be argued that the first olivine to crystallise from a magma which has
originated by partial melting in equilibrium with olivine should reflect
approximately the composition of that refractory olivine. The fact that
in these two basaltic specimens with relatively high Mg numbers the
olivine is relatively Mg poor indicates that they have not originated
by partial melting of normal mantle material.

4-3   Petrogenetic Constraints

A petrogenetic model for the high-K volcanic rocks in south-
eastern Papua must take into account the Tertiary tectonic setting of
the area as well as contemporary andesitic volcanic rocks described
in chapter 5. However, it is appropriate at this stage to review the
physical and geochemical constraints placed by the high-K rocks which
have helped mould the model discussed in chapter 7. These are listed
below.

1)   The high-K volcanic rocks are predominantly basaltic. Although
sampling of the volcanic formations is limited, mapping on a
reconnaissance scale (Smith and Davies, 1976) indicates that the
predominance of basaltic volcanic rocks is a real feature. Nevertheless
the significance of this observation must be tempered by the fact that
associated intrusive rocks (Smith, 1972) are predominantly intermediate
in composition.

2)   High-K intrusive rocks in southeast Papua are closely associated
with large positive gravity and magnetic anomalies (Milsom and Smith,
1975) which indicate the underlying presence of relatively large masses
of high density material.

3)   Initial $^{87/86}$Sr ratios are low indicating that evolved crustal
material has not played a part in their genesis.

4)   Relationships between the Mg/Fe^{2+} ratios of two whole rock samples
and their contained olivine phenocrysts suggest that the whole rock
composition could not have originated by partial melting in equilibrium
with normal mantle material.

5)   The high incompatible element content and in particular the high
Ba and Sr contents and Ba/Sr ratios place constraints on both the nature
of the source material and the processes by which the magmas were
derived from this source.

6)   TiO$_2$, Zr and Nb are typically low but Zr/Nb ratios are high.
Although TiO$_2$ is lower, the abundances of these elements are generally
comparable to abundances in tholeiitic rocks and are unlike those in
alkali basalts.

7)   Cr and Ni contents are variable, are typically lower than those of
basalts thought to be of direct mantle origin (tholeiitic basalts,
alkali basalts), but are higher than those of typical island arc basalts.
V contents are high.

8)   REE patterns show the light/heavy fractionation which is character-
istic of island arc rocks and alkaline rocks but the total REE content is
typically lower than that of alkaline rocks.

4-4   Affinities

        In earlier work (Smith, 1971; 1972) the high-K extrusive and
intrusive rocks in southeast Papua were interpreted as an isolated
magmatic event unrelated to Upper-Miocene to Recent volcanism in the
area; this distinction was implicit in the earlier use of the term
Shoshonite Association. However, reassessment of avialable data
indicate that the middle Miocene volcanic rocks are the southeastern
end of a belt of high-K rocks which extends westward into the Owen
Stanley Range. This southern volcanic belt is paralleled to the north
by a belt of andesitic volcanoes referred to here as the northern volcanic
belt (chapter 5). The following sections discuss the question of a distinct
identity implied by use of the term Shoshonite Association for rocks of the
southern volcanic belt.

The southern volcanic belt.

The southern volcanic belt comprises the Fife Bay and Cloudy Bay Volcanics as well as minor lava flows and pyroclastic interbeds associated with Pliocene sediments in the Musa Valley (Smith and Davies, 1976), volcanic rocks on Managlase Plateau (Ruxton, 1966; Smith and Davies, 1976) and volcanic rocks in the Owen Stanley Range (Pieters, 1974; Blake, 1976). These areas define a gently curving trend extending southeast from the Owen Stanley ranges.

No data is available on the age of the Cloudy Bay Volcanics but because rock types are comparable it has been suggested (Smith and Davies, 1976) that they are the same age as the Fife Bay Volcanics (middle Miocene). To the north, in the Musa Valley area, high-K basaltic rocks have been dated by whole rock K-Ar methods as mid-Pliocene (Ruxton, 1966) and similar rock types interbedded with sedimentary rocks yielded an age of 2.4 m.y. (late Pliocene; Smith and Davies, 1976). Because of their high potassium contents lavas associated with the small Pleistocene to Recent volcanoes (Uoivi Volcanics) described by Ruxton (1966) have been included in the southern volcanic belt despite the fact that they are closely associated with contemporary andesitic rocks of the northern belt. Further west, predominantly basaltic, high-K lavas of Recent age are found as ridge cappings and valley fill deposits in the Owen Stanley Range (Pieters, 1974; Blake, 1976).

The available data indicate that volcanic activity has migrated westward since middle Miocene times within a zone defined by high-K rocks of the southern volcanic belt.

Rock types

Geochemical data on rock types in the southern volcanic belt is limited. Major and trace element data are available from the eastern part of the belt (section 4-2) but only limited major element data are available from the western part (Ruxton, 1966; Blake, 1976; Pieters, unpublished analyses). The most common rock type in the southeast is a basaltic rock high in CaO, K_2O, Ba and Sr but characteristically relatively low in TiO_2, Zr, Nb and Ni. Rock types to the west show more variation in major elements but in general these too are relatively low in SiO_2 and have high K_2O/Na_2O ratios.

The high-K basaltic rocks in southeastern Papua are slightly nepheline normative and in this sense are alkaline rocks but they differ from high-K alkaline rocks of the ocean basins (for example

the high-K alkaline suite from Tristan da Cunha described by Baker and others (1964)) in being relatively low in TiO_2, Zr and Nb. The light REE contents of the Papuan rocks are also characteristically lower and although Ba and Sr contents are high in both suites these elements are more abundant in the high-K alkaline rocks.

The characteristic low TiO_2, Zr, Nb, Ni, Cr of the high-K basaltic rocks in southeastern Papua is shared by the basaltic rocks associated with andesites in the northern volcanic belt. The main differences between the volcanic rock suites in northern and southern belts appears to be that the southern belt contains mainly basaltic rocks which are lower in Al_2O_3 and generally contain higher K_2O/Na_2O ratios than those of the northern belt. Nevertheless, detailed analysis of the major element compositions of these and other comparable rock types in Papua New Guinea (Johnson and others, in prep.) has shown that high-K basaltic rocks such as those in southeastern Papua and in the New Guinea Highlands (Mackenzie and Chappell, 1972) are transitional in chemistry to high-K andesitic suites.

Use of 'Shoshonite Association'

The term shoshonite association was introduced by Joplin (1968) for high-potassium rocks which were demonstrated to have world wide distribution and which hitherto had proved difficult to fit into any scheme of rock classification. Basaltic members of the shoshonite association are alkaline in terms of normative parameters and alkali content but differ from typical alkaline rocks in having low Ti, Zr, and Nb and comparatively lower light REE. The importance of low TiO_2 content in shoshonitic rocks has been emphasised by Kesson and Smith (1972) and can be recognised petrographically in the absence of the titaniferous pyroxene typical of alkaline basalts. These differences in chemical composition between shoshonitic and typically alkaline rocks argue for differing physical conditions and/or source material at the place of origin of the magmas. In a consistent volcano-tectonic petrogenetic model this indicates that shoshonitic rocks should be considered as a distinct group unrelated to alkaline rocks of the ocean basins and continents.

Criticism of the term Shoshonite Association has centered around use of the original rock name shoshonite (Iddings, 1895) for a world wide rock association (Nicholls and Carmichael, 1969a; Prostka, 1973). It can also be argued that the term is difficult to use and that

logically it should include all high-K, low Ti rocks in association
with converging plate boundaries. If shoshonite association was
broadened to include such rocks as the highly alkaline volcanics
of the outer New Guinea arc (Johnson and others, 1976) then its
application to the volcanics in the southern volcanic belt in Papua
would obscure the close relationship to volcanic rocks in the
northern belt. The relationship between volcanic rocks in the northern
and southern belts is discussed in more detail in chapter 7 but it is clear
that the rocks of the two belts together define an association dominated
by andesites but which includes basalts of shoshonitic affinities. In
this context use of the term shoshonite association does not seem
appropriate.

CHAPTER 5

ANDESITIC VOLCANOES IN SOUTHEAST PAPUA

5-1   The Northern Volcanic Belt

Predominantly andesitic volcanoes of late Miocene to Recent age
form a belt extending from the northeast Papuan coast through the
D'Entrecasteaux Islands to the Louisiade Archipelago (Figure 5-1). When
their relative positions are adjusted to allow for the sixteen degrees of
Pliocene to Recent spreading in the Woodlark Basin proposed by Luyendyk
and others (1973) these centres of andesitic activity all lie within
twenty five kilometres of a curvilinear trend extending southeastward
from Mount Lamington. This belt of Miocene to Recent volcanoes is
referred to as the northern volcanic belt and is paralleled to the south
by a southern volcanic belt (chapter 4).

The andesitic volcanic rocks are found in six distinct areas,
namely, the western end of the Calvados Island chain, Egum Atoll,
Normanby Island, the Amphlett Islands, the Moresby Strait area of the
D'Entrecasteaux Islands, and the northeast Papuan coast. Each of these
areas differs from the others with respect to age or distribution of
exposed rock types or both.

Rock nomenclature

The rock suite in the northern volcanic belt is dominated
by andesites but includes a range of rock types from basalt to rhyolite.
A feature of the suite as a whole is high total alkali content,
particularly K_2O, and in general the rocks are comparable to high-K calc-
alkaline suites. The term andesitic is used synonomously with but in
preference to common usage of the term calc-alkaline. Subdivision of
the andesitic rocks is according to arbitary and widely used values
of SiO_2 (chapter 1, Figure 1-2). A problem in nomenclature arises
with several rocks which fall within the dacite SiO_2 range (63-67%);
these rocks contain greater than 7% total alkalies and their composition
is comparable to that of trachytes. However, because of their demonstrably
close relationship to andesites and following the philosophy outlined in
section 1-2 the term alkaline-dacite is used in preference to trachyte.

Variation along the northern volcanic belt.

There are two main sources of bais in the data which might
affect analysis of time/space varition in the distribution and chemical
composition of rocks along the northern volcanic belt. Firstly there
is a field sampling bais; because of outcrop, terraine, or logistic
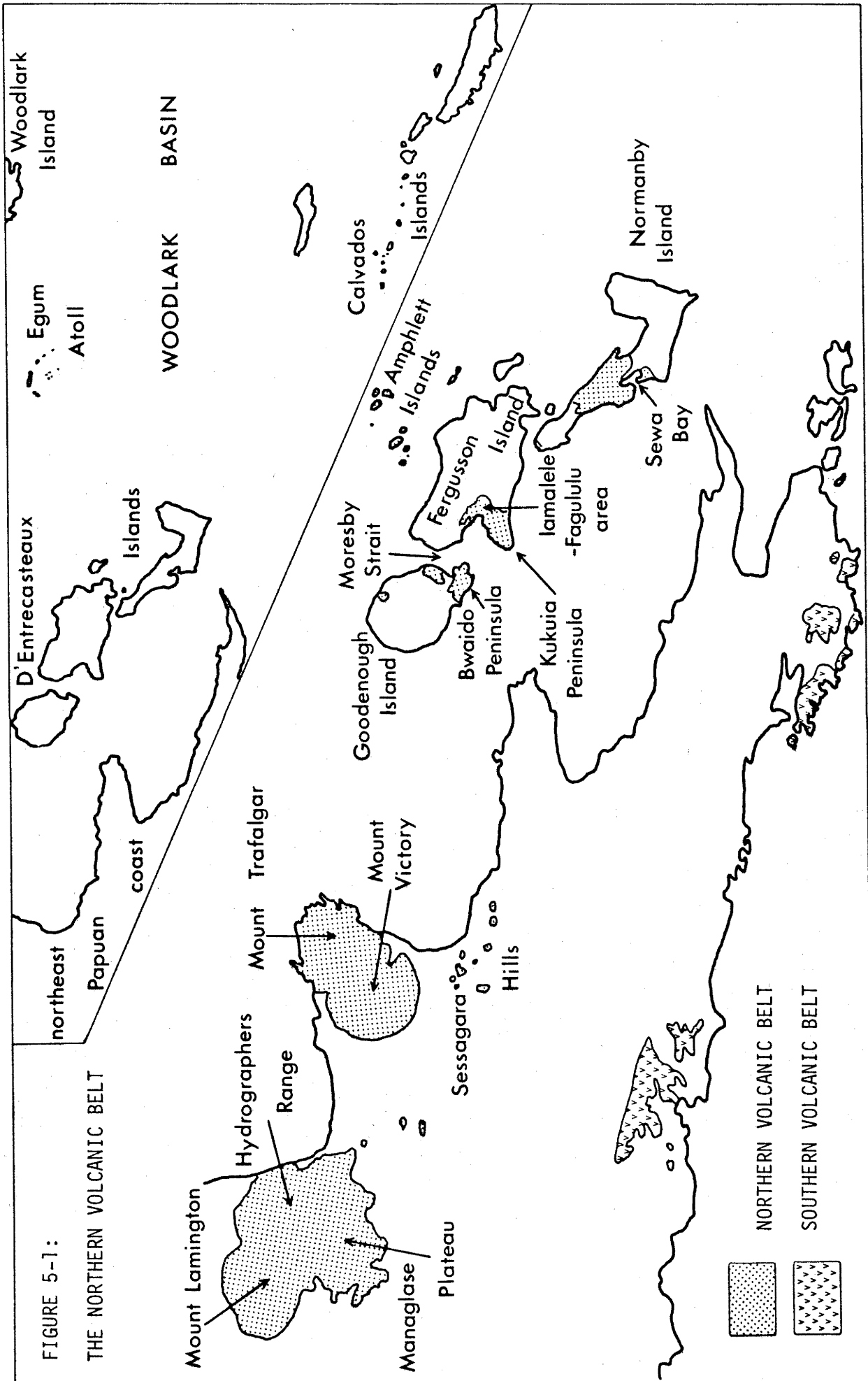
FIGURE 5-1:

THE NORTHERN VOLCANIC BELT

NORTHERN VOLCANIC BELT

SOUTHERN VOLCANIC BELT

limitations the samples collected from any one area may not be representative of that volcano or volcanic episode. For example, although field sampling on Egum Atoll was aimed at a representative collection of the exposed rock types it is unlikely that the limited subaerial exposures are representative of the composition of the whole volcano. In contrast, because of logistic problems the limited sampling of volcanic rocks in the Calvados Islands is unlikely to be representative of even the exposed rock types. A second source of bais is the intentional collection of specific rock types in the field and the preferential selection of these samples for analysis. For example on western Fergusson Island emphasis was placed on collecting rhyolite out of porportion to their volume and on Goodenough Island the younger lavas were more extensively sampled than the older lavas. However, in areas such as Nornamby Island and the Amphlett Islands the exposed rock types have been systematically sampled and the relative abundance of rock types can be estimated with some confidence.

Notwithstanding the problems of representativity, a reasonable estimate of relative abundance of rock types in the offshore part of the northern volcanic belt is basalt 10%, basalt andesite 25%, andesite 45%, dacite 15% and rhyolite 5%. Jakes and Smith (1970) have estimated the relative abundance of rock types in the Cape Nelson complex as basalt 3%, basaltic andesite 37%, andesite 55% and dacite 5%.

Systematic element/SiO_2 variations for TiO_2, Al_2O_3, FeO total, MgO, CaO, Na_2O and K_2O in each of the geographic groupings are illustrated in Figure 5-2. A striking feature of these diagrams is that regression lines for areas represented by rock suites which include a wide range of compositions are overlapping and subparallel. Divergent trends shown by the Egum Atoll and Calvados Islands analyses are due to a small SiO_2 range. FeO total, MgO and CaO show essentially the same abundance and degree of variation in all the different areas, TiO_2 is lower in Egum Atoll and Calvados Islands rocks and Na_2O is lower in Calvados Islands rocks. K_2O is extremely variable especially in the mainland lavas and in those from the Moresby Strait area and Normanby Island. There is a systematic increase in the slope of the K_2O/SiO_2 regression line westward to the Moresby Strait area but to the west the mainland lavas show a reversal of this trend. Considering the broad K_2O variations observed within any one geographic area and the limited nature of the sampling to the east this trend is probably not significant. The regression
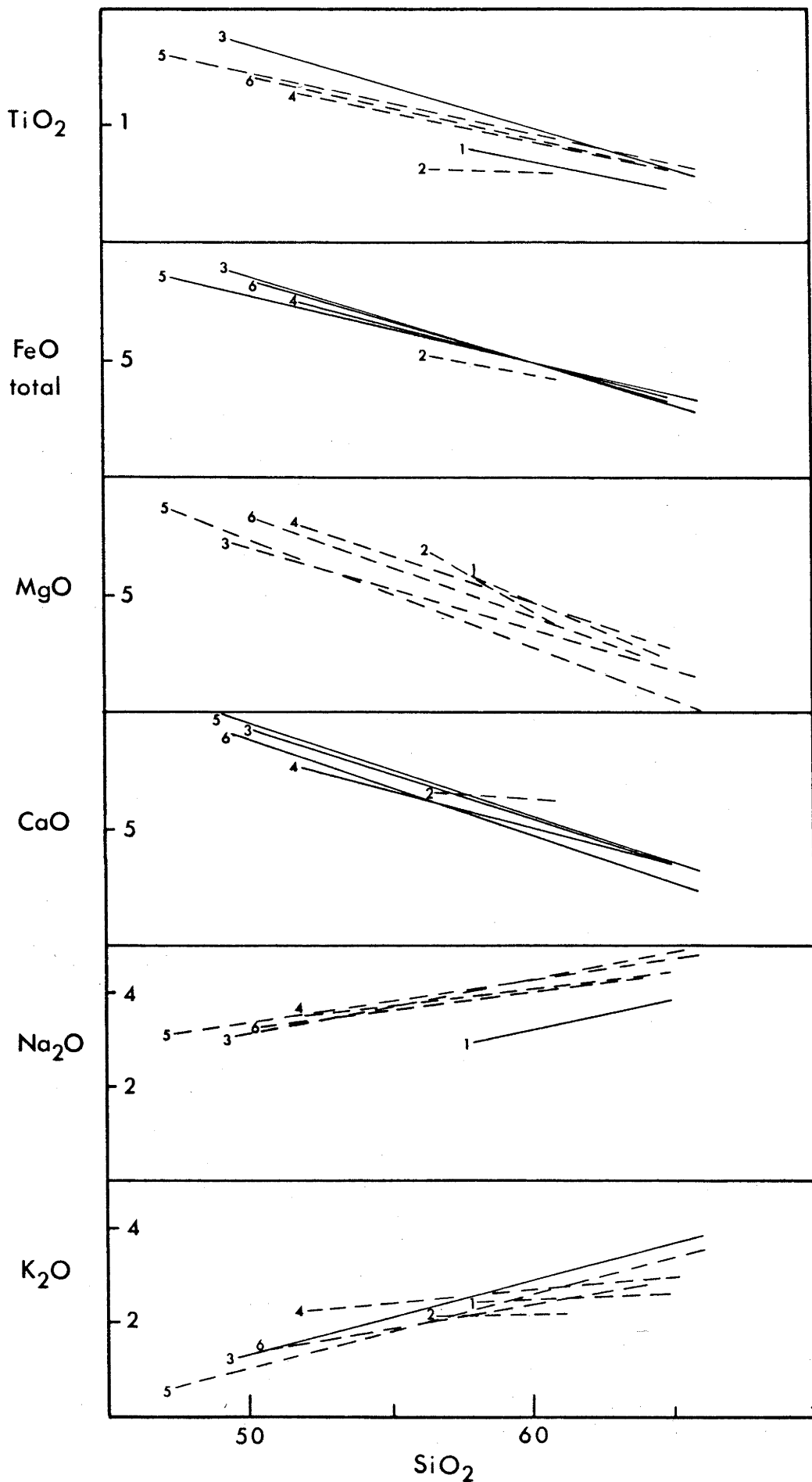
FIGURE 5-2: Regression analysis of major element oxides against SiO_2 (wt.%).

Regression lines with correlations less than 90 shown dashed.
1 - Calvados Islands, 2 - Egum Atoll, 3 - Normanby Island
4 - Amphlett Islands, 5 - Moresby Strait area, 6 - northeast
Papuan coast.

FIGURE 5-3: Q-mode factor analysis of andesitic rocks from the off-shore islands.
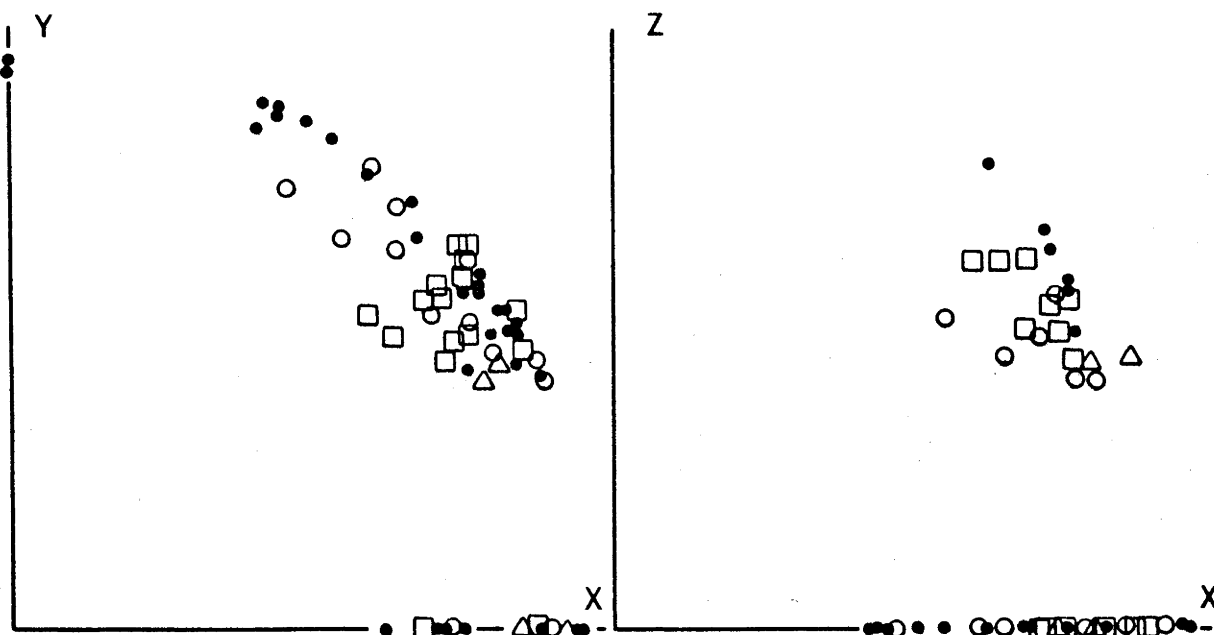
triangles - Calvados Islands and Egum Atoll, circles - Normanby Island, squares - Amphlett Islands, dots - Moresby Strait area. Values of Y and Z less than 40 are plotted along the X-axis.

VERIMAX FACTORS (values less than 40 omitted)

	X.	Y.	Z.
SiO_2	-90		
TiO_2	90	-62	
Al_2O_3	57		
Fe_2O_3	45		70
FeO	90		
MnO	89		
MgO	66	70	
CaO	91		
Na_2O	-45	-42	
K_2O	-91		
P_2O_5	68		46
Rb	-90		
Ba	-46		55
Sr			66
Th	-83		
Zn	65		
Cu	45		
Ni		82	
V	89		
Cr		86	
Pb	-77		

analysis of the data indicates that there are no significant differences in the major element composition of the rock suites making up different centres in the northern volcanic belt.

A further test of east-west variation along the northern volcanic belt is provided by Q-mode factor analysis of major and trace element data from the offshore part of the belt. In the factor analysis eighty six analyses from the offshore islands were treated as a homogeneous group the purpose being to test whether meaningful sub-groups could be established on a geographic basis. Three verimax factors account for all of the significant variation within the data (Figure 5-3). The only factor with any clear petrological significance is Y which contains MgO, Ni and Cr; variation in this factor is probably related to fractionation of olivine or orthopyroxene. Although there is some scatter in plots of the verimax factors for each analysis (Figure 5-3) there is no indication that geographic groupings are important within the data.

Variation in the composition of rock types within individual centres is recognised and is discussed in the following section. However, an important conclusion arising from the regression and factor analysis is that there is no systematic regional variation in rock types along the northern volcanic belt.

5-2   Distribution, Petrography and Chemical Composition

Calvados Islands

Volcanic rocks have been mapped on several of the islands at the western end of the Calvados Island chain in the Louisiade Archipelago (Smith & Pieters, 1969; Smith, 1973b). Rock types are predominantly volcanogenic conglomerate, agglomerate and tuff with subordinate lava flows, which outcrop on a number of islands within a radius of about 8 km and have a present maximum exposed thickness of about 200 m. A single whole rock K-Ar age of 11.4 m.y. on a andesite boulder indicates that these rocks are Upper Miocene.

Limited mapping of the volcanic rocks in the Calvados Chain has revealed a slightly altered series of bedded volcanogenic conglomerate and agglomerate, which possibly represent early submarine volcanic activity in the area, and fresh relatively unconsolidated agglomerate which was erupted subaerially. Specimens of the older rocks are fine grained to slightly porphyritic and consist of clinopyroxene, plagioclase,

iron-titanium oxides and green interstitial material; some contain olivine pseudomorphs. Components of the unconsolidated agglomerate are porphyritic rocks containing phenocrysts of andesine and clino-pyroxene with less common, iron-titanium oxides and rare pseudomorphs after olivine, or of hornblende and biotite, with subordinate iron-titanium oxides. The fine grained groundmass of these rocks is mostly plagioclase, pyroxene, iron-titanium oxides, and in some specimens hornblende,biotite and interstitial glass.

Chemical analysis of three rock types occurring in clasts in unconsolidated agglomerate on Panaroa Island are presented in Table 5-1; these comprise a pyroxene-bearing andesite (603), a hornblende-bearing andesite (604) and a pyroxene-bearing dacite (605). The chemical compositions of this group vary systematically; with increase in SiO_2 there is an increase in Al_2O_3, Na_2O, K_2O, Rb, Pb, La, Ce and a decrease in total iron, MgO, CaO, V, Cr, Cu and Zn. Ba and Sr are variable to high, K/Rb ratios are moderate (260-360), Th/U ratios are high (4-4.5). High Ni in one specimen (603) is correlated with high Cr. Associated dyke rocks intruding the metamorphic basement underlying the volcanics are medium grained and consist of plagioclase (andesine to labradorite), hornblende, and minor iron-titanium oxides; orthoclase and minor biotite and clinopyroxene are present in some specimens. Andesine, hornblende and biotite form phenocrysts in the porphyritic specimens. Chlorite, calcite, sericite, and fine grained secondary material are common in altered rocks.

The one dyke rock analysed (Table 5-1, 606) is a dacite comparable in many respects to other rocks in the Calvados suite but lower in K_2O, Ba, Rb, Th, La, Ce, and Y than dacite 605.

Egum Atoll

Egum Atoll is a typical atoll made up of reefs and low-lying coral islands which rise from the ocean floor at a depth of about 2000 m to enclose a large lagoon containing small (0.5 km^2 or less) volcanic islets. Presumably the basement of the atoll is made up mainly of volcanic rocks but because of subsidence and erosion only an extremely small volume of these remain above sea level. A whole rock K-Ar deter-mination on one sample (608) gave an age of 2.9-2.8 m.y., (Smith, 1973a).

The volcanic islets are composed of jointed porphyritic rock containing phenocrysts of calcic andesine, iron-titanium oxides and clinopyroxene, with less common orthopyroxene. Biotite and hornblende

TABLE 5-1: CALVADOS ISLANDS AND EGUM ATOLL

No.	Calvados Islands				Egum Atoll			
	603*	604*	605*	606*	607	608	609	610
wt%								
SiO_2	58.70	59.20	63.50	65.40	56.63	57.92	59.02	61.09
TiO_2	.71	.82	.48	.48	.60	.61	.65	.56
Al_2O_3	14.60	15.00	16.70	16.50	14.16	15.84	15.78	15.41
Fe_2O_3	1.70	3.90	1.55	1.20	3.54	3.28	4.48	2.77
FeO	4.05	1.75	2.20	2.25	1.91	1.83	1.00	1.50
MnO	.09	.09	.07	.06	.12	.10	.07	.06
MgO	6.45	4.50	2.20	2.80	7.79	5.42	3.89	4.53
CaO	6.15	5.75	4.20	3.20	6.81	6.47	6.03	6.41
Na_2O	3.00	3.20	3.50	4.05	3.76	4.20	4.44	4.18
K_2O	2.15	2.65	3.10	2.30	2.05	2.43	1.96	2.27
P_2O_5	.22	.32	.25	.18	.28	.29	.33	.30
S	nd	nd	nd	nd	nd	.02	nd	nd
H_2O+	1.30	1.26	1.63	1.00	.71	.40	.60	.32
H_2O-	.36	1.26	.19	.12	1.37	.63	1.12	.32
CO_2	.15	.05	.09	.05	.13	.12	.17	.03
Total	99.63	99.75	99.66	99.59	99.86	99.56	99.54	99.75
Fe_2O_3/FeO	.42	2.23	.70	.53	1.85	1.79	4.48	1.85
Mg.No. (Fe_2O_3/FeO=0.2)	70.6	64.0	55.9	63.6	76.0	70.2	61.6	70.2
ppm Ba	613	925	915	766	1116	960	977	1055
Rb	55	60	99	73	41	51	42	39
Sr	914	315	1250	1109	1126	1216	999	1257
Pb	30	34	37	33	12	18	16	10
Th	9	8	13	8	5	11	4	6
U	2	2	3	3	2	3	1	2
Zr	nd	nd	nd	nd	124	149	137	146
Nb	nd	nd	nd	nd	3	4	2	5
Y	18	22	18	14	13	11	18	10
La	18	21	32	17	34	26	31	33
Ce	40	52	63	37	49	54	40	50
Sc	15	17	7	11	11	12	15	11
V	142	138	77	88	97	112	85	90
Cr	310	136	42	76	344	268	268	158
Ni	211	20	26	42	288	170	96	120
Cu	45	25	18	11	192	29	36	66
Zn	81	72	66	61	65	59	57	42
Ga	nd	nd	nd	nd	16	19	17	17
Cl	nd	nd	nd	nd	902	nd	2331	840
K/Rb	324.51	366.65	259.95	261.53	415.07	395.54	387.40	483.19
Ba/Sr	.67	2.94	.73	.69	.99	.79	.98	.84
Th/U	4.50	4.00	4.33	2.67	2.50	3.67	4.00	3.00
Zr/Nb	-	-	-	-	41.33	37.25	68.50	29.20

nd = not determined.   Abundances <0.5 ppm recorded as 0.
* major element analysis by AMDL.

are rare but aggregates of fine grained iron-titanium oxides displaying hornblende and biotite morphology are typically abundant. Analysed rocks (Table 5-1) from Egum Atoll are all andesites of similar composition. Na_2O, K_2O, Ba and Sr are high, K/Rb ratios are moderate (380-415). Cr is moderately high and shows a negative correlation with SiO_2; Ni is more variable but is high in comparison with average andesite values given by Taylor (1969).

Inclusions, abundant in some of the andesites on Egum Atoll, are fine to medium-grained and originally consisted mainly of plagioclase and clinopyroxene. There has been substantial recrystallization of feldspars and alteration of pyroxene to iron-titanium oxides, with some secondary biotite.

Normanby Island

Normanby Island is made up mainly of pre-Tertiary metamorphic and ultrabasic rocks but these are overlain by late Cenozoic volcanics in much of the western part of the island. The maximum thickness of volcanic rocks on the island, (several hundred metres) is in the hills to the north of Sewa Bay. In this area and in the mountains to the northwest, the rocks are more deeply dissected and are typically slightly altered.

A variety of volcanic rock types outcrop on Normanby Island. Basaltic and intermediate lavas are common on southwestern Normanby Island; these are for the most part medium to dark grey sparsely to strongly porphyritic rocks containing phenocrysts of olivine (or pseudomorphs after olivine) and clinopyroxene or of labradorite (An_{50-65}), clinopyroxene and olivine with or without small phenocrysts of iron-titanium oxides. Weakly pleochroic orthopyroxene occurs as phenocrysts in some specimens. The groundmass of these rocks is fine grained and consists mainly of plagioclase, subordinate clinopyroxene iron-titanium oxides, and in some specimens minor olivine; interstitial glass may be abundant. Vesicles, present in some specimens, are commonly lined with finely crystalline zeolite. Some specimens contain clusters of crystals, typically made up of olivine, orthopyroxene and clinopyroxene.

The chemical compositions of these rocks range from basalt to andesite (<59% SiO_2; analyses 611 to 621, Table 5-2). In general there is a systematic correlation between major elements and SiO_2 content. Trace element abundances particularly Ba, V, Cr, Ni and Zn are variable. High V content is correlated with high TiO_2 content which in two specimens

(613, 614) is anomalously high for andesitic rocks. Although Ni and Cr abundances are closely correlated they are not clearly related to MgO content although they do show a correlation with Mg-number.

One specimen (611) stands out from the others in having relatively low Al_2O_3 and Na_2O but high K_2O and a K_2O/Na_2O ratio of 0.9. This specimen is also characteristically higher in Ba, Rb, Zr, Nb, La, Ce, Y, V, Cr and Ni and has a high Th/U ratio but a low Zr/Nb ratio.

Hornblende-bearing lavas are less common. These are typically porphyritic and contain phenocrysts of andesine and hornblende with or without clinopyroxene, biotite, iron-titanium oxides and olivine. Hornblende phenocrysts are invariably surrounded by an opaque rim which is typically matched by a turbid outer rim in coexisting plagioclase phenocrysts. The fine-grained groundmass is made up of plagioclase, clinopyroxene and iron-titanium oxides.

These rocks are exclusively andesites (>59% SiO_2; analyses 622 to 624, Table 5-2). Their compositions in general continue the trends of the lower-Si volcanic rocks on Normanby Island. Element abundances which don't fall into this pattern are Sr, Cr, and Ni; in particular Cr and Ni are anomalously high for rocks with moderate SiO_2 contents.

Porphyritic dacites containing phenocrysts of plagioclase, biotite and less common pale green clinopyroxene and iron-titanium oxides are a minor component of the volcanic rocks on Normanby Island. These dacites contain total alkali contents of over 8% and are referred to as alkali dacites. Compared with the andesites the dacites are high in Rb, Th, Zr, Nb, La, Ce, Y and low in transition elements. These features, and systematic major element variations, are consistent with a model of fractional crystallization from andesite.

The most Si-rich rock collected from Normanby Island is a rhyolite containing phenocrysts of sodic plagioclase in a largely feldspathic groundmass which contains patches of interstitial quartz. The chemical composition of this rhyolite (Table 5-2, 627) is consistent with its position as the most Si-rich member of an andesitic suite. Low ferromagnesian elements, CaO and Sr, and relatively high Ba, Rb, Zr, Nb, La, Ce and Y suggest that this rhyolite could have originated by fractional crystallisation from a parental magma represented by associated andesites and dacites.

Porphyritic light-coloured lavas are common in the northwestern part of Normanby Island. Typical specimens contain phenocrysts of andesine (An_{30}, less commonly An_{40-45}), subordinate biotite or clinopyroxene,

TABLE 5-2: NORMANBY ISLAND

No.	611*	612*	613*	614	615*	616*	617	618	619*	620*	621	622	623*	624*	625	626	627*
wt%																	
SiO_2	48.80	49.60	51.90	51.91	53.60	54.10	54.37	54.62	56.10	58.20	58.70	59.03	59.60	60.60	65.82	66.10	69.10
TiO_2	1.68	1.75	2.00	1.93	1.49	1.12	1.20	1.36	1.11	1.20	.92	.92	.91	.87	.61	.78	.39
Al_2O_3	13.70	17.40	16.50	15.53	16.90	14.70	15.37	16.73	15.20	17.60	14.99	15.79	15.50	15.60	15.97	16.81	15.40
Fe_2O_3	4.3?	3.40	4.00	2.51	2.4?	.69	2.12	2.97	3.00	1.96	1.74	1.00	2.95	3.35	2.27	1.66	1.98
FeO	5.30	5.40	4.50	6.71	5.25	6.45	4.82	3.65	3.30	3.95	3.72	4.35	2.35	1.53	1.21	.8?	.47
MnO	.1?	.18	.13	.15	.14	.14	.11	.12	.12	.12	.08	.09	.09	.08	.07	.02	.0?
MgO	9.6?	5.97	4.20	5.88	3.60	8.0?	6.74	4.17	6.0?	2.95	5.57	5.18	4.70	3.30	.94	1.01	.30
CaO	8.0?	9.7?	7.9?	8.33	7.30	7.70	7.03	7.50	6.3?	6.00	5.76	5.77	5.00	4.15	5.58	2.41	.7?
Na_2O	2.50	3.8?	4.0?	3.59	3.70	3.0?	3.50	4.22	3.5?	4.10	3.28	3.89	3.65	4.20	5.58	4.79	5.9?
K_2O	2.2?	.75	1.61	1.57	1.58	1.58	2.12	2.20	2.10	2.1?	2.81	2.62	2.80	3.00	4.18	4.17	4.2?
P_2O_5	.84	.36	.74	.62	.49	.31	.36	.49	.41	.33	.37	.33	.28	.27	.18	.28	.08
S	nd	nd	nd	nd	nd	nd	.02	nd	nd	nd	nd	.02	nd	nd	.01	nd	nd
H_2O+	1.2?	.98	1.07	.3?	1.34	.71	.66	.52	1.36	.55	1.20	.64	1.36	.76	.34	.44	.38
H_2O-	1.04	.32	1.69	.39	1.04	.77	.78	.71	1.16	.75	.48	.29	.62	2.00	.34	.3?	.58
CO_2	.0?	.0?	.0?	.0?	.78	.42	.32	.18	.0?	.08	.0?	.21	.0?	.0?	.08	.02	.0?
Total	99.6?	99.76	100.40	99.?4	99.66	99.79	99.?2	99.44	99.86	99.94	99.68	100.13	99.86	99.76	99.58	99.69	99.74
Fe_2O_3/FeO	.8?	.6?	.89	.37	.47	.11	.44	.81	.91	.50	.47	.23	1.26	2.19	1.88	1.9?	4.21
Mg-No. ($Fe_2O_3/FeO=0.2$)	68.?	59.4	51.8	57.6	50.0	70.2	67.?	57.8	67.7	51.7	68.6	67.2	66.1	60.1	37.?	47.2	21.7
ppm																	
Ba	132?	333	699	460	844	608	77?	704	98?	856	735	721	876	1046	450	962	1111
Rb	5?	11	26	30	38	41	41	40	33	34	67	60	67	71	102	113	102
Sr	660	442	807	669	786	620	613	803	869	668	762	714	552	600	190	478	97
Pb	9	6	10	8	12	11	1?	18	15	16	20	19	16	18	23	22	20
Th	6	0	3	3	4	3	6	8	6	?	8	8	9	7	17	15	1?
U	1	1	0	1	1	1	2	2	2	1	1	1	2	2	3	3	3
Zr	26?	178	198	182	202	172	198	24?	259	213	216	121	229	263	460	351	502
Nb	14	4	?	?	8	6	8	9	8	6	?	17	7	8	19	11	18
Y	2?	31	26	28	24	21	20	2?	22	22	19	17	19	21	3?	19	34
La	1?	2?	32	22	33	24	32	30	41	31	29	26	34	37	43	37	5?
Ce	6?	3?	59	5?	69	34	5?	68	6?	57	6?	5?	63	66	89	78	97
Sc	2?	27	22	23	17	22	19	19	1?	16	15	14	13	10	5	7	6
V	213	188	257	271	185	160	153	176	122	113	130	124	9?	68	38	69	7
Cr	44?	3?	68	119	46	377	317	?4	262	3?	230	176	253	133	7	1?	19
Ni	260	38	40	87	22	80	6?	43	16?	7	132	113	134	43	?	13	2
Cu	41	2?	36	30	40	17	20	48	35	?	44	27	26	8	6	10	0
Zn	84	?2	88	117	75	80	84	80	74	75	73	77	73	61	65	59	79
Ga	16	17	19	18	19	16	19	20	17	19	19	19	17	18	23	19	21
Cl	32	3?	257	312	5?	155	nd	nd	47	100	nd	nd	212	49	nd	427	45
K/Rb	333.54	566.01	514.0?	434.44	345.17	319.91	429.25	456.58	528.28	330.52	348.17	362.50	346.93	350.77	340.20	306.35	345.90
Ba/Sr	2.01	.72	.87	.69	1.08	.98	1.26	.88	1.13	1.28	.99	1.01	1.59	1.74	2.37	2.01	11.45
Th/U	6.00	-	-	3.00	4.00	3.00	3.00	4.00	3.00	5.00	8.00	8.00	4.50	3.50	5.67	5.00	5.00
Zr/Nb	19.14	44.50	28.29	26.00	25.25	28.67	24.75	27.22	32.38	35.50	43.20	17.29	32.71	32.88	24.21	31.91	27.89

nd = not determined.   Abundances <0.5 ppm recorded as 0.   * major element analysis by AMDL.

chlorite pseudomorphs (probably after mafic phenocrysts) and rare
hornblende. The groundmass is fine-grained and consists of feldspar
(plagioclase and alkali feldspar) quartz, and minor iron-titanium
oxides and chlorite. Epidote, calcite and chlorite are common secondary
minerals. These lavas differ from those found elsewhere in that they
are all moderately altered.

The comparatively high degree of alteration encountered in
the lavas of northwestern Normanby Island suggests that they are
relatively old. Davies (1969) has suggested on tenuous evidence
(microfossils in a limestone boulder linked by association with nearby
rocks) that there was volcanic activity on Normanby Island during the
Lower Miocene (Tertiary 'e' stage).

A Rb-Sr determination of a dacite from Sewa Bay yielded an age
of 3 m.y. (appendix IV). There are no volcanic land forms preserved on
Normanby Island at the present time so it is unlikely that volcanic
activity extended into Quaternary times. On the available evidence
volcanic activity in the Normanby Island area was a Miocene - Pliocene
phenomenon.

Amphlett Islands.

The Amphlett Islands lie to the north and northeast of
Fergusson Island and are entirely volcanic. The group consists of twenty
small (10 m^2 to 4 km^2) rocky islands made up of massive jointed flows
and agglomerate beds intruded by dykes. The islands are arranged in a
roughly circular pattern which suggests that they may represent the
remnants of a large volcanic complex centered in the middle of the
group. Uama and Tewara are two very similar islands which lie twenty
five kilometres southeast of the Amphlett Islands and are conveniently
grouped with them.

K-Ar dating of a hornblende separate from a sample collected
on Wawia Island gave an age of 3.59 to 3.98 m.y. (Smith, 1973a); a Rb-Sr
determination on a second sample (appendix IV) from the same island
yielded an age of 4 m.y.

Rock types in the Amphlett, Uama and Tewara Islands are basaltic
andesite, andesite and dacite; they are typically porphyritic and some
are vesicular. The basaltic andesites contain phenocrysts of olivine,
typically showing brown marginal alteration, and clinopyroxene with less
common minor colourless hypersthene. The groundmass consists mainly

TABLE 5-3: AMPHLETT ISLANDS

No. wt%	628	629	630	631	632	633	634	635	636	637	638	639	640	641	642	643	644
SiO_2	52.39	53.42	54.64	55.07	57.02	57.79	58.43	58.53	58.98	59.44	59.55	59.98	60.84	63.23	64.29	64.45	64.82
TiO_2	1.15	1.23	.94	1.30	1.01	1.09	.81	1.10	.9?	1.00	.75	1.00	.79	.69	.62	.60	.64
Al_2O_3	14.67	14.53	15.20	15.27	15.71	16.49	14.60	15.57	15.74	16.48	14.58	14.47	14.80	15.29	16.20	16.08	15.21
Fe_2O_3	4.51	2.83	4.50	2.69	3.07	3.46	3.01	2.35	4.24	2.48	2.65	2.18	1.71	1.64	2.48	1.91	1.94
FeO	3.04	4.97	2.19	4.05	2.83	2.57	3.26	3.62	1.03	3.33	2.93	3.19	3.46	2.08	1.41	1.92	1.67
MnO	.12	.13	.12	.11	.09	.09	.10	.10	.07	.08	.08	.08	.09	.06	.05	.09	.04
MgO	7.94	8.60	6.96	6.79	4.83	3.71	6.77	4.38	3.94	3.55	6.64	5.45	5.71	3.72	2.60	3.05	3.13
CaO	7.66	7.46	7.34	6.20	6.09	5.71	5.62	5.63	4.94	6.06	4.92	4.82	5.11	3.81	3.87	4.13	3.65
Na_2O	3.56	3.31	3.92	4.01	3.67	3.92	3.64	4.03	4.08	4.34	4.20	3.98	3.89	4.19	4.56	4.54	4.38
K_2O	2.60	1.79	2.33	2.57	3.07	2.82	2.23	2.51	3.28	1.93	2.05	2.99	2.57	4.02	2.42	2.49	3.49
P_2O_5	.22	.37	.40	.45	.46	.41	.20	.39	.39	.21	.20	.32	.29	.28	.20	.22	.26
S	.02	nd	.02	.02	nd	nd	nd	nd	nd	nd	nd	nd	.01	nd	nd	nd	nd
H_2O+	.56	.4?	.50	.41	.87	.94	.54	.44	1.13	.41	.47	.50	.40	.84	.52	.31	.43
H_2O-	.44	.48	.38	.33	.51	.65	.45	.56	.57	.64	.85	.53	.29	.41	.32	.34	.52
CO_2	.0?	.09	.08	.11	.02	.01	.03	.02	.04	.02	.0	.06	.05	.07	.01	.03	.06
Total	99.3?	99.67	99.52	99.38	99.2?	99.66	99.69	99.23	99.38	99.97	99.87	99.5?	100.01	100.33	99.55	100.16	100.24
Fe_2O_3/FeO	1.48	.57	2.0?	.66	1.08	1.3?	.92	.6?	4.12	.74	.90	.68	.49	.79	1.76	.99	1.16
Mg.No. $(Fe_2O_3/FeO=0.2)$	69.9	70.4	69.8	68.5	64.2	57.5	70.2	61.3	62.8	57.0	72.2	68.7	70.3	68.5	59.7	63.5	65.5
ppm Ba	1160	882	1061	933	1219	1026	837	933	13?2	574	707	1014	864	1266	804	943	1161
Rb	6?	33	41	50	74	69	42	64	8?	40	47	75	60	105	62	62	99
Sr	1065	670	929	847	931	781	558	746	100?	612	667	929	657	895	668	651	914
Pb	28	9	22	18	21	17	15	15	3?	14	15	34	21	39	17	17	38
Th	15	4	8	7	11	9	9	7	11	2	4	11	7	16	4	5	15
U	2	0	2	2	3	2	2	1	3	1	1	4	1	4	1	2	4
Zr	211	214	196	208	274	260	17?	230	250	168	160	218	198	253	167	189	20?
Nb	7	7	7	14	7	7	6	7	6	5	4	7	6	6	5	5	4
Y	17	21	17	16	21	23	15	20	16	17	23	16	13	11	21	20	11
La	54	29	44	38	53	45	30	41	54	23	40	46	31	50	45	41	44
Ce	90	53	76	64	90	77	4?	77	84	50	36	56	56	69	57	69	58
Sc	18	20	22	14	14	15	16	16	12	16	14	12	12	8	10	9	9
V	159	162	126	128	111	123	124	129	90	108	91	100	89	70	66	63	64
Cr	536	457	421	289	173	117	488	141	188	10?	393	320	294	147	139	124	156
Ni	288	291	194	181	72	6?	92	61	86	38	291	164	193	79	92	81	80
Cu	39	27	50	33	20	17	16	19	20	29	28	24	26	15	24	14	18
Zn	81	85	77	77	71	73	74	84	75	67	76	78	70	56	70	59	67
Ga	18	18	19	19	18	20	16	19	20	19	18	19	18	20	19	18	20
Cl	nd	124	nd	nd	665	719	571	413	838	503	495	358	nd	816	316	395	nd
K/Rb	362.00	450.29	471.77	426.70	344.40	339.28	440.77	325.57	332.06	400.55	362.09	330.95	355.58	317.83	324.03	333.40	292.65
Ba/Sr	1.09	1.32	1.14	1.10	1.31	1.31	1.50	1.25	1.27	.94	1.06	1.09	1.32	1.41	1.20	1.45	1.27
Th/U	7.50	-	4.00	3.50	3.67	4.50	4.50	7.00	5.00	2.00	4.00	2.75	7.00	4.00	4.00	2.50	3.75
Zr/Nb	30.71	30.57	28.00	14.86	39.14	37.14	29.17	32.86	41.67	33.60	40.00	31.14	33.00	42.17	33.40	37.80	51.25

nd = not determined. Abundances <0.5 ppm recorded as 0.

of plagioclase, subordinate pyroxene, minor iron-titanium oxides and
glass, and rare olivine.

Andesites predominate; typical specimens contain large
phenocrysts of plagioclase (andesine-labradorite) together with smaller
phenocrysts of clinopyroxene and either olivine plus hypersthene or
hornblende. Plagioclase characteristically occurs as multiple, complexly
zoned crystals especially in specimens that contain abundant hornblende.
Hornblende phenocrysts are variable in abundance and are rimed or
completely replaced by opaque material. Less commonly the andesites
contain phenocrysts of clinopyroxene and olivine with subordinate
plagioclase and hypersthene (specimens 637 to 640). In general there
is a correlation between the abundance of hornblende and the abundance
of a group of incompatible elements comprising K_2O, Ba, Sr, La, Ce and
Zr; K/Rb ratios are generally lower in hornblende bearing andesites.

Dacites contain prominent crystals of andesine together with
smaller phenocrysts of clinopyroxene, hypersthene, hornblende and
generally biotite in a fine groundmass of feldspar, pyroxene and minor
iron-titanium oxides. Feldspar phenocrysts typically contain a narrow
turbid zone close to their outer margin; hornblende and biotite
crystals are invariably surrounded or replaced by opaque material.

In general the Amphlett Island suite is high in Na_2O and K_2O
with the exception of specimens 629, 637, 642 and 643 which have lower
K_2O contents. These relatively low-K rocks are lower in Ba, Rb, Sr,
Pb and Th than associated rocks; Zr is lower in the andesite to dacite
range. There is no clear relationship between the low-K characteristic
of these five specimens and any other compositional or petrographic
feature but they were collected from a number of islands within a
contiguous area at the southwestern end of the Amphlett Group and
perhaps represent a distinct eruptive centre.

As a suite, the rocks from the Amphlett, Uama and Tewara Islands
are typically high in V, Ni and Cr. The generally close correlation
between Ni and Cr, and MgO suggests a control by ferromagnesian minerals
which is supported by petrographic observations. High Ni and Cr contents
are correlated with the presence of abundant olivine and clinopyroxene
phenocrysts in basalts, and in basaltic andesites and andesites with the
presence of olivine, orthopyroxene and clinopyroxene typically forming
clusters of large crystals with or without plagioclase.

Moresby Strait

Volcanic rocks occur on western Ferguson Island and
on Goodenough Island in what is referred to here as the Moresby Strait

area. On west Fergusson Island volcanic rocks occur mainly in the south and central west of the island but isolated outcrop extends to the centre of the island. The largest contiguous area of volcanic rocks is on Kukuia Peninsula and it is here that they reach their maximum thickness of about 600 m. No volcanic land forms have been recognized on the peninsula but Davies and Ives (1965) have suggested that some of the peaks at the western end may be volcanic plugs or necks. Whole rock K-Ar dating of a specimen thought to represent the older lavas at the western end of Kukuia Peninsula yielded an age of 1.0 m.y.; a specimen from the central part of the peninsula gave a whole rock K-Ar age of 0.4 m.y. (Smith, 1973a). However, Rb-Sr ages (Appendix IV) of 4-6 m.y. on two rhyolites from Central Kukuia peninsula indicate that the K-Ar results are minimum ages.

The Iamalele-Fagululu area which lies to the north of Kukuia Peninsula is low lying except for several small steep-sided cumulo-domes and volcanic plateaux, and it contains numerous thermal areas which are among the most active in eastern Papua. The largest of these cumulo-domes, to the west of Fagululu village, is made up of rhyolite and obsidian. On the western side of the area there is a cluster of six cumulo-domes with associated lava flows; the lava flows are andesites and limited sampling suggests that the domes are also made up of andesite. Because of the presence of youthful volcanic land forms and the present high level of solfataric activity, the volcanic rocks in the Iamalele-Fagululu area are thought to be Holocene.

Volcanic rocks outcrop around the margins of the metamorphic core of Goodenough Island. They are most extensively developed on Bwaido Peninsula in the southeast where they reach a maximum exposed thickness of about 600 m. Elsewhere they form small cones or flows adjacent to the major faults, or isolated hills on the extensive alluvial apron surrounding the central metamorphic block. These volcanic rocks may be as old as Pleistocene especially in the thick section on Bwaido Peninsula where volcanic landforms are absent. Well developed volcanic land forms including ash cones and blocky lava flows on the northern and eastern flanks of Bwaido Peninsula provide evidence of volcanic activity probably within the past few hundred years.

The predominant rock types in the Moresby Strait volcanic province are basaltic andesite and andesite with subordinate basalt and dacite; rhyolites are locally abundant on Kukuia Peninsula and in the Iamelele-Fagululu area but are rare on Goodenough Island.

The basalts, basaltic andesites and some of the andesites are typically medium to dark grey porphyritic and commonly vesicular rocks containing sparse to abundant phenocrysts. Phenocryst assemblages are plagioclase, clinopyroxene and olivine, less commonly clinopyroxene and olivine and rarely olivine alone; small phenocrysts of iron-titanium oxides are also present in some specimens. Plagioclase phenocrysts (An_{50-75}) commonly show normal zoning and in some specimens are sieved with finely crystalline material. Olivine typically has brown alteration rims. The groundmass of these rocks consists of labradorite, clinopyroxene, iron-titanium oxides less common orthopyroxene and in some specimens olivine; turbid interstitial material or glass may also be present. The lavas in the Iamalele-Fagululu area are characteristically less porphyritic than those on Kukuia Peninsula and contain more abundant olivine and clinopyroxene. One specimen from this area contains rare oxide pseudomorphs after hornblende. A minor rock type on Goodenough Island is made up of abundant labradorite (An_{50-55}) phenocrysts with subordinate clinopyroxene and rare colourless orthopyroxene.

These rocks range from 47 to 57 % SiO_2; in general there is an increase in plagioclase phenocrysts and a decrease in pyroxene and olivine phenocrysts with increase in SiO_2. Al_2O_3 is variable to high (14-19%) and shows a rough negative correlation with SiO_2; there is no obvious plagioclase accumulation. All of these basaltic and intermediate rocks are moderately oxidised and contain moderate Fe total, MgO and CaO contents; in general variation in MgO content is reflected in Ni and Cr abundances. The alkalies, particularly K_2O are variable to high. K/Rb ratios are moderate to high and in three specimens (Table 5-4, 646, 647, 653) are anomalously high for andesitic rocks (690-800). One of these (646) has an unusually high TiO_2 content and is lower in Ba than associated rocks but in other respects is comparable to rocks with similar SiO_2 content.

Hornblende-bearing lavas ranging from andesite (>60 % SiO_2) to dacite are a minor part of the volcanic rocks on Kukuia Peninsula and on Bwaido Peninsula. These are typically porphyritic and contain phenocrysts of plagioclase (An_{30-60}), brown hornblende, biotite, iron-titanium oxides with less common clinopyroxene and orthopyroxene and rare olivine or quartz. Iron-titanium oxides commonly rim or completely pseudomorph hornblende and biotite phenocrysts. The groundmass of these rocks is made up of plagioclase, hornblende, biotite, iron-titanium

TABLE 5-4: MORESBY STRAIT AREA

No.	645	646	647	648	649	650	651	652	653	654	655	656	657	658	659	660	661
wt%																	
SiO_2	47.51	47.91	49.39	50.28	50.47	52.80	53.00	53.53	53.60	53.70	53.88	53.97	54.22	55.22	55.44	55.45	55.86
TiO_2	1.64	2.00	1.43	1.11	1.64	1.26	1.18	1.43	1.08	1.67	1.15	.96	1.02	1.46	1.17	1.18	1.18
Al_2O_3	15.00	17.13	15.53	15.62	19.21	18.00	16.57	14.17	18.51	17.15	15.82	16.51	17.62	17.66	17.80	17.84	17.89
Fe_2O_3	2.39	2.90	3.03	3.77	4.33	2.43	4.39	2.34	2.41	2.34	1.07	2.11	1.79	3.45	1.95	2.49	2.41
FeO	6.41	6.28	5.11	3.94	2.54	4.40	2.75	3.91	5.30	5.40	6.03	5.69	5.87	3.83	4.06	3.84	3.79
MnO	.15	.15	.13	.14	.11	.13	.10	.11	.14	.14	.13	.14	.14	.13	.11	.11	.10
MgO	11.77	7.69	9.76	10.06	4.59	5.01	5.19	6.87	3.99	3.99	7.35	5.62	4.51	3.08	3.61	3.93	3.84
CaO	9.37	10.03	9.34	9.22	8.91	9.17	7.71	9.61	8.28	8.30	7.97	9.45	9.02	6.92	7.67	7.71	7.29
Na_2O	3.40	3.89	3.16	3.44	3.76	3.80	3.93	2.87	3.43	3.97	3.54	2.92	3.09	4.36	4.08	4.00	4.08
K_2O	.52	.48	.98	1.24	1.58	1.27	1.78	2.33	1.66	1.53	1.67	1.25	1.33	2.29	1.84	1.67	1.78
P_2O_5	.37	.37	.76	.52	.51	.39	.41	.62	.31	.34	.34	.29	.30	.56	.31	.30	.31
S	nd	.04	nd	nd	nd	.01	.01	nd	nd	nd	nd	nd	nd	nd	.02	.02	.02
H_2O+	.48	.44	.42	.22	1.27	.37	1.01	.53	.55	.66	.49	.60	.44	.31	.84	.91	.95
H_2O-	.46	.29	.38	.14	.78	.42	1.22	.33	.21	.34	.19	.14	.17	.17	.28	.33	.43
CO_2	.23	.23	.03	.06	.12	.0	.08	.69	.01	.26	.02	.09	.0	.10	.41	.08	.09
Total	99.70	99.83	99.45	99.76	99.82	99.46	99.33	99.32	99.52	99.79	99.65	99.74	99.52	99.54	99.59	99.86	100.02
Fe_2O_3/FeO	.37	.46	.59	.96	1.70	.55	1.60	.59	.46	.43	.18	.37	.30	.90	.48	.65	.64
Mg.No. ($Fe_2O_3/FeO=0.2$)	74.0	64.2	72.1	74.0	59.7	61.2	61.6	70.4	52.4	52.4	68.6	60.6	55.6	47.9	56.3	57.3	57.2
ppm Ba	388	154	549	740	680	579	743	1088	582	596	619	551	582	1011	586	586	581
Rb	13	5	11	23	36	23	42	53	20	38	40	20	20	41	39	36	40
Sr	657	463	675	856	843	666	599	1346	941	493	608	867	922	996	577	594	578
Pb	1	9	5	9	7	13	13	13	9	11	11	9	9	12	13	13	14
Th	0	0	0	6	2	3	5	13	1	4	6	1	1	3	5	5	0
U	1	20	0	1	1	0	0	2	0	1	2	0	1	2	0	1	1
Zr	188	205	161	170	184	161	243	428	174	219	188	140	149	238	191	189	190
Nb	5	4	3	4	5	5	7	6	4	4	6	1	2	6	5	5	5
Y	22	23	22	21	21	22	23	20	19	29	22	17	23	25	19	21	27
La	16	12	25	40	28	26	34	207	22	24	32	22	22	39	23	23	29
Ce	21	48	50	71	39	47	62	311	39	52	61	44	44	69	47	50	47
Sc	24	29	23	25	17	25	21	20	21	21	22	26	23	16	18	19	18
V	156	206	193	204	176	186	161	206	198	180	173	208	215	194	146	153	142
Cr	592	303	457	540	101	46	172	240	0	23	291	61	15	0	37	43	42
Ni	343	109	262	281	72	37	78	110	7	34	98	24	14	5	26	26	25
Cu	48	47	51	47	35	49	49	141	56	68	24	112	139	28	27	28	27
Zn	64	73	71	74	59	45	71	70	75	77	75	70	71	74	73	73	72
Ga	14	17	15	15	18	18	18	17	19	19	17	17	19	20	19	20	19
Cl	129	nd	34	96	33	nd	nd	74	107	114	259	93	208	107	nd	nd	nd
K/Rb	332.06	796.94	739.59	447.56	364.34	458.39	351.82	364.95	689.02	334.24	346.59	518.84	552.05	463.67	391.66	385.10	369.42
Ba/Sr	.59	.33	.81	.86	.81	.87	1.24	.81	.62	1.21	1.02	.64	.63	1.02	1.02	.99	1.01
Th/U	-	-	-	6.00	2.00	-	-	7.50	-	4.00	3.00	-	1.00	1.50	-	5.00	-
Zr/Nb	62.67	51.25	53.67	42.50	36.80	32.20	34.71	71.33	43.50	54.75	31.33	140.00	74.50	39.67	38.20	37.80	38.00

nd = not determined.   Abundances <0.5 ppm recorded as 0.

TABLE 5-4 (CONTINUED)

No.	662	663	664	665	666	667	668	669	670	671	672	673	674
wt%													
SiO_2	56.16	56.20	56.30	56.54	56.97	57.01	57.26	57.45	57.67	60.29	61.55	64.63	65.99
TiO_2	.96	1.15	1.16	1.15	1.15	1.13	1.04	1.00	.69	1.15	.79	.87	.71
Al_2O_3	14.70	17.56	17.65	17.85	17.61	17.61	16.60	14.52	14.65	16.54	16.45	16.02	16.72
Fe_2O_3	3.08	1.58	2.36	2.89	2.89	2.32	2.89	2.78	2.27	2.54	2.43	2.95	1.82
FeO	3.27	4.31	3.93	3.19	3.26	3.59	3.07	2.62	4.29	2.55	2.21	1.46	1.34
MnO	.11	.12	.11	.12	.09	.11	.10	.09	.12	.12	.08	.09	.10
MgO	6.89	3.85	3.80	3.51	3.33	3.72	4.12	5.85	7.16	2.64	2.84	1.51	.94
CaO	8.31	7.50	6.82	6.73	6.44	6.96	6.84	7.59	7.11	4.03	4.94	4.02	2.03
Na_2O	3.09	4.22	4.26	4.36	3.69	4.17	3.58	3.35	3.14	5.19	4.36	4.60	5.56
K_2O	2.13	1.69	1.78	1.72	2.67	1.66	2.63	2.59	1.68	3.14	2.66	2.76	4.14
P_2O_5	.43	.28	.32	.31	.48	.28	.44	.44	.20	.46	.26	.27	.2?
S	nd	nd	.01	.01	.01	nd	.01	nd	nd	nd	.01	nd	nd
H_2O+	.35	.57	.71	.62	.76	.73	.65	.93	.41	.60	.73	.23	.50
H_2O-	.20	.19	.32	.32	.37	.48	.52	.25	.33	.23	.60	.62	.26
CO_2	.03	.23	.1?	.09	.13	.02	.09	.05	.05	.01	.08	.03	.03
Total	99.71	99.45	99.69	99.41	99.85	99.79	99.84	99.51	99.77	99.49	99.99	100.06	100.39
Fe_2O_3/FeO	.94	.37	.60	.91	.89	.65	.94	1.06	.53	1.00	1.10	2.02	1.36
Mg-No. ($Fe_2O_3/FeO=0.2$)	70.3	58.2	56.6	55.7	54.1	57.6	60.1	70.3	70.1	53.1	57.3	43.2	39.6
ppm Ba	99?	584	670	691	1173	612	1164	1145	576	995	822	825	1185
Rb	43	38	35	37	57	39	58	38	39	85	76	71	107
Sr	946	580	560	561	1178	571	1087	1241	650	500	549	486	309
Pb	13	14	17	14	19	9	19	16	12	19	19	16	22
Th	6	5	5	0	11	3	13	4	3	10	11	9	18
U	1	0	3	1	0	1	0	2	1	3	3	2	4
Zr	257	190	196	193	307	197	297	224	130	380	220	201	461
Nb	4	6	5	5	5	4	6	5	2	9	6	3	10
Y	28	19	23	60	54	28	53	16	40	33	73	30	2?
La	104	21	29	40	162	33	138	42	39	36	101	52	57
Ce	114	37	56	56	166	54	146	73	41	99	122	65	79
Sc	21	18	17	17	15	16	15	14	23	11	12	9	4
V	170	143	139	129	181	130	167	126	171	84	89	85	35
Cr	206	39	93	38	13	39	70	172	393	61	96	3	0
Ni	97	27	27	25	20	26	34	146	120	33	125	8	3
Cu	72	29	34	27	90	22	79	63	87	10	27	11	0
Zn	66	71	73	71	74	65	71	80	70	64	96	61	57
Ga	16	18	19	19	21	18	20	17	16	19	18	17	19
Cl	65	nd	nd	nd	nd	238	nd	904	153	216	nd	412	104
K/Rb	411.21	369.20	422.19	385.91	388.86	353.35	376.43	565.81	357.60	306.67	290.55	322.71	321.20
Ba/Sr	1.05	1.01	1.20	1.23	1.00	1.07	1.07	.92	.89	1.97	1.50	1.70	3.83
Th/U	6.00	-	1.67	-	-	3.00	-	2.00	3.00	3.33	3.67	4.50	4.50
Zr/Nb	64.25	31.67	39.20	38.60	61.40	49.25	49.50	44.80	65.00	42.22	36.67	50.25	46.10

oxides, clinopyroxene and, in some specimens minor interstitial glass.

Within the range from 60 to 66 % SiO_2 these rocks show a decrease in total iron, MgO and CaO, and an increase in the degree of oxidation, Na_2O and K_2O. Rb and Ba is higher Sr is slightly lower than in non hornblende-bearing rocks but K/Rb ratios are comparable. Ni and Cr are closely correlated and extremely variable in abundance. Two of these specimens (Table 5-4, 671 and 674) are higher in alkalies, Ba and Zr.

Within the Moresby Strait area there are two groups of rocks which are characteristically higher in K_2O than associated rocks of similar SiO_2 content but have comparable K_2O and Na_2O contents to rock types which predominate in the Amphlett Islands. One group comprises four samples (Table 5-4, 658, 669, 671, 674) from southeastern Goodenough Island; two of these (671, 674) are hornblende-bearing rocks from the older lava flows of Bwaido Peninsula and two (658, 669) are olivine-clinopyroxene-bearing rocks from the Recent cones in the area. The only consistent feature related to the high-K content of these rocks is high Ba content.

The second group of high-K rocks comprises four samples (Table 5-4, 652, 662, 666, 668) all from a restricted area of lava flows and domes on the northern side of the Iamalele-Fagululu area. High K_2O contents in these rocks is consistently correlated with high Ba, Rb, Sr, and Zr and with very high La and Ce. Two of these specimens are high in MgO, Ni and Cr but this is not a consistent feature of the group.

One andesite (672) from the northern side of Kukuia Peninsula is also characterised by high La and Ce abundances but does not share the other chemical characteristics of the group from the Iamalele-Fagululu area. This rock is closely associated with rhyolites which also have high La and Ce abundances (chapter 6).

Rhyolites which are closely associated with andesites on Kukuia Peninsula and in the Iamalele-Fagululu area are described in Chpater 6.

Northeast Papuan coast

Andesitic volcanoes on the northeast Papuan coast have been described in the literature (Taylor, 1958; Ruxton, 1966; Smith, 1969; Jakes and Smith,1970; Smith and Davies, 1976). No new work on these volcanoes was undertaken during the present study however a brief summary of the occurrence and petrography of the volcanoes is given below and data from the literature is used in some of the following

sections.

Andesitic activity on the mainland is essentially a late
Pliocene and Quarternary phenomenon. Two main areas are recognized;
the Cape Nelson volcanic complex (Smith, 1969; Jakes and Smith, 1970)
comprises an extinct Pleistocene strato-volcano, Mount Trafalgar, and on
its southwestern flank an active Pleistocene to Recent volcano, Mount
Victory; 100 km to the west an essentially similar volcanic complex
(Taylor, 1968, Ruxton, 1966) is made up of Hydrographers Range (late
Pliocene to Pleistocene, extinct) and on its western flank Mount
Lamington (Pleistocene-Recent, active). Smaller areas of predominantly
Quaternary volcanism are found in the Sessagara Hills (including Waiowa
Volcano active during 1943 - 44) (Smith and Davies, 1976) and on Managalase
Plateau (Ruxton, 1966).

Rock types making up the mainland volcanoes are predominantly
basaltic andesite and andesite with subordinate basalt dacite and
rhyolite. The basaltic andesites are either moderately porphyritic or
fine and even grained rocks. In the porphyritic varieties, plagioclase
(An_{35-65}) forms the dominant phenocrysts (up to 3 mm across) accompanied
by smaller phenocrysts of clinopyroxene, orthopyroxene, iron-titanium
oxides, olivine and, rarely, amphibole and biotite. The groundmass
consists of devitrified glass with plagioclase,clinopyroxene,
orthopyroxene and iron-titanium oxides. Non porphyritic basaltic
andesite consists of clinopyroxene, altered olivine, flow-oriented
plagioclase, iron-titanium oxides and rare orthopyroxene.

The andesites and dacites are strongly porphyritic. Plagioclase
(andesine - labradorite) and amphibole are common phenocrysts whereas
biotite,clinopyroxene, iron-titanium oxides and rarely K-feldspar are
less abundant as phenocrysts. The fine-grained groundmass consists of
abundant glass with crystals of plagioclase, amphibole, biotite, iron-
titanium oxides and minor clinopyroxene.

The basalts are typically porphyritic rocks containing
phenocrysts of plagioclase (An_{65-75}), clinopyroxene and olivine set
in a fine-grained groundmass of plagioclase, clinopyroxene, minor
olivine, iron-titanium oxides and a small amount of glass. Rhyolites
are only known from the Managlase Plateau area and have been described
by Ruxton (1966) as light grey rocks containing phenocrysts of plag-
ioclase, biotite, hornblende, pyroxene and rarely apatite in a
groundmass of pink glass with perlitic cracks and microlites. Tridymite

occurs in cavities and is common in the ash-flow tuffs of the area.

5-3   Geochemistry of the Northern Volcanic Belt

All of the centres of the northern volcanic belt have erupted andesite; in most centres andesite is accompanied by basaltic andesite with or without subordinate basalt and dacite. Considered as a whole the rocks form an andesitic suite characterised by high alkali contents and comparatively high K_2O/Na_2O ratios. This section discusses abundances and variations in abundance among groups of elements which constrain petrogenetic models for these andesitic rocks. The discussion is based in part on the correlation matrix presented in Table 5-5.

Barium, rubidium and lead

Ba, Rb and Pb are characteristically high in the east Papuan andesitic suite. Ba is typically higher than the andesitic rock average calculated by Taylor (1969) but falls within the range for high-K andesites given by Jakes and White (1972). Ba displays a weak positive correlation with K_2O, Pb, Th, and Ce, but shows no systematic relationship to SiO_2 content.

Rb contents are high and are highly correlated with K_2O (+97) and with SiO_2 (+93); this group of elements is also well correlated with Th (+69). K/Rb ratios show wide variations but with the exception of a few anomalously high values (>600) in basalts, are comparable to those in other suites; there is a systematic decrease in both the K/Rb ratio and amount of variation from basalt (mean = 500, standard deviation $(\bar{x})$=170, through basaltic andesite (425, $\bar{x}$ = 90) and andesite 375, $\bar{x}$ = 60 to dacite (310, $\bar{x}$ = 30).

Pb abundances are high, are moderately well correlated with SiO_2, K_2O, Rb and Th but are only poorly correlated with Ba.

Ba, Rb and Pb are highly incompatible in an upper mantle residual mineral assemblage and are typically low in abundance in undepleted primary mantle. The typically high incompatible element content of the east Papuan andesitic rocks is highly significant in terms of the constraints placed on petrogenetic models.

Strontium

Sr is high in all of the analysed rocks but shows wide variations. Sr is moderately correlated with Fe_2O_3, MgO, CaO, P_2O_5, V, Ni, Cu, Zn. This close relationship with a group including typically ferromagnesian elements is suprising in view of the fact

TABLE 5-5: ANDESITIC ROCKS FROM THE OFFSHORE ISLANDS - CORRELATION MATRIX

	SiO_2	TiO_2	Al_2O_3	Fe_2O_3	FeO	MnO	MgO	CaO	Na_2O	K_2O	P_2O_5	Rb	Ba	Sr	La	Ce	Y	Th	U	Zr	Nb	Zn	Cu	Ni	V	Cr	Ga	Pb
SiO_2	100	-90	-48	-70	-84	-89	-84	-97	61	91	-82	93		-60				78				-76	-53	-51	-92	-55		62
TiO_2		100	52	58	83	84	64	85	-45	-79	83	-80						-70				71			89			-62
Al_2O_3			100			42		47		-52		-52						-53							45			
Fe_2O_3				100		51	54	62		-54	69	-62		59								55		43	57	43		-64
FeO					100	87	74	84	-62	-84	63	-80	-46					-74				67	40		87	42		-68
MnO						100	74	88	-51	-85	70	-86						-74				65	47	83	86	42		-50
MgO							100	82	-73	-77	67	-78		55				-61			-47	61	52		73	88		-65
CaO								100	-68	-93	77	-94		62				-79				67	61	46	94	49		
Na_2O									100	56	-54	54		-56				42		48	48		-52	-50	-68	-56		
K_2O										100	-61	97	44	-49				90		44	52	-64	-51	-43	-85	-46		69
P_2O_5											100	-67		60				-50				65	43	43	83	41		-45
Rb												100		-57				89			45	-69	-55	-45	-87	-48		69
Ba													100			46		45				52						47
Sr														100									59	42	57			
La															100	83	68			44								
Ce																100				60								
Y																	100											
Th																		100		43	47	-56			-72			74
U																			100									
Zr																				100	68						41	
Nb																					100		-41					
Zn																						100		40	72	42		
Cu																							100		56			
Ni																								100				
V																									100	91		-61
Cr																										100		
Ga																											100	
Pb																												100

Correlations less than 40 are omitted.

Table 5-6: $^{87}Sr/^{86}Sr$ initial ratios, rubidium and strontium values for late Cenozoic andesites and associated rocks from eastern Papua.

No.	Center	Rock type	Rb(ppm)	Sr(ppm)	Rb/Sr	$^{87}Sr/^{86}Sr$
608	Egum Atoll	andesite	51	1216	.042	.70414± 2
614	Normanby Island	basalt	30	669	.045	.70399±4
626		dacite	113	478	.236	.70436±7
628	Amphlett Islands	basaltic andesite	61	1063	.057	.70431±3
638		andesite	47	667	.070	.70425±6
641		dacite	105	895	.117	.70443±4
646		basalt	5	463	.011	.70321±3
655		basaltic andesite	40	608	.066	.70398±4
658	Moresby Strait	basaltic andesite	41	996	.041	.70381±2
664		andesite	35	560	.063	.70381±1.5
669*		andesite	38	1241	.031	.7043
674	area	dacite	107	309	.346	.70409±5
676		rhyolite	120	269	.446	.70409±6
678		rhyolite	98	326	.301	.70406±2
679		rhyolite	107	259	.413	.70399±8
3514*	Cape Nelson Complex	andesite	61	856	.071	.7047
3544*		basalt	21	506	.042	.7054

* data from Page and Johnson (1974)

that theoretically at least Sr is too large to substitute for Ca in
the 6-fold coordination sides of pyroxenes (Taylor, 1966). Ba/Sr
ratios are high and show a small positive correlation with SiO_2
(basalt .85, $\bar{x}$ = .47; basaltic andesite 1.0, $\bar{x}$ = .21; andesite
1.22, $\bar{x}$ = .42; dacite 1.67, $\bar{x}$ = .92), and also with K_2O.

$^{87}Sr/^{86}Sr$ initial ratios

$^{87}Sr/^{86}Sr$ initial ratios for fifteen samples from the offshore
islands and two from the Cape Nelson complex are presented in Table 5-6.
Excluding an anomalously low value for a basalt (646) from the Moresby
Strait area the initial ratios show a range of .7038 to .7044 with a
mean of .7041 (standard deviation .0002). These values do not appear
to be correlated with either geographic location or whole rock chemical
composition. They are typical of $^{87}Sr/^{86}Sr$ ratios for many island arc
rocks (e.g. Pushkar, 1968; Gill and Compston, 1973; Whitford, 1975),
are higher than the mean value (.7036 $\pm$ .0001) reported by Page and
Johnson (1974) for the Bismarck Arc in northern New Guinea and are
within the range reported for oceanic island basalts (Gast, 1967).

The uniformity of $^{87}Sr/^{86}Sr$ initial ratios in the andesitic
rocks from the offshore islands conflicts with the suggestion based on
only three measurements that the magma source for the east Papuan lavas
may be heterogeneous (Page and Johnson, 1974). Nevertheless the two
ratios reported for the Cape Nelson volcanic complex (Page and Johnson,
1974; Table 5-6) are significantly higher than those from the offshore
islands which raises the possibility of a more evolved source or of a
contaminated source for andesitic rocks on the Papuan mainland.

One specimen (646) from the Moresby Strait area has an initial
$^{87}Sr/^{86}Sr$ ratio which is markedly lower than any other measurements on
an andesitic rock in eastern Papua. Several other features of the
chemical composition of this rock are unusual when compared with other
basalts in the northern volcanic belt. Rb, Ba and Sr are low, TiO_2 and
K/Rb ratio are high. This specimen has been dated at 1.2 m.y. and is
comparable in composition to transitional basalts associated with
Recent peralkaline rhyolites in eastern Fergusson Island (Chapter 9).
The tectonic significance of this comparison is discussed in Chapter 10.

Rare earth elements (REE)

La, Ce and Y abundances for all the analysed andesitic rocks
are presented in tables 5-1 to 5-4; complete REE abundances for eight

selected samples are presented in Table 5-7. Relative La and Y
abundances and the complete REE data and show a typical pattern of
enrichment in light relative to heavy REE (Figure 5-4). REE
abundances and chondrite normalised patterns are, with the exception
of a group of samples from west Fergusson Island, comparable to those
of andesitic suites in other areas of the southwest Pacific (e.g. Jakes
and Gill, 1970).

La displays a strong correlation (+83) with Ce and weaker
correlations with Ba (+46) and Zr (+44). Ce shows a moderate
correlation with Zr but no significant correlation with Y. The eight
samples for which more complete data are available show no clear
relationship between REE abundances and any other parameter. The data
indicates that the REE element content of these andesitic rocks is
essentially independent of chemical composition for a wide range of
rock types. A second feature of the data is absence of an Eu anomaly
even in the more Si-rich types.

A distinct group of rocks within the Moresby Strait area is
characterised by very high La and Ce abundances. The group is
represented by a basaltic andesite (653) and three andesites (622, 666,
668) from the Iamalele-Fagululu area, and by an andesite (672) and two
rhyolites (676, 677) from the northern side of Kukuia Peninsula.

The La/Y ratios of this group indicate strong fractionation
of light REE relative to heavy REE. There is an increase in the Y
abundances but a decrease in La/Y ratios which is correlated with
increase in SiO_2. Ce is strongly depleted relative to La in the two
rhyolites; because both of these rocks are strongly oxidised (Fe_2O_3/
FeO = 1.8 and 6) one possibility is that the low Ce abundances are due
to alteration.

Complete REE abundance data are available for basaltic
andesite 652 (Table 5-7) and for rhyolite 676 (Table 6-2). The
basaltic andesite shows an extremely fractionated pattern with strong
enrichment of light REE relative to chondritic abundances. The
rhyolite data shows a strongly inflexed pattern with enriched fraction-
ated light REE and enriched but unfractionated heavy REE. The data
indicate that the chondrite normalised REE patterns of this group of
rocks will form a family of curves with enriched fractionated light
REE but with progressive increase in abundance and reduction in degree
of fractionation heavy REE correlated with increase in SiO_2 (Figure 5-5).
The REE abundances suggest a close genetic link between these rock types.
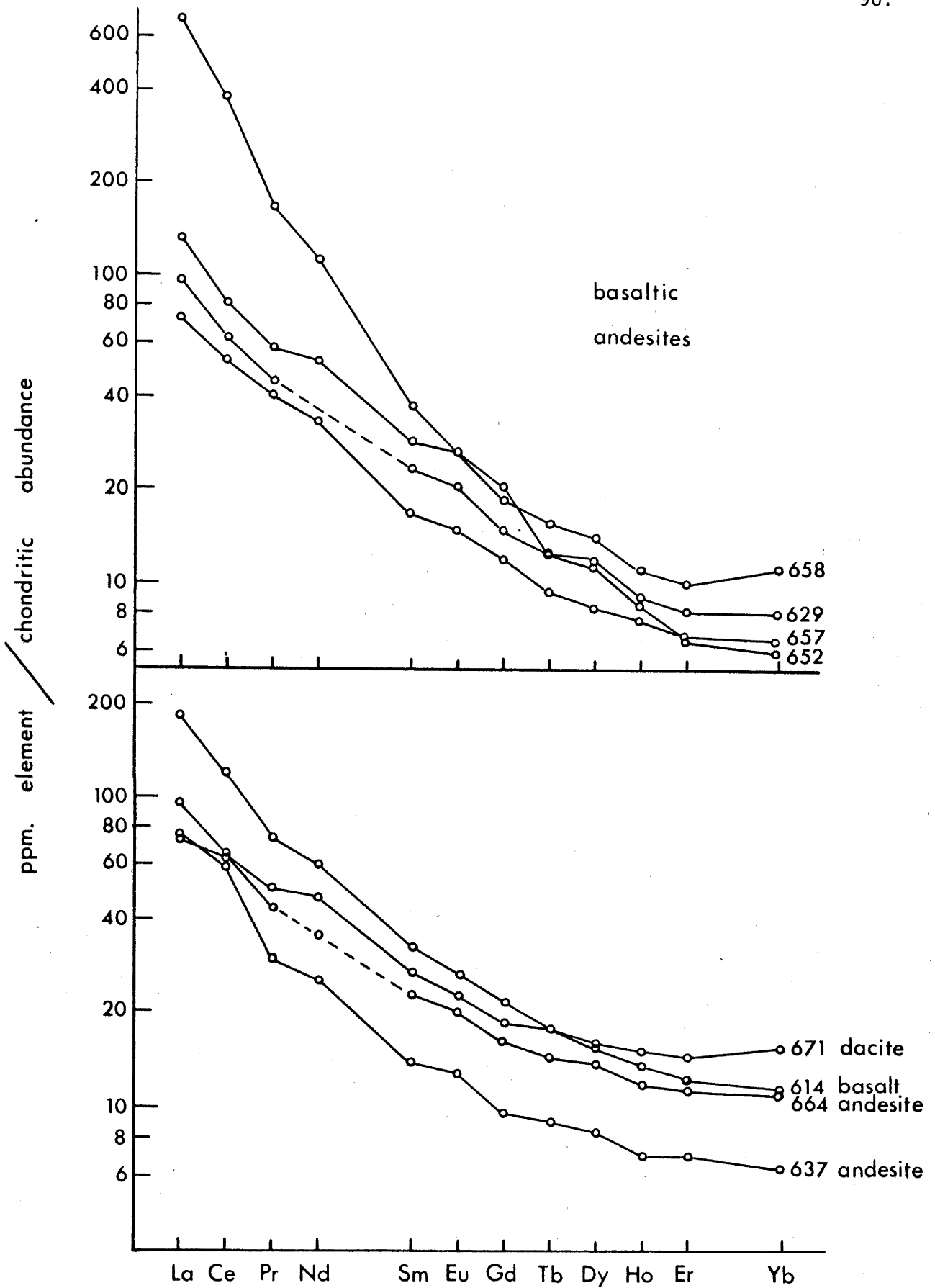
FIGURE 5-4: Chondrite normalised rare earth patterns of representative
andesitic rocks from the northern volcanic belt.
Numbers refer to analyses in Table 5-7.
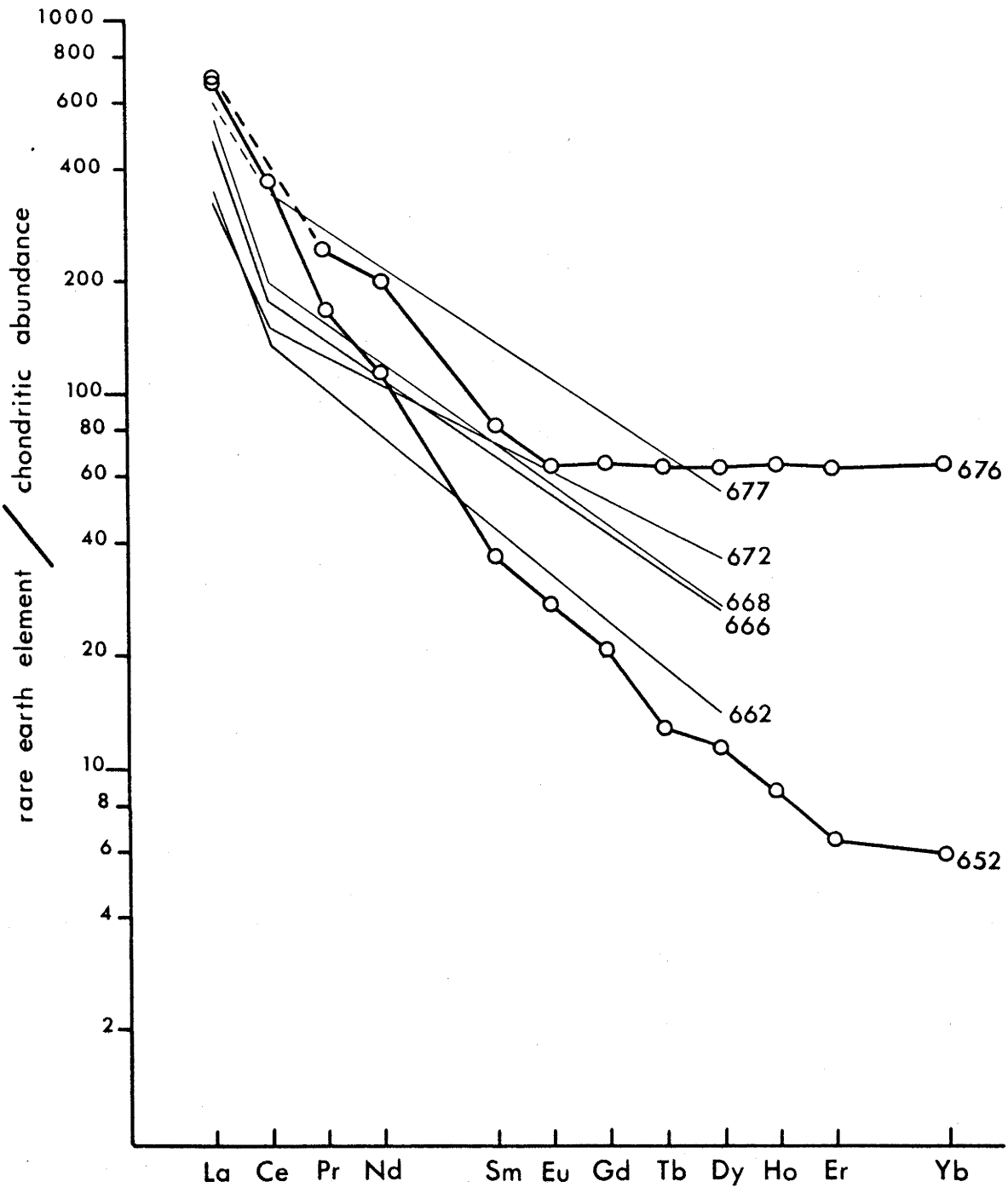
FIGURE 5-5: Chondrite normalised rare earth patterns of andesitic
rocks from Kukuia Peninsula and the Iamalele-Fagululu
area which have unusual rare earth element abundances.
(data from Tables 5-4,5-7,6-1 and 6-2.)

TABLE 5-7: RARE EARTH ELEMENT AND OTHER TRACE ELEMENT ABUNDANCES IN SELECTED ANDESITIC ROCKS

ppm	No rock type	614 basalt	629 basaltic andesite	657 basaltic andesite	658 basaltic andesite	637 andesite	664 andesite	671 andesite	652 basaltic andesite
	La	22	29	22	39	23	29	56	207
	Ce	54	53	44	69	50	56	99	311
	Pr	6.1	5.5	4.9	7.0	3.6	5.3	8.9	19.7
	Nd	27.6	-	19.4	30.9	14.9	-	35.3	65.1
	Sm	5.7	4.9	3.5	6.1	2.9	4.8	6.9	7.8
	Eu	1.7	1.5	1.1	2.0	.94	1.5	2.0	2.0
	Gd	4.9	3.8	2.8	4.8	2.5	4.2	5.7	5.3
	Tb	.87	.61	.46	.76	.44	.70	.88	.62
	Dy	4.8	3.7	2.6	4.3	2.6	4.3	4.9	3.5
	Ho	1.0	.66	.56	.8	.51	.87	1.1	.63
	Er	2.6	1.7	1.4	2.1	1.5	2.4	3.0	1.4
	Tm	.37	.27	.21	.36	.22	.36	.52	.19
	Yb	2.3	1.6	1.3	2.2	1.3	2.2	3.1	1.2
	Lu	.35	.25	.20	.34	.21	.34	.48	.18
	La/Yb	9.6	18.1	16.9	17.7	17.7	13.2	18.1	172.5
	Eu/Eu*	1.00	1.07	1.08	1.13	1.08	1.04	.99	.94
	Cs	1.3	.40	.49	1.1	1.4	1.4	2.8	.64
	Pb	9.8	5.9	8.7	10.8	11.1	12.8	18.8	8.8
	Th	3.8	4.5	2.9	5.9	3.3	4.8	9.8	10.5
	U	.98	.86	.59	1.8	.94	3.0	2.9	2.4
	Th/U	3.9	5.2	4.9	3.3	3.5	1.6	3.4	4.4
	Hf	4.1	4.0	3.7	4.6	3.2	4.3	7.3	7.9
	Zr/Hf	44.4	53.5	40.3	51.7	52.5	45.6	52.1	54.2
	Sn	1.2	1.3	.70	1.5	1.1	1.7	2.2	1.4

La and Ce measured by XRF, remainder by spark source mass spectrometry. [1]estimated abundance

Thorium, Uranium, Zirconium and Niobium

These four elements are the common large highly charged cations. Th shows a good correlation with SiO_2, K_2O, and Rb and a weaker correlation with Na_2O, Ba, Pb, Zr and Nb. Th/U ratios are variable within the range 1 to 8 but are typically higher (4.1, $\bar{x}$ = 1.6) than the crustal average of 3.5.

Zr abundances are typically high, Nb abundances are low. Zr/Nb ratios are moderate to high and are roughly constant throughout the SiO_2 range (basalt 40.5, $\bar{x}$ = 14; basaltic andesite 42.3, $\bar{x}$ = 10; andesite 40.4, $\bar{x}$ = 12; dacite 39.6, $\bar{x}$ = 10). Zr contents and Zr/Nb ratios are higher in the high-La group of samples from the Moresby Strait area. Zr and Nb are a moderately correlated (+68) pair of elements which show a weak correlation with Na_2O, K_2O and Th.

Ferromagnesian elements

There is a well correlated group of major oxides comprising TiO_2, FeO, MnO and MgO which show a clearly defined negative correlation with SiO_2 K_2O and related elements. CaO and P_2O_5 are correlated with this group. Trace elements which are well correlated in this group are V, Cr and Ni, those which are less well correlated are Zn and Cu.

V abundances are moderate to high in low-Si specimens but decrease as SiO_2 increases. Sc abundances are low (typically 15-20) and appear to be related to V. TiO_2 and V are well correlated with FeO and MnO which suggests that iron-titanium oxides play an important role in determining their abundance. V/Ni ratios are low typically <5; this is due to high Ni contents discussed in the following paragraph but is atypical of the andesitic rocks described by Taylor (1969) and Taylor and others (1969).

Ni abundances in the east Papuan andesitic suite are variable and in general are unusually high for andesitic rocks. Ni is well correlated with Cr (+91) and with MgO (+83). On a Ni/MgO variation diagram (Figure 5-6) most of the rocks plot in a broad field with Ni<220 ppm and MgO 1 to 8%; there is a small but clearly definable gap in this field which divides the analyses into a relatively low-Ni group (Ni<20x MgO) and a high-Ni group (Ni>20xMgO). A third group of mainly basaltic rocks is defined by very high Ni content (>260 ppm) and high MgO (8-12%). These rocks contain relatively abundant olivine phenocrysts which typically display a narrow alteration rim but in some specimens are completely altered. The high MgO, Ni and Cr content of these specimens is thought to be due to accumulation of olivine and to a lesser extent ortho-and clinopyroxene.
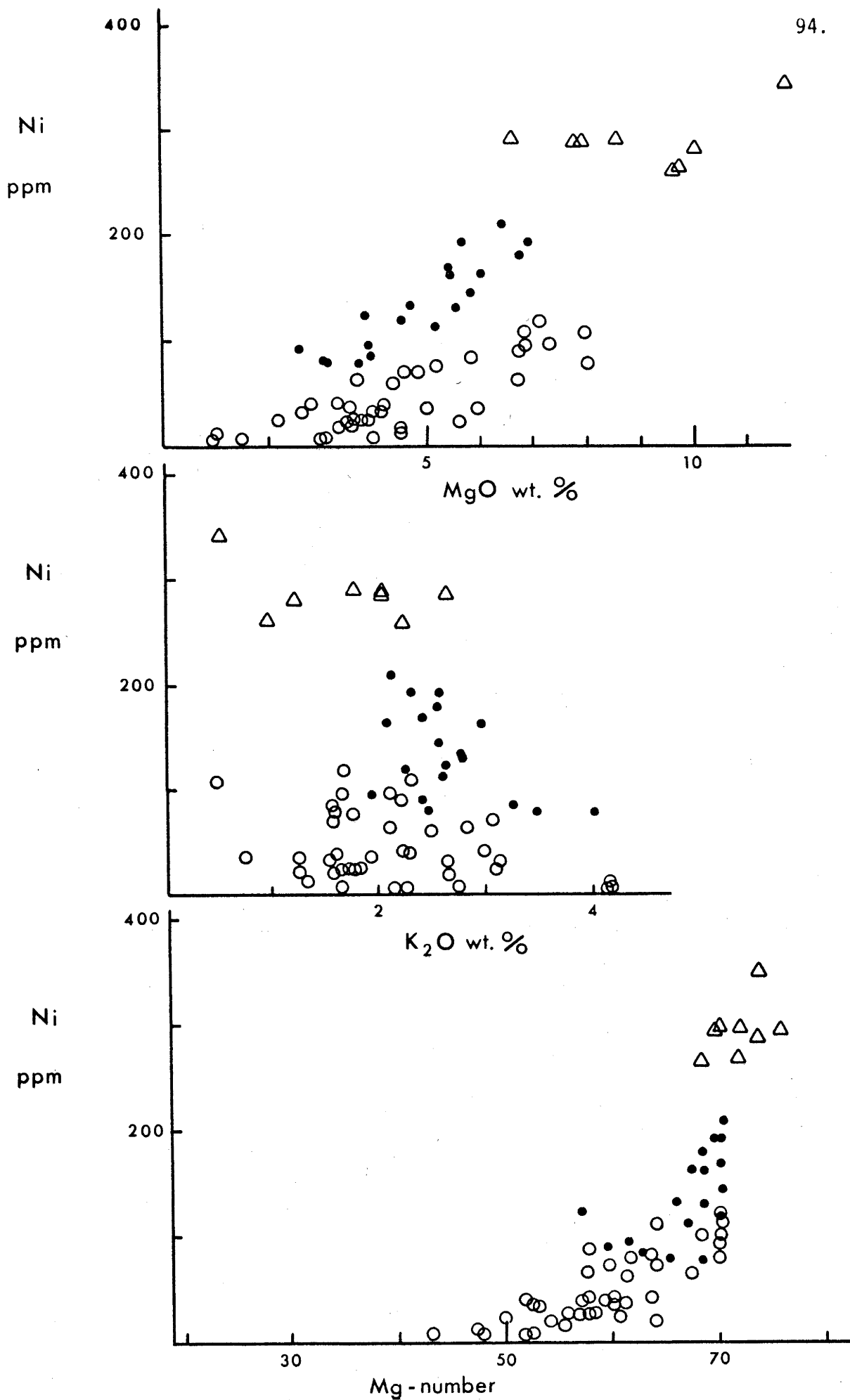
FIGURE 5-6: Variation of Ni abundances with respect to MgO, K₂O and

Mg-number in andesitic rocks from the off-shore islands.

Triangles - accumulative specimens, dots - high-Ni specimens, circles - (relatively) low-Ni specimens.

TABLE 5-8:   Ni-RICH ANDESITIC ROCKS FROM THE NORTHERN VOLCANIC BELT

	No	SiO$_2$	Ni	Mg.No(Fe$_2$O$_3$/FeO = 0.2)
Accumulative Group				
	607	56.63	288	76.0
	611	48.80	260	68.5
	628	52.39	288	69.9
	629	53.42	291	70.4
	638	59.55	291	72.2
	645	47.51	343	74.0
	647	49.39	262	72.1
	648	50.28	281	74.0
High-Ni Group				
	603	58.70	211	70.6
	608	57.92	170	70.2
	609	59.02	96	61.6
	610	61.09	120	70.2
	619	56.10	165	67.6
	621	58.70	132	68.6
	622	59.03	113	67.2
	623	59.60	134	66.1
	630	54.64	194	69.8
	631	55.07	181	68.5
	636	58.98	86	62.8
	639	59.98	164	68.7
	640	60.84	193	70.3
	641	63.23	79	68.5
	642	64.29	92	59.7
	643	64.45	81	63.5
	644	64.82	80	63.5
	669	57.45	146	70.3
	672	61.55	125	57.3

The high-Ni group (Table 5-8) comprises rocks ranging from basaltic andesite to dacite but is dominated by andesites. All of the group have relatively high K_2O contents and only three analyses of low-Ni rocks (634, 652, 662) plot within the field defined by the high-Ni rocks on a Ni/K_2O variation diagram (Figure 5-6). All of the high-Ni rocks with less than about 59% SiO_2 contain abundant olivine and clinopyroxene with less common orthopyroxene; intergrown pyroxene aggregates and orthopyroxene phenocrysts showing clear evidence for reaction with the surrounding matrix are moderately common. Above 59% SiO_2 the phenocryst assemblages become more varied but all of these rocks contain pyroxene and many contain olivine or pseudomorphs after olivine with or without plagioclase amphibole or biotite. Crystal clusters are common and amphibole occurs with clino-pyroxene and olivine in some specimens.

Magnesium numbers

Magnesium numbers (mol. 100 MgO/MgO + FeO; Fe_2O_3/FeO = 0.2) in the andesitic rocks range from 43 to 76. As a group the accumulative basaltic specimens have the highest numbers (68 to 76) but because the high MgO contents are related to accumulation of ferromagnesian phases these high numbers have no significance. Apart from these specimens the highest Mg-numbers are in the range 68-71 and are found in both high-Ni and low Ni rocks over a wide range of composition. High Mg-numbers are found within the range 55-63% SiO_2 in low Ni specimens.

A striking feature of variation in Mg-numbers is that with the exception of the accumulative specimens there is a continuous range of numbers up to but not beyond about 71; this cut off in values is remarkably sharp (Figure 5-6) and implies that the relative FeO and MgO contents of magmas have been buffered over a wide range of SiO_2.

The significance of high Mg-numbers

Estimates of the chemical compsoition of undepleted upper mantle (Ringwood, 1966; Carter, 1970) give Mg-numbers ranging from 87.5 to 89.3 implying a similar range for upper mantle olivine (Kesson, 1973). If the data from refactory ultrabasic inclusions are considered, the composition of olivine in the mantle probably ranges from $Fo_{87.5}$ to at least Fo_{92}. $Mg/Mg+Fe^{2+}$ ratios of orthopyroxene in the upper mantle probably show a similar range.

The relationship between the $Mg/(Mg+Fe^{2+})$ ratios of liquid and coexisting crystalline residuum (olivine and/or orthopyroxene) is given by the expression $X_{ol} = (X_{liq} \times 100)/[X_{liq} + K_D (100 - X_{liq})]$ (Irving, 1971) where X = Mg-number. In terms of the widely accepted value of $K_D = 0.3$ (Roeder and Emslie, 1970) the comparatively high Mg-numbers of non accumulative east Papuan andesitic rocks imply equilibrium with olivine (or orthopyroxene) compositions up to $Fo_{88.8}$ ($En_{\sim 89}$), which is within the range of upper mantle compositions. This conclusion is in general agreement with the $Mg/(Mg+Fe^{2+})$ ratios in olivine and/or orthopyroxene phenocrysts analysed in seven andesitic rocks including accumulative (607, 638, 645) and high-Ni (640, 642) specimens (Table 5-9).

At face value this data places the constraint on the Papuan andesitic rocks that for a wide range of compositions (basalt to andesite), magmas must have been in equilibrium with highly magnesian olivine and/or orthopyroxene. However, although the value $K_D = 0.3$ is probably applicable to natural systems at low temperatures and pressures and at liquid compositions close to those of Roeder and Emslie's (1970) original experimental work, extrapolation to higher temperatures and pressures may not be valid. For example Nicholls (1974) reports a range in K_D of .33 to .50 in olivine-glass pairs produced in experimental work on quartz-normative basaltic to andesitic compositions under hydrous conditions and Mysen (1975) has shown experimentally that in the presence of H_2O K_D must increase with increasing pressure at a rate of about 6.5% /Kb between 10 and 30 Kb at $1100^{\circ}C$. On the basis of this work the assumption that high Mg-numbers necessarily imply equilibrium with highly magnesian residual phases comes into serious doubt.

Increasing oxygen fugacity (fo_2) will lead to an increase in the $Fe^{3+}/(Fe^{3+}+Fe^{2+})$ of a system which results in an increase in the $Mg/(Mg+Fe^{2+})$ and, since Fe^{3+} cannot be accommodated to any significant extent in olivine, an increase in the Fo content of coexisting olivine (Mysen 1975). In this situation the $Mg/(Mg+Fe^{2+})$ of the liquid increases with increasing fo_2 but the total percentage of iron also increases so that the liquid will have relatively low $Mg/(Mg+\Sigma Fe)$. Although the east Papuan andesitic rocks have comparatively high $Mg/(Mg+\Sigma Fe)$ ratios both generally and in comparison to other island arc type rocks in Papua New Guinea they show a spread in $Mg/(Mg+\Sigma Fe)$ ratios which may indicate variable fo_2 conditions in the source.

TABLE 5-9: REPRESENTATIVE ANALYSES OF ORTHOPYROXENE AND OLIVINE PHENOCRYSTS FROM SELECTED ANDESITIC ROCKS.

ORTHOPYROXENE

Rock No.	642							638						667			
SiO_2	56.15	54.93	53.75	54.14	54.19	54.16	52.98	56.95	56.96	57.64	56.58	56.35	55.60	53.08	53.09	52.75	52.47
TiO_2	.0	.0	.21	.11	.19	.12	.0	.0	.0	.0	.0	.0	.0	.75	.35	.60	.57
Al_2O_3	.76	1.20	2.28	1.46	1.24	.63	.68	1.13	1.05	.73	1.36	1.23	1.60	1.98	2.14	.96	.67
FeO	9.97	13.47	13.53	13.78	14.45	17.39	20.15	5.98	5.97	5.74	7.04	7.71	9.42	14.93	15.03	18.34	19.63
MnO	.14	.16	.12	.19	.17	.47	.36	.0	.0	.0	.0	.0	.14	.23	.28	.48	.46
MgO	31.56	29.05	28.98	28.39	28.28	26.10	24.84	34.82	34.90	35.05	33.60	33.29	31.66	27.53	27.45	24.61	23.93
CaO	1.32	1.18	1.14	1.69	1.49	1.12	.98	.62	.65	.61	1.05	1.12	1.17	1.49	1.66	2.26	2.27
Cr_2O_3	.11	.0	.0	.24	.0	.0	.0	.51	.47	.23	.38	.31	.41	.0	.0	.0	.0
Mg No.	84.9	79.4	79.2	78.6	77.7	72.8	68.7	91.2	91.2	91.6	89.5	88.5	85.7	76.7	76.5	70.5	68.5

OLIVINE

Rock No.	607			638			640			
SiO_2	40.28	40.21	40.33	40.54	40.19	40.48	40.35	40.20	39.85	39.79
FeO	11.23	11.47	11.52	10.66	11.00	11.02	11.65	12.01	13.31	14.24
MnO	.19	.16	.12	.0	.0	.0	.0	.0	.0	.0
MgO	48.30	48.16	48.03	48.80	48.81	48.51	47.93	47.79	46.84	45.96
CaO	.0	.0	.0	.0	.0	.0	.07	.0	.0	.0
Mg No.	88.5	88.2	88.1	89.1	88.8	88.7	88.0	87.6	86.2	85.2

Rock No.	645							649				638					
SiO_2	40.00	40.10	39.66	38.61	38.04	37.31	37.11	40.38	39.71	38.99	38.22	39.23	38.94	38.88	38.76	38.07	38.10
FeO	11.93	11.93	13.72	18.65	21.71	24.34	25.62	12.54	13.92	17.54	21.85	16.42	17.82	18.80	19.17	21.27	22.41
MnO	.0	.16	.0	.22	.37	.43	.46	.0	.0	.14	.17	.0	.15	.17	.17	.24	.16
MgO	47.93	47.82	46.44	42.28	39.69	37.67	36.56	46.99	46.21	43.24	39.63	44.35	43.09	42.15	41.91	40.34	39.18
CaO	.14	.14	.17	.23	.18	.26	.25	.10	.16	.09	.13	.0	.0	.0	.0	.09	.15
Mg No.	87.8	87.7	85.8	80.2	76.5	73.4	71.8	87.0	85.5	81.4	76.4	82.8	81.2	80.0	79.6	77.2	75.5

analyses by electron microprobe, normalised to 100%. Fe measured as FeO.

In the upper mantle under conditions of fo$_2$ buffered by iron-wustite and magnetite-haematite equilibria, liquids derived from peridotitic mantle could have Mg/(Mg+ΣFe) ratios within the range 0.9 to 0.3 depending on temperature, fo$_2$ and the Mg/(Mg+ΣFe) ratio of the source (Mysen and Boettcher, 1975; Mysen, 1975). In practice this means that at least for rocks such as andesitic rocks in which water is thought to play a significant genetic role it is not possible to use either the Mg/(Mg+ΣFe) or the Mg-number to make predictions about the composition of the residual source mineralogy. The arguements in Mysen's (1975) paper also suggest that the widely accepted practice of using an arbitary value of the ratio Fe_2O_3/FeO can lead to erroneous interpretations of the data. For example the arguement presented earlier that an apparent limitation to the Mg-numbers in east Papuan andesitic rocks indicated that the compositions were buffered with respect to Fe/Mg ratios is based on the assumption that the Fe_2O_3/FeO ratios in a suite of andesitic rocks can meaningfully be assumed to be constant.

5-4   Discussion

The degree of preservation of volcanic land forms in the northern volcanic belt indicates that centres within the belt become systematically younger westward. In the east, scant volcanic remnants of volcanoes are found in the Calvados Islands and at Egum Atoll; on Normanby Island and in the Amphlett Islands there are substantial volcanic piles but there is no preservation of volcanic land forms. Well preserved volcanic land forms and the presence of solfataric activity testify to Quaternary volcanic activity in the western D'Entrecasteaux Islands (Moresby Strait area) and along the northeast Papuan coast. The recent eruptions of Mount Victory (1890's; Smith 1969), Waiowa Volcano (1943-44; Baker, 1946) and Mount Lamington 1951 ; Taylor, 1958) are indicative of a continuing moderate level of activity in the western part of the northern volcanic belt.

This observation is not entirely substantiated by the available radiometric ages (Table 5-10). Activity on the mainland appears to have been essentially a Quaternary phenomenon and is continuing at a moderate level at the present time. Volcanic activity in the D'Entrecasteaux Islands and Egum Atoll is older (late Miocene to Quaternary) and there is geomorphic evidence of Recent activity in the western part of this area. On the available data there is a distinct time break between volcanic activity in the D'Entrecasteaux Islands and that in the Calvados Islands

TABLE 5-10:   AGE RELATIONSHIPS IN THE NORTHERN VOLCANIC BELT

CENTRE	AGE	PRESERVATION
Calvados Islands	11 m.y. (K-Ar)	Island remnants
Egum Atoll	3 m.y. (K-Ar)	Island remnants
Normanby Island	3 m.y. (Rb-Sr)	Extensive volcanic pile no volcanic land forms
Amphlett Islands	4 m.y. (K-Ar) 4 m.y. (Rb-Sr)	Extensive volcanic pile no volcanic land forms
Moresby Strait	1 m.y. ⎫ (K-Ar)	Extensive volcanic pile
Kukuia Peninsula	4 m.y. ⎭	no volcanic land forms
	6 m.y. ⎫ (Rb-Sr)	
	4 m.y. ⎭	
Iamalele-Fagululu area		Moderate development of Volcanic landforms, extensive solfataric activity
Goodenough Island		Well developed volcanic landforms
Papuan Coast	1.5 m.y. - present (K-Ar)	Deeply disected Pleistocene volcanics. Active volcanoes.

(Upper Miocene) but in view of the limited number of age determinations this may not be real.

Despite these qualifications there is some evidence for a westward migration of andesitic activity during the late Cenozoic which has important tectonic implications. A similar migration of activity can also be documented for centres in the southern volcanic belt.

Petrogenetic constraints

This section reviews the physical and chemical features of the andesitic suite forming the northern volcanic belt which constrain the petrogenetic model developed in Chapter 7.

1) The northern volcanic belt shows systematic differences in age from east to west. The western and central parts of the belt roughly coincide with a weak seismic zone interpreted as representing the present boundary between the Solomon Sea and the Indian-Australian plates, and are closely associated with ultramafic rocks which lie roughly along the zone of the lower Tertiary plate boundary.

2) The northern volcanic belt is paralleled to the south by the southern belt which also shows systematic age relationships. Although there are differences in the rocks of the two belts, they are clearly related in space and time. A model is required which can explain this relationship in terms of the Tertiary tectonism of the area.

3) Initial $^{87}Sr/^{86}Sr$ ratios are low and, with the possible exception of the mainland lavas, remarkably uniform. This argues for a young source which has not suffered contamination by evolved Sr and also indicates that the source is laterally homogeneous.

4) In common with rocks of the southern volcanic belt the andesitic suite is characterised by high incompatible element content and high Ba/Sr ratios, which place constraints on the mineralogy of the source region and the partial melting process.

5) TiO_2 contents are variable but in general are comparable to those of tholeiitic basalts but are significantly higher than those in basalts of the southern volcanic belt. Similarly Zr and Zr/Nb ratios are higher in the northern volcanic belt.

6) Ni and Cr are high in comparison with andesitic rocks in general. Typical values are comparable to those oceanic basalts. V is high but V/Ni ratios are low. High Ni contents are associated with high K_2O; this is a surprising feature which has important genetic implications.

7) REE patterns show light/heavy fractionation and total REE abundances typical of andesites with the exception of a small group of

samples from western Fergusson Island; the REE content of these rocks suggests that they have a slightly different origin to those in the rest of the belt.

In general terms these constraints are similar to those imposed by the composition of rocks in the southern volcanic belt although in detail there are significant differences which further constrain the petrogenetic model discussed in Chapter 7.

CHAPTER 6

AN ANDESITE RHYOLITE ASSOCIATION

The andesite association of modern island arcs and active continental margins is characterised by predominance of andesites (basaltic andesite, andesite) typically accompanied by subordinate basalt and dacite; only rarely are basaltic rocks abundant (e.g. the South Sandwich Islands, (Baker, 1968)). Rhyolites in association with andesites are comparatively rare and are almost exclusively restricted to the continental segments of island arcs (e.g. the Aleutians, North Island New Zealand) or to active continental margins (e.g. the South American Andes). The andesite-rhyolite association in currently active arcs appears to be related to specific geological environments which suggests that their origin is linked to the presence of relatively thick crust.

In southeastern Papua, rhyolites are associated with andesites on west Fergusson Island, on Managlase Plateau (Ruxton, 1966) and to a lesser extent on Goodenough and Normanby Island. Comprehensive geochemical data are available for a suite of rhyolites from west Fergusson Island and this provides the basis for the discussion of their petrogenesis presented in this chapter.

6-1   Rhyolites on West Fergusson Island

Rhyolite (including obsidian) flows are widespread near the northern and southern coasts of Kukuia Peninsula, and rhyolite and obsidian form cumulo-domes in the Iamalele-Fagululu area. These rhyolites are typically very fine grained to sparsely prophyritic; all have oligoclase as rare to abundant phenocrysts or as microlites. Quartz has only been observed as phenocrysts in one specimen (687). Ferromagnesian assemblages are varied; most commonly the rhyolites contain amphibole and/or biotite together with iron-titanium oxides, less commonly, and only in relatively low-Si specimens (<70% SiO_2) hornblende occurs together with orthopyroxene, clinopyroxene and iron-titanium oxides. Rare microlites of zircon have been observed in several specimens but there is no correlation between their presence and the SiO_2 or Zr content of the whole rock.

The rhyolites from west Fergusson Island range from 68 to 76% SiO_2 (Table 6-1). With increase in SiO_2 there is a systematic decrease in Al_2O_3 and also TiO_2, total Fe, MgO and CaO which together make up less than 2% of the most Si-rich specimens. Alkalies, especially Na_2O

TABLE 6-1: RHYOLITES FROM WEST FERGUSSON ISLAND

No.	675	676	677	678	679	680	681	682	683	684	685	686	687	688
wt%														
SiO_2	67.89	68.14	69.75	69.82	70.16	72.30	72.56	72.77	73.66	74.43	75.56	75.71	75.84	76.12
TiO_2	.62	.58	.40	.48	.34	.26	.25	.26	.24	.23	.16	.16	.17	.17
Al_2O_3	15.47	16.25	14.40	15.64	14.70	14.20	14.68	14.19	14.05	13.86	12.93	13.10	13.25	13.12
Fe_2O_3	1.08	2.21	1.59	1.02	1.50	.38	1.03	.42	.39	.56	.23	.16	.66	.32
FeO	2.13	.35	.86	1.10	.53	.95	.16	.94	.90	.56	.64	.18	.26	.60
MnO	.06	.02	.03	.04	.06	.06	.05	.05	.04	.04	.03	.04	.02	.04
MgO	1.01	.14	.40	.71	.44	.22	.15	.22	.18	.06	.08	.11	.05	.10
CaO	2.63	1.86	1.99	1.91	1.52	.72	.80	.71	.63	.79	.63	.63	.56	.66
Na_2O	4.77	4.39	3.58	4.69	4.90	5.19	4.65	5.05	5.01	4.86	4.17	4.13	4.06	4.08
K_2O	3.41	3.76	4.34	3.89	3.66	4.45	3.99	4.44	4.51	4.07	4.57	4.65	4.69	4.67
P_2O_5	.17	.12	.09	.18	.09	.04	.03	.04	.03	.04	.08	.01	.08	.10
H_2O+	.27	1.21	1.87	.40	.57	.52	1.14	.41	.38	.50	.27	.34	.25	.33
H_2O-	.11	.49	.73	.28	.41	.16	.45	.11	.09	.12	.15	.12	.21	.13
CO_2	.03	.14	.02	.02	.13	.06	.05	.03	.03	.07	.00	.07	.09	.02
Total	99.65	99.66	100.05	100.18	99.01	99.51	99.99	99.64	100.14	100.19	99.50	99.41	100.19	100.46
Fe_2O_3/FeO	.51	6.31	1.85	.93	2.83	.40	6.44	.45	.43	1.00	.36	.89	2.54	.53
ppm Ba	771	926	778	954	908	956	923	778	937	875	676	680	691	673
Rb	109	120	129	98	107	128	109	128	131	129	146	145	143	144
Sr	316	269	243	326	259	76	111	77	66	107	73	71	68	71
Pb	21	25	21	20	24	22	30	23	23	31	24	23	24	22
Th	11	14	14	10	13	14	21	13	15	18	18	20	19	19
U	3	5	3	3	2	3	4	3	4	0	4	4	4	4
Zr	309	301	260	271	264	325	214	329	308	207	138	133	136	133
Nb	8	8	6	9	8	9	8	9	9	9	7	6	6	7
Y	22	294	111	18	12	23	14	22	22	16	10	10	8	9
La	34	217	183	39	36	40	41	31	39	43	30	30	29	30
Ce	64	164	72	62	64	73	58	71	71	71	56	38	38	42
Sc	6	6	4	5	3	3	2	3	3	2	1	1	1	1
V	41	38	26	28	21	3	9	9	5	10	5	4	6	4
Cr	0	0	0	0	0	0	0	0	0	0	2	1	0	0
Ni	2	0	1	1	1	1	0	0	2	0	0	0	1	0
Cu	4	6	0	1	8	0	0	0	0	1	0	0	0	0
Zn	52	62	35	49	41	39	31	39	38	34	21	22	17	22
Ga	18	20	16	18	17	17	17	17	17	15	15	14	15	15
Cl	117	nd	169	323	nd	243	115	247	253	nd	227	231	520	221
K/Rb	259.71	260.11	279.29	329.52	283.96	288.61	303.88	287.96	285.80	261.92	259.85	266.22	272.27	269.22
Ba/Sr	2.44	3.44	3.20	2.93	3.51	12.58	8.32	10.10	14.20	8.18	9.26	9.58	10.16	9.48
Th/U	3.67	2.80	4.67	3.33	6.50	4.67	5.25	4.33	3.75	-	4.50	5.00	4.75	4.75
Zr/Nb	38.63	37.63	43.33	30.11	33.00	36.11	26.75	36.56	34.22	23.00	19.71	22.17	22.67	19.00

nd = not determined.   Abundances <0.5 ppm recorded as 0.

are variable and high. Although the major element abundances in general show smooth variation with respect to SiO_2 trace element abundances are more variable. Ba abundances divide the rhyolites into two groups, one with high Ba (>900 ppm) and the other with comparatively low Ba (<800 ppm). Within each of these two main groups increase in SiO_2 is correlated with an increase in Rb and to a lesser extent Th and U, and a decrease in Sr, Zr, Sc, V, Zn and Ga. K/Rb ratios of all the rhyolites fall within a comparatively narrow range (260-330) and show no consistent variation with SiO_2 content. Cr, Ni and Cu are low to absent.

Rare earth elements (REE)

Relative La, Ce and Y abundances in all of the rhyolites indicate chondrite normalised patterns in which the light REE are strongly enriched relative to heavy REE. La/Y ratios are typically in the range 1.4 to 3.6; typical enrichment factors relative to chondrites are La 95-140, Ce 45-90 and Y 0.5 - 1. Two atypical rhyolite specimens from the northern side of Kukuia peninsula (676, 677) contain anomalously high contents of La, Ce and Y which clearly set them apart from other rhyolites on west Fergusson Island.

Complete REE abundance data for four 'typical' rhyolites are tabulated in Table 6-2; these comprise two glassy (680, 688) and two crystalline (675,687) specimens. Chondrite normalised patterns of these specimens (Figure 6-1),display the strong light/heavy fractionation predicted from La/Y ratios; all the patterns are essentially parallel and show a sharp inflexion between a steep La-Eu curve and a flat Eu-Yb curve. All show a small but distinct negative Eu anomaly (Eu/Eu* .88 to .73). Light REE abundances are comparable to those in associated andesitic rocks (chapter 5) but heavy REE display a small relative depletion. Two important features of the abundance patterns are the overall decrease in total REE correlated with increase in SiO_2 and the fact that the curves are essentially parallel.

The REE normalised to average north American shale abundances (Figure 6-1) display flat patterns with a small positive Eu anomaly. The rhyolites are all slightly depleted relative to the shale abundances.

The REE data from one of the 'atypical' specimens (Table 6-2; 676) shows a chondrite normalised abundance pattern comparable to those of 'typical' specimens but enriched by a factor of about 10. Ce is notably depleted in both atypical specimens although because they are
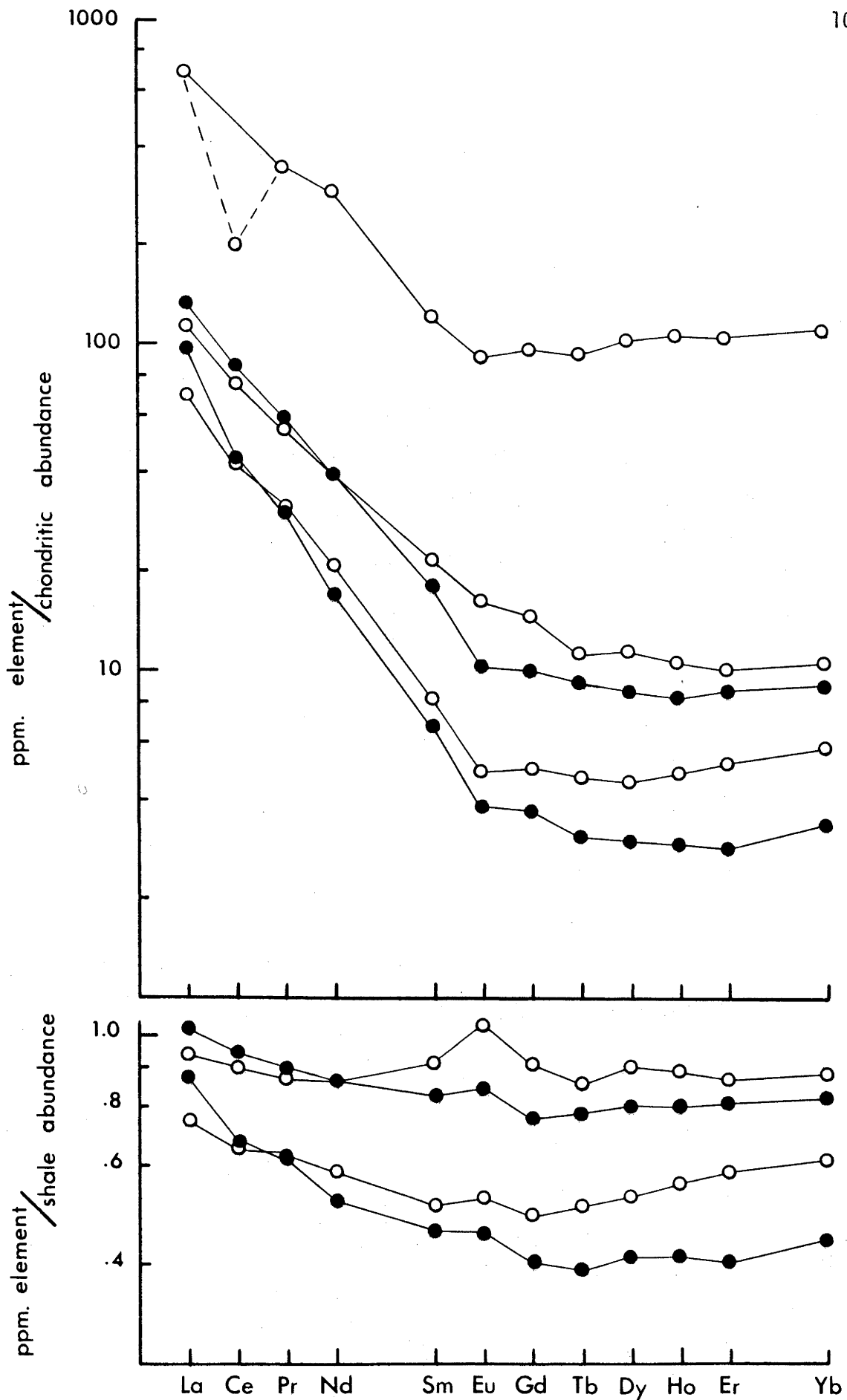
FIGURE 6-1: Rare earth patterns in rhyolites from west Fergusson Island.
Upper - element abundances normalised against chondritic
abundances, lower - element abundances normalised against
north American shale abundances. Numbers refer to analyses
in Table 6-2.

TABLE 6-2: RARE EARTH ELEMENTS AND SOME OTHER TRACE ELEMENTS IN
RHYOLITES FROM WEST FERGUSON ISLAND.

No.	675	680	687	688	676
ppm					
La	34	40	29	21	217
Ce	64	73	38	36	164
Pr	6.6	7.2	3.7	3.8	42
Nd	23	23	9.8	12	170
Sm	4.6	3.7	1.4	1.7	25
Eu	1.2	.76	.28	.36	6.7
Gd	3.8	2.6	.96	1.3	25
Tb	.54	.45	.15	.23	4.5
Dy	3.5	2.7	.93	1.4	32
Ho	.77	.60	.21	.35	7.8
Er	2.1	1.8	.59	1.1	22
Tm[1]	.30	.26	.09	.17	3.2
Yb	2.1	1.8	.67	1.16	22
Lu[1]	.28	.28	.10	.18	3.4
La/Yb	16.2	22.2	43.3	18.1	9.9
Eu/Eu*	.88	.74	.73	.74	.84
Cs	5.6	5.1	5.1	8.0	5.1
Pb	21	16	18	18	25
Th	11	9.8	13	13	14
U	3	2.9	3.6	4.0	5
Th/U	3.7	3.4	3.6	3.3	2.8
Hf	6.7	6.3	2.9	3.6	6.6
Zr/Hf	46.1	51.6	46.9	36.9	45.6

[1] estimated abundance. La and Ce determined by XRF.

highly oxidised this may be due to alteration. These unusually high-REE
rhyolites pose a problem which is all the more intriguing because they
are comparable to the typical rhyolites in all other aspects of their
compositions. High-REE andesites are found in association with these
rhyolites on Kukuia Peninsula and also outcrop in the Iamalele-Fagululu
area (chapter 5); together these rocks form a distinct group possibly
related to a REE enriched source.

$^{87}Sr/^{86}Sr$ initial ratios

$^{87}Sr/^{86}Sr$ initial ratios of three rhyolites from West Fergusson
Island are presented with initial ratios of associated andesitic rocks
in Table 5-6. These three ratios are identical (.7040) to within
experimental error and are closely comparable to ratios in andesitic
rocks of the northern volcanic belt which average .7041. This
uniformity of values indicates either that the source for both andesites
and rhyolites is common or that andesites have provided a source for
rhyolitic magmas which are either partial melts or fractional
derivatives.

6-2 Trace Element Patterns

Initial $^{87}Sr/^{86}Sr$ ratios of the west Fergusson Island rhyolites
are essentially the same as those in associated andesite and in the
andesitic rocks of the northern volcanic belt generally. This constrains
hypotheses for the origin of the rhyolites to two models; either the
rhyolites are the end members of one or more fractionation series from
associated andesite or they are the products of partial melting of a
source which at least in terms of isotope chemistry is comparable to
that which produced the andesites.

Crystal fractionation

The behaviour of trace element abundances during crystal
fractionation can be described in terms of residual elements, feldspar
controlled elements, and depleted elements.

Residual elements

Elements which do not significantly enter any of the fraction-
ating phases and which as a result become concentrated in derivative
liquids have been termed residual elements (Harris, 1967). If SiO_2
content is taken to provide an index of fractionation the only elements
which show residual behaviour are Rb and Th. In some peralkaline
rhyolite suites (e.g. Weaver and others, 1972; Barberi and others,
1975; chapter 9) Zr and Nb show well developed residual behaviour and

La and Ce appear also to have behaved as residual elements. In the west Fergusson Island rhyolites these elements show a negative correlation with SiO_2 (figure 6-2) which is not easily explained by a crystal fractionation hypothesis. It is true that some rhyolite specimens contain minute crystals of zircon which if separated from magma could account for derivative liquids depleted in Zr but the separation of such small crystals from high-Si magmas which are demonstrably viscous seems intuitively unlikely.

La, Ce,Y and, based on the data from four samples (Table 6-2) total REE, show a decrease in abundance with increasing SiO_2 although light/heavy fractionation remains approximately the same. Because the light REE are typically concentrated in different minerals than the heavy REE, production of similar REE patterns for a range of decreasing total REE contents cannot be explained by removal of crystals.

Feldspar controlled elements

The most important feldspar controlled elements are Ba and Sr although Rb and Pb will also enter feldspars. Ba will enter the K-sites of alkali feldspar and is also known to be concentrated in biotite. Fractionation of either of these phases will result in Ba depletion in derivative liquids. Alkali feldspar is not an early crystallising phase in the west Fergusson rhyolites but biotite is moderately common. The fact that Ba abundances are high in all of the rhyolites argues that fractionation of biotite can not have taken place.

Sr is known to readily enter Ca-sites in plagioclase and K-sites in alkali feldspar (Taylor, 1966; Brooks, 1968) and its behaviour will be dominated by the behaviour of feldspar. The decrease in Sr with increase in SiO_2 in the west Fergusson Island rhyolites is consistent with removal of feldspar and with the observation that plagioclase is an early crystallising phase.

Eu is known to be preferentially concentrated by feldspar either in Ca-sites or K-sites. Removal of feldspars from a magma will lead to depletion in Eu (Haskin and others, 1966; Philpotts and Schnetzler, 1968). The very small Eu anomalies (Eu/Eu* 7-9) observed in the west Fergusson Island rhyolites indicate that little if any feldspar fractionation has taken place.

Depleted elements

The depleted elements are typically those which are

110.
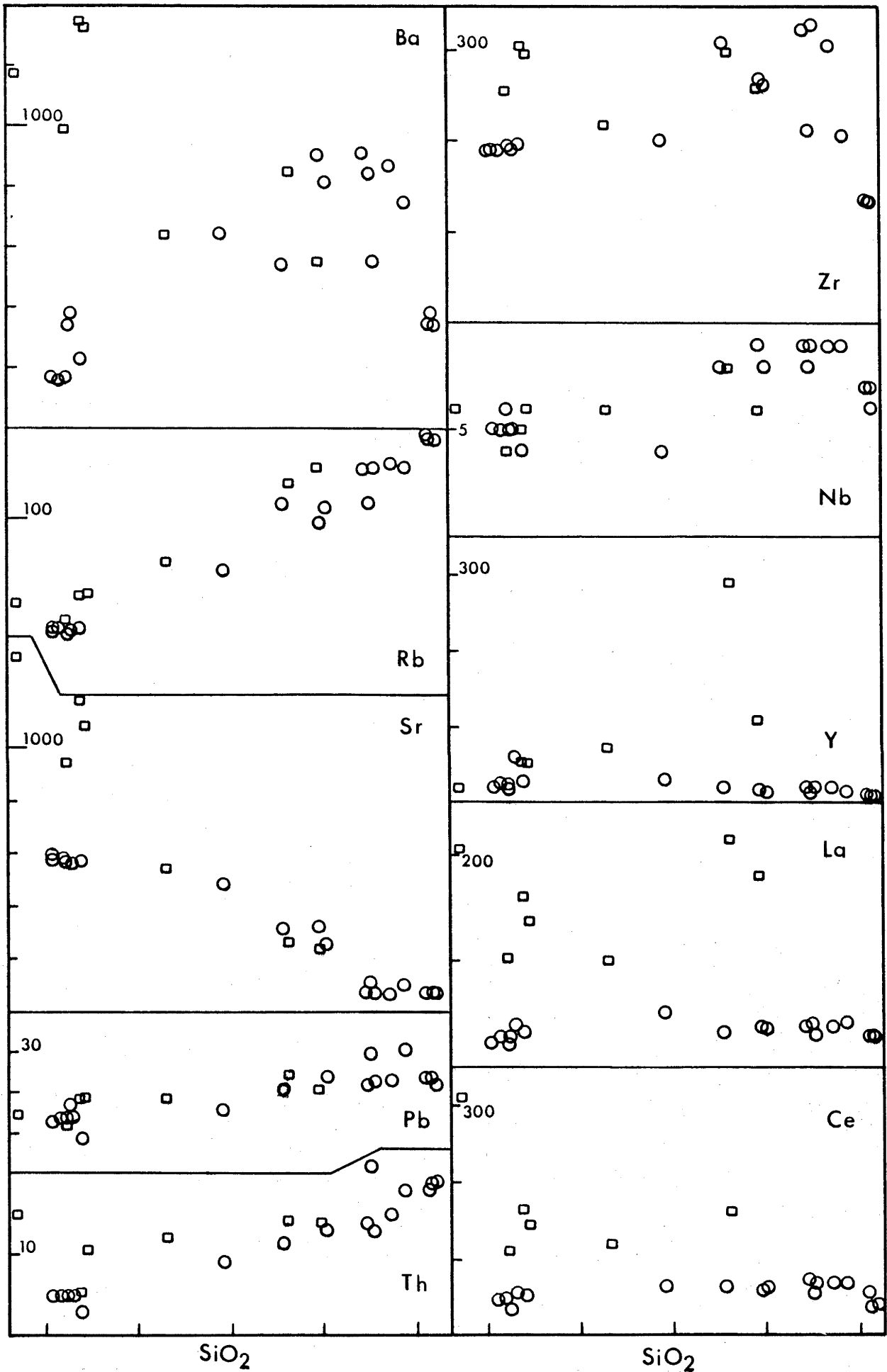
FIGURE 6-2: Variation diagram for rhyolites and associated andesites
and dacites from west Fergusson Island.
rectangles - specimens with unusually high rare earth elements.

concentrated in the early crystallising minerals of parental magmas and
with fractionation become totally depleted in derivative liquids.
Typical examples are Ni and Cr which are low to absent in these
rhyolites and Sr,V and Zn which show a negative correlation with SiO_2.
the abundance patterns of these elements can be explained in terms of
crystal fractionation.

Partial melting

The relative and absolute concentrations of trace elements in
a partial melt will be controlled by the degree of partial melting and
by liquid/solid partition equilibria but will depend on the absolute
abundance of the element in the source composition and on the mineralogy
of the residuum. A second order effect will be the nature of the partial
melting process which in the extreme can be considered as equilibrium
(batch) melting - melt in total equilibrium with residual phases - or
as ideal fractional melting - melt forms by successive small increments
each isolated from contact with the residuum from the moment of
formation. There are some aspects of crystal fractionation which can
be considered as the converse of partial melting but there are important
differences in the two processes which allow the behaviour of certain
groups of trace elements to be predicted.

Elements which are strongly partitioned into an early melt
phase are essentially incompatible in the residual mineral assemblage;
these elements are equivalent to those termed residual elements in a
crystal fractionation model. Incompatible elements in the source rock
will be present in low melting mineral phases or as dispersed elements
(along grain boundaries, in crystal defects etc.) and will tend to
enter the melt at an early stage. During partial melting an incompatible
element could be predicted to increase up to the stage when all of the
element in the source composition has entered the melt phase; continued
melting in the source region will then effectively dilute the concen-
tration of the element in the melt. In a series of batch melts
developed within a source area different amounts of partial melting
could give rise to a series of related magmas; in this situation an
incompatible element when plotted against an index reflecting
increasing degrees of partial melting will display an inflexed trend
characterised by an initial increase in abundance followed by a
decrease in abundance.

An essential part of this model is the notion that elements
which are highly incompatible in the source will enter the melt over a
finite melting interval. This notion is difficult to quantify but is

intuitively more plausable than a model in which all the incompatible elements enter the first melt fraction.

Arguments which are developed in section 6-3 indicate that major element variation in the west Fergusson rhyolites can be explained by conditions within the quartz-feldspar ternary system. Partial melts within this system will show a trend of decreasing SiO_2 with increasing degree of partial melting. The negative correlation with SiO_2 displayed by elements such as Zr, Nb and REE can thus be interpreted in terms of the model outlined in the preceeding paragraphs.

Of particular importance is the parallel nature of the chondrite normalised patterns. Fractional crystallisation of phases such as feldspar which, with the exception of Eu do not significantly fractionate light from heavy REE and which have low crystal/liquid partition coefficients would result in essentially parallel patterns which increase with the degree of fractionation (i.e. with SiO_2 in this case). Such patterns can be demonstrated in rock series for which there is good evidence for crystal fractionation (e.g. chapter 9, figure 9-5). The negative correlation with SiO_2 observed in REE patterns from the west Fergusson Island rhyolites argues strongly against a model of fractional crystallisation.

An obvious exception to this arguement is rhyolite 676 which has a highly enriched REE pattern. This rhyolite is closely associated in the field with andesite 672 (Table 5-4) which has La Ce and Y abundances which are high relative to other andesites but which are lower than rhyolite 676. These relative abundances do not preclude an origin for the rhyolite by fractional crystallisation from andesite although the small magnitude of the Eu anomaly (Eu/Eu* = .84) argues against extensive fractionation of feldspar. Apart from REE abundances the chemical composition of rhyolite 676 is closely comparable to that of the other rhyolites and in view of this it is consistent to model for partial melting rather than fractional crystallisation. In a partial melting model the pronounced Ce anomaly of rhyolite 676 may imply a residual Ce-bearing phase.

Under appropriate conditions of partial melting Ba and Sr abundances will be controlled by partition equilibria. In the absence of a residual Ba-bearing phase, all of the Ba in the source will have entered the melt when the last alkali feldspar (+ biotite) has melted; continued melting will effectively dilute the concentration of Ba in the melt. The behaviour of Ba in this situation is that of an

incompatible element and with relatively small degrees of partial melting could be expected to show the negative correlation with SiO_2 observed in the west Fergusson Island rhyolites. Sr abundances in successive melts will be controlled by melting of both plagioclase and alkali feldspar and can be expected to rise even with moderate degrees of partial melting.

For very small degrees of partial melting, partition equilibria will ensure that some Ba and Sr are partitioned into the melt phase. In contrast, the affinity of Ba for alkali feldspars (and biotite) and of Sr for both plagioclase and alkali feldspar means that with extensive removal of feldspar (and biotite) crystals derivative liquids can be completely depleted in these elements. The efficacy of feldspar fractionation to deplete melts in Sr and Ba has been demonstrated for peralkaline rhyolite series (e.g. Barberi and others, 1975; chapter 9). Moderate Sr contents and high Ba contents suggest that crystal fractionation has not been an important process in the origin of the west Fergusson Island rhyolites.

The small Eu anomalies observed in these rhyolites are consistent with partition equilibria involving residual plagioclase.

6-3   Feldspar - Quartz Relationships

The end members of the quaternary system SiO_2 - Na Al Si_3O_8 - K $AlSi_3O_8$ - Ca $Al_2Si_2O_8$ make up over 90% of the compositions of the west Fergusson Island rhyolites. In projections of this system the rhyolites form a trend extending toward the ternary minimum at P_{H_2O} = 1000 bars (Figure 6-3). This trend is slightly displaced from the experimentally determined minimum in the system SiO_2 - Na $AlSi_3O_8$ - K $AlSi_3O_8$ but this is consistent with the presence of a small anorthite component (10 to 3 wt %) in the rhyolite compositions (cf Barth, 1966). The position of the rhyolites within the system is in agreement with the petrographic observation that plagioclase is the only near liquidus phase in all of the rhyolites except 687 which plots closest to the ternary minimum and contains plagioclase and quartz phenocrysts.

In the ternary feldspar projection (Figure 6-3) the rhyolite compositions lie within, or on the plagioclase side of, the low temperature trough proposed by Kleeman (1965) separating the orthoclase field from the plagioclase field. Two groups of points lie close to the lines representing the locus of compositions in equilibrium with two feldspars and water vapour at 5000 and 1000 bars.
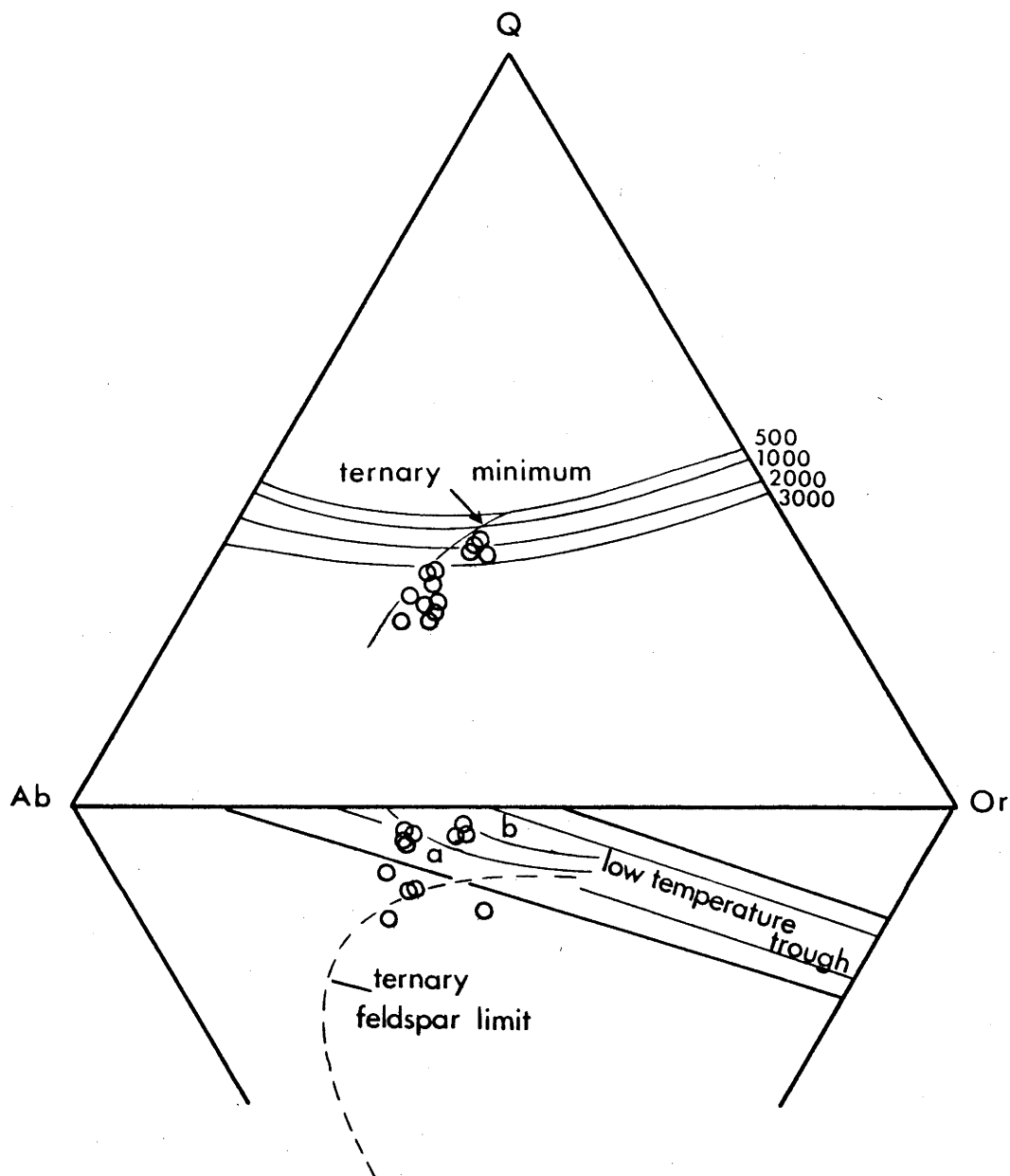
FIGURE 6-3: The ternary systems Q-Ab-Or (upper) and Ab-Or-An (lower)
(weight percentages).
Q-Ab-Or shows the position of the quartz/feldspar field
boundary and the ternary minimun for a range of water
vapour pressures between 500 and 3000 kg/cm², (from
Tuttle and Bowen,1958).
Ab-Or-An shows the limit of ternary solid solution in
natural feldspars and Kleeman's (1965) proposed low
temperature trough separating the plagioclase from the
orthoclase field. Curve a is the locus of liquids in
equilibrium with two feldspars and water vapour at 5000
kg/cm²; curve b is the locus of liquids in equilibrium
with two feldspars, water vapour and quartz, at 1000 kg/cm².

In the quaternary system SiO_2-Al_2O_3-Na_2O_3-K_2O the west Fergusson Island rhyolites plot in an elongate zone trending close to and at an acute angle with the median line ($Na_2O + K_2O/Al_2O_3$ =1) dividing aluminous from peralkaline compositions, (Figure 6-4). A feature of projections in this system is that they show changes in the ratio of alkalies to Al_2O_3 within a suite of rocks and this can be used to illustrate the control of feldspar on development of a series. For example the trend shown by the rhyolites on Figure 6-4 indicates that fractionation of feldspar with compositions in the range An_{20} to An_{30} could explain the observed variations in SiO_2, Al_2O_3, Na_2O and K_2O. An equally acceptable alternative is that the rhyolites form a partial melting series with compositions buffered by residual sodic plagioclase.

On a plot of CaO against the ratio $(Na_2O+K_2O)/Al_2O_3$ (peralkalinity index) the west Fergusson Island rhyolites show a well defined (r = .89) trend toward an index of one when CaO is zero (Figure 6-4). This trend implies that the rhyolite compositions have been buffered with respect to the molecular proportions of CaO, Al_2O_3, Na_2O and K_2O. Because minerals containing these oxides (plagioclase, amphibole, biotite, clinopyroxene) would be expected to fractionate in varying proportions during crystal fractionation it would be a remarkable coincidence if the last CaO was removed from the melt as the alkali/alumina ratio reached one. On the other hand the relationships illustrated in Figure 6-4 are to be anticipated in a rock series produced by progressive equilibrium partial melting. Under such conditions the relative proportions of CaO, Al_2O_3, Na_2O and K_2O would be buffered initially by alkali feldspar ($(Na_2O + K_2O)/Al_2O_3$ = 1) and at a later stage by plagioclase ($(CaO + Na_2O + K_2O)/Al_2O_3$ = 1).

In summary, their position close to the ternary minimum in the system SiO_2 - $NaAlSi_3O_8$ - $KAlSi_3O_8$, variations in alkali/alumina ratio with respect to SiO_2 and evidence for feldspar-buffered compositions indicate that the west Fergusson rhyolites are partial melting products.

Almost all of the west Fergusson Island rhyolites contain a small amount of corundum in the CIPW norm (typically <1%). The presence of normative corundum shows a deficiency in CaO + Na_2O + K_2O with respect to Al_2O_3 which is abnormal in igneous rocks and is surprising in this case because Al_2O_3 contents are not markedly high although Na_2O + K_2O are moderately high. Clearly the calculation of normative corundum in these rocks is related to the very low CaO
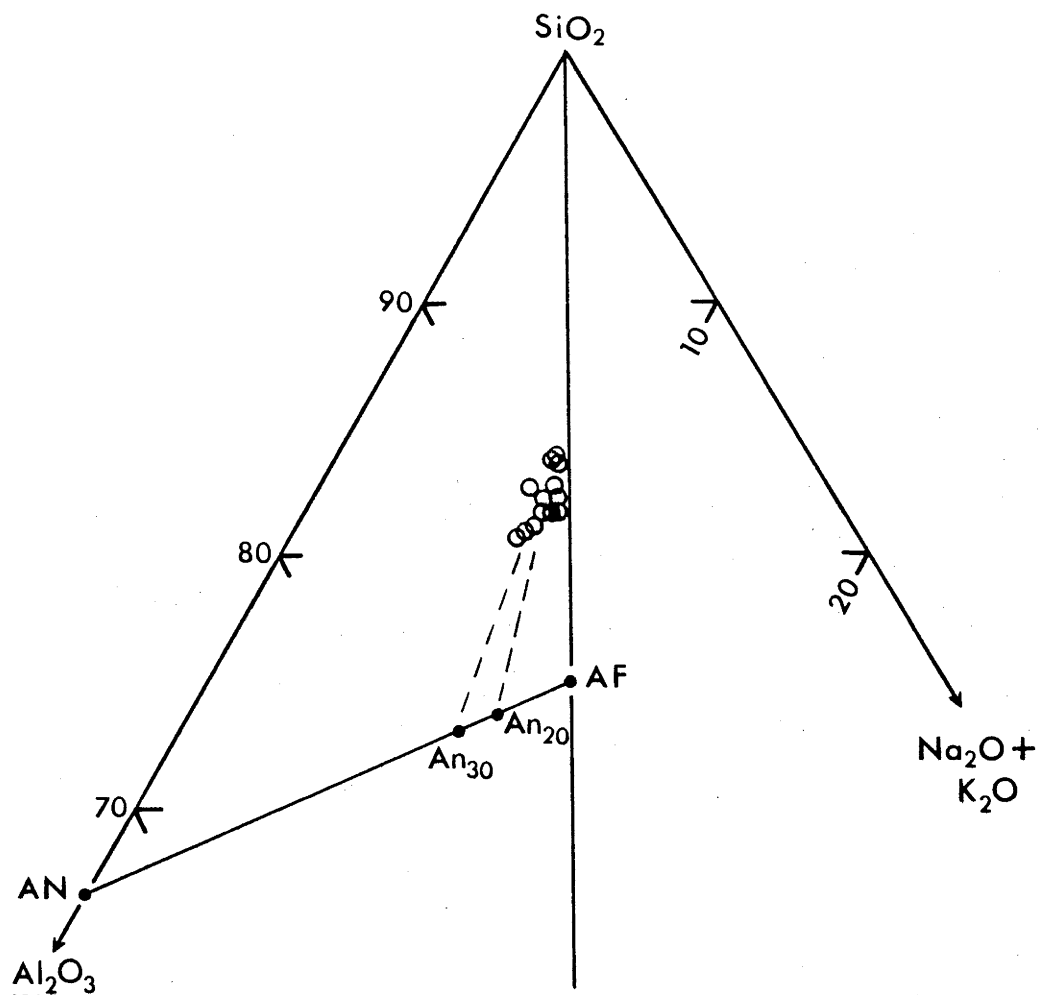
FIGURE 6-4: Part of the system SiO_2-Al_2O_3-Na_2O+K_2O (molecular percentages).

AN is anorthite, AF is alkali feldspar. The line connecting AN and AF represents the plagioclase solid solution series; the positions of two members of the series with possible genetic significance to the west Fergusson Islands are indicated.
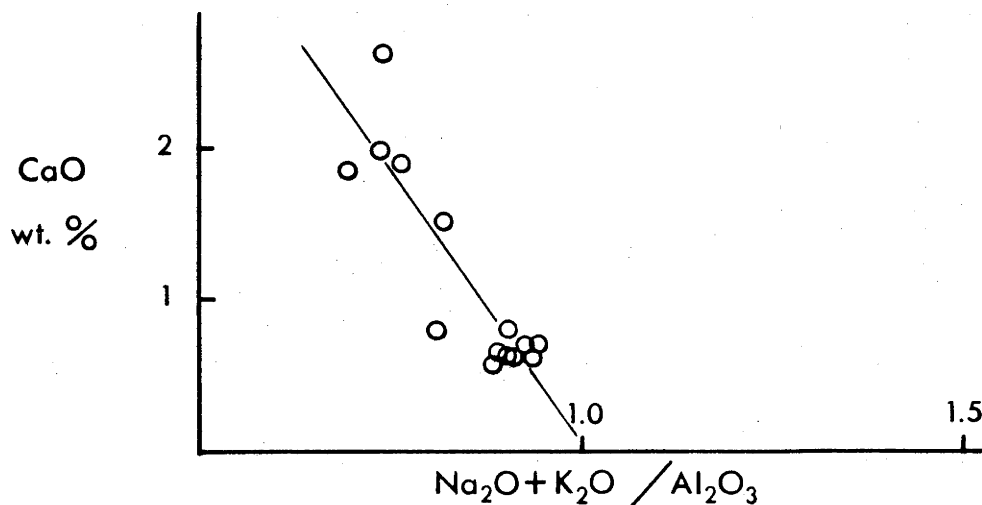
Weight percent CaO plotted against peralkalinity index [mol.% $(Na_2O$+$K_2O)/Al_2O_3$]. The line drawn through the points has a correlation coefficient of -89.

contents, a feature which suggests that plagioclase was not extensively involved in the melting process.

6-4   Discussion

The trace element abundance patterns observed in the rhyolite suite from the Moresby Strait area indicate a model of partial melting rather than of crystal fractionation from low-Si magma. This conclusion is based on REE abundance patterns, relatively high Sr contents and moderate K/Rb ratios but is also the preferred explanation for abundance patterns of elements which have been shown to have residual behaviour in some crystal fractionation processes.

Relationships within the quartz-feldspar system, and variation patterns of feldspathic elements show that the rhyolite compositions are close to a minimum melt composition and could have originated by melting of quartz, K-feldspar and a relatively small amount of plagioclase at comparatively low water pressures. Because the composition of initial melts are controlled by crystal-liquid equilibria near the eutectic within the granite-feldspar system (e.g. Tuttle and Bowen, 1958; Luth and others, 1964) physical conditions in the source region are constrained to pressures and temperatures at which the mineral assemblage quartz plus two feldspars is stable. Experimental work (e.g. Luth and others, 1964; Merrill and others, 1970; Stern and Wyllie, 1973; Figure 6-5) shows that because of this constraint liquids of rhyolitic composition cannot be generated at pressures greater than about 10-15 kb.

Above about 3 kb, melting within the temperature range 700-1200°C will be determined by the water content of the source region (figure 6-5). Water contents in the melt of 2-5 wt % bring the liquidus temperature for relatively low pressures within the range 750-900°C. These water contents are well below the estimated limit of solubility of water in melts of rhyolitic composition at pressures greater than a few kilobars (Stern and Wyllie, 1973; Brunham, 1975). The lower half of this temperature range at least, is within the range of temperatures attained during regional metamorphism (Turner 1968). The spatial association of rhyolites on west Fergusson Island with metamorphic rocks of amphibolite and granulite grade (Davies and Ives, 1965) shows that the temperatures close to those required for partial melting have been reached at high crustal levels. Given the presence of sufficiently high temperatures the major factor controlling the production of rhyolite magmas will be the presence of sufficient water in the source region.

FIGURE 6-5: Experimental rhyolite - water systems.
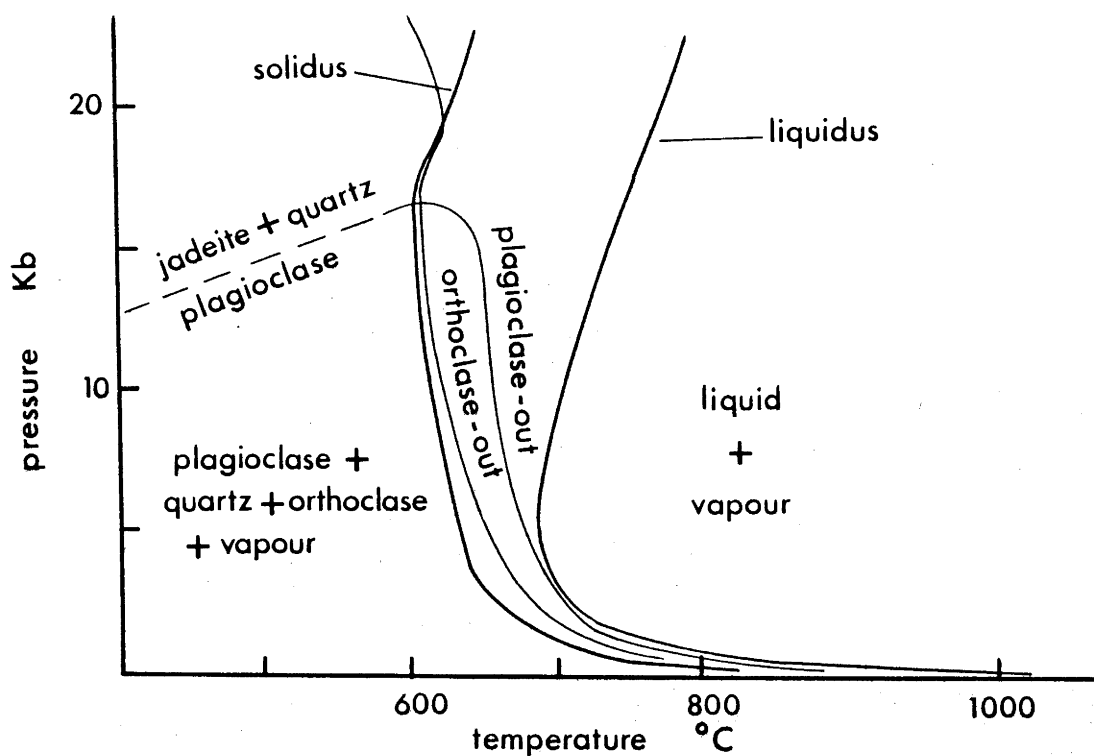
Simplified phase relationships for rhyolitic (granitic) compositions with excess water. (modified from Stern and others, 1975).
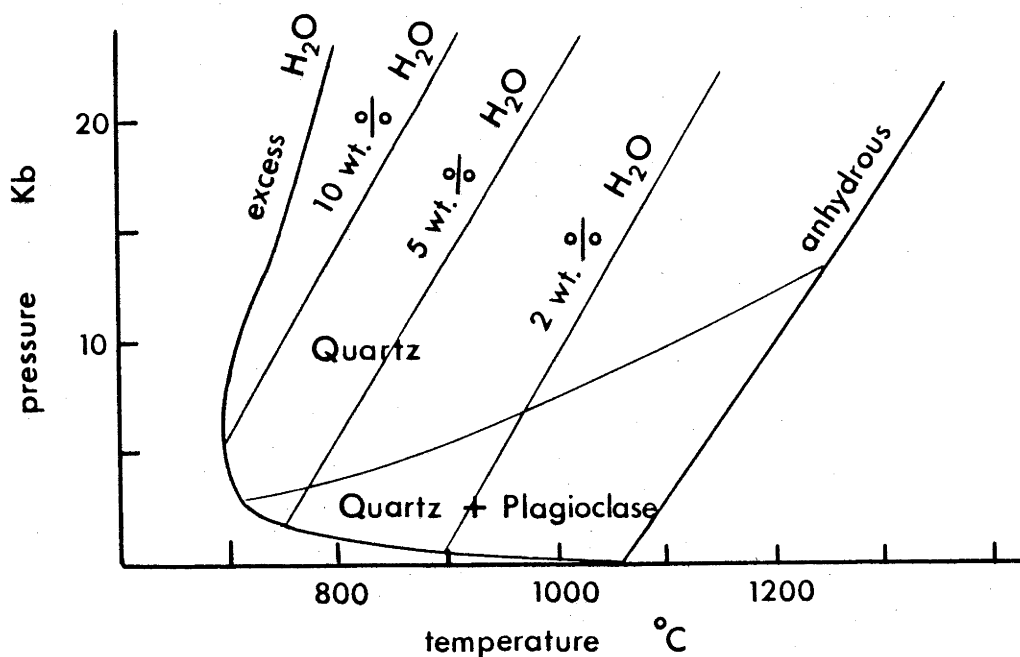
Contoured map of the water undersaturated liquidus surface for rhyolite showing liquidus and near liquidus minerals. (after Stern and others, 1975).

It was suggested that the west Fergusson Island rhyolites originated by partial melting involving only a small amount of plagioclase. Phase relationships for granitic compositions (Figure 6-5) show that if this is the case then melting temperatures required are only slightly above that of the solidus. The amount of melting of the source to produce the west Fergusson Island rhyolite composition would have been dependent on the K-feldspar (and K_2O) content of the source region.

Current models of crustal structure beneath the D'Entrecasteaux Islands (discussed in chapter 10) are extremely complex. Within constraints imposed by these models potential source materials for the west Fergusson Island rhyolites are either the former sediments making up the metamorphic cores of the islands or material of intermediate composition intruded into the base of the crust as part of the cycle of igneous activity represented by the andesitic rocks in the area. Because $^{87}Sr/^{86}Sr$ initial ratios in both the andesites and the rhyolites are comparable and because trace element abundances and ratios suggest a close relationship, the favoured alternative is that the rhyolites originated by partial melting of dioritic (andesitic) material at crustal pressures.

CHAPTER 7

ANDESITIC PETROGENESIS IN EASTERN PAPUA

Late Cenozoic tectonism in southeast Papua is extremely complex
and the relationship between tectonic events and the genesis of andesitic
rocks is more equivocal than it is in typical island arc situations.
The tectonic history modelled in chapter 10 is based at least in part on
the interpreted significance of andesitic volcanism in the area. The
interpretation rests on constraints which their chemical compositions
place on models for the origin of andesitic rocks in the light of
currently popular petrogenetic hypotheses. This chapter discusses
relevant aspects of the petrochemistry of the late Cenozoic andesitic
lavas described in Chapters 4 and 5 in relation to these petrogenetic
hypotheses.

7-1 Petrogenesis of Andesitic Rocks: A Review

Geochemical constraints, experimental studies and plate tectonic
models have led to the development of a consistent petrogenetic model
for a wide range of mantle derived basaltic compositions in both oceanic
and continental settings where the plate tectonic regime can be
described as diverging (e.g. D. Green, 1971; 1972). To a first approx-
imation variation in the compositions of these magmas is controlled by
the depth (pressure) and degree of melting of the source material which
is considered to be undepleted mantle containing minor (< 0.4%) water.
In fact, in view of evidence for fractionation events which preceed the
magma generative event (e.g. Sun and Hanson, 1975) and for heterogeneous
distribution of incompatible elements in the upper mantle (Kesson, 1973)
the notion that the typically alkaline rocks of diverging plate boundaries
represent very small degrees of partial melting of unfractionated
primitive mantle is probably an oversimplification. A model in which
the source of alkaline rocks is fractionated mantle relatively enriched
in incompatible elements appears more plausible and overcomes the
physical objection to removing very small amounts of melt from the
residuum. There is some evidence (e.g. Kesson and Price, 1972) that
amphibole is an accessory phase in the upper mantle source region of
alkaline rocks and that it plays a major role in determining their
chemical composition.

A primary assumption on which petrogenetic hypotheses have been
founded is that andesitic rocks are in some way significantly different

from those associated with converging plate boundaries and therefore require either a source or a process which is different from that which produced rocks of the other volcanic associations. In fact, as geochemical data accumulate, the uniqueness of andesitic rocks has become blurred and gaps in the compositional spectrum of volcanic rocks less clearly defined. Although there are clearly definable differences between andesites and oceanic tholeiites or between andesitic and alkaline rocks, the island arc tholeiites and the island arc alkaline rocks (shoshonites) largely complete the compositional spectrum.

Compared with tholeiitic rocks andesitic rocks are higher in K-type incompatible elements, have light enriched and heavy depleted REE patterns; Ba/Sr Rb/Sr and Th/U ratios are higher, Zr/Nb ratios are comparable and K/Rb ratios are lower. Characteristic features of andesitic rocks are low Ni and Cr, and high V/Ni ratios but data from eastern Papua show that this is not always the case. The high incompatible element content, including the relatively high K/Na ratios observed in some andesitic rocks can be matched in alkaline rocks but the alkaline rocks differ in having characteristically high TiO_2 contents and, although Zr content is comparable, Zr/Nb ratios are low. The main feature which sets island arc type volcanic rocks (andesitic and tholeiitic) apart from the tholeiitic and alkaline rocks of the continents and ocean basins is their relatively high SiO_2 mode. Both alkaline and tholeiitic rocks are characteristically basaltic and, although there is evidence for primary more Si-rich compositions (e.g. Green and others, 1974) Si-rich alkaline and tholeiitic rocks can generally be explained by low pressure fractionation. In contrast the volcanic rock associations of island arcs (including the island arc tholeiites) are dominated by intermediate rocks and andesitic suites with a SiO_2 mode of about 55% are typical.

Although it has been suggested that the particular features of andesitic rocks can be explained by fractional crystallisation under special conditions (e.g. Osborn, 1959) or by contamination with crustal rocks (e.g. Clark, 1960) this is not supported by trace element compositions (e.g. Taylor and others, 1969), isotopic ratios (e.g. Gill and Compston, 1973; Whitford, 1975) or by the relative abundance of rock types in andesitic associations. An important conclusion of recent work on volcanic rocks of the island arcs and active continental margins is the concept of a primary andesite magma.

If the assumption that the volcanic rocks which characterise

diverging plate boundaries represent the range of compositions which can
be derived from primitive (including fractionated) mantle is correct,
what is the significance of the apparently different andesitic association?
The active volcanoes associated with modern active converging plate
boundaries, recognised as either island arcs (e.g. Marianas, Tonga-
Kermadec) or active continental margins (e.g. the American Cordillera),
invariably erupt arc-tholeiitic or andesitic lavas. Although it is not
true to say that andesitic rocks are always associated with active
converging plate boundaries (recognised by the presence of Benioff zones)
andesitic rocks can generally be related to a geological environment
which includes past tectonic convergence. The available evidence indicates
that andesitic (and arc-tholeiitic) rocks represent the characteristic
magma type of converging plate boundaries and originate under pressure-
temperature conditions appropriate to the lower crust and upper mantle
from a source material which is evolved in terms of incompatible elements
and enriched in SiO_2 but which is isotopically relatively primitive.

The global distribution of andesitic rocks indicates a source
which is independent of the vagaries of regional geology. The most likely
source for andesitic rocks is primitive upper mantle material which has
been modified by a process unique to converging plate boundaries.

The role of subduction

Active andesitic arcs are characterised by inclined zones of
earthquake hypocenters (Benioff zones) which are systematically related
in space to the volcanoes of the arcs. The erupted lavas of many
volcanic arcs show systematic compositional variations (e.g. Sugimura,
1961; 1968) which have been correlated with depth to an underlying
Benioff zone (Dickinson and Hatherton, 1967; Dickinson, 1968; 1975).
Although this relationship is not always as close as these workers have
suggested (e.g. Johnson, 1976) it has been observed in many andesitic
arcs and has become an accepted generalisation. As a result modern
petrogenetic models for andesitic rocks are dominated by the concept
of subduction involving thrusting of basaltic oceanic crust beneath
the volcanic arc to depths at which an incompatible component is released
to trigger the production of andesite magma. Three groups of models are
currently popular.

1)   Direct melting of subducted oceanic crust. Direct melting of
subducted oceanic basalt has been proposed by T. Green and Ringwood (1968),

Jakes and White (1969; 1972), Fitton (1971) and Marsh and Carmichael (1974). In this model the range of island arc type magmas is explained by successively smaller amounts of melting in equilibrium with successively higher pressure mineral parageneses as the basaltic slab is thrust deeper into the mantle.

2)   Melting of modified mantle. Dehydration reactions in the subducted oceanic slab add water to the overlying wedge of mantle peridotite resulting in modification of the mineral assemblage and melting to produce andesite magmas (e.g. McBirney, 1969; Kushiro, 1973; Mysen, 1973).

3)   Multiple source hypotheses. Water and a melt rich in SiO_2 and incompatible elements produced by dehydration and melting of subducted oceanic crust modifies the overlying mantle. Subsequent melting of this material leads to the production of a range of andesitic magmas (e.g. Nicholls and Ringwood, 1973; Nicholls, 1974).

Discussion

If the magmas generated at the converging plate boundaries are primary melts of a subducted slab their compositions will be dominated by the low melting faction of that slab i.e. basaltic crust. Rocks of basaltic composition probably occur in eclogite facies mineral assemblages at pressures greater than 20-25 Kb the upper stability limit of amphibole (e.g. Lambert and Wyllie, 1970; Essene and others, 1970; Hill and Beottcher, 1970). If temperatures in this pressure range are less than $700^{o}C$ the amphibolite to eclogite transformation may be kinetically retarded (Boettcher, 1973) but at temperatures high enough to allow partial melting garnet is likely to be present. D. Green and Ringwood (1972) have shown that garnet will occur at relatively lower pressures in drier more undersaturated and less magnesian compositions.

Magmas which originate by direct partial melting of the down going slab are thus required by the nature of the thermal regime, in subduction zones (Oxburgh and Turcotte, 1970 ; Minear and Toksoz 1970) to have been in equilibrium with residual garnet. This require-ment places a severe constraint on possible REE patterns of the magmas especially considering the low amount of melting implied by the high content of incompatible elements in island arc rocks relative to the rocks forming oceanic crust. Because garnet is strongly enriched in heavy REE the complementary patterns of melts which have been in

equilibrium with garnet will show extreme depletion in these elements. Where such patterns have been recognised (Arth and Hanson, 1972; chapter 8) Yb abundances are typically less than chondritic abundances; this compares with typical andesitic abundances (Jakes and Gill, 1970; chapter 5) of 5 to 10 times chondritic.

The constraint that the REE patterns of derived melts must be complementary to those of garnet precludes direct partial melting of a down going slab as a general process for the origin of andesitic rocks. This conclusion was arrived at quantitatively by Gill (1974) who considered a range of trace element abundances in the light of the experimentally determined high pressure mineralogy of a 'typical' andesite.

A second constraint on direct partial melts of subducted oceanic basalt is placed by the high $^{87}Sr/^{86}Sr$ initial ratios of andesitic rocks relative to ocean floor basalt. Because the Rb contents of ocean floor basalt are extremely low the rate of evolution of the $^{87}Sr/^{86}Sr$ ratio is low. In direct partial melting of subducted basalt the $^{87}Sr/^{86}Sr$ ratios in the melt will be the same as those in the parental basalt and provided that the melt gains reasonably rapid access to the surface will be the same as those in the erupted magma. Relatively high $^{87}Sr/^{86}Sr$ ratios in island arc rocks imply unacceptably old subducted crust. Thus the strontium isotope data also argues against direct melting of oceanic crust (cf. Hedge and Lewis, 1971; Gill and Compston, 1973).

A third constraint which is relevant to andesitic rocks in eastern Papua and to typically high-K andesitic suites (Andean type of Jakes and White, 1972) is the high incompatible element content characteristic of these rocks. Direct melting of oceanic basalt could only produce high incompatible element contents if the degree of melting was unacceptably low. In the present context this is a qualitative observation but it is supported by the quantitative calculations of Gill (1974).

Although the relationship between andesitic volcanoes and an underlying Benioff zone argues for a genetic link between subducted oceanic crust and magma genesis it is clear that direct melting of this subducted material cannot account for the compositions of lavas erupted at converging plate boundaries. An acceptable alternative is that andesitic magmas are produced within mantle which has been modified by interaction with subducted material.

7-2   Toward a Petrogenetic Model

Crystal fractionation is traditionally a process which looms large in any discussion of the causes of variation in igneous rocks. If the strongly porphyritic nature of andesitic rocks is a true reflection of the state of the magma prior to solidification then some degree of fractionation of crystals and melt could be expected. However, because of the complex phenocryst assemblages which characterise andesitic rocks, such differentiation patterns are difficult to quantify. In general, because of the regional scale of sampling in eastern Papua it would be fortuitous if a particular group of samples represented a differentiation series but in some cases the observed patterns of variation can be modelled on such a process. Although it would be a fallacy to deny the possibility of crystal fractionation in the andesitic rocks from eastern Papua a basic tenet to the following discussion is that at least part of the observed chemical variation in the suite is primary and can be related to physical and chemical variations in the source region.

Andesitic rocks in eastern Papua are associated with mainly shallow, weak seismicity, there is no seismic evidence for subduction at the present time. Nevertheless because the compositions of the andesitic rocks are comparable to rocks in modern island arcs and continental margins which are associated with Benioff zones and by inference with subducted material it is consistent to suggest that subduction has also played a role in the origin of andesitic rocks in eastern Papua. The tectonic rationale for subduction in eastern Papua is discussed in Chapter 10; for the present discussion it is assumed that subduction under eastern Papua has acted to produce the source material for the late Cenozoic andesitic volcanism.

During subduction, thermal retardation of the downgoing slab of oceanic crust will allow the amphibolite to eclogite transition to take place below the solidus with the result that water will be released into the overlying mantle wedge. McBirney (1969), Kushiro (1973) and Mysen (1973) suggest that melting of the hydrous peridotite resulting from this process will produce andesitic magmas at depths of up to 80 km. The main problem with such a model is to explain the high incompatible element content and light enriched REE patterns typical of andesites. The experimental work of Nicholls and Ringwood (1972, 1973) and Nicholls (1974) has shown that a more likely product of partial melting of hydrous peridotite is an oversaturated tholeiitic magma which on fractionation could produce the island arc tholeiite association characterised by

relatively low incompatible element content and unfractionated REE patterns.

At depths greater than about 100 km the mineralogy of the subducted basaltic crust will be essentially quartz eclogite. When temperatures within this material exceed about $750^{\circ}C$ partial melting will occur producing high-Si melts (T. Green and Ringwood, 1968; Stern and Wyllie, 1973) which will contain most of the K-type, large and highly charged cation and light rare earth trace elements. Residual phases complementary to the partial melt will be mainly garnet and omphacite. Residual garnet will cause extreme depletion of heavy REE in the melt and preferential retention of Na in residual pyroxene will produce relatively high K/Na ratios. The nature of low melting phases (one or more of mica, sanidine, quartz, kyanite) and the amount of partial melting will control the minor compositional features of the melt.

That melts with the chemical characteristics predicted for partial melts of subducted oceanic basalt are virtually unknown in association with andesites indicates that they do not retain their distinctive composition as they rise through the overlying mantle wedge. Nicholls and Ringwood (1973) and Nicholls (1974) suggest that the Si-rich slab melts will rise into the overlying mantle wedge and will react to form garnet bearing pyroxenite. They argue that the existence of a body of relatively less dense material, aided by the presence of minor water, will initiate diapiric uprise of the garnet pyroxenite which will undergo partial melting to produce andesitic magmas.

Despite the common occurrence of garnet on the liquidus in experimental work on andesitic compositions (T. Green and Ringwood, 1968, T. Green, 1972; Stern and others, 1975) the REE patterns of almost all andesitic rocks preclude the existance of garnet as a residual phase in equilibrium with andesite magma. If the source of andesitic melts is a mixture of slab melt and primative mantle then this material has equilibrated at pressures less than the stability field of garnet (i.e. < 20 - 25 kb) prior to segregation of andesitic melts. At these pressures amphibole is likely to dominate the low melting fraction in the source and will influence the composition of partial melts both as a low melting phase and as a buffering phase. Because quartz will probably also be a low melting phase under these conditions, partial melts will be more Si-rich than partial melts involving amphibole bearing primary mantle (the alkaline rocks) but incompatible element contents and ratios will be comparable.

A major difference between the alkaline rocks of the continents and ocean basins, and andesitic rocks is their high TiO_2 and Nb content and low Zr/Nb ratios. In this respect andesitic rocks are comparable to the tholeiitic rocks of ocean basins. If high TiO_2 contents and low Zr/Nb ratios in alkaline rocks are due to direct involvement of a titaniferous amphibole such as kaersutite as suggested by Kesson and Price (1972) and if amphibole is also important in the source region of andesitic magmas what is the cause of the differences in Ti and Nb contents of the two magma types? Either the composition of the amphibole in andesitic sources is different from that found as inclusions in alkaline rocks, or andesitic magmas are buffered by a high Ti low Zr/Nb amphibole, or Ti and Nb are fractionated from the low melting component of the source by a refractory phase.

An alternative to reaction between slab melt and overlying mantle is the siutation in which the slab melt triggers melting in the mantle. Melts produced in this way will combine the characteristics of slab melt and minimum mantle melt and would probably have andesitic characteristics. This model offers more potential for production of Si-rich melts (andesitic) because SiO_2 will not be locked up in residual orthopyroxene resulting from reaction between siliceous melt and olivine. Slow migration toward the surface by such a melt would allow a zone refining (Harris, 1957) process which would further enrich the incompatible content of the melt but which would probably constrain the $Mg/(Mg+Fe^{2+})$ ratio to a value consistent with equilibrium with mantle ferromagnesian phases. Although andesitic rocks generally have $Mg/(Mg+Fe^{2+})$ ratios which are apparently so low as to preclude equilibrium with residual phases this is not the case with the east Papuan andesites but in view of Mysen's (1975) paper questioning the assumed Mg/Fe portion coefficient under mantle conditions low $Mg/(Mg+Fe^{2+})$ ratios may not be an important constraint.

Either of these models or perhaps a combination of the two offer an explanation for the observed chemical compositions of andesitic rocks and for their close association with converging plate boundaries. However the tectonic history for eastern Papua modelled in chapter 10 requires that the andesite source be in existence for a significant period of time after the subduction event. In view of this it is perhaps more likely that the source is a reaction product which undergoes partial melting at a later stage rather than a liquid-solid system lying dormant for an extended period.

7-3   Discussion

The model outlined in section 7-2 offers a process by which
incompatible element and Si-rich magmas can originate in an upper mantle
source which has been modified by interaction with subducted oceanic
crust. The characteristic variability of andesite associations can be
explained by variation in a number of parameters the most important of
which are the proportion of slab melt which has contributed to the
andesite source, the degree of melting in the source and the depth of
segregation. Because the source is essentially composed of two components,
variation in the relative proportions of either component can cause primary
heterogeneity in the source and can account for much of the variability
observed in andesitic rocks. Thus variation in Th/U and Rb/Sr or K/Rb
ratios among the andesitic rocks of eastern Papua are probably a reflection
of source heterogeneity rather than an indication of unusual and variable
residual phases.

The single feature which is most difficult to explain in the
compositions of the east Papuan andesites is the high Ni and Cr content,
this is an anomalous feature in relation to andesites (e.g. Taylor, 1969)
and to island arc type rocks generally. In any model involving melting
in equilibrium with,or fractionation of,olivine and orthopyroxene,derivative
melt compositions should show an antipathetic relationship between Ni and
Cr on the one hand and K-type incompatible elements on the other. It is
therefore surprising to find that apparently nonaccumulative high Ni
andesitic rocks in eastern Papua typically have relatively high K_2O contents.
This relationship suggests that there is another important factor which acts
to produce variability in the compositions of andesitic magmas in Papua.

Two component mixing

Chappell (1966) has suggested that the spectrum of compositions
observed within individual plutons of granite batholiths arises from the
mixing in varying proportions of source or residual source material with a
partial melt. A range of compositions is produced by varying degrees of
melting and by variable amounts of primary source or residuum being
included with the melt to form an intrusive magma. This two component
mixing model has provided a consistent hypothesis to explain the linear
correlation between the chemical compositions of cognate inclusions
(identified as residual source material) and whole rock granite compositions.

Two component mixing can explain several unusual features in

granitic rocks but recognition of the process has relied substantially on observed linear correlations between the various phases of individual plutons which, because they form a single body, are assumed to be cogenetic. The hypothesis is an interesting one which A.J.R. White (pers. comm.) has suggested could be extended to account for some of the unusual petrographic and chemical features of andesites. A major problem in recognising whether two component mixing has operated in a suite of volcanic rocks is the difficulty in establishing a cognetic relationship between lava flows especially in areas of relatively poor exposure such as Papua. However two features suggest that it may be an alternative to simple partial melting involving complete segregation of melt and residuum.

1)   In some andesites (e.g. Mount Victory, Jakes and Smith, 1970) amphibolite inclusions are common. These may be comparable to source inclusions in granitoids.

2)   Although many andesites do not contain inclusions they are character- ised by the presence of complexly zoned and commonly corroded feldspar phenocrysts, and also by clusters or clots of early formed crystals. One explanation for these is that they represent fragments of source material. Similarly the occurrence of complex phenocryst assemblages (hornblende, biotite, pyroxene, olivine, plagioclase) may also point to the inclusion of residual crystals from the source. Some of the syenites associated with the   high-K   volcanic rocks in southeastern Papua contain abundant inclusions of biotite bearing pyroxenite which by analogy with the granitoid model could represent source material.

A two component mixing model offers an explanation for the occurrence of high Ni and Cr andesitic rocks in eastern Papua. If the high content of these elements is related to inclusion of residual source material then the incompatible element content of the melt is independent of the Ni and Cr contents of the whole rock (melt plus some crystaline residuum). The fact that high Ni rocks are also high K rocks suggests that, possibly because of a higher volatile content or possibly because a smaller proportion of melt cannot segregate from the residuum as readily, relatively high K melts are more likely to carry residual crystals from the source. The close correlation between Ni and Cr in these rocks suggests that orthopyroxene or a mixture of olivine plus pyroxene form the most important included components and it is significant that the high Ni rocks are also those in which ferromagnesian crystal clusters are observed.

Two component mixing is not contamination of a melt by pre-existing

material it is a mixing of a partial melt with components of the
crystalline residuum with which it is in equilibrium. The process offers
a way in which chemical components that are normally antipathetic can
become correlated. The way in which two component mixing will produce
variations in a suite of magmas will clearly be very sensitive to the
residual mineralogy of the source and the depth of magma segregation.

The two component mixing model has two important implications.
Firstly, because the magmas so formed are a mixture of partial melt and
residual solid, arguements based on the assumption that they were at one
time entirely liquid are not valid. This may be important to crystallisation
experiments in which liquidus phases are assumed to represent residual
crystals in a partial melting process. Secondly the residual mineralogy
has an important control over the composition of a series of rocks not
only as a buffering residual phase but as a physical component of the
magma.

7-4   The Late Cenozoic Andesite Association

Miocene to Recent andesitic rocks in southeastern Papua form two
distinct volcanic belts referred to as the northern and southern volcanic
belts. The northern volcanic belt contains rock types ranging from
basalt to rhyolite but is dominated by andesite; the southern volcanic
belt contains mainly high-K basaltic rocks (trachybasalts). The chemistry
of the rocks in the two belts is comparable and they are together referred
to as the late Cenozoic andesite association, nevertheless there are
differences between rocks of the two belts which have undoubted genetic
significance.

The most important difference lies in the range of $^{87}Sr/^{86}Sr$
isotope ratios. In the northern belt the ratios are extremely constant
over a wide range of rock compositions and this must imply an isotopically
homogeneous source. In contrast the $^{87}Sr/^{86}Sr$ ratios over a range of
rock compositions in the southern volcanic belt show wide variation. To
be consistent with the proposed petrogenetic and tectonic models it is
suggested that the differences in the isotope ratios of rocks in the two
belts are related to differences in the source which can be traced to
the subduction event which initially produced an evolved source material.
The andesites are related to a source formed by mixing of the early break-
down products of eclogite mineralogy in the subducted slab and this will
probably include most of the quartz in the assemblage. At deeper levels
the melts given off the slab will be lower in Si and on interaction with
the overlying mantle will produce a source which is different from that

produced by interaction with an early slab melt. This model is one way in which a heterogeneous source can be produced by a continuous subduction process and it can explain the predominantly basaltic character of rocks in the southern volcanic belt. Further the $^{87}Sr/^{86}Sr$ ratios also show that Rb and by inference K-type imcompatible elements have not been homogeneously distributed in the source. It is suggested that at a level in the subduction zone below that at which the first quartz rich melt is given off the slab, the volume of melt produced is much lower and mixing of this melt with overlying mantle less complete.

The structural setting of the two belts is different. The northern belt is closely associated with ultramafic rocks marking a former collision zone between saiïc material (the Owen Stanley Metamorphics) and oceanic crust and upper mantle (the Papuan ultramafic belt). The southern volcanic belt overlies tholeiite submarine basalts thought to be related to sea floor spreading in the Coral Sea. This difference in setting is illustrated in Figure 7-1. It is suggested that differences in the structural setting may be a secondary cause of the differences between the northern and southern belts. Milsom and Smith (1975) have, on the basis of geophysical anomalies, suggested that intrusive rocks related to the volcanic rocks of the southern volcanic belt are underlain by masses of relatively dense material. If these masses represent diapirs of source material then the high-K basaltic rocks of the southern volcanic belt are possibly products of a moderate degree of melting of the source at comparatively shallow depths.

FIGURE 7-1: Structural setting of the late Cenozoic Andesitic
Volcanoes.
Generalised geological sections - not to scale.

Late Cenozoic andesitic magmas.

Tholeiitic basalts (related to Cenozoic sea floor spreading).

Metamorphic rocks.

Old oceanic crust (Papuan ultramafic belt)
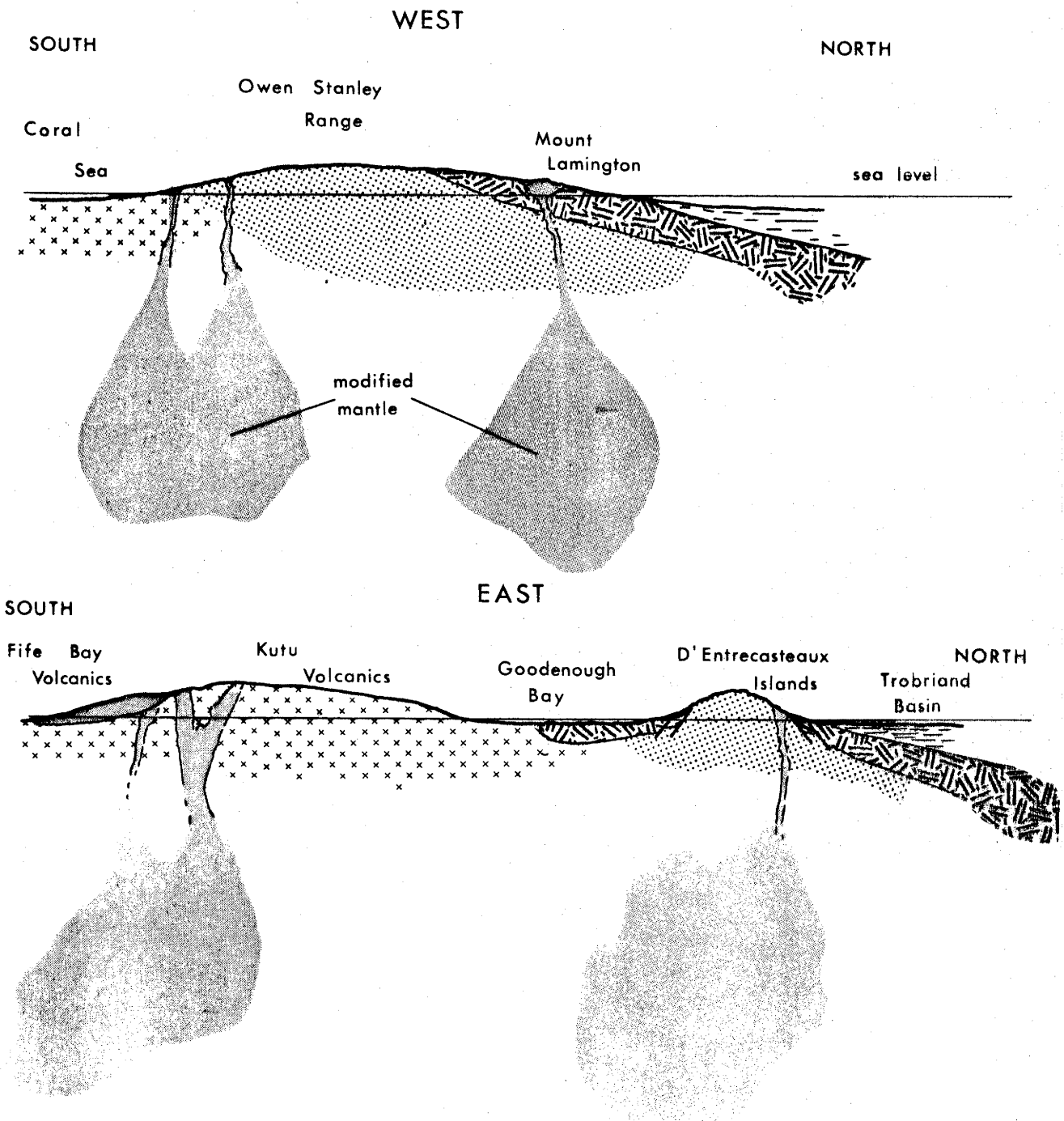
CHAPTER 8

QUATERNARY HIGH-K TRACHYTES IN THE LUSANCAY ISLANDS

The Lusancay Island group is part of a reef complex lying on a basement high (the Woodlark Rise) which extends along the southern margin of the Solomon Sea. Islands on this basement high are composed mainly of coral limestone although aeromagnetic data (CGG, 1973) indicate the presence of underlying basement. Only on Woodlark Island and on a few small islands in the Lusancay Group are volcanic rocks exposed; tholeiitic submarine basalts on Woodlark Island underlie a thick Miocene-Pliocene limestone sequence and represent old sea floor (chapter 3); in contrast, the rocks in the Lusancay Islands are high-potassium trachytes of Quaternary age.

North of the Lusancay Isalnds the sea floor slopes steeply into the Kiriwina Trough on the southern edge of the Solomon Sea basin; to the south is the Trobriand Island basin containing 4000 to 5000 m of late Tertiary and Quaternary sediments and which is characterised by very low heat flow values (Stoen and Garside, 1973). The volcanic islands themselves are small (less than 0.5 km^2) but the magnitude of their underlying aeromagnetic anomalies indicates that they are the surface expression of much larger volcanic piles.

Fine-grained strongly jointed volcanics form steep rocky knolls (presumably volcanic necks) on Nauria, Simsim and Wagalasa Islands; similar rocks are also found on the predominantly limestone islands Kawa, Boinagi and Ioana (Figure 8-1). Some of the outcrops on Nauria and Simsim islands contain abundant basaltic inclusions.

Whole rock K-Ar dating of specimens from Simsim and Wagalasa islands yielded ages of 1.1 and 1.08 m.y. respectively and a further whole rock K-Ar determination of 2.3 m.y. on a specimen from Simsim Island was supplied by Amoco, Australia (Smith, 1973a).

8-1   The High-K Trachytes

Typical specimens of the high-K trachyte from the Lusancay Islands are fine grained, medium to dark grey or less commonly red rocks. In thin section they are porphyritic and contain well-formed sparse to abundant phenocrysts of clinopyroxene (up to 0.5 mm across) and less commonly biotite, in a fine grained groundmass. Clinopyroxene phenocrysts are commonly zoned from colourless core to pale green or yellow brown rims. The groundmass in these rocks is made up of

FIGURE 8-1: The Lusancay Islands.
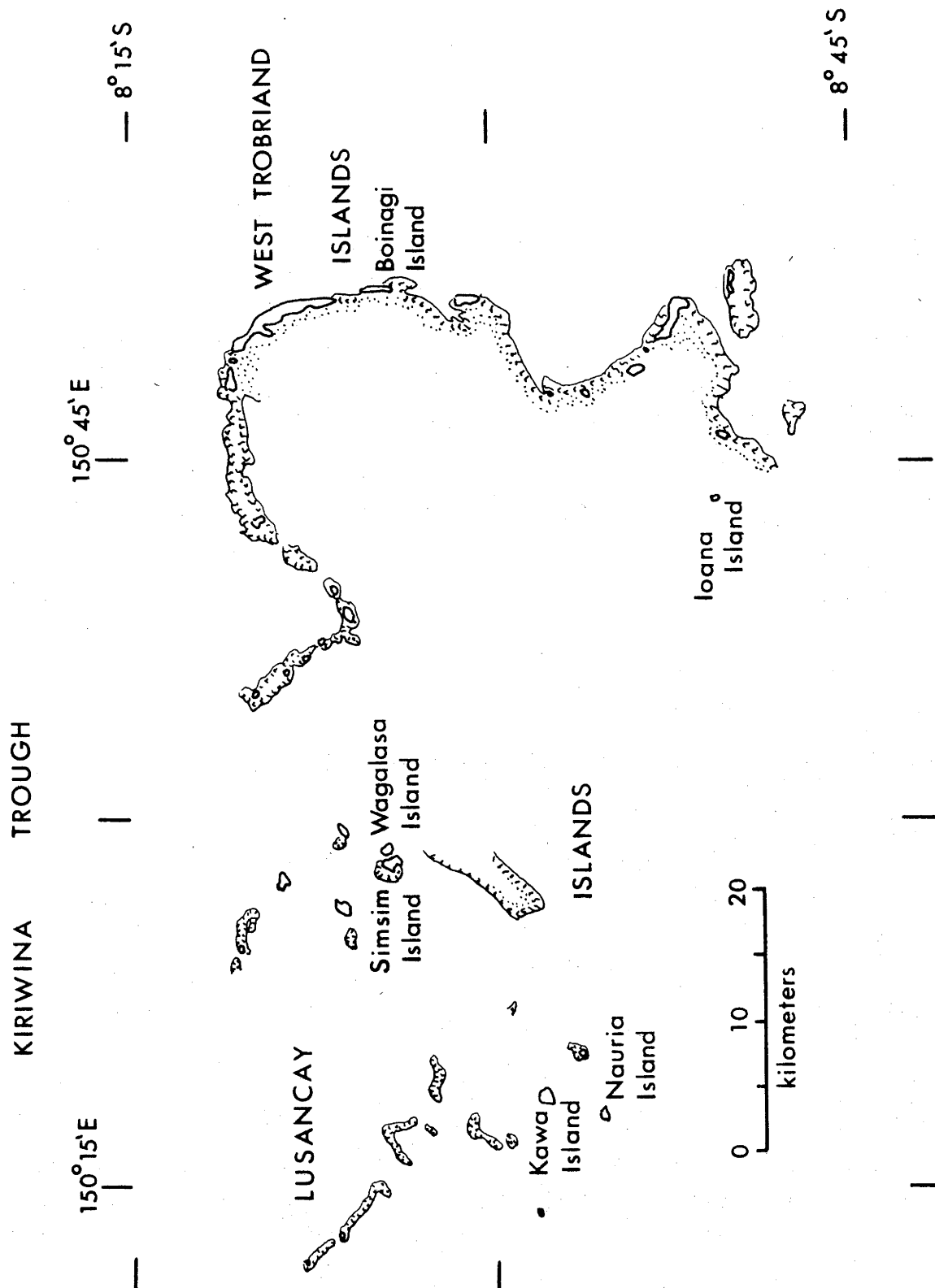
plagioclase and probably alkali feldspar (?sanidine) with minor iron-
titanium oxides. Biotite and small equant quartz crystals are present
in the groundmass of many of the specimens collected. Quartz also
occurs as sparse xenocrysts rimmed by an opaque reaction rim in a few
specimens.

Chemical composition

Major and trace element analyses of eleven trachytes are
presented in Table 8-1. The analysed rocks comprise four from
Wagalasa Island, five from Simsim Island, one from Nauria Island and
one collected from a large boulder on Kawa Island. These rocks are
moderately rich in SiO_2 (62 - 66%) and have high total alkali contents
(8 - 11%); for these reasons they are termed trachytes.

The main features of the major element compositions are high
K_2O/Na_2O and Fe_2O_3/FeO, and low Al_2O_3. Because of the high alkali
content the high degree of oxidation of these rocks is probably due
at least in part to the alkali-ferric iron effect noted by Carmichael
and Nicholls (1973). Generally fresh appearance and low water content
indicate that the rocks have not suffered secondary alteration.

Ba, Sr, Th and Zr are unusually abundant, U,Nb and Y are
low. Rb abundances are moderate to high (70 - 160 ppm) but so too
are the K/Rb ratios (390 - 600). La and Ce are strongly enriched
relative to chondritic abundances and the La/Y ratios indicate a
light/heavy REE enrichment pattern. V, Cr, Ni and particularly Cu are
high relative to average dacite abundances (Taylor, 1969) and are also
higher than typical trachyte abundances. Ba/Sr and Th/U ratios are
high, Zr/Nb ratios are unusually low.

For comparable SiO_2 content, specimens from Wagalasa Island
are lower in Al_2O_3, CaO and Na_2O than those from Simsim Island but
are higher in all other major elements and all measured trace elements
except Sr. The specimen from Nauria Island (699) is of this 'Wagalasa'
type and the specimen from Kawa Island (694) is of the 'Simsim' type.
If the outcrops on Wagalasa and Simsim Islands each represent
distinct volcanic necks these differences in chemical composition
between islands less than 0.5 km apart have no particular importance.
However, it is significant that rocks which can be chemically related
to one or other of these types are found on Nauria and Kawa Islands
20 km to the south west, indicating a wider distribution of two similar
but distinct magma types.

TABLE 8-1: HIGH-K TRACHYTES AND ACCIDENTAL INCLUSIONS FROM THE LUSANCAY ISLANDS

No.	'Sinsin' Type				High-k Trachytes			'Magalasa' Type						Inclusions		
wt%	689	690	691	692	693	694	695	696	697	698	699	700	701	702	744
SiO2	62.89	64.71	65.37	65.45	65.71	66.07	63.12	63.21	63.90	64.75	65.51	44.85	45.74	47.51	49.32
TiO2	.96	.93	.88	.87	.90	.77	1.01	1.04	1.02	1.01	.99	1.01	.89	.85	.83
Al2O3	15.11	14.73	14.64	14.83	15.03	14.39	13.97	13.81	13.72	13.97	14.92	17.00	19.12	17.34	17.50
Fe2O3	2.13	2.79	2.00	2.50	2.13	2.09	2.23	2.23	2.06	2.49	3.07	7.54	6.93	6.38	5.04
FeO	.84	.22	.72	.46	.53	.74	1.53	1.35	1.39	.99	.22	6.48	6.11	5.32	4.76
MnO	.03	.03	.03	.03	.03	.03	.04	.04	.04	.04	.03	.21	.13	.13	.17
MgO	1.76	1.56	1.54	1.21	1.10	1.65	2.29	2.32	2.39	2.09	.87	7.62	6.36	6.34	12.29
CaO	5.40	4.93	5.06	4.21	4.20	3.97	4.12	4.25	4.00	3.51	2.08	11.31	11.01	11.17	12.21
Na2O	2.97	2.90	3.06	3.11	2.59	3.07	2.42	2.25	2.23	2.50	2.63	1.21	1.17	1.67	1.41
K2O	5.28	5.60	5.48	5.29	5.48	5.99	6.85	7.08	7.22	7.33	7.98	.13	.13	.23	.36
P2O5	.43	.42	.38	.39	.39	.31	.45	.44	.42	.42	.45	.03	.04	.08	.17
S	.01	.02	nd	.02	.02	nd	.02	.02	.03	nd	nd	.02	.01	.01	.02
H2O+	.55	.48	.19	.44	.58	.42	.94	1.01	.74	.26	.47	1.29	.53	.53	.76
H2O-	.37	.19	.19	.62	.37	.14	.35	.24	.43	.32	.56	.93	.04	.48	.69
CO2	.24	.22	.11	.12	.10	.08	.26	.16	.03	.02	.04	.16	.11	.11	.35
Total	98.97	99.73	99.65	99.55	99.51	99.72	99.59	99.41	99.69	99.70	99.82	99.69	99.71	99.24	99.88
Fe2O3/FeO	2.54	12.68	2.78	5.43	4.68	2.82	1.46	1.65	1.48	2.52	13.95	1.26	1.33	1.38	1.06
Mg.No. (Fe2O3/F=0.2)	57.0	54.2	55.9	48.1	45.2	56.6	57.2	58.9	60.4	57.3	37.7	54.4	53.4	53.5	73.3
ppm Ba	2131	1957	1831	1830	1397	2131	2686	2767	2693	2657	2562	130	41	157	21
Rb	71	95	91	90	90	85	143	155	134	156	164	1	1	1	2
Sr	2652	2280	2405	2226	2177	1923	1566	1534	1513	1541	1726	255	244	245	197
Pb	27	26	20	26	26	26	29	28	23	23	26	8	1	9	8
Th	20	19	10	19	17	12	31	30	27	25	25	0	0	0	0
U	1	2	2	4	1	1	9	4	3	3	3	0	0	0	1
Zr	436	430	410	401	393	397	655	672	680	668	645	7	3	1	40
Nb	5	5	5	6	4	3	5	4	3	3	2	1	0	1	4
Y	5	6	6	5	5	7	8	7	1	11	7	6	5	8	19
La	69	67	63	60	63	58	70	71	70	71	90	0	0	2	4
Ce	100	103	98	93	96	80	102	90	105	92	134	15	21	28	34
Sc	6	6	6	6	6	5	10	9	9	9	9	47	41	44	58
V	117	105	114	104	111	110	167	176	169	156	108	546	436	430	226
Cr	23	27	21	43	23	18	163	78	79	64	43	22	43	74	909
Ni	23	23	23	22	20	22	40	39	41	39	29	50	40	59	164
Cu	42	191	127	159	153	77	136	156	200	176	205	473	352	2095	1885
Zn	56	55	56	62	53	48	64	63	60	63	52	131	89	131	126
Ga	26	24	24	25	25	24	27	27	25	25	25	16	19	16	13
Cl	nd	nd	709	nd	nd	1064	nd	nd	763	273	820	nd	nd	nd	nd
K/Rb	617.35	489.35	499.91	487.94	505.47	585.01	392.17	379.19	399.98	390.06	403.94	1079.19	1079.19	254.67	1494.27
Ba/Sr	.80	.86	.76	.82	.87	1.11	1.72	1.78	1.78	1.73	1.48	.51	.12	.64	.11
Th/U	20.00	9.50	5.00	4.75	17.00	12.00	3.44	7.50	9.00	8.33	8.33	-	-	-	-
Zr/Nb	87.20	86.00	82.00	66.83	98.25	132.33	131.00	168.00	227.33	222.67	322.50	7.00	-	7.00	10.00

nd = not determined.   Abundances < 0.5 ppm recorded as 0.

TABLE 8-2: HIGH-K TRACHYTES FROM THE LUSANCAY ISLANDS – CORRELATION MATRIX.

	SiO_2	TiO_2	Al_2O_3	Fe_2O_3	FeO	MnO	MgO	CaO	Na_2O	K_2O	P_2O_5	Rb	Ba	Sr	La	Ce	Y	Th	U	Zr	Nb	Zn	Cu	Ni	V	Cr	Ga	Pb
SiO_2	100																											
TiO_2	-72	100																										
Al_2O_3			100																									
Fe_2O_3			-82	100																								
FeO	-70	73	-92	-67	100																							
MnO	-61		-87		86	100																						
MgO	-73		-60		91	86	100																					
CaO								100																				
Na_2O		-86	79		-71	-90	-69		100																			
K_2O		67	-61			65		-78	-83	100																		
P_2O_5	-67	91							-63		100																	
Rb	-69	77	-68			76		-69	-89	96	60	100																
Ba		78	-76		68	85	65		-93	90			100															
Sr			82			-81			85	-88		-90	-87	100														
La		67						-67				76	73	70	100													
Ce				63							62				86	100												
Y			-68							69		69	70	-74			100											
Th	-68	89							-89	72	80	81	86	-72			69	100										
U																		69	100									
Zr		86	-74		61	85			-95	93	67	96	97	-87	67		69	88		100								
Nb								76		-76				60							100							
Zn	-61	66			63	75	62											68		70		100						
Cu				60								65											100					
Ni	-60	81	-88		79	97	79		-95	80		87	93	-86			71	85	63	95		70		100				
V	-68	74	-90		92	98	89		-91	62		72	85	-76				78		83				95	100			
Cr		73	-64		73	76	61		-68			60	67	-65				77		95				68	74	100		
Ga	-79	67			67	60			-60		64		61					78		65		63			71	67	100	
Pb																											66	100

Correlations less than 60 are omitted.

$^{87}Sr/^{86}Sr$ ratios in two of the Lusancay trachytes are .70457
(694) and .70432 (695)   (Appendix IV). These ratios are slightly
higher than those of andesitic rocks to the south (chapter 5) but are
within the range of both island arc rocks and ocean island rocks.

An inter-element correlation matrix for the trachytes is
presented in Table 8-2. Four well correlated (> 80) groups of elements
are recognised; namely, a K-group (K_2O, Rb, Ba), a Ti-group (TiO_2,
P_2O_5, Th Zr), a Mn-group (FeO, MnO, MgO, V, Ni) and a Sr-group (Al_2O_3,
Na_2O, Sr). A surprising feature of the trace element abundance pattern
is the generally good correlation between elements of the K, Ti and Mn
groups, and the strong negative correlation between most of the
elements in these groups and those of the Sr-group. This pattern,
linking as it does, typically ferromagnesian elements (the Mn-group)
with typically felsic elements (the K-group) places severe genetic
constraints on petrogenetic processes for the Lusancay rocks.

Rare earth elements (REE)

Complete REE data for three specimens are presented in
Table 8-3 and chondrite normalised abundances are plotted in Figure
8-2. A striking feature of the REE patterns is the smooth curve linking
moderately enriched light REE with strongly depleted heavy REE. All
three patterns show a small but distinct positive Eu anomaly (Eu/Eu*
1.1 to 1.3). The patterns are essentially parallel over most of
their length but Ho, Er and Yb are lower in specimen 689.

Light REE abundances in the Lusancay trachytes are higher
than in andesitic rocks (Jakes and Gill, 1970; chapter 5) but are close
to those in alkaline rocks (e.g. Price and Taylor, 1973). The heavy
REE are unusually low for igneous rocks and are among the lowest values
recorded for igneous rocks (Arth and Hanson, 1972).

Fractional crystallisation

It is possible that the two trachyte types in the Lusancay
Islands represent successive members of a crystal fractionation
series. The 'Wagalasa' type contains phenocrysts of clinopyroxene
and biotite and because of relatively higher contents of MgO Cr and
Ni could be considered the more primitive type. Fractionation of
clinopyroxene would account for the observed increase in Sr/Ca ratio, and
decrease of MgO content but not for the higher CaO of the 'Simsim' type;
fractionation of biotite could explain the lower K_2O, Ba, Rb and higher
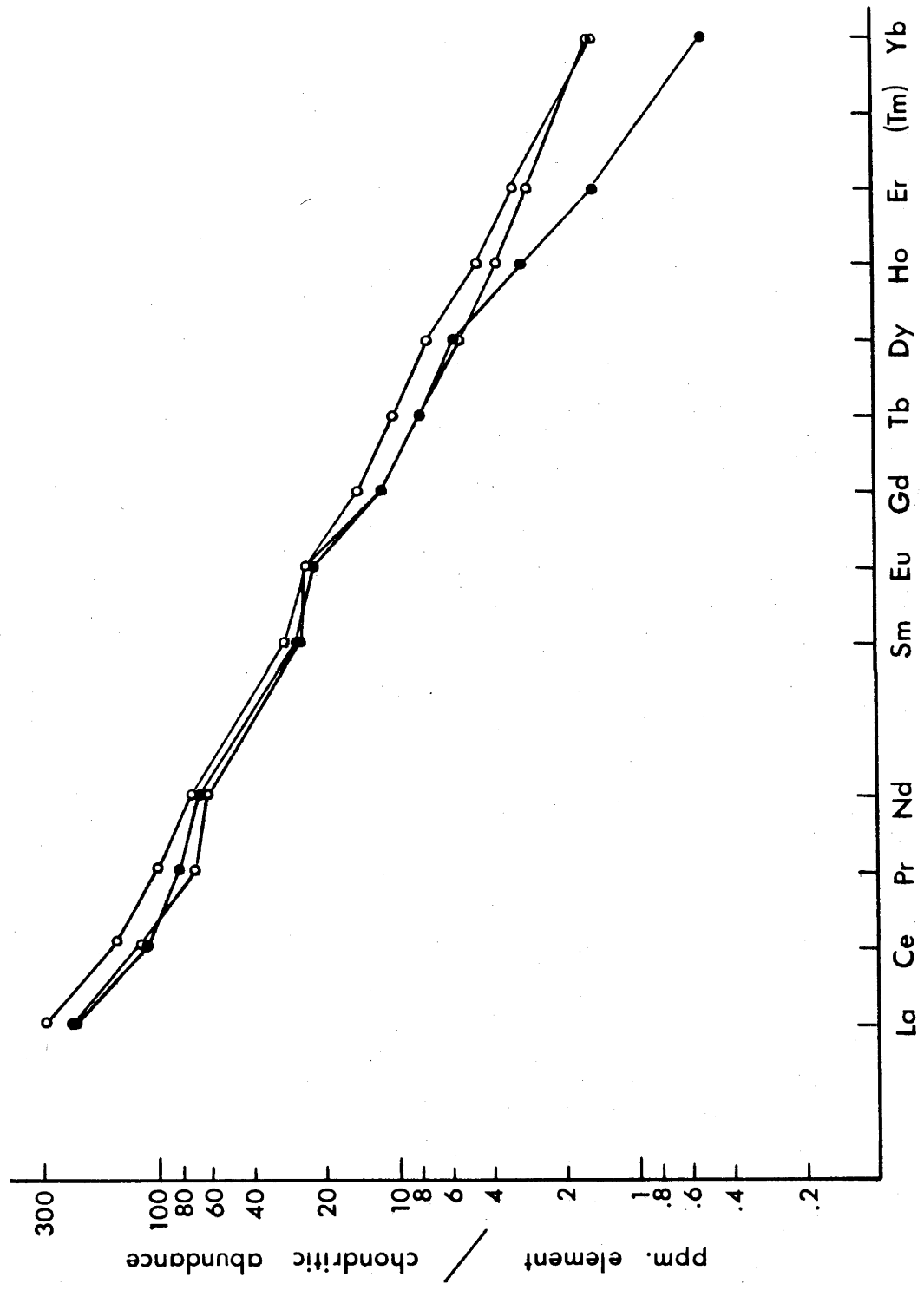
FIGURE 8-2: Chondrite normalised rare earth patterns in high-K trachytes from the Lusancay Islands. Numbers refer to analyses in Table 8-3.

TABLE 8-3:   RARE EARTH ELEMENT AND SOME OTHER TRACE ELEMENT
ABUNDANCES IN TRACHYTES FROM THE LUSANCAY ISLANDS.

	689	697	699
La	69	70	90
Ce	100	105	134
Pr	10.1	8.5	12.3
Nd	40.2	37.0	43.1
Sm	5.5	5.4	6.2
Eu	1.7	1.8	1.8
Gd	3.0	3.1[1]	3.8[1]
Tb	.39	.39[1]	.51
Dy	1.8	1.74[1]	2.3
Ho	.21	.28	.33
Er	.31	.59	.67
Yb	.10	.3	.29
La/Yb	690	233	310
Eu/Eu*	1.22	1.29	1.10
Cs	.46	1.2	.81
Pb	20.3	25.3	16.6
Th	12.1	19.5	18.3
U	1.6	3.3	2.6
Th/U	7.6	5.9	7.0
Hf	9.4	12.8	13.0
Zr/Hf	46.4	53.3	49.6

[1]estimated abundance. La and Ce determined by XRF

K/Rb in the "Simsim" type. What cannot be explained if the 'Simsim' type evolved by fractionation of clinopyroxene and biotite from the 'Wagalasa' type is the decrease in abundance of elements such as Th, U, Zr, La and Ce which because they cannot be linked to any early crystallising phase present in the rocks would be expected to behave as residual elements. Fractionation from 'Simsim' to 'Wagalasa' type is precluded because it would involve an increase in typically ferromagnesian elements which enter the early crystallising phases and could therefore be expected to become depleted. The lack of a close chemical relationship between the two trachyte types is embodied in the surprising correlation between K-type and Mn-type elements noted earlier.

8-2   Inclusions

Rounded gabbroic inclusions are abundant in some of the trachyte outcrops of Nauria, Simsim and Wagalasa Islands. The inclusions are medium to fine-grained (average grainsize 0.5 - 1.5 m) and typically consist of plagioclase (An_{65-70}) and clinopyroxene accompanied by minor iron-titanium oxides. The feldspar is commonly partly altered and pyroxenes are in most cases rimmed by fine grained semi-opaque reaction products. There is also some evidence of reaction with the host rock at the margins of the inclusions.

Analyses of four inclusions from Simsim and Wagalasa Islands are presented in Table 8-1. All are basaltic and are slightly over-saturated(Q 2-4, Fe_2O_3/FeO as measured) or slightly under-saturated (Q 0-9, Fe_2O_3/FeO = 0.2) depending on the assumed degree of oxidation. Chemical compositions are variable; in general Al_2O_3, total iron and CaO are high and TiO_2, Na_2O and K_2O are low. Specimen 744 differs from the others in being relatively lower in Al_2O_3 and higher in MgO. Rb, Th, U, Zr, Nb, La are very low in abundance, Ba is high for basaltic compositions. The Ce/Y ratio indicates a slightly fractionated light/heavy REE pattern; La is depleted relative to this pattern. V, Cr, Ni and Cr abundances are highly variable and in particular Cr is unusually abundant in two of the inclusions. Relatively higher abundances of MgO, Cr and Ni in specimen 744 suggest that it may be accumulative in origin.

Although not typical, the modal and normative mineralogy, high total iron and low K_2O and Rb contents in the inclusions are indicative of tholeiitic compositions. Anomalous features are the relatively high Al_2O_3 and Ba and low Na_2O. These inclusions are not

generally comparable to the tholeiitic basalts on the east Papuan
Mainland to the south (Kutu Volcanics) but do bear some resemblance
to tholeiitic submarine basalts exposed on Cape Vogel Peninsula
(Dabi Volcanics).

The chemical compositions of the inclusions show no
relationship to the compositions of the host trachytes and on this
basis they are interpreted as accidental inclusions picked up by the
trachyte magma during ascent to the surface. In this interpretation
an $^{87}Sr/^{86}Sr$ ratio of .70437 measured on one inclusion (744) and
which is closely comparable to values measured in the trachytes is
anomalous. It is possible that there has been equilibration of Sr
between host and inclusion but this appears unlikely in view of the
lack of recrystallisation in the inclusion. Further, $^{87}Sr/^{86}Sr$ ratios
measured on basaltic inclusions in comendite flows in the Dawson
Strait area (chapter 9; appendix IV) do not show any evidence of
equilibration on this scale.

The presence of oceanic tholeiites on Woodlark Island
(chapter 3) suggests a general model for the Woodlark Rise in which
late Cenozoic reefal deposits are underlain by former ocean floor. If
the $^{87}Sr/^{86}Sr$ ratio of inclusion 744 is not an artefact of equilibration
of the host trachyte then it implies that the Woodlark Rise beneath
the Lusancay Islands includes evolved basaltic material.

8-3   Origin of the Lusancay Trachytes

A singular feature of the chemical composition of the Lusancay
trachytes is the extremely low abundance of heavy REE. On the basis
of presently known distribution coefficients (Schnetzler and Philpotts,
1970; K. Harris pers. comm. 1976) this suggests that the trachyte
magma was in equilibrium with garnet at some stage during its formation.
Garnet becomes strongly enriched in heavy REE and slightly depleted in
light REE relative to a coexisting melt. Depending on its composition,
hornblende can also have the effect of depleting coexisting liquids in
heavy relative to light REE although not to the same extent as garnet
(Nagasawa and Schnetzler, 1971). Because hornblende accpets K in
preference to Rb (Philpotts and Schnetzler, 1970; Nagasawa and
Schnetzler, 1971) liquids in equilibrium with amphibole will have
relatively low K/Rb ratios so the high K/Rb ratios in the Lusancay
trachytes indicate that garnet rather than hornblende is responsible
for the heavy REE depletion. Although depleted heavy REE patterns

might have resulted by separation of zircon, apatite or sphene,
consideration of presently known distribution coefficients (Nagasawa,
1970; Nagasawa and Schnetzler, 1971) and relatively high abundances of Zr,
P_2O_5 and TiO_2 in the Lusancay trachytes shows that this was not a signif-
icant process.

Evidence for the influence of garnet in the petrogenesis of
the Lusancay trachytes suggests that they originated either by
fractionation of garnet at comparatively shallow depths or by partial
melting in equilibrium with garnet and hence by implication with an
eclogite mineral assemblage of depths greater than 20 - 25 Kb load
pressure equivalent (>60 km). Although garnet does crystallise at
crustal levels under conditions of decreasing water pressure according
to the reaction biotite + muscovite + quartz → almandine + sanidine +
H_2O garnet is not present in any of the trachytes, and the high Sr and Ba
and lack of negative Eu anomaly preclude feldspar as a fractioning
phase. This, and evidence discussed below favours an origin by partial
melting in equilibrium with an eclogite mineral assemblage.

An eclogite mineral assemblage consists essentially of garnet
plus clinopyroxene (omphacite) with accessory mica (phlogopite) and
possibly sanidine kyanite and quartz. As Gill (1974) has pointed out,
the subsolidus eclogite mineralogy will depend on pressure, bulk
composition, iron oxidation and the grossular content of the garnet;
increasing oxidation of iron favours kyanite rather than quartz and
as the grossular component of garnet increases the clinopyroxene/
garnet ratio decreases so that more quartz is formed. The presence
of water is probably also important since experimental work (T. Green,
1972; T Green and Ringwood, 1972) has shown that with melting in the
presence of a significant partial pressure of water vapour (P_{H_2O} = 3
to 5 kb) garnet becomes more important relative to clinopyroxene in
the residuum and the minimum melt is more siliceous.

A second feature of the Lusancay trachyte compositions is
the unusually high abundances of K, Ba, Rb and Sr. Those elements
have low bulk equilibrium distribution coefficients (< 1) with
garnet and clinopyroxene are incompatible in a residual eclogite
assemblage, and will be contained almost entirely within accessory
minerals such as phlogopite and sanidine. The abundance of these
elements in the melt will be controlled initially by the amount of

melting of accessory phases and, as melting continues, by the degree
of dilution caused by melting of residual clinopyroxene and garnet.
Only Sr with slightly higher equilibrium coefficients might be
modified by melt-residuum equilibria. At a stage in melting when
all of the accessory but none of the residual minerals have melted,
such incompatible elements will have their greatest abundance in the
melt equal to the total element content in the source rock. With
continued melting and consequent dilution the relative element concen-
tration will be reduced but interelement ratios will not.

Elements which could be expected to show similar behaviour
are Pb, Th, U, Zr and, in the absence of a residual oxide phase TiO_2
and V. Light REE should also display the same sort of behaviour and
light/heavy fractionation will be enhanced by equilibrium exchange
with garnet. Partition equilibrium with clinopyroxene will also fraction-
ate the light REE into the melt. The low heavy REE contents in the
Lusancay trachytes suggests that neither garnet or clinopyroxene have
contributed significantly to the melt.

The major K-bearing phase in an eclogite mineralogy within
the upper mantle is commonly considered to be a mica such as phlogopite
(e.g. Jakes and White, 1970). Melting of a mica phase will produce melts
which are high in potassium but which will have low K/Rb ratios (Jakes
and White, 1970); because Sr will not readily enter micas (Taylor,
1966) such melts will be characteristically low in Sr and will have
very high Ba/Sr ratios.

An alternative to mica as the major K-bearing phase has been
suggested by Marsh and Carmichael (1974) who argue that the experimentally
determined field of sanidine is compatible with its occurrence in an
eclogite mineral paragenesis. Because feldspars have a greater affinity
for K rather than Rb, melts to which sanidine has been a major contrib-
utor might be expected to have relatively high K/Rb ratios; Ba/Sr
ratios would be lower and would more closely reflect the bulk source
ratio. If this reasoning is approximately correct then the geochemistry
of the Lusancay trachytes is more compatible with melting involving
sanidine than with melting involving mica. The presence of positive
Eu anomalies in the chondrite normalised REE patterns also points to
melting involving feldspar.

Notwithstanding the known facts of mineral trace element
compositions there is a possibility that the element abundances and

ratios in the Lusancay trachytes bear no relationship to the low melting phases in the source. The arguments presented above presuppose that the incompatible content of a melt is controlled entirely by low melting mineral phases. However, if incompatible elements are held largely in intergranular films or lattice defects etc. their abundance will be controlled mainly by degree of melting and source rock abundances, and will provide no evidence of low melting phases in the primary mineral assemblage of the source.

The relatively high Cr and Ni content of the trachytes pose another problem. In a 'normal' mantle mineral assemblage partial melts will be in equilibrium with phases which strongly partition ferromagnesian elements so that for very low degrees of partial melting the melts will contain very small amounts of these elements. In contrast, using Shaw's (1970) equation for calculating trace element behaviour during equilibrium partial melting and using partition coefficients for clinopyroxene and garnet summarised by Gill (1974) it can be calculated that about 25 - 30% of the Cr and Ni contents of the source will enter the melt for small degrees of partial melting in equilibrium with eclogite. Thus it appears feasable to produce incompatible-rich melts with ferromagnesian element contents which are relatively high.

Conclusion

The REE patterns and high content of incompatible elements in the Lusancay trachytes is consistent with a small degree of partial melting involving accessory phases in equilibrium with residual clinopyroxene and garnet. High K/Na ratios are probably due in part to retention of Na in omphacitic clinopyroxene. The Al content of the trachytes is low in relation to other rock types of comparable Si content but is higher than might be expected for a melt in equilibrium with relatively high Al phases such as garnet and omphacitic clinopyroxene. This can be explained if kyanite or sanidine formed part of the accessory mineral assemblage of the parent eclogite so that a significant proportion of the Al in the source entered the melt.

Chemical composition of the source

In the tectonic setting of the Lusancay Islands one potential source material is basaltic oceanic crust which has been depressed to appropriate P-T conditions. If it is assumed that the incompatible element content of the trachytes represents the total content of the

source rock and that the source rock was unaltered oceanic basalt
then the observed enrichment in K (20 - 30 times), Sr (12 - 22
times) and particularly Ba (150 - 230 times) appear unacceptably
high even for extremely low degrees of partial melting (< 5%)
Although low degrees of partial melting of an altered oceanic
basalt composition in which K and Ba are increased, offers a
more acceptable solution Ba/Sr ratios of close to one (.8 - 1.8)
in the trachytes indicate that oceanic basalt is not a feasable
source material.

$^{87}Sr/^{86}Sr$ ratios show that the source composition was more
evolved than typical oceanic basalts; high Th/U and very high Zr/Nb
ratios indicate that the source had probably undergone at least one
fractionation event prior to the partial melting episode which
produced the Lusancay trachytes.

8-4   Discussion

The Lusancay trachytes are not clearly comparable with any
other igenous rock type described in the literature. Nevertheless
they closely resemble the predicted composition of partial melts
produced by a small degree of partial melting of quartz eclogite (T.
Green, 1972; T. Green and Ringwood, 1972). Such melts have been
interpreted as a part of the process by which andesitic magmas are
produced from subducted oceanic crust in spite of the fact that they
have yet to be recognised in the andesite associations of island arcs
and continental margins. Geochemical constraints indicate that the
Lusancay trachytes originated by partial melting in equilbirium with
eclogite but that the chemical composition of the parental rock was
more evolved in terms of incompatible element content and strontium
isotopes than oceanic basalt.

The indicated chemical characteristics of the source of the
Lusancay trachytes suggest that it may be comparable to the source of
andesitic rocks in the D'Entrecasteaux Islands to the south. If this
is the case then the differences in the chemical compositions between
the trachytes and the andesites provide an illustration of the
influence that the source mineralogy can have on the partial melting
products of the same source composition. Further, the distinctive
compositions of the Lusancay trachytes indicate that typically
andesitic rocks cannot represent partial melts of eclogite.

CHAPTER 9

A PERALKALINE RHYOLITE ASSOCIATION

9-1   Introduction

High-Si peralkaline volcanic rocks, unique among the volcanic
products of west Melanesia, occur in the Dawson Strait area of the
D'Entrecasteaux Islands. These rocks, which appear to form part of a
transitional basalt - peralkaline rhyolite series, overlap in time with
the Quaternary andesitic volcanism in the western D'Entrecasteaux Islands
and on the east Papuan mainland. Mildly peralkaline rhyolites (comendites)
are the characteristic high-Si rocks of oceanic islands (Baker, 1975),
and are also typically found on the continents in close association with
major rift structures such as the east African rift (Bailey and Macdonald,
1970). Peralkaline rhyolites are rare in the vicinity of andesitic arcs
and their occurrence in the D'Entrecasteaux Islands has important
implications for Quaternary tectonics in the area.

Published work on the comendites in the D'Entrecasteaux Islands
is limited to brief mention of their occurrence and chemical composition
in work dealing with patterns of regional volcanism in Papua New Guinea
(Morgan, 1966; Johnson and others, 1973); details of their field
occurrence are given in Smith (1973a).

Rhyolitic volcanic rocks form the southeastern part of Fergusson
Island, the neighbouring island of Dobu and a large part of Sanaroa
Island; small outcrops are also found on Oiaobe Island (Figure 9-1).
The rocks are predominantly fragmental. Fine to coarse unconsolidated
pumice ash predominates, but welded and non-welded ash-flow tuffs are
common in some areas, notably the area to the west and southwest of
Sebutuia Bay, much of Sanaroa Island and in basal coastal exposures on
Dobu Island. Lava forms less than five percent of the volcanic products
in the area and typically occurs as small steep-sided lava domes or
lobate lava flows indicating that the lava was viscous at the time of
eruption. Almost all of the lava is either glassy (obsidian) or
crystalline comendite. Boulders of trachyte found in the area southeast
of Mount Lamonai may be either lava blocks from ash deposits or remnants
of trachyte lava flows.

Davies and Ives (1965) described an outcrop of basalt in the
lower reaches of the Salamo River in southeastern Fergusson Island but
its relationship to the high-Si rocks in the area is unknown. Apart

FIGURE 9-1: Distribution of comendites and associated
rocks in the Dawson Strait area (shown
stippled). Numbers refer to analyses in Tables
9-4 and 9-6.

from this, basic and intermediate volcanic rocks have been found only as inclusions in comendite lava flows and as blocks in ash deposits.

There are three recognisable volcanic centres in the Dawson Strait area, namely Mount Lamonai and Mount Oiau, both on Fergusson Island, and Dobu Island. These cones are between 300 m and 500 m high; they are roughly aligned north-south. These three centres display youthful volcanic landforms suggesting eruptive activity in the very recent past. Taylor (in Davies, 1973) suggests on the basis of devitrification rates that Mount Oiau was last active about 600 years ago.

Small hills in the area between Mounts Lamonai and Oiau probably represent plugs or crater rim remnants from an earlier period of activity. A near-circular bay 5 km southeast of Mount Lamonai has the appearance of a former volcanic centre, and arcuate steep cliffs and thermal activity in the northern part of Numanuma Bay suggest that this is also an extinct eruptive centre. Similarly the volcanic rocks on northern Sanaroa Island show no development of volcanic landforms and are also representative of an earlier period of activity.

The lower age limit for volcanic activity in the Dawson Strait area is difficult to estimate. Because of the high rainfall, consequent high erosion rates and abundant unconsolidated pyroclastic rocks in the area the absence of volcanic landforms on the older volcanic rocks is not significant. Volcanic activity in the Dawson Strait area is thought to have extended from late Pleistocene through Holocene times.

9-2   Comendites

Petrography and Mineralogy

The crystalline comendites are light grey to green-grey porphyritic rocks; the glassy comendites are typical porphyritic obsidians. Individual lava flows are predominantly crystalline or predominantly glassy, a few with intercalations of crystalline and glassy material are banded. Phenocrysts are mainly anorthoclase (up to 16%) with subordinate (<1%) pyroxene and iron-titanium oxides; fayalitic olivine, less commonly amphibole or aenigmatite are present as phenocrysts in some specimens. The groundmass of the crystalline comendites is composed mainly of feldspar and irregular interstitial patches of quartz with fine grained aggregates of amphibole, clinopyroxene and iron-titanium oxides. Aenigmatite (confirmed by X-ray diffraction) is

present in the groundmass of many specimens but is typically fine grained and difficult to identify optically.

Anorthoclase

Anorthoclase forms large (0.5 - 2 mm) phenocrysts in all of the porphyritic comendites; chemical compositions of phenocrysts from 15 representative specimens are presented in Table 9-1. In general anorthoclase phenocrysts in the comendites are either slightly calcic ($An_{0.9 - 2}$) with compositions ranging from Or_{25} to Or_{30} or are essentially Ca free ($An_{0.5}$, typically 0) and have compositions ranging from Or_{30} to Or_{36} (Figure 9-2). The more sodic phenocrysts are uniquely found in comendites associated with the young eruptive centers Lamonai, Oiau and Dobu, whereas the more potassic anorthoclases form phenocrysts in comendites from the area of older volcanic activity to the north of Numanuma Bay. In the following sections it is convenient to refer to Oiau type, and Numanuma type comendites respectively.

A crystalline comendite from the northern shore of Sebutuia Bay (specimen 713) contains anorthoclase phenocyrsts which are markedly more sodic and calcic ($Or_{13.6}$, $An_{4.7}$) than those in any of the other comendites. This specimen is also unique in several other mineralogical features but is closely similar in chemical composition to Oiau type comendites. Anorthoclase phenocrysts from two comendite samples from Sanaroa Island are relatively potassic (Or_{33-35}) but are more calcic ($An_{.5}$) than those in all but one Numanuma type comendite (740).

The anorthoclase phenocrysts are typically zoned but core to rim variations observed in phenocrysts from any one specimen are less than 5.3 mol % Or. In general the compositional zoning observed increases as the silica content of the host rock increases. The same pattern of variation is observed between the composition of phenocrysts and coexisting microlites.

The feldspar compositions in twenty one comendites were estimated by X-ray diffraction using the three peak method of Wright (1968). In general the feldspar compositions of glassy specimens as determined by X-ray diffraction are comparable to the phenocryst compositions determined by electron microprobe. However, the feldspar compositions of the crystalline samples are in almost every case more sodic than the compositions of their phenocrysts. The diffraction work was carried out on a separated light (D<2.9) fraction of the crushed whole rock and may thus give a closer approximation to the bulk feldspar

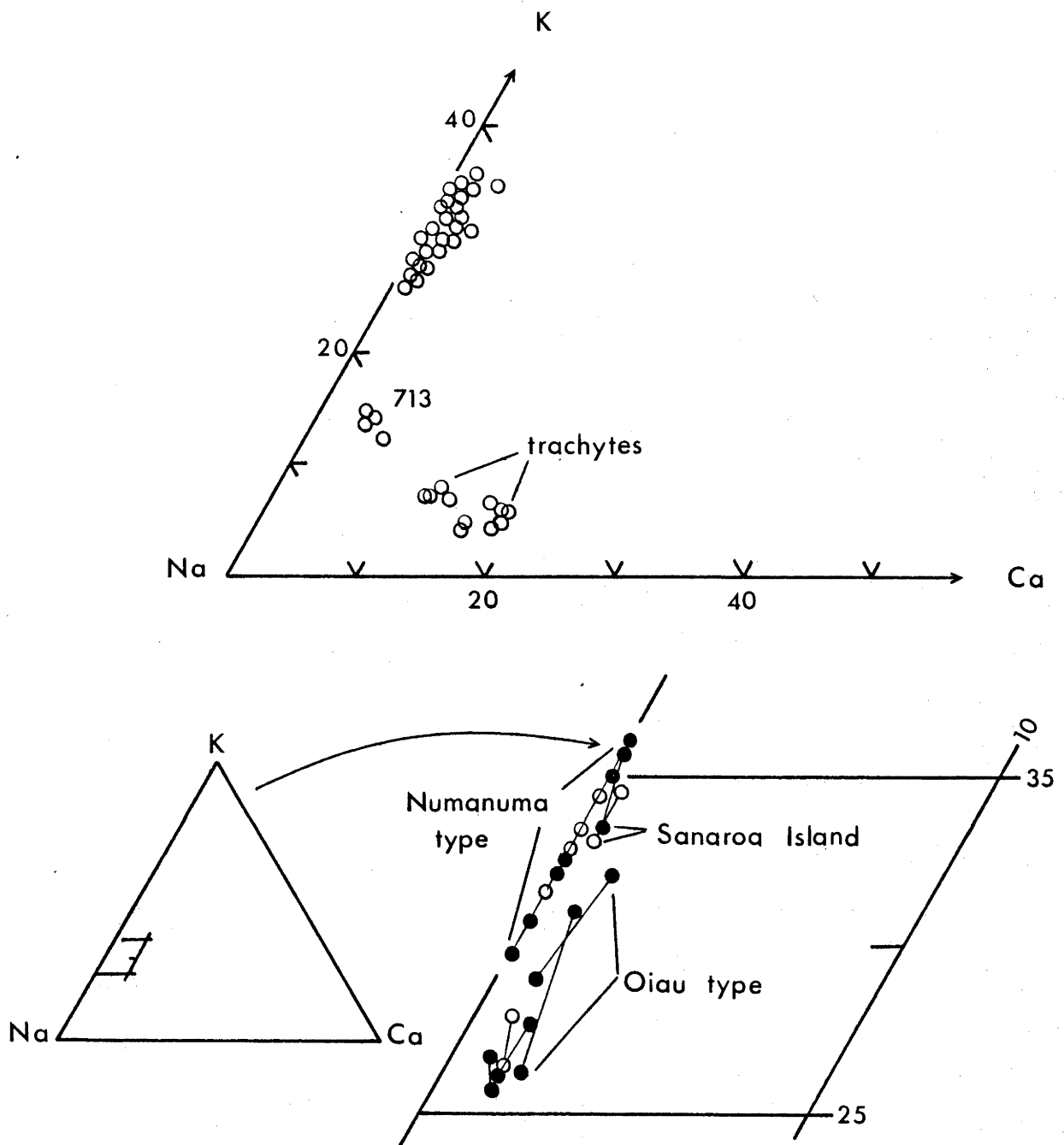FIGURE 9-2: Composition of feldspar phenocrysts and microlites in two trachytes and fifteen representative comendites from the Dawson Strait area.

In the upper part of the figure all analyses are plotted, in the lower part of the figure representative analyses (Table 9-1) are plotted; tie lines join coexisting core-rim and phenocryst-microlite pairs. Solid circles - glassy, open circles - crystalline specimens.

TABLE 9-1: REPRESENTATIVE ANALYSES OF FELDSPAR PHENOCRYSTS
IN THE DAWSON STRAIT COMENDITES

		OIAU TYPE COMENDITE												SANAROA ISLAND COMENDITES			
		Crystalline					Glassy							Crystalline		Glassy	
Rock No.		713	718		719		722		727		728	729		730		732	
		C	C	R	C	R	C	R	R	M	C	C	R	C	R	R	M
wt%	SiO$_2$	67.2	67.5	67.4	67.3	67.2	67.3	67.6	67.2	67.8	65.4	67.8	67.2	67.5	67.4	67.2	67.5
	Al$_2$O$_3$	20.1	19.4	19.5	19.6	19.4	19.5	19.3	19.5	18.6	21.4	19.1	19.2	19.0	19.1	18.9	19.0
	Fe$_2$O$_3$	.2	.2	.3	.2	.3	.2	.2	.3	.7	.4	.2	.3	.2	.2	.5	.4
	CaO	.9	.3	.2	.3	.2	.3	.3	.4	.2	.2	.2	.3	.1	.1	.1	.0
	Na$_2$O	9.3	8.1	7.9	8.2	8.2	8.2	7.9	8.1	7.5	7.9	7.8	7.5	7.5	7.3	7.5	7.2
	K$_2$O	2.3	4.5	4.7	4.4	4.6	4.5	4.7	4.5	5.2	4.7	4.9	5.5	5.7	5.9	5.8	5.9

Number of ions on the basis of 32 oxygens.

	Si	11.84	11.96	11.95	11.93	11.94	11.93	11.98	11.92	12.05	11.63	12.02	11.96	12.01	12.00	11.98	12.01
	Al	4.18	4.05	4.08	4.10	4.06	4.08	4.03	4.08	3.90	4.49	3.99	4.03	3.99	4.01	3.97	3.99
	Fe^{3+}	.03	.03	.04	.03	.04	.03	.03	.04	.09	.05	.03	.04	.03	.03	.07	.05
	Ca	.17	.06	.04	.06	.04	.06	.06	.08	.04	.04	.04	.06	.02	.02	.02	.0
	Na	3.18	2.78	2.72	2.82	2.82	2.82	2.72	2.79	2.58	2.72	2.68	2.59	2.59	2.52	2.59	2.48
	K	.52	1.02	1.06	.99	1.04	1.02	1.06	1.02	1.18	1.07	1.11	1.25	1.29	1.34	1.32	1.34
	Z	16.04	16.04	16.07	16.05	16.04	16.04	16.04	16.04	16.04	16.17	16.04	16.03	16.02	16.03	16.02	16.05
	X	3.86	3.86	3.82	3.87	3.90	3.89	3.83	3.88	3.80	3.83	3.83	3.89	3.90	3.88	3.93	3.82
mol%	Or	13.38	26.37	27.85	25.71	26.70	26.14	27.71	26.24	31.01	27.85	28.96	32.07	33.17	34.55	35.56	35.03
	Ab	82.22	72.15	71.15	72.82	72.33	72.40	70.80	71.80	67.98	71.15	70.05	66.46	66.34	64.96	65.95	64.97
	An	4.40	1.48	1.00	1.47	.97	1.46	1.49	1.96	1.00	1.00	.99	1.47	.49	.49	.49	.0
XRD % Or		32.6	6.8				29.8				30.0	34.5		15.8			

NUMANUMA TYPE COMENDITES

		Crystalline				Glassy							
Rock No.		734		737		739	740		742		743		
		C	R	C	R	C	C	M	C	R	C	R	
wt%	SiO$_2$	67.4	67.5	67.4	67.6	67.6	67.5	67.7	67.6	67.7	67.3	67.4	
	Al$_2$O$_3$	18.6	18.7	18.7	18.8	18.7	18.8	18.6	18.8	18.5	18.9	18.8	
	Fe$_2$O$_3$	.6	.5	.8	.7	.8	.6	.8	.6	.8	.9	.8	
	CaO	.0	.0	.0	.0	.0	.1	.0	.0	.0	.0	.0	
	Na$_2$O	7.6	7.4	7.7	7.4	7.5	7.4	7.0	7.9	7.5	7.7	7.0	
	K$_2$O	5.8	5.9	5.4	5.5	5.4	5.6	5.9	5.1	5.5	5.2	6.0	

Number of ions on the basis of 32 oxygens.

													FELDSPAR DETERMINATION BY XRD ONLY		
	Si	12.02	12.03	12.0	12.02	12.03	12.01	12.05	12.02	12.05	11.98	12.01			
	Al	3.91	3.93	3.93	3.94	3.92	3.95	3.90	3.94	3.88	3.97	3.95	Oiau type	No.	% Or
	Fe^{3+}	.08	.07	.11	.09	.11	.08	.11	.08	.11	.12	.11	crystalline	712	29.8
	Ca	.0	.0	.0	.0	.0	.02	.0	.0	.0	.0	.0		714	2.6
	Na	2.63	2.56	2.66	2.55	2.59	2.55	2.42	2.72	2.59	2.66	2.42	glassy	720	28.6
	K	1.32	1.34	1.23	1.25	1.23	1.27	1.34	1.16	1.25	1.18	1.36		721	29.5
														725	26.1
	Z	16.01	16.02	16.04	16.06	16.05	16.04	16.06	16.04	16.04	16.06	16.07			
	X	3.95	3.90	3.89	3.80	3.81	3.89	3.76	3.88	3.84	3.84	3.78	Sanaroa type		
mol%	Or	33.43	34.41	31.57	32.84	32.15	33.08	35.67	29.81	32.55	30.76	36.06	glassy	731	41.6
	Ab	66.57	65.59	68.43	67.16	67.85	66.45	64.33	70.19	67.45	69.24	63.94	Numanuma type		
	An	.0	.0	.0	.0	.0	.96	.0	.0	.0	.0	.0	crystalline	736	2.2
XRD % Or		12.0		8.4		38.1	45.9		36.6		31.8		glassy	738	34.2
														741	40.1

analyses by electron microprobe, Fe determined as FeO, all analyses normalised to 100%.
C - phenocryst core, R - phenocryst rim, M - microlite.

composition of the rock than do phenocryst or coexisting microlite
analyses. The discrepancy between the diffraction and microprobe
results suggests that the groundmass feldspars in the crystalline
comendites are more sodic than their coexisting phenocrysts despite
the fact that zoning in the phenocrysts is from relatively sodic
core to more potassic rim.

Ferromagnesian assemblages

Ferromagnesian phenocrysts are present in all of the porphyritic
comendites although they are generally small (<.5 mm across) and sparse
(<.5 vol %). Clinopyroxene phenocrysts are present in almost all of the
comendites and are typically accompanied by either iron-rich olivine or
amphibole. Only in specimen 713 from the northern side of Sebutuia Bay,
have olivine phenocrysts been observed to coexist with amphibole pheno-
crysts; this specimen is also unique in that the coexisting pyroxene
phenocrysts are ferrohypersthene.

Clinopyroxene phenocrysts from twelve representative comendites
(Table 9-2) show a compositional range from ferro-augite to sodic ferro-
hedenbergite to (in one specimen, 734) aegirine. The small degree of
compositional zoning within individual phenocrysts and between phenocryst
and coexisting microlite is toward enrichment in Fe^{2+} relative to Mg and
Fe^{3+} relative to Fe^{2+}; Ca is generally slightly enriched in phenocryst
rims and coexisting microlites but this is not always so. The pyroxene
compositions from Numanuma and Oiau type comendites fall into distinct
fields (Figure 9-3) although taken as a whole they define a trend which
lies close to the pyroxene crystallisation path described for the Sakhalin
alkaline province (Yagi, 1953). Increase in silica content of the host
rock is correlated with an increase in the Fe^{2+}/Mg and $(Na + Fe^{3+})/Fe^{2+}$
ratios and to a lesser extent with increase in Ca content in the pheno-
crysts. There is a break in the range of pyroxene phenocryst compositions
between the sodic ferrohedenbergite found in most of the Numanuma type
comendites and the aegirine of specimen 734 which roughly corresponds to
the miscibility gap between sodic diopside-hedenbergite and aegirine-
rich pyroxenes suggested by Aoki (1964) although there is some overlap
of Numanuma type pyroxene compositions into the immiscible field. The
existence of this gap has been subsequently questioned by Yagi (1966).

The extent of acmite enrichment in clinopyroxenes is controlled
by the oxygen fugacity of the magma. Crystallisation under conditions of
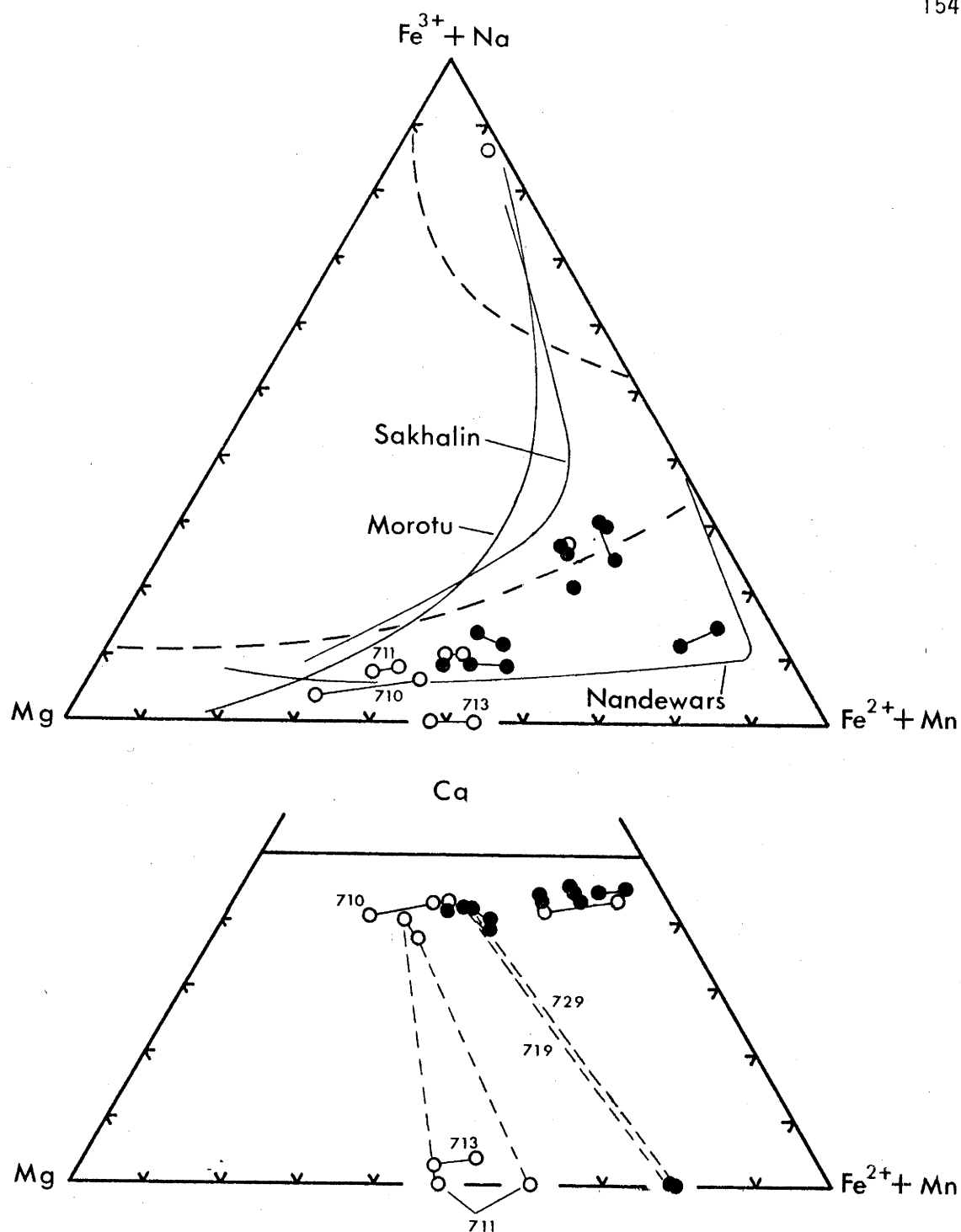
FIGURE 9-3: Composition of pyroxene and olivine phenocrysts in trachytes and representative comendites from the Dawson Strait area.

The upper part of the figure compares the pyroxene compositions with pyroxene crystallisation paths from Sakhalin (Yagi, 1953), Morotu (Yagi, 1966) and Nandewar Volcano (Abbott, 1969); the miscibility gap proposed by Aoki (1964) is defined by the dashed line.
The lower part of the figure shows Ca, Mg, Fe+Mn variation among the pyroxenes and coexisting olivines.

Solid tie lines join core-rim pairs of zoned crystals, dashed tie lines join pyroxene with coexisting olivine crystals. Solid circles - glassy, open circles - crystalline comendites

TABLE 9-2: REPRESENTATIVE ANALYSES OF FEROMAGNESIAN PHENOCRYSTS
IN THE DAWSON STRAIT COMENDITES

PYROXENES

		OIAU TYPE									SANAROA TYPE		NUMANUMA TYPE			
Rock No.	713		718		719		727	728	729		732		734	737	739	
	C	M	C	R	C	M	C	C	C	R	C	R	C	C	C	R
SiO_2	51.8	50.8	51.7	51.7	50.8	50.5	51.5	51.5	51.5	51.1	49.0	48.7	52.0	50.1	50.5	50.6
TiO_2	.2	.2	.0	.0	.2	.2	.2	.2	.2	.0	.3	.3	.8	.4	.1	.3
Al_2O_3	.0	.3	.4	.6	.4	.5	.4	.4	.3	.2	.2	.1	.4	.4	.3	.2
FeO	27.0	29.2	17.4	18.3	19.4	21.4	17.5	17.4	18.2	20.5	26.8	28.2	30.7	24.7	24.1	23.8
MnO	2.0	2.4	1.1	1.1	1.3	1.3	1.2	1.3	1.4	1.4	1.3	1.5	.5	1.3	1.2	1.2
MgO	17.6	15.2	9.4	8.9	8.4	8.1	9.7	9.7	8.8	8.0	2.6	1.4	.5	4.7	4.6	4.6
CaO	1.4	1.9	19.2	18.6	18.4	17.0	18.8	18.8	18.9	18.1	18.9	18.7	4.6	16.1	17.1	17.1
Na_2O	.0	.0	.8	.8	1.1	1.0	.7	.7	.7	.7	.9	1.1	10.5	2.3	2.1	2.2

Number of ions on the basis of 6 oxygens.

Si	1.99	1.98	2.00	2.01	1.99	1.99	2.00	1.99	2.00	2.01	2.00	2.00	2.11	2.01	2.02	2.02
Ti	.01	.01	.0	.0	.01	.01	.01	.01	.01	.0	.01	.01	.02	.02	.0	.01
Al	.0	.01	.02	.03	.02	.02	.01	.02	.01	.01	.01	.0	.02	.02	.01	.01
Fe^{3+}	.0	.0	.06	.06	.08	.08	.05	.05	.05	.05	.07	.09	.83	.18	.16	.17
Fe^{2+}	.87	.95	.50	.53	.55	.63	.52	.51	.54	.62	.84	.88	.22	.65	.64	.62
Mn	.07	.08	.04	.04	.04	.04	.04	.04	.05	.05	.04	.05	.02	.04	.04	.04
Mg	1.01	.89	.54	.51	.49	.48	.56	.56	.51	.47	.16	.09	.03	.28	.27	.27
Ca	.06	.08	.80	.77	.77	.72	.78	.78	.79	.76	.82	.82	.20	.69	.73	.73
Na	.0	.0	.06	.06	.08	.08	.05	.05	.05	.05	.07	.09	.83	.18	.16	.17
mol % Di	2.9	4.0	39.9	39.1	38.1	35.5	39.0	39.0	39.6	38.0	41.0	40.8	9.5	34.2	36.3	36.4
En	50.4	44.3	27.1	26.0	24.2	23.6	28.0	28.0	25.6	23.4	7.8	4.2	1.4	13.9	13.6	13.6
Fs	46.7	51.7	27.0	28.8	29.4	33.3	28.0	27.7	29.4	33.3	44.1	46.3	11.0	34.3	33.9	33.1
Ac			6.0	6.1	8.3	7.6	5.0	5.3	5.3	5.3	7.1	8.7	78.1	17.7	16.2	16.9

PYROXENES					OLIVINES	
	NUMANUMA TYPE					
Rock No.	740	742	743		719	729
	R	C	C	R		
SiO_2	50.0	49.9	49.9	49.5	31.3	30.4
TiO_2	.2	.3	.2	.3		
Al_2O_3	.2	.1	.5	.7		
FeO	24.4	26.0	25.9	26.6	57.0	57.3
MnO	1.4	1.0	.9	1.2	3.0	3.3
MgO	5.0	3.3	3.2	3.1	8.5	8.8
CaO	17.1	17.4	16.9	16.1	.2	.2
Na_2O	1.7	2.0	2.5	2.5		

Number of ions on basis of 6 oxygens and 4 oxygens.

Si	2.00	2.02	2.01	2.00	1.00	.97
Ti	.01	.01	.01	.01		
Al	.01	.0	.02	.03		
Fe^{3+}	.13	.16	.20	.20		
Fe^{2+}	.69	.72	.68	.70	1.52	1.54
Mn	.05	.03	.03	.04	.08	.09
Mg	.30	.20	.19	.19	.40	.42
Ca	.73	.75	.73	.70	.01	.01
Na	.73	.16	.20	.20		
mol % Di	36.2	37.3	36.1	34.5		
En	14.7	9.8	9.5	9.2		
Fs	36.1	37.4	35.0	36.8		
Ac	13.0	15.5	19.3	19.4		
Fa					79.9	79.5

AMPHIBOLES						AENIGMATITE
Rock No.	713	718		734		739	737
		C	R	C	R		
SiO_2	50.6	49.0	49.8	46.6	50.2	46.7	41.0
TiO_2	1.2	4.0	.8	2.0	.8	2.4	7.5
Al_2O_3	1.6	.7	.9	2.2	.2	1.6	.6
FeO	19.5	32.7	32.6	27.7	27.2	26.9	42.2
MnO	.8	1.0	1.2	.8	1.0	1.0	1.2
MgO	11.4	.9	2.1	6.7	1.6	5.4	.7
CaO	6.5	2.5	1.7	6.2	12.1	5.4	.2
Na_2O	5.0	7.1	7.2	5.5	5.7	4.8	7.1
K_2O	.9	1.2	1.2	1.0	.1	1.0	.1

Analyses by electron microprobe. Fe determined as FeO.
Fe^{3+} in pyroxene estimated from Na content. C - phenocryst
core, R - phenocryst rim, M - microlite.

increasing and high oxygen fugacities yields clinopyroxene trends from
augite through sodic augite and aegirine-augite to aegirine as
illustrated by the Sakhalin (Yagi, 1953) and Morotu (Yagi, 1966)
pyroxene trends. Crystallisation under lower oxygen fugacities will
produce trends dominated by $Fe^{2+}/Fe^{2+} + Mg$ variations at the expense
of enrichment in acmite as in the Nandewar series (Abbott, 1969). The
Dawson Strait pyroxenes display a trend intermediate between the
Sakhalin-Morotu and Nandewar trends (Figure 9-3) although enrichment
in the acmite component of Numanuma type pyroxenes suggests that these
crystallised under conditions of relatively higher oxygen fugacity.
Variation in the oxygen fugacity during crystallisation may explain
why pyroxene phenocrysts from one Sanaroa Island comendite (732) plot
away from the Oiau type - Numanuma type trend and closer to the Nandewar
trend.

Orthopyroxene phenocrysts in specimen 713 are zoned from
En_{50} to En_{44}. They are typically surrounded by a brown alteration
zone but as they are evenly distributed throughout the rock there is no
reason to believe that they have not crystallised as early crystals from
a liquid with approximately the analysed whole rock composition. Marginal
alteration of these early formed crystals may have taken place in response
to a change in oxygen fugacity in the crystallising magma.

Iron-rich olivine occurs as rare (< 1 vol %) phenocrysts in
many of the glassy comendites but is uncommon in crystalline specimens.
Analyses of olivine phenocrysts from two Oiau type glassy comendites
have compositions of $Fa_{79.5}$ and $Fa_{79.9}$ (Table 9-2).

Amphibole is present as sparse phenocrysts in crystalline
comendites but is rare in glassy specimens. It does not occur as pheno-
crysts coexisting with olivine but is found as a groundmass phase in
specimens containing olivine phenocrysts. Phenocrystic and groundmass
amphiboles are typically pleochroic in shades of brown, brown to green,
or blue green to blue; groundmass amphiboles may also be pleochroic
in shales of blue. Analyses of amphibole phenocrysts from three
crystalline and one glassy specimen are given in Table 9-2. These
amphiboles are Al_2O_3-poor types, low in K_2O with variable to relatively
high content of iron, MgO, CaO and Na_2O; blue and blue-green colour
is associated with higher content of iron and Na_2O. The chemical
compositions of the amphiboles indicate that they belong to the
ferrorichterite-arfvedsonite series.

Aenigmatite is rare as phenocrysts although it is relatively
widespread in the groundmass of crystalline comendites. Phenocrysts
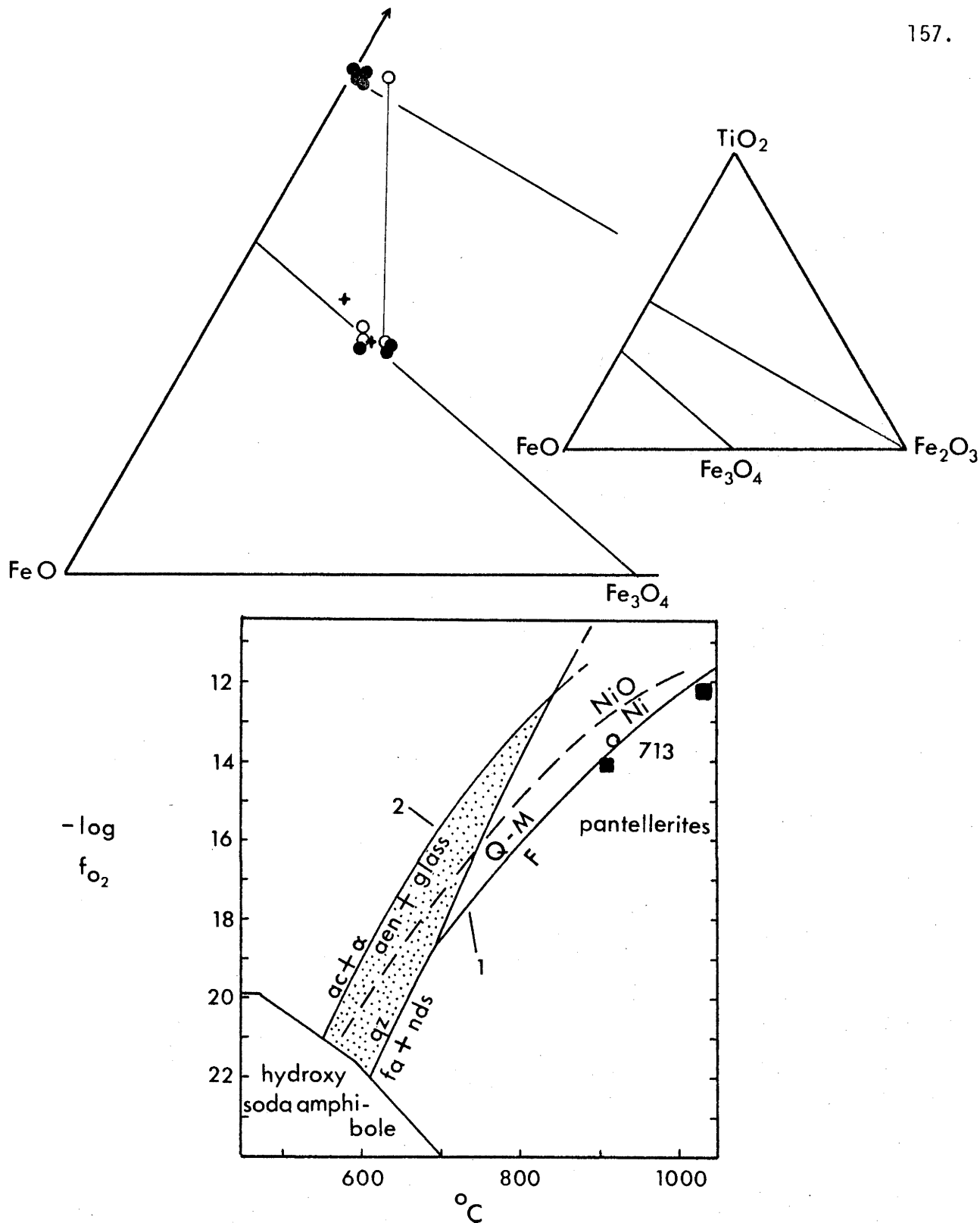
FIGURE 9-4: Composition of iron-titanium oxide phenocrysts in trachytes and comendites from the Dawson Strait area.

Upper - ternary TiO_2-FeO-Fe_2O_3 plot; FeO and Fe_2O_3 calculated on an ulvospinel basis (method of Carmichael, 1967). Tie line joins coexisting α and β phases in sample 713.

Lower - oxygen fugacity against temperature diagram after Nicholls and Carmichael (1969b); Ni-NiO buffer curve from Buddington and Lindsley (1964). Open circle - sample 713, solid squares - pantellerite data from Carmichael (1967). The no oxide field (stippled) is bounded by curves representing
1) β phase + Na metasilicate (nds) + quartz (qz) $\rightarrow$ acmite (ac)
2) aenigmatite (aen) + Na metasilicate + O_2 $\rightarrow$ acmite + α phase.

TABLE 9-3: REPRESENTATIVE ANALYSES OF IRON TITANIUM OXIDE PHENOCRYSTS
IN THE DAWSON STRAIT COMENDITES

Rock No.	713	718	719	722	728	729	.730	732	737	739	742	743
SiO_2	.0	.7	1.0	.0	1.3	.4	.0	.3	.8	.6	2.1	.9
TiO_2	20.7	21.7	20.6	19.9	19.8	19.9	22.1	49.6	52.3	49.9	49.2	50.0
Al_2O_3	.3	.3	.7	.7	2.1	.6	.2	.2	.3	.2	.3	.3
FeO	74.9	75.0	73.0	73.9	71.7	75.2	71.1	44.9	44.7	45.4	45.5	46.2
MnO	1.7	1.2	1.3	1.4	1.3	1.5	1.6	1.9	2.3	1.8	1.7	1.6
MgO	.3	.1	.7	.8	.5	.6	.0	.2	.2	.4	.3	.3
CaO	.1	.1	.1	.0	.2	.1	.0	.1	.1	.1	.6	.1

Recalculated analyses (after the method of Carmichael 1967).

Ilmenite basis

	713	718	719	722	728	729	.730	732	737	739	742	743
Fe_2O_3	43.3	41.5	41.1	43.2	39.5	43.8	39.0					
FeO	35.9	37.7	36.0	35.0	36.2	35.8	36.0					
Total	102.3	103.3	101.5	101.0	100.9	102.7	98.9					

Ulvospinel basis

	713	718	719	722	728	729	.730	732	737	739	742	743
Fe_2O_3	29.5	26.4	26.5	30.0	25.2	30.2	24.3					
FeO	48.3	51.3	49.2	46.9	49.1	48.0	49.2					
Total	101.1	101.7	100.1	99.7	99.4	101.3	97.4					
mol % Usp	58.1	62.9	61.7	56.4	61.1	57.0	64.3					

	713	718	719	722	728	729	.730	732	737	739	742	743
Fe_2O_3	6.87							2.45	.0	2.59	1.73	2.48
FeO	41.62							42.69	45.38	43.07	43.94	43.97
Total	100.79							97.45	100.62	98.66	99.87	99.65
mol % R_2O_3	6.56							2.54	.0	2.64	1.86	2.59

analyses by electron microprobe.   Fe determined as FeO.

of aenigmatite have been found in coexistance with titanomagnetite in one specimen (730) and with phenocrysts of sodic ferroaugite, ilmenite and amphibole in another (740); (Table 9-2).

Iron-Titanium oxides

Iron-titanium oxides are almost invariably present in the comendites as very small (< .1 mm) sparse phenocrysts typically in close spatial association with pyroxene and olivine phenocrysts. These oxide phenocrysts are of two distinct types; the Oiau type comendites contain phenocrysts of an α phase (magnetite-ulvospinel series) and the Numanuma type comendites contain phenocrysts of a β phase (haematite-ilmenite series) (terminology of Verhoogen, 1962). Comendites from Sanaroa Island may contain either an α or a β phase. In only one specimen, the orthopyroxene-bearing comendite from Sebuluia Bay (713) do both α and β phases coexist as phenocrysts.

Representative analyses of oxide phenocrysts from thirteen comendites are presented in Table 9-3. Exsolution is absent from both phases and microprobe analysis shows that there is little, if any, variation in composition between coexisting phenocrysts. Ulvospinel contents of the β phases range from 58 to 64 mol. %, and the α phases contain between 0 and 6 mol. % R_2O_3 (mainly Fe_2O_3) (Figure 9-4).

Chemical composition

Major and trace element abundances of thirty two comendites are presented in Table 9-4. These analysed comendites comprise nineteen obsidians and thirteen crystalline specimens.

The comendites display a range in SiO_2 from 69 to 74 % which is greater than that previously reported for any comendite suite (e.g. Macdonald and Bailey, 1973) and this feature accounts for many of the differences in chemical composition observed between the Dawson Strait comendites and comendites described in the literature. In general the TiO_2, total Fe, MnO, CaO, K_2O and P_2O_5 contents of the Dawson Strait comendites are comparable, but Na_2O and, in the less siliceous comendites, Al_2O_3 are significantly higher than in comendites described from other localities; high Na_2O/K_2O ratios appear to be a feature of the Dawson Strait suite. The peralkalinity index (mol. $(Na_2O + K_2O)/Al_2O_3$) also shows a wider range (1 to 1.4) than other comendite suites.

The Dawson Strait comendites show regular variations in chemical composition which can be correlated with increase in SiO_2. Thus total iron and peralkalinity index increases and Al_2O_3, MgO, CaO

TABLE 9-4: COMENDITES FROM THE DAWSON STRAIT AREA

No.	Crystalline 'Oiau' Type							Glassy 'Oiau' Type										
	712	713	714	715	716	717	718	719	720	721	722	723	724	725	726	727	728	729
wt%																		
SiO_2	68.78	68.89	69.03	69.13	69.40	69.84	70.29	69.60	69.65	69.73	69.80	69.84	69.87	69.93	70.14	70.27	70.43	70.68
TiO_2	.37	.47	.33	.32	.38	.35	.29	.30	.42	.29	.29	.29	.29	.30	.30	.29	.28	.28
Al_2O_3	14.39	14.87	14.64	14.32	14.20	14.35	14.32	14.01	14.03	14.30	14.09	14.14	14.08	14.18	14.11	14.29	14.35	14.09
Fe_2O_3	2.13	2.01	2.42	1.74	1.35	2.34	1.44	1.17	1.20	1.07	1.12	1.12	1.12	1.11	1.19	1.04	1.05	.99
FeO	1.42	1.27	.97	1.69	2.00	.90	1.65	2.11	2.09	2.06	2.05	1.97	1.90	2.09	2.08	1.96	1.95	1.86
MnO	.10	.10	.10	.10	.10	.09	.09	.10	.21	.10	.09	.10	.09	.10	.10	.09	.09	.09
MgO	.52	.24	.32	.16	.40	.30	.21	.06	.07	.17	.18	.18	.11	.26	.22	.21	.23	.15
CaO	.88	.55	.41	.62	.73	.37	.35	.35	.41	.35	.35	.35	.36	.44	.36	.37	.34	.33
Na_2O	6.20	6.49	6.46	6.28	6.25	6.70	6.14	6.41	6.41	6.39	6.38	6.33	6.32	6.36	6.42	6.26	6.33	6.16
K_2O	4.64	4.06	4.84	4.79	4.90	3.83	4.95	4.74	4.80	4.82	4.82	4.89	4.85	4.89	4.90	4.85	4.92	4.94
P_2O_5	.04	.04	.04	.05	.05	.05	.04	.03	.03	.02	.03	.02	.03	.03	.03	.02	.02	.02
H_2O+	.09	.13	.05	.24	.18	.18	.09	.39	.50	.32	.14	.24	.16	.19	.33	.18	.29	.36
H_2O-	.10	.12	.09	.11	.18	.25	.09	.12	.12	.11	.09	.07	.14	.10	.29	.20	.08	.14
CO_2	.19	.01	.15	.06	.05	.13	.07	.04	.04	.09	.04	.05	.17	.13	.02	.17	.05	.11
Total	99.85	99.25	99.85	99.61	100.17	99.69	100.02	99.45	99.98	99.82	99.47	99.59	99.49	100.11	100.49	100.20	100.41	100.20
Mol. $\frac{(Na_2O+K_2O)}{Al_2O_3}$	1.06	1.01	1.08	1.08	1.10	1.06	1.08	1.12	1.12	1.10	1.11	1.11	1.11	1.11	1.12	1.09	1.10	1.10
ppm Ba	89	601	173	100	99	465	53	89	80	83	67	64	41	83	82	40	59	12
Rb	102	102	101	113	105	90	116	115	115	113	116	115	117	117	115	117	119	129
Sr	24	14	10	8	20	19	3	2	3	3	3	3	4	3	2	5	4	3
Pb	24	29	24	32	25	170	28	28	29	28	28	28	0	28	29	29	28	30
Th	20	22	20	22	19	20	23	21	21	20	22	21	22	22	21	22	22	24
U	4	4	3	4	4	3	3	5	5	5	5	5	5	5	5	5	5	5
Zr	997	872	953	1054	979	838	1117	1057	1054	1025	1041	1042	1055	1054	1061	1037	1062	1057
Nb	23	21	22	24	22	20	25	24	24	23	25	24	24	24	23	23	24	25
Y	66	40	57	70	65	81	26	71	71	68	69	69	70	70	71	69	70	72
La	74	33	56	71	64	91	34	68	66	69	67	70	69	69	68	69	62	73
Ce	136	99	108	141	133	114	140	138	131	131	131	137	139	141	135	144	132	140
Sc	6	8	4	6	7	8	5	6	6	6	6	6	6	6	6	6	5	4
V	9	5	4	4	12	9	1	2	3	2	2	2	1	2	2	1	0	1
Cr	2	0	0	0	26	0	0	0	0	0	0	0	0	0	0	0	0	0
Ni	2	0	0	0	1	0	0	0	0	0	0	0	0	0	0	0	0	0
Cu	1	1	0	6	2	0	0	1	1	1	0	1	0	41	1	1	1	1
Zn	96	84	98	103	101	87	65	108	107	104	104	103	105	108	108	107	103	104
Ga	26	24	27	25	23	23	27	26	26	25	25	26	26	25	26	26	26	26
Cl	98	nd	388	nd	32	nd	21	1178	1175	1143	1135	1124	1114	1189	1147	1110	1128	1296
K/Rb	377.64	330.43	397.81	351.89	387.40	353.27	354.24	342.17	346.50	354.10	344.94	352.99	344.12	346.96	353.72	344.12	343.22	317.90
Zr/Nb	43.35	41.52	43.32	43.92	44.50	41.90	44.68	44.04	43.92	44.57	41.64	43.42	43.96	43.92	46.13	45.09	44.25	42.28

nd = not determined. Abundances <0.5 ppm recorded as 0.

TABLE 9-4 (CONTINUED)

No.	Sanaroa Island			Crystalline 'Numanuma' Type						Glassy 'Numanuma' Type					
	730	731	732	733	734	735	736	737	738	739	740	741	742	743
wt%														
SiO_2	69.68	70.73	72.40	70.18	70.95	71.10	71.55	71.62	71.65	71.79	71.98	72.43	72.62	73.57
TiO_2	.27	.26	.27	.29	.30	.35	.30	.34	.29	.33	.27	.25	.25	.25
Al_2O_3	13.79	12.97	11.77	12.52	11.94	11.50	12.28	11.18	12.04	11.07	11.54	10.50	10.67	10.69
Fe_2O_3	3.30	1.24	1.53	3.19	3.07	3.55	2.30	3.00	1.52	1.99	1.72	2.00	1.91	1.99
FeO	.73	2.30	2.51	1.55	1.71	1.80	1.67	2.11	2.54	3.11	2.45	2.58	2.61	2.62
MnO	.07	.13	.12	.15	.08	.15	.08	.24	.12	.15	.12	.11	.11	.11
MgO	0.00	.19	.14	.13	.12	.21	.14	.24	.14	.15	.15	.04	.18	.05
CaO	.17	.37	.28	.42	.39	.33	.21	.28	.26	.22	.19	.17	.20	.17
Na_2O	5.14	5.87	5.74	5.46	5.49	5.15	5.60	5.27	6.07	6.32	5.90	5.91	5.93	5.98
K_2O	4.85	4.95	4.72	4.59	4.73	4.70	4.83	4.68	4.76	4.63	4.64	4.35	4.45	4.47
P_2O_5	.02	.02	.01	.03	.03	.02	.01	0.00	.02	.02	.01	.01	.02	.01
H_2O+	.80	.33	.24	.39	.27	.33	.24	.40	.36	.23	.41	.31	.56	.08
H_2O-	.63	.12	.06	.56	.35	.79	.30	.40	.10	.05	.11	.09	.08	.11
CO_2	.02	.05	.04	.08	.09	.05	.17	.07	0.00	.02	.07	.07	.06	.04
Total	99.47	99.53	99.83	99.54	99.52	100.03	99.68	99.71	99.87	100.08	99.56	98.82	99.65	100.14
Mol. $\frac{(Na_2O+K_2O)}{Al_2O_3}$	.99	1.16	1.24	1.11	1.18	1.18	1.18	1.23	1.26	1.39	1.28	1.37	1.37	1.37
ppm Ba	30	0	0	0	0	0	0	0	0	0	0	0	0	0
Rb	128	134	152	153	160	150	151	153	158	157	174	195	191	193
Sr	13	3	2	12	7	8	3	5	2	1	1	2	1	2
Pb	21	25	28	46	40	46	37	43	40	42	46	51	51	51
Th	19	19	23	30	30	31	32	31	31	34	34	37	37	38
U	2	4	5	0	0	7	3	8	7	7	8	9	8	10
Zr	696	699	799	1627	1632	1687	1572	1696	1547	1682	1753	2136	2100	2130
Nb	21	21	23	35	34	37	36	36	34	37	38	44	43	45
Y	43	58	68	133	89	46	44	142	106	117	118	134	132	134
La	49	60	69	139	77	51	47	109	97	103	107	120	118	120
Ce	74	116	129	249	126	193	106	209	209	198	216	255	247	258
Sc	7	6	4	6	5	6	4	6	3	6	3	2	2	2
V	4	2	2	1	1	3	1	2	2	2	1	1	0	1
Cr	0	0	0	0	0	35	0	0	0	0	0	0	0	0
Ni	0	0	0	0	0	1	0	0	0	0	0	0	0	0
Cu	2	0	0	7	5	3	0	3	1	3	0	4	3	3
Zn	77	111	138	206	166	189	109	209	162	188	175	200	199	201
Ga	28	25	24	30	30	23	28	28	27	27	27	28	28	28
Cl	nd	308	344	nd	nd	57	348	29	1601	1401	1601	1323	1338	1336
K/Rb	314.55	306.66	257.78	249.04	245.41	260.11	265.54	253.93	250.10	244.81	221.37	185.19	193.41	192.27
Zr/Nb	33.14	33.29	34.74	46.49	48.00	45.59	43.67	47.11	45.50	45.46	46.13	48.55	48.84	47.33

and to a lesser extent TiO_2, Na_2O and K_2O decrease as SiO_2 increases; total iron decreases slightly in the Oiau type comendites and increases through the Numanuma type comendites and a similar pattern is observed in MnO abundances. Of particular importance is the extremely low MgO and CaO of the most Si-rich rocks. The high-Si comendites are all of the type recognised petrographically as Numanuma type (71-74 % SiO_2) and the Oiau type comendites are all relatively low in SiO_2 (68-71 %), comendites from Sanaroa Island have intermediate SiO_2 contents.

Trace element abundances in the comendites are highly distinctive. Pb, Th, U, Zr, Nb, Y, La, Ce, Zn, Ga and Cl are generally high compared to other rhyolites and V, Cr and Ni are low, both absolutely and relative to Fe content. Perhaps the most conspicuous feature of the trace element compositions is the extremely low Ba and Sr contents. The trace element contents are generally comparable with those in comendites described from other localities (summarised by Macdonald and Bailey, 1973) although they typically show a greater range of abundances. For equivalent SiO_2 content, the Dawson Strait comendites have typical concentrations of Sr and Ce, are higher in Rb, Zr and to a lesser extent Th, U and La, and lower in Ba, Nb, Y, Ca and Cl.

There is a strong positive correlation of Rb, Pb, Th, U, Zr, Nb, Y, La, Ce, Zn, Ga and Cl with SiO_2; Ba and apparently Sr (although abundances are close to detection limits) show a negative correlation with SiO_2. Ba, which is present in Oiau type comendites at levels of 12-80 ppm was not detected in Numanuma type and Sanaroa Island comendites.

Although apparently transitional in major element chemistry between Oiau and Numanuma type comendites the specimens from Sanaroa Island have distinctive trace element abundances. In particular the Sanaroa Island comendites are relatively depleted in Rb, Pb, Zr, Y, La, Ce, Ga and Cl.

Rare earth element abundances

Rare earth element (REE) data for the Dawson Strait comendites has been derived from two sources. La and Ce which together with Y provide information on the abundance and degree of relative fractionation of light and heavy REE have been measured in all of the analysed
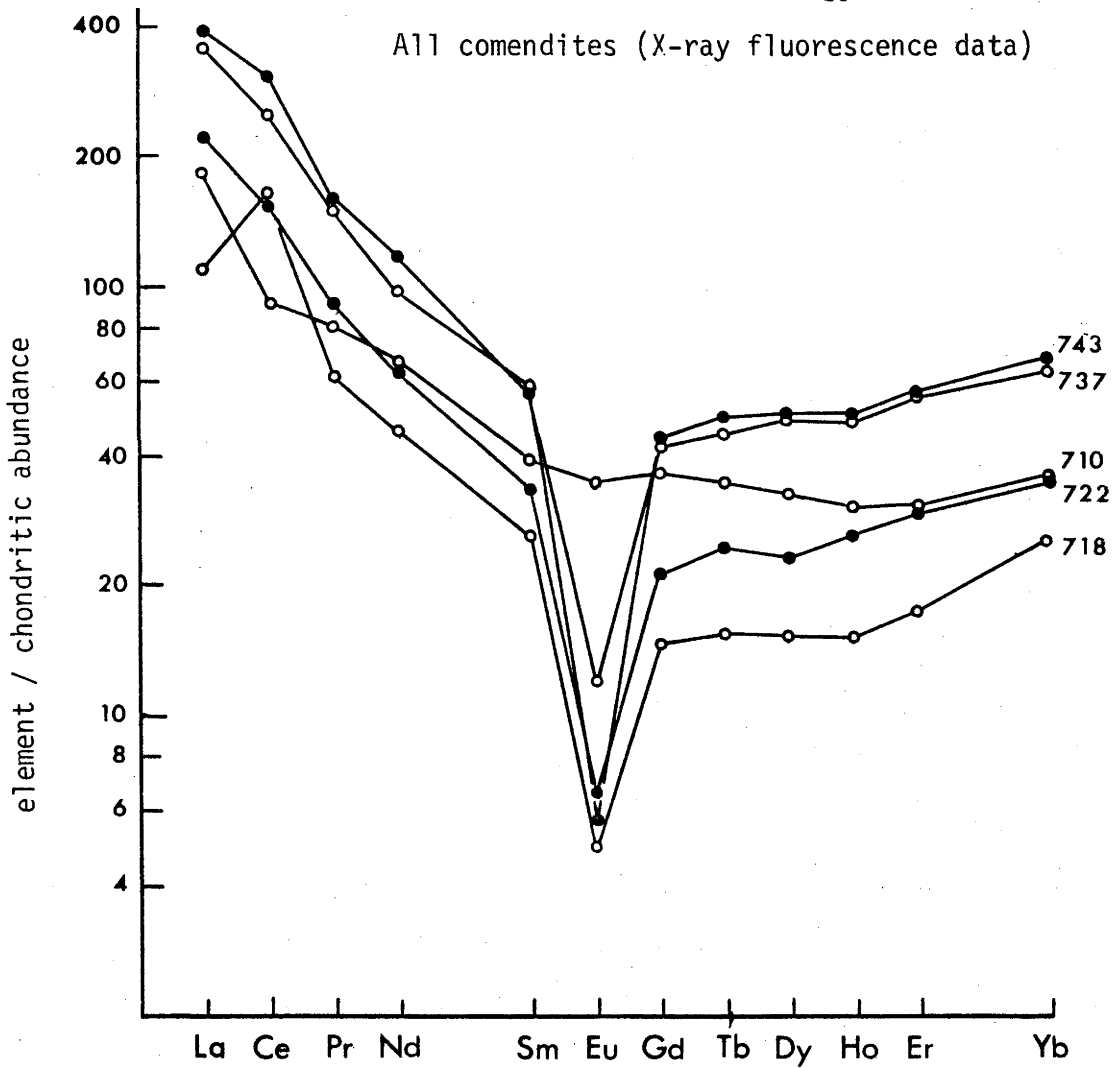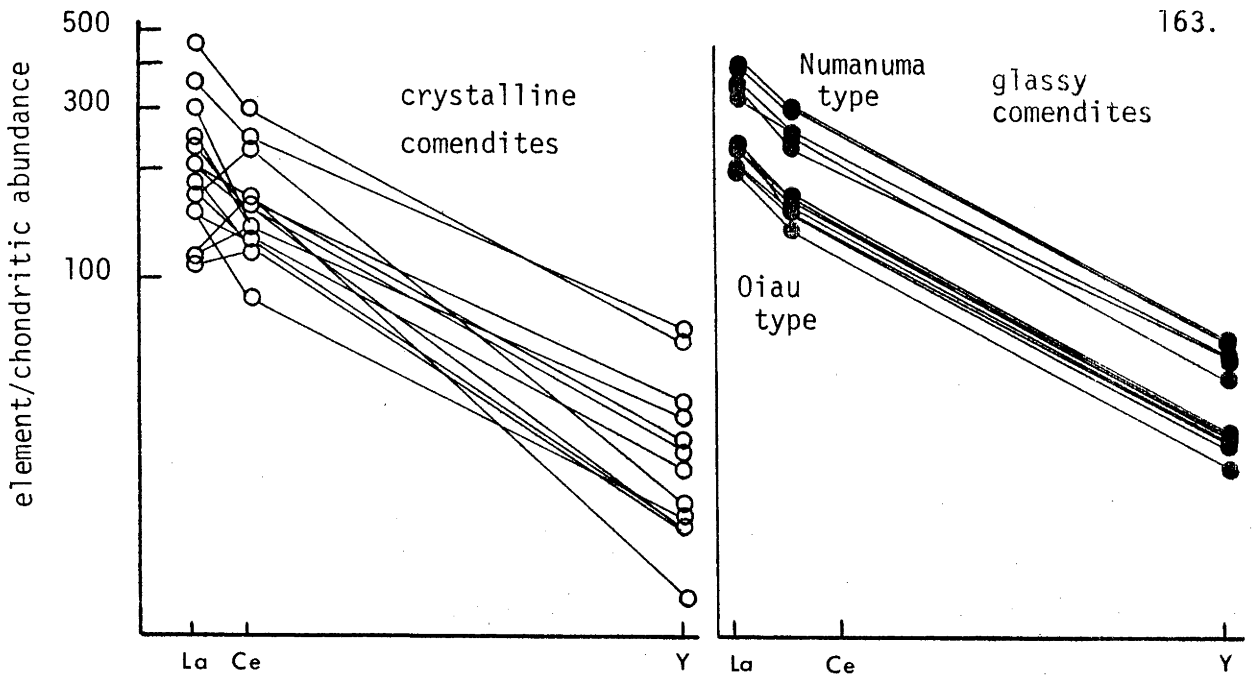
FIGURE 9-5: Chondrite normalised rare earth element patterns
in four comendites and a trachyte (710) from the
Dawson Strait area.
Open circles - crystalline specimens
Solid circles - glassy specimens

TABLE 9-5   RARE EARTH ELEMENT AND SOME OTHER TRACE ELEMENT ABUNDANCES
              IN FOUR COMENDITES AND A TRACHYTE FROM THE DAWSON STRAIT
              AREA

	Trachyte 710	718	722	737	743
La	55	34	67	109	120
Ce	78	140	131	209	258
Pr	10.0	7.5	11.1	18.5	19.4
Nd	39.2	26.7	36.7	57.5	68.7
Sm	8.3	5.5	7.1	12.5	12.0
Eu	2.6	.36	.49	.89	.43
Gd	9.4	3.8	5.5	11.0	11.6
Tb	1.7	.75	1.2	2.2	2.2
Dy	10.0	4.7	7.2	15.1	15.5
Ho	2.2	1.1	1.9	3.5	3.6
Er	6.4	3.7	6.1	11.7	12.0
Tm[1]	1.2	.84	1.1	2.1	2.2
Yb	7.1	5.1	6.9	12.6	13.4
Lu[1]	1.1	.79	1.1	2.0	2.1
La/Yb	7.7	6.7	9.7	8.7	9.0
Eu/Eu*	.93	.24	.24	.24	.11
Cs	.81	.80	5.8	1.5	11.5
Pb	14.4	16.6	23.2	22.0	51.0
Th	8.0	14.7	15.6	16.7	25.9
U	1.5	2.4	4.5	6.7	7.8
Th/U	5.4	6.1	3.5	2.7	3.3
Hf	12.9	19.2	16.8	25.0	32.4
Zr/Hf	53.8	58.2	62.0	67.8	65.7

[1]estimated abundance. La and Ce determined by XRF.

comendites by means of X-ray fluorescence. More detailed data are analyses by mass spectrometry of REE in two crystalline and two glassy comendites (Table 9-5).

The X-ray fluorescence data show that overall the abundance of REE in the comendites are high and that there is significant enrichment of the light REE (La, Ce) relative to heavy REE (represented by Y). Although relative enrichment patterns are the same, the Numanuma type comendites contain greater abundances than do the Oiau type or the Sanaroa Island comendites. REE abundances of crystalline and glassy specimens are generally comparable but the crystalline comendites display marked variations in interelement ratios which contrasts with the smooth patterns shown by glassy types (Figure 9-5). This effect is due mainly to variation in the relative abundances of Ce thought to be due to late stage crystallisation effects discussed in the following section.

The main features of the REE patterns determined by mass spectrometry are enrichment in the light REE (La, Ce, Pr, Nd, Sm) relative to the heavy REE (Gd, Tb, Dy, Ho, Er, Yb), strong development of a negative Eu anomaly (Eu/Eu* = .24 - .11), and a small but distinct progressive enrichment of the heavy REE from Gd to Yb (Figure 9-5). Again there is a contrast between the smooth pattern between La and Pr shown by the glassy specimens and the variable patterns shown by the crystalline comendites. In general the behaviour of the REE is comparable in all four comendites although there is an overall increase in abundance which is correlated with increase in SiO_2.

Chemical effects of crystallisation

Peralkaline rhyolites are notably susceptible to chemical changes related to crystallisation and to secondary hydration of groundmass glass. It is generally assumed in suites including both, that the non hydrated glassy rocks represent the composition of the magma and that chemical differences between these and associated crystalline rocks reflect late stage processes in the crystallisation history. A similar effect could also be produced by hydration of glassy specimens. Both of these processes are reasonable for the Dawson Strait rocks where crystalline and glassy comendites of comparable chemical composition are closely associated.

The available data (summarised by Macdonald and Bailey, 1973) indicates that late crystallisation processes in peralkaline rhyolites

can result in loss of Na_2O, F, Cl and U and this is correlated with increased oxidation of iron. The main changes accompanying secondary hydration are loss of Na_2O and gain or loss of SiO_2, K_2O, halogens and alkaline earth elements.

Water contents of the Dawson Strait comendites are low (typically <.5 %). Combined water (H_2O+) contents are variable but are generally higher in Numanuma type comendites. There is no consistent difference in H_2O+ content between crystalline and glassy rocks although there are indications that the crystalline rocks are slightly lower. It could be anticipated that secondary alteration or hydration would be reflected by uncombined water (H_2O-) contents. The H_2O- contents of all the obsidians and of Oiau-type crystalline comendites are uniformly low (typically <.2 % H_2O-). However the Numanuma type crystalline comendites are slightly higher which may be partly due to post crystallisation alteration.

The most obvious differences between crystalline and glassy comendites in the Dawson Strait area are increased iron oxidation and lower Na_2O in crystalline specimens (Figure 9-6). The crystalline comendites generally have lower SiO_2 contents than their associated glassy rocks and this is particularly the case with the Oiau type comendites; there is thus some evidence for loss in SiO_2 during crystallisation. Differences in trace element abundances between crystalline and glassy comendites are minimal; only U which is slightly more variable and abundant in crystalline specimens and Cl (Figure 9-6) which is low and extremely variable in crystalline specimens are notably affected. These Cl abundances agree with the observations of Carmichael (1962), Nobel (1965) and Nobel and others (1967) that the halogens are generally depleted in crystalline peralkaline rhyolites compared with the glassy peralkaline rhyolites in which they are typically enriched. Although the REE are generally considered to be stable in rocks that have undergone even moderate amounts of secondary alteration, variable La/Ce ratios (Figure 9-6) in the crystalline comendites compared with glassy specimens suggests that these two REE at least have been affected by late crystallisation processes.

Lipman (1965) has suggested that leaching by groundwaters can account for much of the chemical variation observed in comendites from western North America. As the Numanuma type comendites are the oldest in the Dawson Strait area, one possible explanation for the difference between glassy and crystalline specimens could be that there has been more time
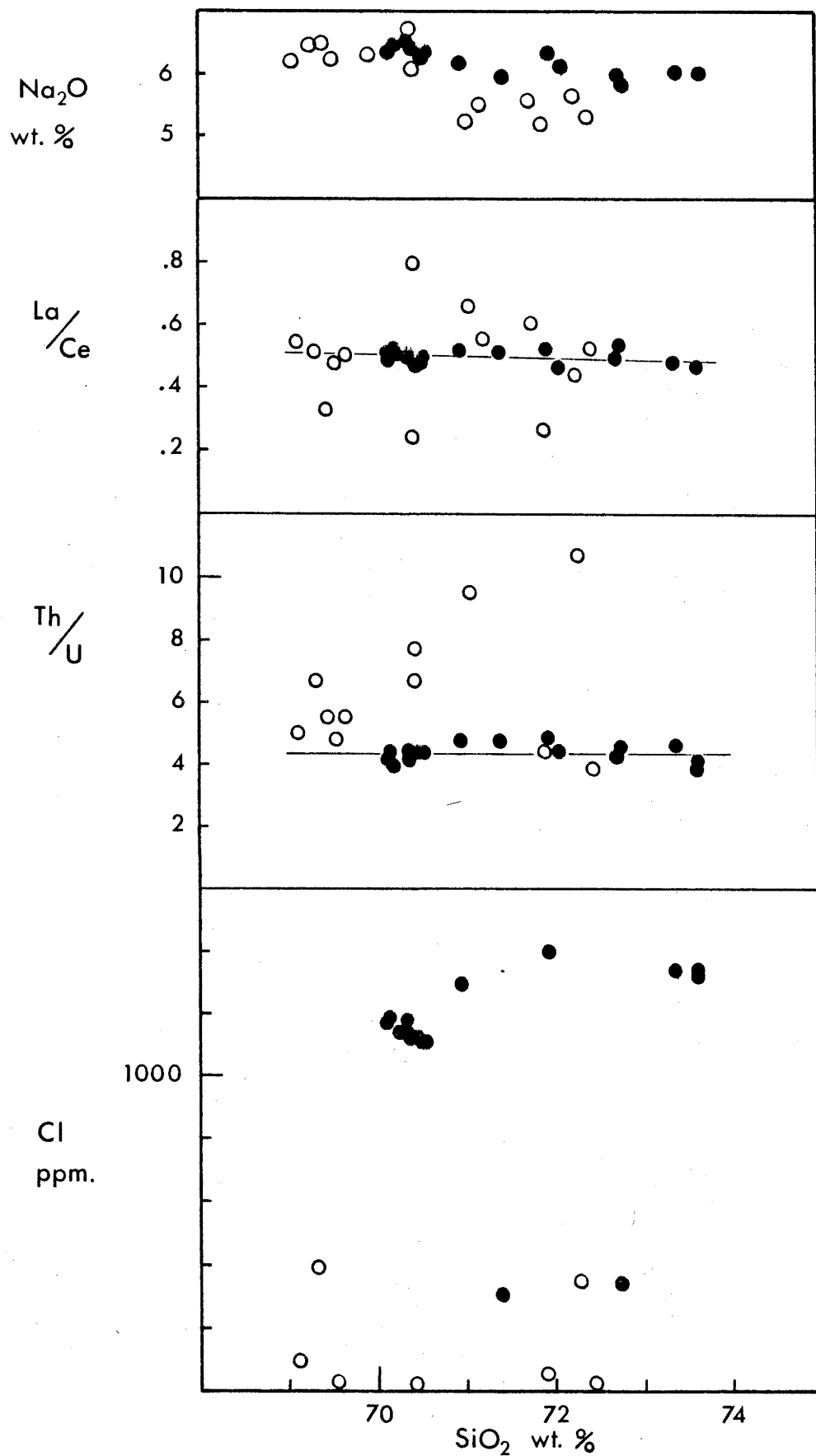
FIGURE 9-6: Compositional variations between crystalline and glassy
comendites from the Dawson Strait area.

Open circles - crystalline comendites, solid circles
- glassy comendites.

for such leaching to take place. The fresh appearance and low water
contents of all of the comendites in the Dawson Strait area precludes
leaching by groundwater as a significant process but leaching by a
late stage siliceous, sodium and halogen rich fluid remains a feasible
alternative.

A late stage volatile component

There are small but consistent differences between glassy and
crystalline comendites in the Dawson Strait area which argue for a
more general process than the localised leaching of lava flows by
groundwaters. Although the Numanuma type comendites are older and
therefore have had more opportunity to be modified by groundwater leaching
it is perhaps more significant that they are the most peralkaline rocks
in the area. Toward the close of crystallisation and in the absence of
an abundant sodic ferromagnesian phase, residual liquids will become
enriched in Na. This is because of the fact that as peralkaline liquids
become more peralkaline the crystallising feldspars become more potassic
thus increasing the Na/K ratio of residual liquids.

It is suggested that the chemical difference between crystalline
and glassy comendites in the Dawson Strait area point to the existance of
a volatile phase which develops late in the crystallisation process and
has the effect of leaching elements which are not held in crystal
structures such as the halogens, Na, U possibly Si and apparently also
La and Ce. That such a volatile phase has not operated during cooling of
glassy specimens is evidenced by the extremely stable and consistent Cl
abundances in the obsidians despite the fact that Cl is demonstrably mobile
in the presence of a volatile phase (Fyfe and others, 1958, p. 143). The
effects of this volatile phase are enhanced in more peralkaline rocks, and
the leaching process is thought to occur during cooling after extrusion
of lava flows.

An important implication of the existance of a volatile phase
during crystallisation of peralkaline magmas is that it has the effect of
leaching sodium from the system thus rendering the rock less peralkaline.
This could lead to problems of interpretation in slightly peraluminous or
slightly peralkaline suites in which non hydrated glassy rocks are
absent.

Discussion

Carmichael (1967) has shown that non-peralkaline rhyolites
containing olivine coexisting with α and β oxide phases lie close to the

curve defined by the quartz-magnetite-fayalite (QMF) buffer in f_{O_2}-T space at 1 atm. total pressure (Wones and Gilbert, 1967). It follows that the Oiau-type comendites containing the ferromagnesian phenocryst assemblage pyroxene-olivine-β phase, which presumably crystallised in equilibrium with silica-rich liquid (the quartz of the buffer system) would also lie close to this curve. The temperature and oxygen fugacity of equilibrium of the coexisting α and β phases in specimen 713 can be estimated using the curves of Buddington and Lindsley (1964). For this specimen a near liquidus temperature of about 920°C and a position close to the curve of the QMF buffer in f_{O_2}-T space is indicated. Equilibrium data for coexisting iron-titanium oxide microphenocrysts in two pantellerites (Carmichael, 1967) also plot close to this curve (Figure 9-4).

Nicholls and Carmichael (1969b)have commented on the common absence of both α and β oxide phases in glassy pantellerites, an observation which is in marked contrast to the widespread occurrence of oxides as phenocrysts in the comendites from the Dawson Strait area. They suggest that the absence of iron-titanium oxides in peralkaline rhyolites can be explained by the existence in f_{O_2}-T space of a no oxide field bounded by curves controlled by equilibrium reactions representing the common occurrence of aenigmatite and sodic pyroxene in a siliceous peralkaline rock (Figure 9-4). The extent of this no oxide field will be controlled in part by the activity of $Na_2Si_2O_5$ in the liquid and Nicholls and Carmichael (1969b)suggest that peralkalinity can be taken as a measure of this activity. In the less peralkaline comendite systems the no oxide field would be reduced relative to its extent in the more peralkaline pantellerite system and the more common occurrence of oxides in comendites is therefore to be expected.

Experiments by Lindsley (1971) have shown that in a vacuum aenigmatite melts incongruently at $880-900^{\circ}$C and is stable under conditions of f_{O2} bounded by curves defined by the nickel-nickel oxide and QMF buffers. The presence of aenigmatite in the groundmass and as rare phenocrysts in some specimens of the Dawson Strait comendites suggests that much of their crystallisation path will be constrained in f_{O2}-T space by the Ni-NiO and QMF buffer curves, and that the oxygen fugacity of peralkaline liquid is independent of composition for any given temperature.

As comendites in the Dawson Strait suite become more peralkaline

there is an increase in the K/Na ratio of early feldspars and by
implication in the Na/K ratio of the residual liquid; the data indicate
that only in late stages of crystallisation do the feldspars become
relatively sodic. These features are apparently characteristic of
comendites and pantellerites in general (Nicholls and Carmichael, 1969b.
In nature, peralkalinity can be taken as a measure of the activity of
alkalies, but increase in the K/Na ratio of early feldspars in more
peralkaline rocks implies a lowered activity of Na relative to K.

Increase in the peralkalinity index is also correlated with
increase in the total Fe content in the Dawson Strait comendites and
in other peralkaline suites (e.g. Bailey and Macdonald, 1970; Barberi
and others, 1975). This suggests that the Fe activity is relatively low
in peralkaline liquids and Fe is therefore preferentially retained in
residual liquids to become enriched in the more peralkaline liquids.
The absence of iron-titanium oxides in more peralkaline rocks can be
explained by this lowering of Fe activity. This also accounts for the
crystallisation of a β phase in the less peralkaline and Fe-rich Oiau
type comendites and of a α phase in the more peralkaline and Fe-rich
Numanuma type comendites.

An apparent anomaly in this discussion is that as the total Fe
concentration rises the Fe activity is lowered. Comendites and
pantellerites contain abundant halogens and the concentration of these
elements increases with peralkalinity index. It is possible that low
Na and Fe (as Fe^{3+}?) activities in peralkaline rocks result from the
formation of complexes in the melt.

During the later stages of crystallisation of peralkaline magma
the concentration of   Na and Fe will rise and so too will their
activities. At this stage conditions will favour the precipitation of
arfvedsonite, aenigmatite and aegirine. The typical occurrence of these
minerals as 'mossy' aggregates suggests that this occurs rapidly and at
a late stage in the crystallisation history.

9-3   Associated Rocks

Basaltic and intermediate rocks

The comendite flows at the eastern end of Dobu Island contain
abundant rounded inclusions of dark grey porphyritic basaltic rock
ranging from a few millimetres to tens of centimetres in diameter. The
margins of these inclusions are sharp and there appears to have been

TABLE 9-6: BASALTIC, INTERMEDIATE AND TRACHYTIC ROCKS IN THE DAWSON STRAIT AREA

		Transitional Basalt		Hawaiite				mugearite	Trachyte	
No.		703	704	705	706	707	708	709	710	711
wt%										
	SiO_2	47.63	48.91	50.02	50.16	52.00	54.22	54.93	63.70	64.25
	TiO_2	1.12	1.17	2.01	2.58	1.98	1.62	2.30	.89	.81
	Al_2O_3	20.61	20.77	17.07	16.09	16.65	15.65	15.30	16.33	16.49
	Fe_2O_3	2.98	3.94	3.67	4.96	3.40	3.96	2.38	3.13	1.98
	FeO	3.24	2.30	6.16	5.45	5.37	3.85	6.15	1.44	2.54
	MnO	.11	.12	.17	.13	.16	.14	.16	.09	.12
	MgO	6.57	5.21	4.85	5.01	4.57	5.04	3.01	.87	.77
	CaO	12.15	11.08	8.69	9.40	8.66	7.89	6.00	2.45	2.09
	Na_2O	2.91	3.24	3.97	4.50	4.63	4.31	5.21	7.79	7.21
	K_2O	.33	.74	1.03	.79	1.19	1.14	1.49	2.79	2.49
	P_2O_5	.20	.24	.41	.45	.38	.27	.72	.25	.30
	H_2O+	.70	.88	.84	.01	.25	.38	.62	.29	.24
	H_2O-	.95	.68	.40	.11	.16	.71	.61	.26	.24
	CO_2	.22	.24	.16	.18	.12	.17	.89	.03	.20
Total		99.72	99.52	99.45	99.87	99.52	99.35	99.77	100.31	99.73
Fe_2O_3/FeO		.92	1.71	.60	.91	.63	1.03	.39	2.17	.78
Mg.No. ($Fe_2O_3/FeO=0.2$)		69.7	64.9	51.5	51.2	52.9	58.5	43.0	29.8	27.0
ppm	Ba	54	89	427	129	151	138	468	1127	1253
	Rb	3	18	12	10	23	39	23	56	41
	Sr	524	487	456	391	403	372	359	156	157
	Pb	2	10	7	4	18	8	11	12	14
	Th	0	3	2	1	4	6	5	9	10
	U	0	0	0	1	2	2	2	1	2
	Zr	121	176	198	275	333	340	397	694	788
	Nb	2	5	5	6	8	9	11	13	11
	Y	17	21	36	39	41	37	48	58	41
	La	7	12	28	20	27	28	38	55	42
	Ce	20	37	56	46	68	60	81	78	66
	Sc	0	21	29	31	28	23	20	11	11
	V	160	145	237	331	243	188	211	44	23
	Cr	231	242	12	28	35	68	0	0	0
	Ni	113	79	15	21	22	48	4	1	1
	Cu	56	55	40	37	32	39	15	3	1
	Zn	45	56	78	86	96	69	97	100	82
	Ga	16	16	18	16	21	18	20	22	22
	Cl	279	nd	1432	739	nd	852	409	59	290
K/Rb		913.16	341.28	712.54	655.82	429.51	242.66	537.79	413.59	504.16
Ba/Sr		.10	.18	.94	.33	.37	.51	1.30	7.22	7.98
Th/U		-	-	-	1.00	2.00	3.00	2.50	9.00	5.00
Zr/Nb		60.50	35.20	39.60	45.83	41.63	37.78	36.09	53.38	71.64

nd = not determined.   Abundances <0.5 ppm recorded as 0.

little or no reaction with the surrounding comendite. These inclusions contain large (1-3 mm) phenocrysts of labradorite, clinopyroxene and olivine in a fine grained groundmass composed of plagioclase, clino- pyroxene (in some specimens lilac coloured) and abundant iron-titanium oxides.

A similar rock collected from a rounded boulder on the west coast of Sanaroa Island contains sparse small phenocrysts of labradorite in a fine grained groundmass of plagioclase, clinopyroxene, altered olivine and abundant iron-titanium oxides. The groundmass olivine in this rock typically forms larger grains than the other groundmass minerals and textural relations show that it was an early crystallising phase.

Orthopyroxene has not been recognised in any of these rocks and there is no evidence of reaction of olivine phenocrysts to form pyroxene.

Features of the major element chemistry of these basaltic rocks (Table 9-6) are variable Al_2O_3, low (for basaltic compositions) total iron and MgO and high CaO and Na_2O/K_2O. High Al_2O_3 content in two specimens is correlated with abundant plagioclase indicating that their composition has been influenced by plagioclase accumulation; these two specimens are also high in CaO. Three specimens which are not obviously accumulative are moderately high in Al_2O_3 (16-17 %) and TiO_2 (2-2.5 %), the two apparently accumulative specimens contain lower TiO_2 contents (1.2 %). All of the basaltic inclusions are oxidised possibly because of their mode of occurrence. Water contents are low to moderate and this, with their generally fresh appearance in thin section indicates that they have undergone little secondary alteration.

The non-accumulative specimens contain moderate to high abundances of Ba, Sr, Zr, V, Cl and relatively low Cr and Ni; K/Rb ratios are moderate (400-700). The two apparently accumulative specimens are notably higher in Cr and Ni which suggests that ferro- magnesian minerals, probably olivine and clinopyroxene may also have been cumulative phases. High to very high Cl contents provide some ndication of chemical interchange with the surrounding comendite magma or more probably a late fluid or volatile phase. Abundances of La, Ce and Y indicate that the light REE have been fractionated relative to the heavy REE.

When corrected for oxidation, three of these basaltic rocks plot on or to the left of the low temperature thermal divide in the normative 'iron free basalt tetrahedron' (Figure 9-7) and are therefore transitional

FIGURE 9-7: Associated rocks in the Dawson Strait area.
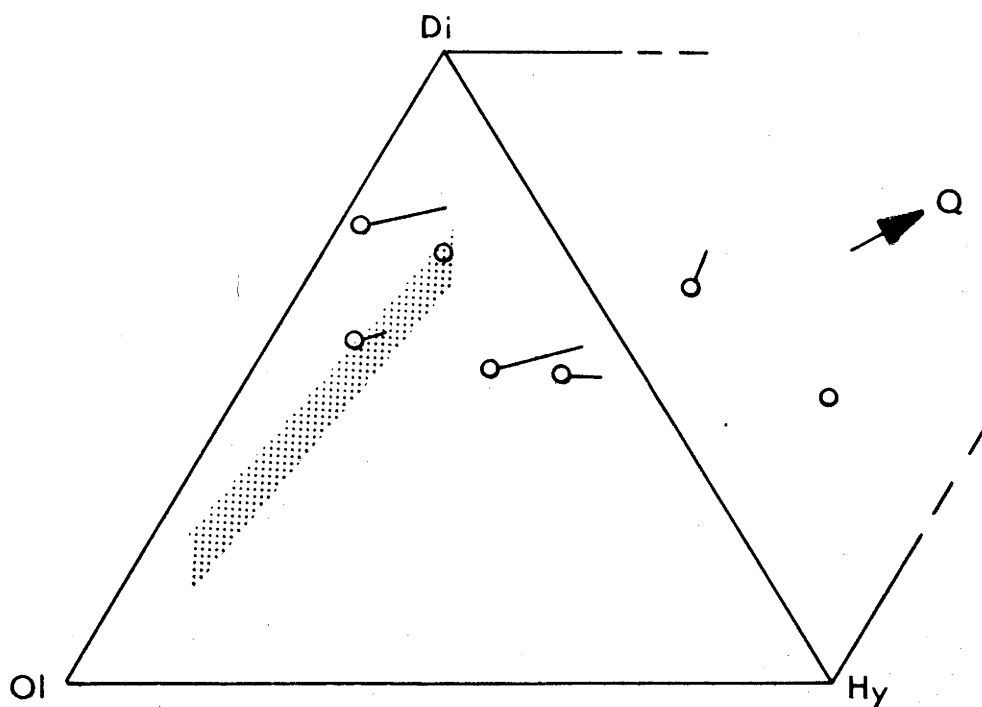
Normative mineralogy plotted on a Di-Ol-Hy-Q diagram.
Open circles represent the position of the samples after
recalculation of iron content according to the method of
Irvine and Baragar (1971); the end of the solid line
extending to the right of the circles marks their position
using FeO and Fe_2O_3 as measured. The position of the one
atmosphere thermal divide separating tholeiitic from
alkaline basalts (shown stippled) is taken from Bass (1971).
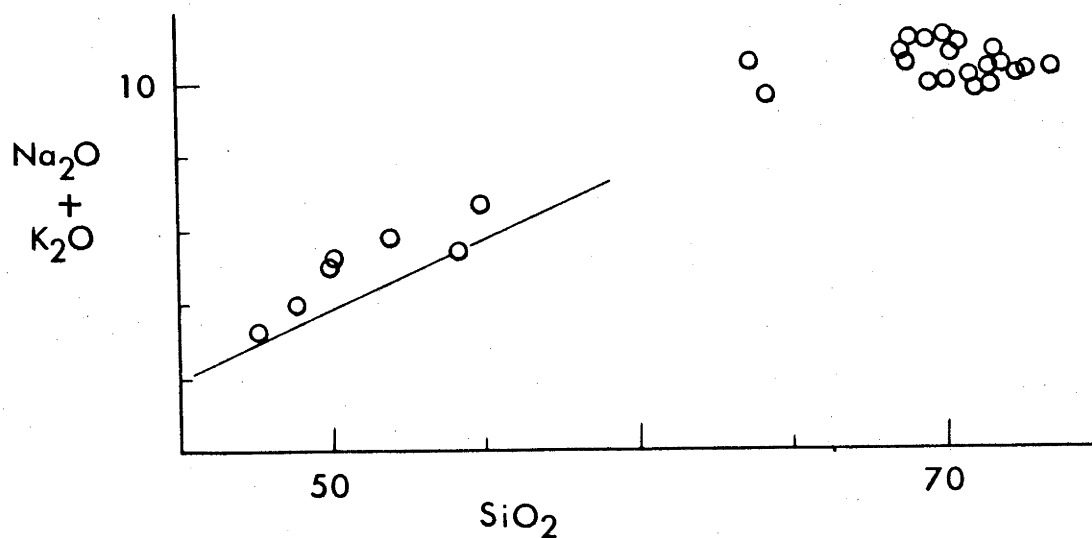
Total alkalies against SiO_2 plot for the comendites and
associated rocks from the Dawson Strait area. Solid line
divides Hawaiian tholeiitic lavas from Hawaiian alkaline
lavas (Macdonald and Katsura, 1964).

in the sense of Coombs (1963) and Bass (1971). The transitional character of all of the basalts is demonstrated on an alkalies-silica diagram (Figure 9-7).

Sparsely porphyritic lava blocks collected from basal pyroclastic deposits on the northern side of Dobu Island contain phenocrysts of calcic andesine, clinopyroxene and rare olivine in a fine grained groundmass of plagioclase, clinopyroxene, iron-titanium oxides, fine green-brown interstitial material and minor secondary calcite. Plagioclase and clinopyroxene crystals, with or without olivine crystals, form clusters of possible accumulative origin in some specimens. A similar rock type has also been found as inclusions in comendite flows at the eastern end of Dobu Island.

Chemical analysis of two of these specimens (Table 9-6) shows them to be generally intermediate in composition between the basaltic rocks and the trachytes described in the following section. The two analysed specimens differ in TiO_2, MgO, Ba, Ni and Cr contents, and K/Rb ratio; the relatively high MgO, Ni and Cr in one (708) which has higher phenocryst content may be due to accumulation of early formed crystals.

Nomenclature of these basaltic rocks follows well established rules based on normative feldspar content. Two specimens with normative labradorite (703,704) are transitional basalts comparable to Abbott's (1969) big feldspar basalts. Three specimens containing normative andesine (705-707) and one containing normative andesine and quartz (708) fit Macdonald's (1960) definition of hawaiite. The remaining specimen (709) contains oligoclase with quartz in the norm and can be termed quartz mugearite.

Trachyte

Trachyte has been collected from boulders at two localities in the area to the north of Numanuma Bay. It is not known whether the trachytes were erupted as lava flows or whether they are lava blocks from pyroclastic deposits, it is assumed that they are related to the associated Numanuma type comendites.

The trachytes are grey porphyritic rocks containing medium sized (<2 mm) phenocrysts of oligoclase (An_{16}) with a few smaller (<1 mm) phenocrysts of augite, titano-magnetite, and olivine (zoned from Fo_{51} to Fo_{39}) in a fine grained groundmass composed of plagioclase with subordinate quartz, clinopyroxene and brown amphibole. Chemical analyses

TABLE 9-7: REPRESENTATIVE ANALYSES OF PHENOCRYSTS IN TWO TRACHYTES FROM THE DAWSON STRAIT AREA

FELDSPARS

Rock No.	710 C	710 R	711 C	711 R
SiO_2	63.6	64.9	64.2	63.1
Al_2O_3	22.9	21.8	22.4	22.7
Fe_2O_3	.2	.3	.3	.7
CaO	3.9	2.9	3.4	3.9
Na_2O	8.6	8.9	8.9	8.6
K_2O	.8	1.2	.8	1.0

Number of ions on basis of 32 oxygens.

	710 C	710 R	711 C	711 R
Si	11.25	12.34	12.24	12.12
Al	4.77	3.26	3.37	3.43
Fe^{3+}	.03	.03	.03	.07
Ca	.74	.59	.69	.80
Na	2.95	3.28	3.29	3.20
K	.18	.29	.19	.24
Z	16.05	15.63	15.64	15.62
X	3.87	4.16	4.17	4.24
Or (mol %)	4.7	7.0	4.6	5.7
Ab	76.2	78.8	78.9	75.5
An	19.1	14.2	16.5	18.8

PYROXENES

Rock No.	710 C	710 R	711 C	711 R
SiO_2	51.8	51.2	50.6	50.4
TiO_2	.7	.0	.8	.8
Al_2O_3	1.6	.4	2.2	1.8
FeO	12.0	16.4	15.0	17.0
MnO	.5	.9	.5	.6
MgO	13.8	10.5	11.9	11.7
CaO	19.3	20.1	17.4	17.0
Na_2O	.3	.5	.6	.7

Number of ions on basis of 6 oxygens and 4 oxygens.

	710 C	710 R	711 C	711 R
Si	1.95	1.98	1.93	1.94
Ti	.02	.0	.02	.02
Al	.07	.02	.10	.08
Fe^{3+}	.02	.04	.04	.05
Fe^{2+}	.36	.49	.43	.49
Mn	.02	.03	.02	.02
Mg	.77	.60	.68	.67
Ca	.78	.83	.75	.70
Na	.02	.04	.04	.05
Di (mol %)	39.6	40.9	38.2	35.2
En	39.3	29.7	34.4	33.7
Fs	18.9	25.7	22.9	25.8
Ac	2.2	3.7	4.5	5.2
Fa				

OLIVINES

Rock No.	711 C	711 R
SiO_2	35.2	33.8
FeO	39.3	46.6
MnO	1.2	1.6
MgO	24.0	17.7
CaO	.3	.3
Si	1.00	1.00
Fe^{2+}	.94	1.16
Mn	.03	.04
Mg	1.02	.78
Ca	.01	.01
Fa	48.6	60.5

IRON-TITANIUM OXIDES

Rock No.	710	711
SiO_2	.3	.8
TiO_2	23.9	20.9
Al_2O_3	1.7	1.4
FeO	65.1	72.3
MnO	1.6	.9
MgO	1.6	1.4
CaO	.5	.2

Recalculated after Carmichael (1967)

Ilmenite basis

	710	711
Fe_2O_3	34.9	40.9
FeO	33.7	35.5
Total	98.2	102.0

Ulvospinel basis

	710	711
Fe_2O_3	18.8	26.3
FeO	48.2	48.7
Total	96.6	100.5
Usp (mol %)	70.3	61.3

Analyses by electron microprobe.   Fe determined as FeO. Fe^{3+} in pyroxene estimated from Na content.   C - phenocryst core, R - phenocryst rim.

of these phenocryst phases are presented in Table 9-7 and plotted on Figures 9-2 to 9-4.

The trachytes are sodic oversaturated rocks. They are enriched in Rb and particularly Ba and Zr relative to the associated low-Si rocks and are relatively depleted in Sr; Cr and Ni are below or close to detection limits.

Rare earth element abundances in trachyte 710 are presented with the comendite abundances in Table 9-5; chondrite normalised abundances are plotted in Figure 9-5. REE abundances show an overall enrichment relative to chondritic abundances and show a degree of light/ heavy fractionation which is comparable to that of the associated comendites. The trachyte shows a small negative Eu anomaly (Eu/Eu* = .93) which contrasts with the well developed anomaly developed in the comendites. REE abundances in the trachyte are higher than those in Oiau-type comendites but are lower than those in Numanuma-type comendites.

9-4   Petrogenesis

Peralkaline rhyolites from many parts of the world in both oceanic and continental settings show remarkable similarity in major and trace element chemical composition which argues for a common petrogenetic process. In general, processes such as melting of country rocks at the margins of basic intrusions or partial melting of crustal material would appear to be unlikely because the crustal rocks in different areas of peralkaline volcanism are demonstrably different. The most popular alternative to hypotheses of partial melting is a process of fractional crystallisation from a basaltic parent involving removal of early formed plagioclase to produce a silica-rich slightly peralkaline liquid (e.g. Bowen, 1945; Carmichael and Mackenzie, 1963; Noble, 1965; Thompson and Mackenzie, 1967; Ewart and others, 1968; Noble, 1968; Weaver and others, 1972; Barberi and others, 1975). Subsequent evolution of such slightly peralkaline liquids will be controlled by fractional crystallisation of alkali feldspars (e.g. Roux and Varet, 1975). Evidence for the occurrence of series controlled by fractional crystall- isation has been provided from the east African rift (Weaver and others, 1972) and from the Afar region, Ethiopia (Barberi and others, 1975).

Experimental work (e.g. Bailey and Schairer, 1964; 1965) has

shown that there is no way by which simple melting of normal crustal materials would yield peralkaline liquids directly. However, enrichment in alkalies and incompatible late stage elements by means of a volatile phase has been suggested as one process by which peraluminous siliceous liquids derived by partial melting could become peralkaline (Nicholls and Carmichael, 1969b, Macdonald and others, 1970; Sutherland, 1971).

A comagmatic series?

The available data indicate that the basaltic and intermediate rocks found as inclusions within, and in pyroclastic rocks associated with, the comendites in the Dawson Strait area are closely related to them. It is significant that inclusions of country rock are unknown in the comendites and that all of the associated basaltic and intermediate rocks are of a type similar to basaltic and intermediate lava flows on volcanoes which have also erupted comendites. In the following sections the transitional basalt-comendite association of the Dawson Strait area are discussed in terms of a series of rocks related to each other by a process of fractional crystallisation.

A test of the cogenetic relationship of a suite of rocks can be made by examination of the relative abundances of elements which have residual behaviour. As Weaver and others (1972) have pointed out, the relative abundance of a pair of elements in any solid-liquid reaction or series of reactions will be constant if the bulk distribution coefficients between the crystalline and liquid phases during the reactions remains approximately constant. Elements which have bulk distribution coefficients close to zero and which are therefore partitioned almost exclusively into the melt have residual behaviour and have been termed residual elements (Harris, 1967).

Zirconium does not enter any of the major crystallising phases of natural silicate melts except perhaps to a small extent into clino-pyroxene (Chao and Fleischer,1960). Zirconium is characteristically enriched in comendites relative to typical granites and is known to have a high solubility in peralkaline melts (Dietrich, 1968). As neither zircon or any other zirconium bearing mineral have been detected in any of the Dawson Strait rocks and as zirconium is clearly enriched in the more siliceous rocks the element is likely to have residual behaviour.

Among other elements observed to have residual behaviour in volcanic suites which include peralkaline rhyolites are Nb, Rb, Ce and La (Weaver and others, 1972; Barberi and others, 1975). A Zr/Nb plot
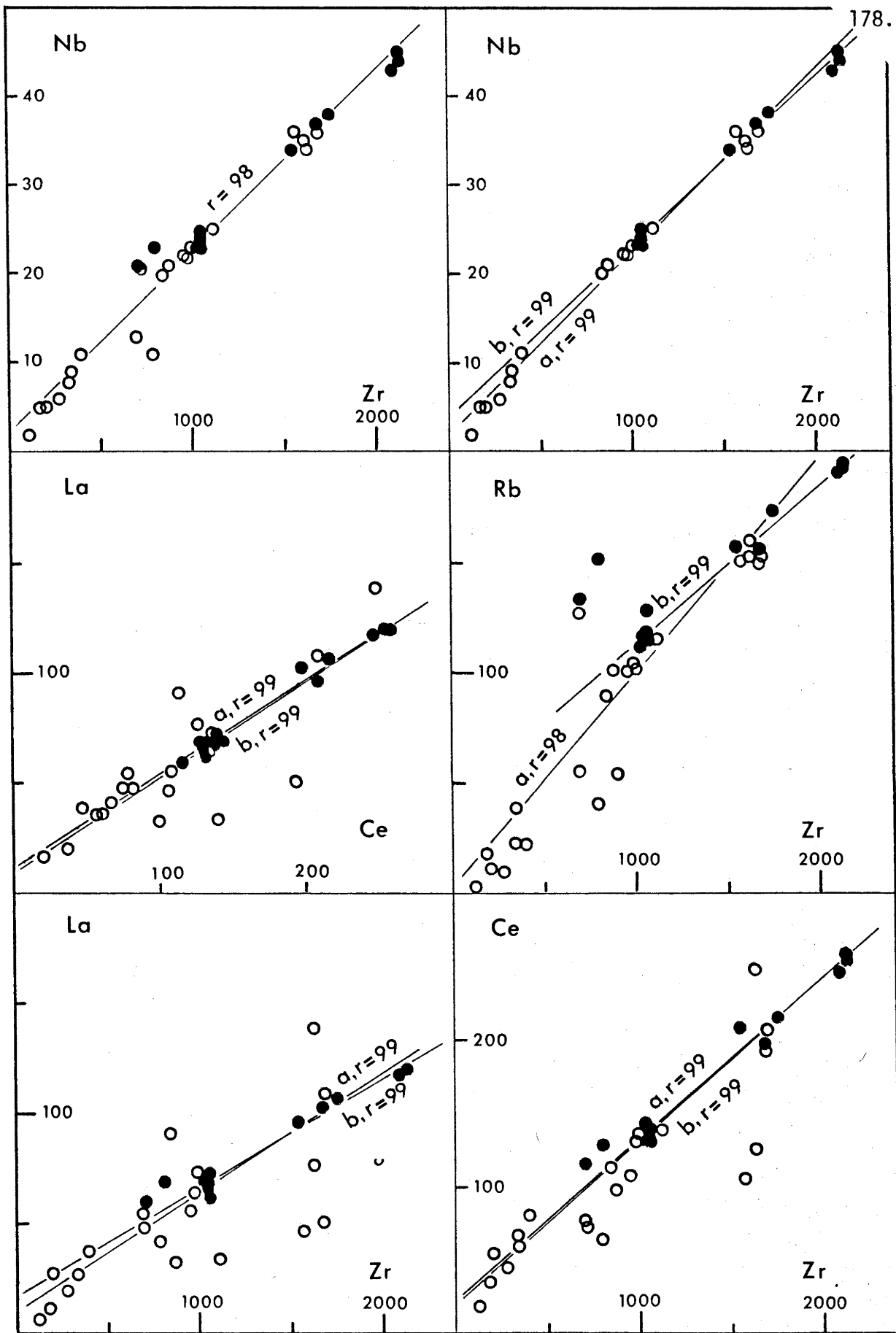
FIGURE 9-8: Residual elements in the Dawson Strait suite.

a-least squares regression line for basaltic and
intermediate rocks and glassy comendites.
b-least squares regression line for glassy
comendites only.
r=correlation coefficient.
Open circles-crystalline, solid circles-glassy rocks.

(Figure 9-8) of the Dawson Strait rocks shows the linear correlation to be expected of a residual element pair in a comagmatic suite although the two trachytes and two comendites from Sanaroa Island plot slightly off the correlation line. La/Zr, Ce/Zr and La/Ce plots (Figure 9-8) also display a moderately good linear correlation if the data from crystalline comendites is disregarded. Weaver and others (1972) have also suggested that Rb can behave as a residual element, the approximately linear Rb/Zr correlation observed (Figure 9-8) in the glassy Dawson Strait rocks supports the contention. The apparently anomalous behaviour of La and Ce in crystalline specimens is due to late crystallisation processes discussed earlier.

The relative abundances of Zr and Nb provides evidence for the close geochemical relationship of the basaltic and intermediate rocks to Oiau and Numanuma type comendites which is in general supported by the abundances of Rb, La and Ce. The trachytes and the comendites from Sanaroa Island are closely related but may form a distinct series.

Crystal fractionation?

The demonstrably close relationship between the volcanic rocks in the Dawson Strait area suggests a genetic link which cannot be explained if the comendites originated by partial melting of crustal material in the area. It follows that the basalts can only be related to the comendites by either progressive partial melting of some type of mantle material (e.g. Cox and others, 1970) or by fractional crystallisation of a basaltic parent.

Although progressive partial melting of basaltic source material can in theory produce a series of liquids which show regular compositional variations such as those observed in the Dawson Strait series; such a process cannot explain either the relative abundances of the residual trace elements or the extreme depletion in Ba and Sr relative to the basalts.

Within multi phase systems (such as natural magmas) residual element behaviour implies that the solid/liquid partition coefficient must be very small so that the element is partitioned entirely into the melt. Residual behaviour of several elements in a series of liquids derived by progressive partial melting could only occur if either all the residual elements resided in one crystalline phase and were released together or, if several residual element bearing crystalline phases broke down

simultaneously. Both of these situations are highly unlikely. In fact, it can be demonstrated (Ferrara and Treuil, 1975) that residual behaviour of a pair of elements can only result from a fractional crystallisation process. Any other processes (e.g. gaseous transfer, partial melting) while producing a sequence of closely related liquids of different composition will modify the relative concentration of residual elements preventing the linear correlation from being maintained.

A reasonable partial melting model giving rise to highly siliceous rocks must involve some degree of feldspar-liquid equilibrium; the abundances of typically feldspathic elements such as Ba and Sr can therefore place constraints on the nature of the reaction. Approximate distribution coefficients for Sr and Ba between feldspar and melt phases have been calculated by Korringa and Noble (1971) using data available for volcanic rocks. Plagioclase-liquid distribution coefficients for Sr vary between 1 and 7 and for Ba from about .4 to .1 depending on the plagioclase composition. Distribution coefficients for Sr and Ba between sodic feldspar and siliceous melt vary from about 3 to 4 and 3 to 5 respectively. Given these partition coefficients, the extremely low abundances of Ba and Sr measured in the Dawson Strait comendites could only be achieved by partial melting if their abundance in the source material was unrealistically low (of the order of 20 ppm).

Volatile enrichment

It has been suggested (Ewart and others, 1968; Nicholls and Carmichael, 1969b, Bailey and Macdonald, 1975) that a process of volatile enrichment may enhance a trend toward peralkalinity initiated by fractional crystallisation and may also explain the extreme enrichment in some trace elements (e.g. Zr, Cl, REE) which typifies peralkaline rhyolites. There is some evidence for the operation of a volatile phase during the late stages of crystallisation of the Dawson Strait rocks however, the net effect of this is to lower rather than raise peralkalinity. Elements such as Zr which have residual behaviour are unaffected.

Bailey and Macdonald (1975) have argued that the behaviour of 'residual' elements in a suite of pantellerites from Eburru volcano cannot be explained by closed system crystal fractionation. The implication from their work is that the observed rock compositions are mixtures of a fluid (vapour) phase rich in 'residual' elements, and a silicate melt which has presumably originated by either fractional

crystallisation or partial melting. There are two fundamental
objections to such a model. Firstly, what is the origin of the residual-
enriched fluid phase? Secondly if such a phase exists what is the
nature of the process by which it is homogeneously mixed with the
silicate melt? Neither of these problems are considered by advocates
of fluid phase enrichment. In particular with reference to the mixing
problem it would be remarkable if the proportions of fluid phase and
silicate melt always combined to give constant element/SiO_2 correlations
in a variety of peralkaline rhyolite suites. This problem remains even
if the mixing process is considered as an equilibrium exchange in a
system buffered by the fluid phase.

As discussed in section 9-7 peralkaline rhyolites represent one
of the most complex natural magma systems and some aspects of their
chemical composition may imply a unique petrogenetic process. However,
although volatile enrichment at depth cannot be altogether discounted
as a process contributing to the orign of the Dawson Strait comendites
the observed variations within the suite can be adequately explained by
crystal fractionation alone.

Quantitative modelling

Quantitative modelling of the fractionation process in the
siliceous rocks of the Dawson Strait suite was undertaken using the Petmix
computer program developed following the scheme of Wright and Doherty (1970)
by M. Gorton (RSES, ANU). The Petmix program operates to obtain a least
squares best fit between two end member whole rock compositions by adding
or subtracting varying proportions of mineral compositions. Mineral
compositions can be entered as either a single composition, or, in the
case of solid solution series as end member compositions. The calculation
can be biased to give the best fit for particular elements.

Using the Petmix program a series of calculations were made using
the two trachyte compositions, crystalline comendite 713 and glassy
comendites 719, 722, 729 (Oiau type) and 739, 743 (Numanuma type).
Mineral compositions used were probe analyses of phenocrysts or, in the
case of the trachyte analyses of crystals occurring as clusters
(accumulative?) in trachyte 710. Weighing of the oxides was biased
toward achieving a better fit for SiO_2, Al_3O_3, CaO, Na_2O and K_2O because
feldspar is the main mineral which forms phenocrysts in all of these
rocks.

The results using trachyte 710 as a parental composition were

TABLE 9-8: <u>PETMIX</u> CALCULATIONS

A. Trachyte 711 to comendite 713

	weight	711	calc	diff	713	feld.	cpx	ol
SiO_2	10.0	65.14	65.02	-.2%	69.70	65.42	52.01	35.63
TiO_2	1.0	.82	.90	9.5%	.47	.00	.65	.00
Al_2O_3	10.0	16.72	16.76	.3%	15.05	21.36	2.12	.00
Fe_2O_3	2.5	2.01	1.95	-2.7%	2.04	.32	.00	.00
FeO	2.5	2.58	2.58	.1%	1.28	.00	10.93	39.78
MgO	1.0	.78	.79	.8%	.24	.00	14.32	24.29
CaO	10.0	2.12	2.12	.2%	.55	2.25	19.57	.30
Na_2O	5.0	7.31	7.35	.5%	6.56	9.50	.41	.00
K_2O	10.0	2.52	2.53	.3%	4.1	1.14	.00	.00
Proportions:					49.81%	42.74%	4.50%	-.08%
Sensitivity:					3.45	3.50	3.06	2.26

B. Trachyte 711 to comendite 722

	weight	711	calc.	diff.	722	feld	cpx	ol
SiO_2	10.0	65.14	65.32	.3%	70.45	61.22	50.85	35.63
TiO_2	1.0	.82	.76	-7.6%	.29	.00	.80	.00
Al_2O_3	10.0	16.72	17.03	1.9%	14.22	24.66	2.21	.00
Fe_2O_3	2.5	2.01	1.60	-20.2%	1.13	.48	.00	.00
FeO	2.5	2.58	3.04	18.1%	2.07	.00	15.08	39 78
MgO	1.0	.78	.38	-51.3%	.18	.00	11.96	24.29
CaO	10.1	2.12	2.14	1.2%	.35	6.05	18.49	.30
Na_2O	5.0	7.31	7.17	-2.0%	6.44	9.49	.60	.00
K_2O	10.0	2.52	2.56	1.2%	4.89	-1.89	.00	.00
Proportions:					64.80%	31.55%	.01%	.92%
Sensitivity:					2.76	2.76	2.16	1.58

C. Trachyte 711 to comendite 739

	weight	711	calc.	diff.	739	feld.	cpx	ol
SiO_2	10.0	65.14	65.19	.1%	72.08	63.91	47.89	35.63
TiO_2	1.0	.82	.91	10.3%	.33	.00	8.85	.00
Al_2O_3	10.0	16.72	16.67	-.3%	11.11	22.39	24.05	.00
Fe_2O_3	2.5	2.01	1.94	-3.4%	1.99	.34	.00	.00
FeO	2.5	2.58	2.57	.1%	3.13	..00	-91.60	39.78
MgO	1.0	.78	.78	-.6%	.15	.00	95.58	24.29
CaO	10.0	2.12	2.12	-.2%	.22	3.50	32.06	.30
Na_2O	5.0	7.31	7.31	.0%	6.34	8.94	-16.83	.00
K_2O	10.0	2.52	2.52	-.2%	4.65	.92	.00	.00
Proportions:					43.93%	51.79%	.62%	.30%
Sensitivity:					4.42	4.46	8.97	3.04

D. Comendite 719 to comendite 739

	weight	719	calc.	diff.	739	feld	cpx
SiO_2	10.0	70.48	69.70	-1.1%	72.08	67.50	50.67
TiO	1.0	.30	.21	-31.2%	.33	.00	-.02
Al_2O_3	10.0	14.19	14.45	1.8%	11.11	18.99	.18
Fe_2O_3	2.5	1.18	1.39	17.5%	1.99	.61	.00
FeO	2.5	2.13	2.14	.1%	3.13	.00	30.28
MgO	1.0	.08	.08	1.1%	.15	.00	-.14
CaO	10.0	.35	.35	1.0%	.22	.10	15.65
Na_2O	5.0	6.49	6.91	6.5%	6.34	7.72	3.38
K_2O	10.0	4.80	4.78	-.4%	4.65	5.08	.00
Proportions:					54.40%	44.25%	1.22%
Sensitivity:					-.47	-.39	-.42

calc - calculated composition, diff - difference between observed and calculated compositions, feld - feldspar, cpx - pyroxene,
ol - olivine.

poor; similarly attempts to model a fractionation series from trachyte through Oiau type to Numanuma type comendites were not successful. Moderately good results were achieved in deriving crystalline comendite 713 and glassy comendite 739 from trachyte 711. The calculations (Table 9-8) indicate that fractionation of 40-50% of feldspar could produce these comendite compositions from the trachyte. The discrepancy between calculated and natural derivative end member in both of these calculations is better than 1% for all oxides except Fe_2O_3 and TiO_2. Derivation of glassy comendite 722 (Oiau type) from trachyte 711 (Table 9-8) was less successful and in particular the ferromagnesian oxides showed large discrepancies. Large discrepancies were also obtained in deriving comendite (Numanuma type) 739 from comendite 719 (Oiau type). It is significant that a single stage trachyte-comendite series was reasonably closely modeled and that it was not possible to calculate a reasonable multi stage fractionation series from trachyte through to the most siliceous comendite.

Chemical variations in the Dawson Strait suite.

The Dawson Strait suite displays regular variations in chemical composition (Figure 9-9); thus with increase in SiO_2 there is a decrease in TiO_2, Al_2O_3, total iron, MnO, MgO, CaO and P_2O_5 and an increase in K_2O, from the basalts to the Oiau type comendites. Na_2O increases with SiO_2 from the basalts to the trachytes and then decreases; total iron and MnO trends also show a reversal and are positively correlated with SiO_2 in the Numanuma type comendites. Trace element abundances show a similar pattern. Rb, Pb, Th, U, Zr, Nb, Y, La, Ce, Zn and to some extent Ga show a positive correlation with SiO_2. Ba increases through the series from basalts to trachytes and then undergoes a spectacular reversal in trend and is absent from the most siliceous comendites. K/Rb ratios decrease from variable but generally moderately high values (mainly 400-700) in the basalts to lower values (200-400) in the comendites.

Some insight into the process of crystal fractionation which may have produced the Dawson Strait series can be gained by an examination of the behaviour of individual elements on variations diagrams using the concentration of a residual element as the absissa. This approach was suggested by Barberi and others (1975) and has an advantage over more commonly used indices of differentiation (solidification index, differentiation index, SiO_2) in that it more closely reflects the position of a particular rock in the series. On such diagrams, elements
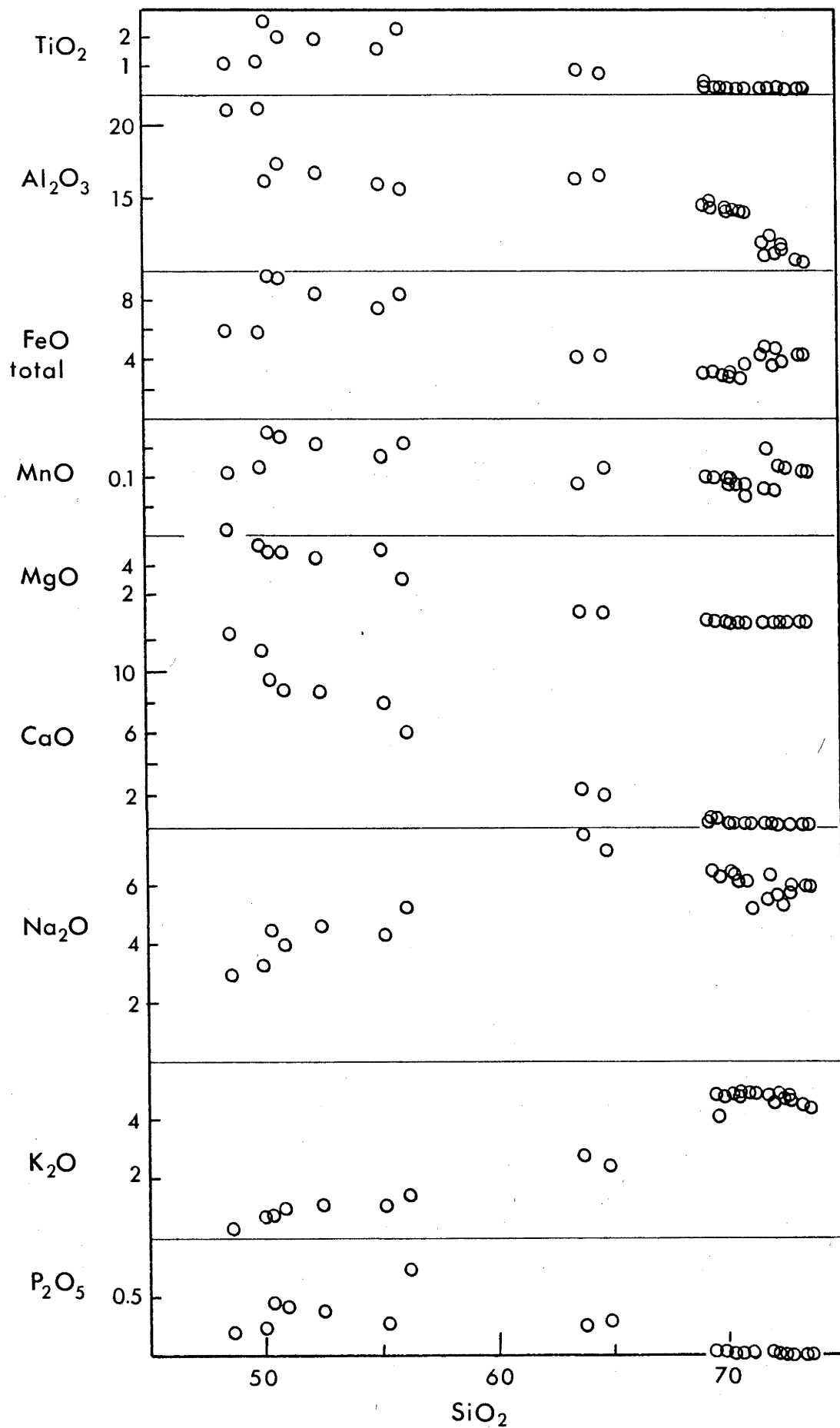
FIGURE 9-9: Compositional variations in the Dawson Strait suite.
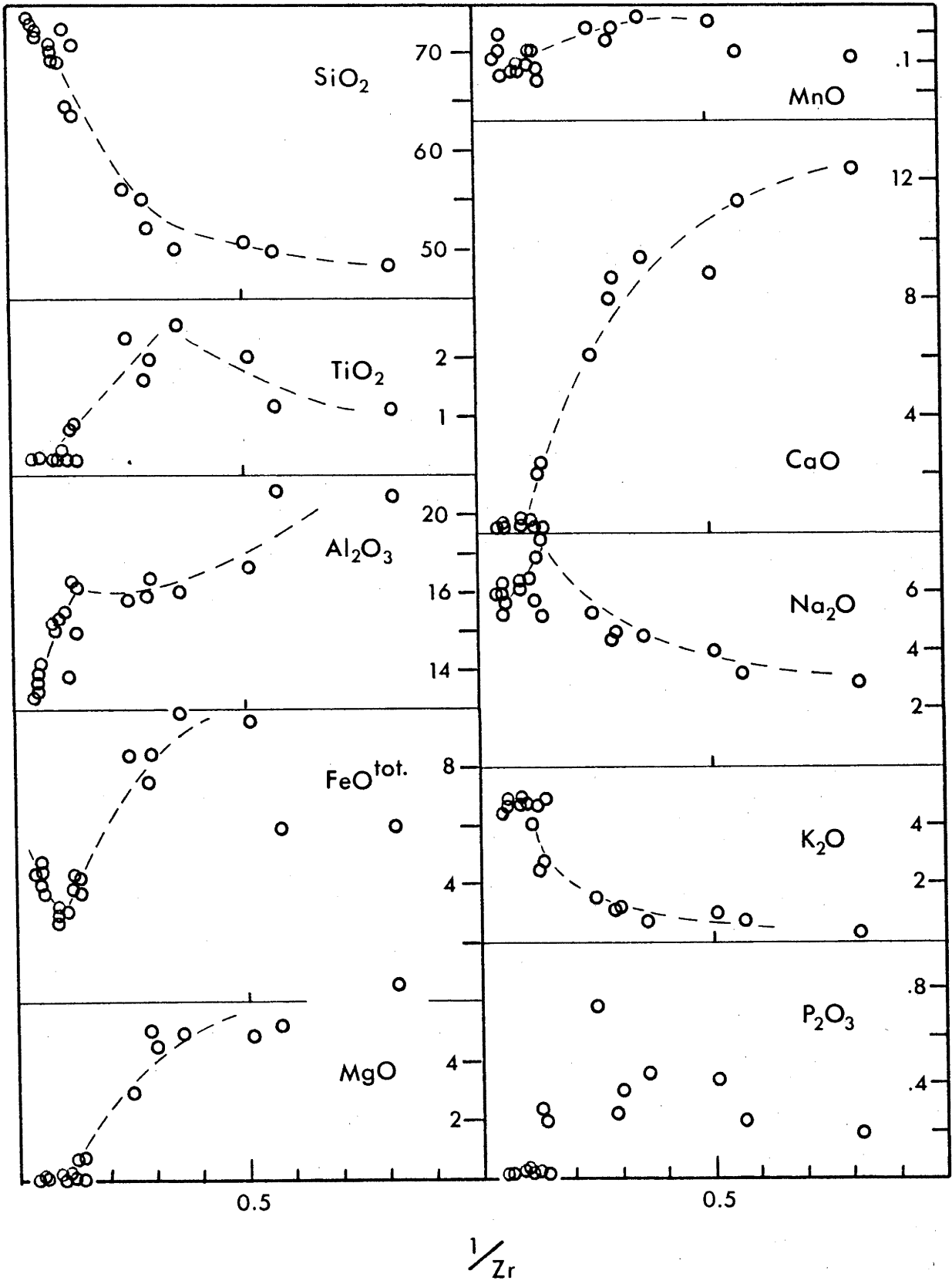Major elements against SiO_2 (wt.%)

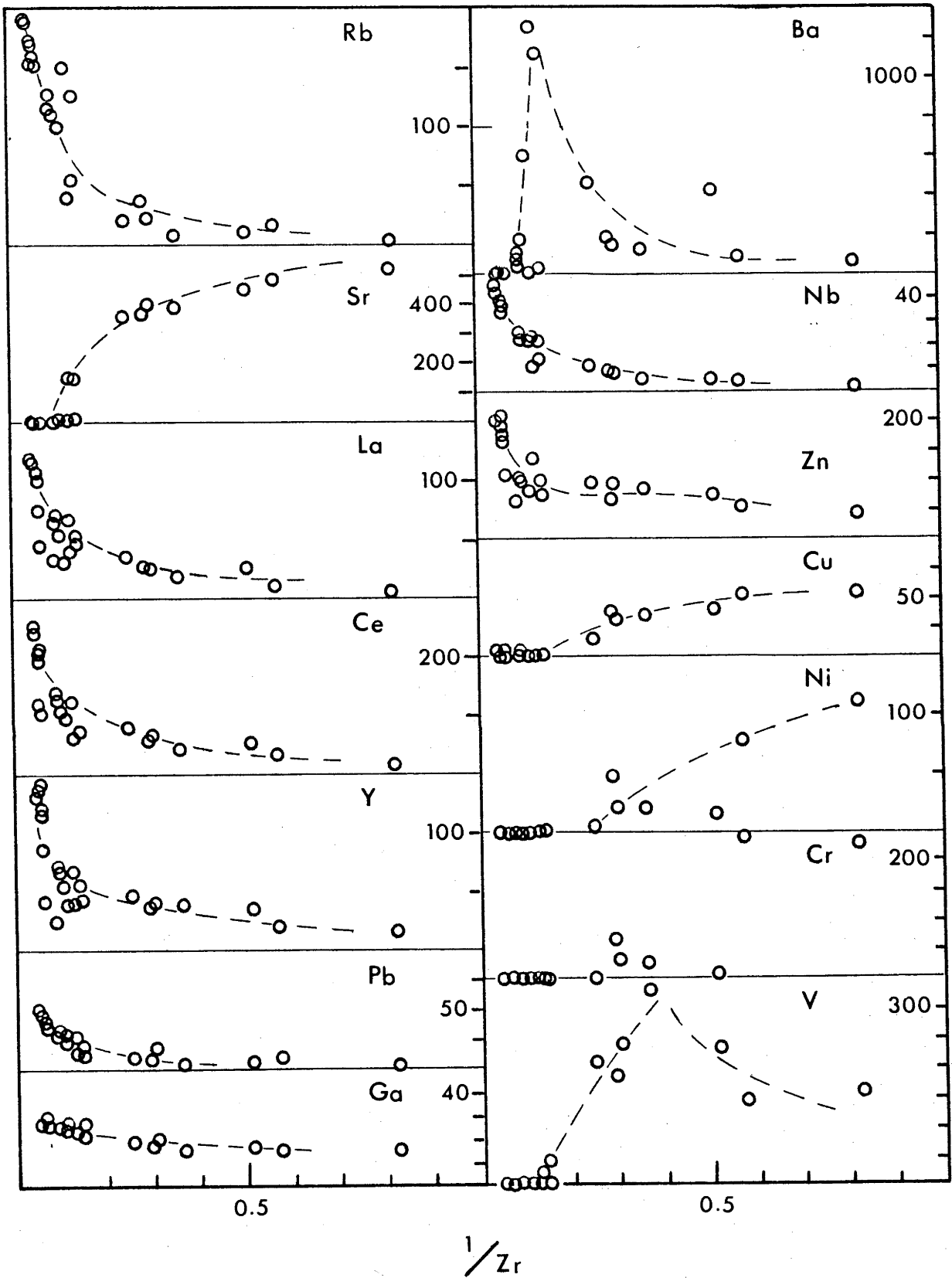FIGURE 9-10: Compositional variations in the Dawson Strait suite. Major elements (wt.%) against 1/Zr.

FIGURE 9-10 (continued): Compositional variations in the Dawson
Strait suite.
Trace elements (ppm) against 1/Zr.

with essentially residual behaviour show smooth variation curves whereas
the distribution of non residual elements is marked by discontinuities.
These discontinuities reflect changes in the solid-liquid partition
coefficients which are due to changes in the nature of the crystallising
phases.

The main chemical variations in the Dawson Strait rocks are illust-
rated in Figures 9-9 and 9-10. Variation curves through the most fractionated
rocks (comendites) are drawn through glassy specimens. A significant
trend on these diagrams is the smooth trend for CaO and Sr toward extreme
depletion in the comendites. MgO shows a similar pattern to CaO reflecting
fractionation by olivine or pyroxene or probably both. Both TiO_2 and V
show similar patterns of behaviour each showing an increase to the
mugearite and a decrease to the comendites. Although V is known to
enter pyroxenes (Taylor, 1966) this parallel behaviour suggests that in
this case its relative abundance has been controlled by the appearance
and subsequent fractionation of an oxide phase probably titanomagnetite.
There is a marked discontinuity in the Al_2O_3, Na_2O and Ba patterns at the
trachyte stage. This is particularly the case with Ba which shows extreme
enrichment in the trachytes and then becomes totally depleted in the
comendites. Ba will enter both biotite and alkali feldspar (Taylor, 1966)
but, biotite is not known from any of the Dawson Strait rocks and so Ba is
progressively enriched in successive melts until anorthoclase becomes an
early crystallising phase. The discontinuity in the Ba distribution
curve is due to a change in the nature of the major fractionating phase
from plagioclase to anorthoclase. Extreme Ba depletion in the comendites
reflects the strong preference of Ba for early K sites (Taylor, 1966).
Change in the nature of the fractionating feldspar is probably also the
cause of the discontinuities in the Al_2O_3 and Na_2O curves.

Late enrichment in both total iron and MnO in the comendites
suggests a change in the nature of fractionating ferromagnesian phases
which is not easy to correlate with petrographic observations. A likely
explanation is that because of low activities these elements have behaved
in a residual fashion and have been retained in the melt.

Behaviour of trace elements during fractionation

The behaviour of individual trace elements during fractionation
of the Dawson Strait series can in general be described as residual,
feldspar controlled, ligand field stabilised or ligand field unstabilised.
Residual behaviour is clearly demonstrated by Zr and Nb; Th, U, Y, La,
Ce and Cl, also display residual behaviour but their abundances in

crystalline comendite appear to have been modified by late stage processes.

The behaviour of Sr and Ba is closely related to feldspars and sensitive to feldspar composition. Sr enters plagioclase in preference to clinopyroxene (Brooks, 1968) and will also readily enter alkali feldspar. Fractionation of feldspar results in almost total depletion of Sr even in the less siliceous comendites (Oiau type). Ba on the other hand will not readily enter plagioclase so that early fractionation of the series produced progressive enrichment. Ba has strong affinity for alkali feldspar so with the appearance of anorthoclase as an early crystallizing phase in the Dawson Strait series the element is fractionated out of the liquid. Only in the more siliceous comendites (Numanuma type) does Ba become completely depleted. It could be expected that with the appearance of early crystallizing anorthoclase Rb might also be preferentially partitioned out of the liquid. However, in this suite and in other peralkaline suites (Weaver and others, 1972) Rb does appear to have residual behaviour.

Ca is a major element in both plagioclase and pyroxene. If plagioclase is the only fractionating phase then preferential incorporation of Sr into plagioclase will reduce the Sr/Ca ratio in successive liquids but if plagioclase is accompanied by calcium bearing pyroxene which will not take up Sr then the Sr/Ca ratio in successive liquids may remain constant or even increase depending on the relative rate of removal of the crystalline phases. Olivine fractionation will not affect the Ca/Sr ratio but because both are Mg-bearing phases, similar arguments can be used to estimate the relative importance of these two elements.

In the Dawson Strait suite, trends of Sr/Ca and Ni/Mg when plotted against Zr indicate that clinopyroxene and olivine have been significant fractionating phases in the early evolution of the series (basalt to hawaiite) but in the later stages (hawaiite-trachyte) plagioclase has become dominant. Relatively high Cr and Ni in the two accumulative basalts support the fractionation of pyroxene and olivine.

The transition elements have two types of behaviour. Those which are highly stabilised by the ligand field in octahedral sites are strongly partitioned into early crystallising minerals and become depleted in more fractionated members of the series. Ni and Cr exhibit this type of behaviour although among the more basic members of the series accumulation of olivine and pyroxene may distort the trends. Ni and Cr are totally

depleted in the trachytes and the comendites. V might be expected to display similar behaviour because it is known to enter pyroxene structures (Taylor, 1966). However, in these rocks it shows initial enrichment to the mugearite followed by total depletion in the comendites. TiO_2 behaves in a similar fashion and this parallel behaviour suggests a control by the appearance and subsequent fractionation of an oxide phase probably titanomagnetite. Precipitation of an oxide phase and subsequent removal of V at an intermediate stage in differentiation can probably be correlated with a change in P_{H_2O} and f_{O_2} conditions.

Cu and Zn provide examples of transition elements which are weakly or not stabilised in the Ligand field and which will therefore show variable behaviour during fractionation (Barberi and others, 1975). In the Dawson Strait series Cu behaves in an orderly fashion becoming progressively depleted through the series to the trachytes in which Cu was below detection limits. This behaviour essentially parallels that of total iron which can theoretically be expected to show similar behaviour (Burns, 1970). Although Treuil and others (1971) have observed that Cu is not readily incorporated into silicates the regular variation displayed by the element in the Dawson Strait Series suggests a control by one of the major fractionating phases; it is suggested that in this suite the behaviour of Cu is controlled by the behaviour of oxide phases. Zn in the Dawson Strait series has behaved essentially as a residual element and becomes enriched in the most fractionated comendites. From theoretical considerations Zn might be expected to enter late Fe^{2+} positions so that although the behaviour of the two elements should be closely correlated the Zn/Fe^{2+} ratio should increase during fractionation. However, there is some doubt about the amount of Zn which actually enters silicate mineral structures and it is possible that much of the content of the element measured in rocks is held in a sulphide phase (Taylor, 1966). The later stages of fractionation of the Dawson Strait series are thought to have taken place under conditions of relatively low f_{O_2} which have been shown experimentally (Haughton and others, 1974) to decrease the solubility of sulphur in magmas and inhibit the formation of a sulphide phase. The observed behaviour of Zn in the Dawson Strait comendites is thus consistant with conditions of falling f_{O_2} assuming that Zn does not enter significantly into silicate phases. Pb appears to behave in much the same manner as Zn probably for similar reasons.

Ga shows a trend of minor enrichment through the Dawson Strait

series, which is surprising because of the generally assumed coherence between Al and Ga (Taylor, 1966). The work of Goodman (1972) has shown that Ga can enter both Fe^{3+} and Al^{3+} sites and that the Ga-Al coherence is not as pronounced as has been hitherto assumed. Ga has strong affinities for tetrahedral coordination and is typically concentrated in early formed plagioclase and magnetite. Although Ga enters plagioclase the Ga x 10^4/Al ratio is typically low (0.96 - 1.89) indicating a preference for Al. This data (Goodman, 1972) has been determined for basaltic volcanic rocks and is at variance with the pattern of enrichment observed in late differentiates of the Dawson Strait series. Although Goodman has observed that Ga is increasingly concentrated in later plagioclase the enrichment in late differentiates controlled by removal of alkali feldspar suggests that anorthoclase/liquid partition coefficients are >1.

REE elements show progressive enrichment and progressive fractionation of light relative to heavy REE throughout the comendites. The extreme enrichment in La and Ce in the most fractionated comendites is consistent with the apparent residual behaviour of these elements. The negative Eu anomaly in the comendites supports an hypothesis of extreme plagioclase fractionation and the relative enrichment of Yb relative to Gd indicates that pyroxene has been a significant fractionating phase.

A limitation on the extent to which crystal fractionation processes could have operated is indicated by REE abundances in trachyte 710 (Figure 9-5). Although the REE abundance patterns in the Numanuma-type comendites are consistent with fractionation from the trachyte, the abundances in the Oiau-type comendites are lower than those in the trachyte and cannot be explained by removal of crystals.

Feldspar-liquid relationships

When the effects of feldspar fractionation are considered in three dimensions one important constraint which emerges is that any liquid fractionating a binary solid solution must remain within the compositional plane defined by itself and the two end members of the solid solution (Bailey and Macdonald, 1969). This means that in a series fractionating only alkali feldspars the initial liquid composition, the feldspar compositions and the compositions of successive derivative liquids must be colinear. The series is thus constrained to a

triangular plane, based on the Ab-Or join, in which the three variables are SiO_2, Al_2O_3 and total alkalies; the position of this plane within the quaternary system can be described by the molecular ratio of excess alkalies (mol. $(Na_2O + K_2O - Al_2O_3)$ / mol. $(SiO_2 - 6Al_2O_3)$) (Bailey and Macdonald, 1969).

In the ternary projection SiO_2-Al_2O_3-Na_2O+K_2O the alkali feldspar join plots as a point, and planes radiating from the join project as lines. A series of liquids whose compositions are controlled by fractionation of alkali feldspar from a common parent will form colinear series of points on this projection. When plotted on this ternary projection (Figure 9-11) the Numanuma type comendites form a trend which is colinear with tie lines to coexisting feldspar phenocyrsts; the Oiau and Sanaroa type comendites lie on this trend but tie lines to coexisting feldspar phenocyrsts lie at a small angle. The comendites with the trachytes define a trend curving from the non-peralkaline field into the peralkaline field; a similar trend is defined by coexisting feldspar phenocrysts. Successive compositions within the peralkaline field are controlled by fractionation of alkali feldspars with peralkalinity indices only slightly less than one, and define a trend which leads into the Ab-Or cotectic zone.

The increase in SiO_2 and peralkalinity in the Dawson Strait rocks is correlated at least in the less fractionated comendites by an increase in K_2O relative to Na_2O in both whole rocks and their feldspar phenocrysts. In contrast the alkali ratios of feldspar phenocrysts in the Numanuma type comendites are either the same or slightly more potassic than their host whole rock compositions (Figure 9-11). This phenomenon places severe restrictions on the K_2O/Na_2O ratios of more evolved liquids and it has been suggested (Thompson and Mackenzie, 1967) that crystallisation and fractional crystallisation under these conditions is controlled by a low temperature zone in the system SiO_2-Al_2O_3-Na_2O-K_2O.

The shape of this low temperature zone can be indicated using methods of projection developed by Roux and Varet (1975) assuming that it lies on the albite rich side of the fractionation curve (Figure 9-13). An important feature of the fractionation curve (and by implication the low temperature zone) is the suggestion of a negative slope for the upper part of the curve. In other words fractionation in the Dawson Strait rocks leads to an increase in K_2O/Na_2O ratio in more peralkaline rocks but once the series enters into the low temperature zone this
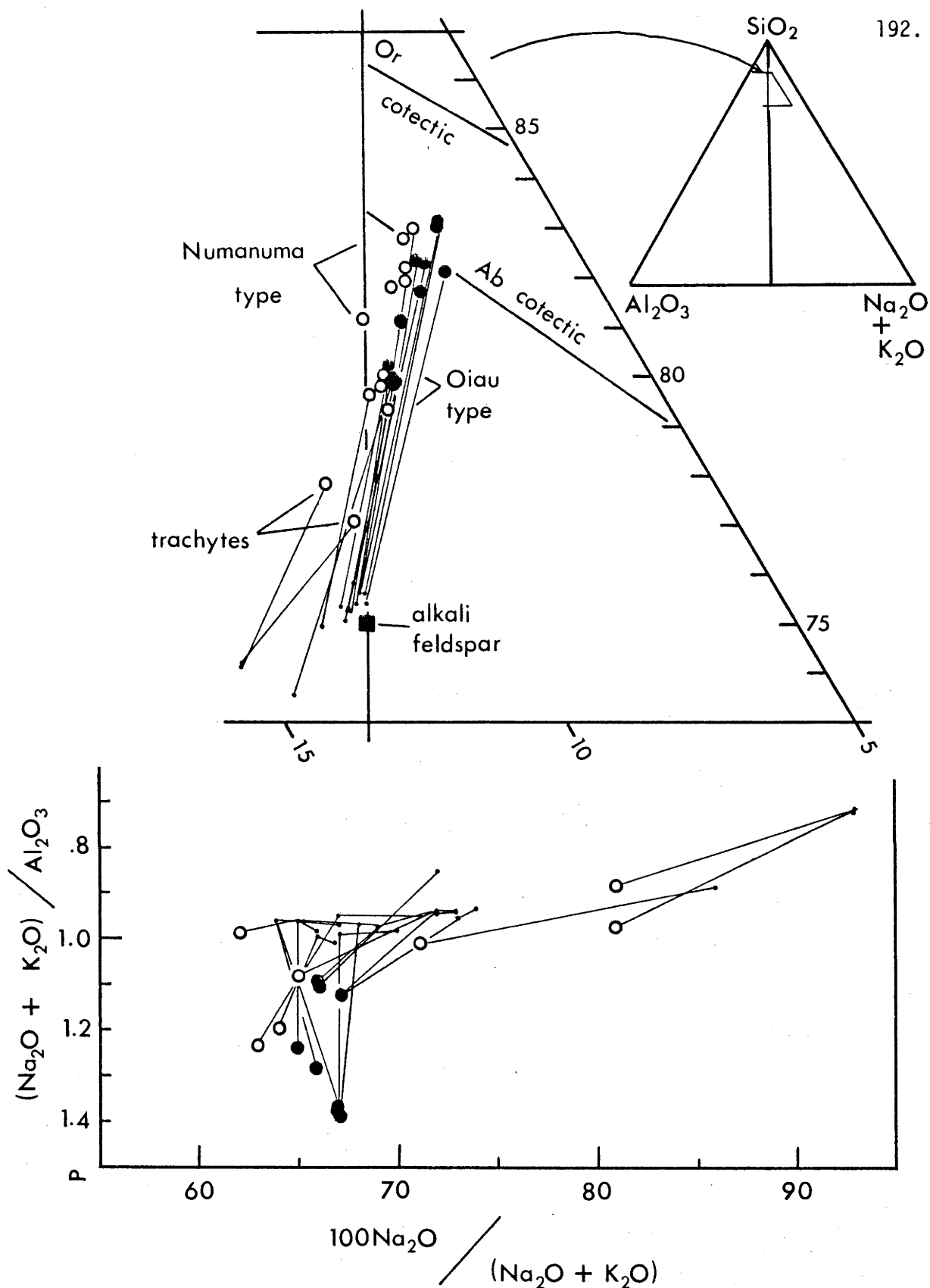
FIGURE 9-11: Feldspar - liquid relationships.

Upper-part of the ternary system SiO_2-Al_2O_3-Na_2O+K_2O (molecular percentages) showing the relationship between whole rock and feldspar phenocryst compositions. Tie lines join feldspar compositions with the composition of their host rock

Lower-variation in sodium/potassium ratio (molecular percent) with respect to peralkalinity. Tie lines join feldspar compositions with the composition of the host rock.

Open circles-crystalline, solid circles-glassy specimens.

DAWSON STRAIT COMENDITES
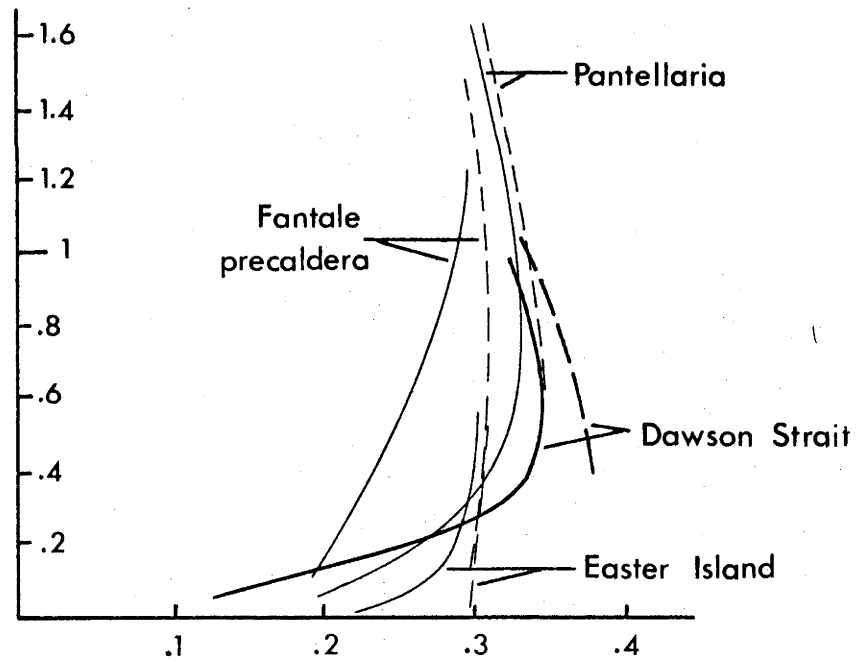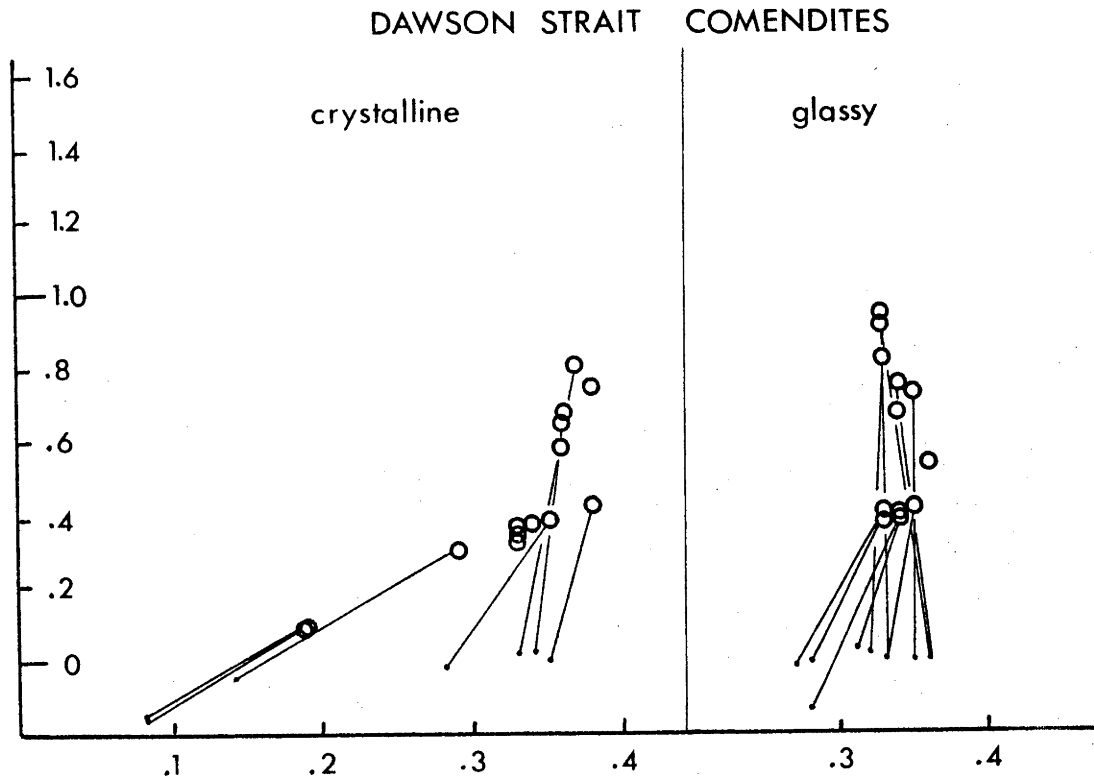
FIGURE 9-12: Variation in alkali ratio with respect to the excess
SiO_2 relative to an alkali feldspar composition. (after
Roux and Varet, 1975).

X axis - $K/(Na+K)$, Y axis - $(Si/3Al)-1$.
In the upper part of the figure tie lines join feldspar
compositions with the composition of the host rock.
In the lower part of the figure solid lines are the
inferred fractionation curve for each series and the
dashed lines represent their respective thermal valleys.

trend is reversed and successive liquids will become more sodic. Thus the most peralkaline liquids would be expected to be highly sodic and to contain relatively potassic feldspar. This behaviour has been observed in peralkaline rhyolite suites from Mayor Island, N.Z. (Ewart and others,1968) Pantelleria (Nicholls and Carmichael, 1969b) Fantale, Ethopia (Gibson, 1972) and Boina (Barberi and others, 1975).

Fractionation curves in the system SiO_2-Al_2O_3-Na_2O-K_2O can enter the low temperature zone from both sodic and potassic parental compositions (Thompson and Mackenzie, 1967) and there are natural examples of both sodic and potassic suites leading to peralkaline rhyolitic compositions (section 9-6). However regardless of their parentage, strongly peralkaline liquids will apparently always crystallise relatively potassic feldspar so that successive liquids will become strongly sodic.

9-5   One Series?

The major and trace element compositions of the comendites in the Dawson Strait area are consistent with a model of fractional crystall-isation and this process has been tacitly assumed in much of the preceeding disucssion. The fact that fractional crystallisation can be so closely modelled is an important feature of the suite but there are several lines of evidence which indicate that the comendites with their associated rocks represent a number of closely similar but nevertheless distinct series.

Basaltic and intermediate rock types are found only associated with Oiau type comendites on Dobu Island and probably represent fragments of related but older basalt rather than parental magma. Trachyte is found only associated with Numanuma type comendites and quantitative calculations show that they may represent a parental composition. Although the Numanuma type comendites are more fractionated than the Oiau type they are older so it is unlikely that they represent a series of increasingly fractionated liquids. The comendites from Sanaroa Island are in many respects intermediate between Oiau and Numanuma type comendites but anomalous abundances of some trace elements (e.g. Zr, Nb, Cl, Rb) suggest that they may form a distinct group.

If the Numanuma-type comendites are related to a trachyte parent similar to the composition of trachyte 710 then the REE pattern of this specimen offers a limitation on the operation of a fractional crystall-isation process. The distinctive features of the chemical compositions of comendites, namely, peralkalinity, very low Ba and Sr and the large negative Eu anomaly can only be explained by extensive feldspar

fractionation. It is commonly assumed that these features develop only in series which fractionate feldspar from an early stage. However, the small Eu anomaly measured in trachyte 710 indicates that feldspar fractionation has not been a significant fractionating phase in low-Si members if the trachyte is a derivative composition. It is suggested that the distinctive features of the comendites can be explained by fractionation of feldspar from a trachytic composition and that there is no need to invoke removal of feldspar from basaltic compositions.

The relative REE abundnaces preclude fractionation of a composition represented by trachyte 710 leading to the Oiau-type comendite composition. Fractionation of the early crystallising phases in the trachyte will inevitably enrich derivative liquids in the REE whereas the Oiau-type comendites have REE abundances which are lower than those in the trachyte.

$^{87}Sr/^{86}Sr$ ratios

$^{87}Sr/^{86}Sr$ ratios of three Oiau-type comendites and three of the associated rocks are presented in Table 9-9. In view of the strong geochemical evidence for a close genetic relationship the spread in ratios shown by these samples is surprising. The two basaltic specimens (706, 708) show ratios which are identical to within experimental error. These ratios are close to the lower end of the range for basaltic rocks in the oceanic islands reported by Gast (1967). Strontium in trachyte 710 is significantly more radiogenic than that in the basaltic rocks. Model age calculations based on an initial $^{87}Sr/^{86}Sr$ ratio of .7031 give an unacceptably high age (46 m.y.) for this trachyte which shows clearly that it is not comagmatic with the basaltic rocks. Comparable differences in the $^{87}Sr/^{86}Sr$ ratios of basaltic rocks and closely associated more 'evolved' rocks are common in Gast's (1967) documentation of ocean island values; these are clearly not due to differences in age and suggest that the source region for ocean island lavas has undergone an early fractionation event and is isotopically heterogeneous. This conclusion is supported by the work of Sun and Hanson (1975) who present evidence for a fractionation event which preceeded the magma generative event by 1000 to 3000 m.y. It is suggested that the differences between the $^{87}Sr/^{86}Sr$ ratios in the trachyte and those in the associated basaltic rocks are not inconsistent with either the close geochemical relationship or the notion that all three are members of a genetically significant association.

The most surprising feature of the data presented in Table 9-9 is the spread in values measured in the three Oiau-type comendites. The

TABLE 9-9   STRONTIUM ISOTOPE DATA ON ROCKS FROM THE DAWSON STRAIT AREA

Rock No	Rock type	Rb	Sr	Rb/Sr	$^{87}Rb/^{86}Sr$	$^{87}Sr/^{86}Sr$	model age
706	basalt	10	391	.026	.074	.70312±2	
708	hawaiite	39	372	.105	.303	.70309±2	
710	trachyte	56	156	.359	1.039	.70378±3	46 m.y. (assumed initial ratio .7031)
718	comendite	107.3*	2.021*	53.093	153.2	.7104±4	2.8 m.y. (assumed initial ratio .7042)
725	comendite	114.2*	3.084*	37.030	106.9	.7042±3	(assumed initial ratio .7042)
728	comendite	114.5*	3.250*	35.138	101.6	.70513±2	.65 m.y. (assumed initial ratio .7042)

* Rb and Sr determined by mass spectrometry, remainder by X-ray fluorescence

three samples are from Dobu Island and were collected from topographic features which appear to be related to the most recent volcanic activity on the island; specimen 718 is from a small cumulo dome in the main crater, 725 is from a lava flow at the eastern end of the island and 728 is from a lava flow on the northern flank of the main cone which probably represents the most recent magmatic event from the volcano.

These three Oiau-type comendites have calculated model ages which are quite distinct (Table 9-9). The absolute values of these ages are not significant because of the uncertainty in initial ratios. Because of topographic evidence which shows that the comendite flows are very young the initial ratio is probably close to that of comendite 725 (.7042) and the indicated ages of comendites 725 and 728 are consistent with the available evidence that they were erupted in very recent times. If the assumed initial ratio is approximately correct then the model 2.9 my age for comendite 718 is inconsistent both with the geomorphic evidence that it was erupted in very recent times and with the geochemical evidence that it is closely related to the other comendites.

Variable $^{87}Sr/^{86}Sr$ ratios in suites of apparently comagmatic rocks are apparently a feature of peralkaline rhyolite associations (e.g. Dickinson and others, 1969; Dickinson and Gibson, 1972; Ferrara and Treuil, 1975). Explanations for this feature involve contamination by equilibration with crustal rocks or ground water (e.g. Noble and Hedge, 1969) or fractionation of Sr isotopes during a late stage in fractionation of the magma (Dickinson and Gibson, 1972; Ferrara and Treuil, 1975). Dickinson and Gibson (1972) suggested that the variation they observed in $^{87}Sr/^{86}Sr$ ratios of pantellerites from Fantale volcano could be explained by enrichment in Rb relative to Sr and hence ^{87}Sr relative to ^{86}Sr during feldspar fractionation and that this enrichment could become measureable in peralkaline rhyolites because of their characteristic extreme Sr depletion. This model which requires that members of a comagmatic series linked by feldspar fractionation lie along an isochron cannot be applied to the three comendites from Dobu Island.

Comendite 718 with an apparently anomalously high $^{87}Sr/^{86}Sr$ ratio (.7104) is crystalline, the other two are obsidians. Although comendite 718 is apparently fresh, geochemical evidence was presented earlier which showed that mobile components are lost from comendite magma during crystallisation. The high $^{87}Sr/^{86}Sr$ ratio cannot be explained by differences in age because of topographic evidence which indicates that the comendite was erupted in very recent times and it is suggested that

the late magmatic processes associated with crystallisation of the comendite may also have modified the initial strontium isotope ratio.

The hypothesis that Sr isotopes can be fractionated as a result of petrogenetic processes which give rise to peralkaline rhyolites is attractive because of the extremely high Rb/Sr ratios and very low Sr contents which characterise these rocks. Although Dickinson and Gibson's (1972) simple feldspar fractionation model does not appear relevant to the Dawson Strait comendites there may be fractionation in the source region. The Sr isotope data available to this study are not sufficient to allow discussion of this possibility, but the alternative that three comendites of closely comparable chemical compositions collected from demonstrably youthful topographic features forming part of a small Recent volcano are not closely related is unacceptable.

9-6   Nandewar Volcano - A Comparison

The Nandewar Mountains, N.S.W., Australia are the remains of a Miocene alkaline volcano whose products range from olivine basalts to peralkaline rhyolites. The volcano has been studied by Abbott(1965, 1969) and provides an interesting comparison to the Dawson Strait series and to other suites which include high-Si peralkaline rocks. To this end, trace element abundances have been measured on Abbott's rock powders (housed in the collection at Department of Geology, A.N.U.) and these are presented with previously published major element analyses (Abbott, 1969) in Table 9-10.

Nandewar Volcano consists of a basaltic shield made up mainly of hawaiite, mugearite and benmoreite with rare olivine basalts; trachyte was erupted during the later stages of shield development, and trachyte, comendite and alkali rhyolite were associated with a final post-caldera episode of activity. The whole sequence of rocks has been interpreted as a series controlled by fractional crystallisation leading from basaltic parental compositions to   peralkaline high-Si end-members. Abbott suggested two series in the Nandewar volcano,one through peralkaline trachyte to comendite and the other toward 'alkali rhyolite' (with mol $(K_2O+Na_2O)/Al_2O_3<1$).

Trace element abundances

Trace element abundances in the Nandewar rocks are in general comparable to abundances found in the Dawson Strait series. Extreme depletion in Ba and Sr coupled with marked enrichment in Th, U, Zr, Nb, Y, La, Ce and Ga support the hypothesis of an origin by prolonged crystal

TABLE 9-10: MAJOR AND TRACE ELEMENT ANALYSES OF ROCKS FROM NANDEWAR VOLCANO.

Rock No.	789	790	792	791	793	795	796	799	800	801	802	803	806	808	809
wt.%															
SiO_2	47.51	47.98	49.30	49.31	50.35	53.36	53.76	56.42	60.14	62.90	65.59	68.26	72.70	73.46	73.82
TiO_2	2.82	2.40	2.76	2.20	2.48	1.80	1.80	1.46	.77	.41	.41	.34	.13	.25	.26
Al_2O_3	16.85	17.53	17.60	14.82	15.89	16.04	16.27	16.93	17.07	16.15	16.45	13.95	13.20	13.91	14.31
Fe_2O_3	4.25	4.06	5.12	4.27	5.92	5.71	4.75	3.50	2.63	1.37	2.11	2.47	2.60	.96	.60
FeO	6.71	5.09	4.78	6.40	5.07	3.73	4.99	4.07	2.98	3.09	1.62	2.34	.54	.09	.07
MnO	.15	.15	.13	.16	.17	.20	.21	.09	.16	.14	.08	.14	.05	.0	.0
MgO	5.62	5.27	3.03	7.45	4.10	2.73	1.89	2.71	.78	.61	.14	.07	.08	.13	.45
CaO	9.28	9.70	8.58	7.83	6.68	5.10	5.16	5.06	2.76	1.83	.36	.68	.09	.04	.11
Na_2O	3.47	3.73	4.17	3.60	4.68	4.24	5.80	5.65	4.87	6.17	7.02	6.26	6.01	5.33	4.73
K_2O	1.08	1.43	2.06	1.90	2.51	3.36	3.19	3.07	5.26	5.57	5.57	5.17	4.50	5.27	5.35
P_2O_5	.93	.69	1.04	.75	1.30	.92	.96	.52	.31	.17	.07	.03	.04	.08	.11
Loss	.60	2.31	.90	1.20	.70	1.93	1.05	.97	.50	.39	.27	.39	.50	.30	.22
Total	99.27	100.34	99.47	99.89	99.85	99.12	99.83	100.45	98.23	98.8	99.69	100.10	100.44	99.82	100.03
ppm.															
Ba	822	505	579	592	735	1338	623	1606	1385	475	0	0	0	0	26
Rb	17	33	36	39	49	66	42	68	69	102	111	124	327	180	154
Sr	787	831	847	607	740	625	607	408	202	66	2	2	4	3	8
Pb	42	113	23	18	6	12	8	15	12	16	15	15	36	25	13
Th	0	1	2	3	5	4	3	10	6	15	14	16	48	24	20
U	0	1	1	1	2	1	1	3	2	4	3	2	10	10	7
Zr	129	200	226	213	324	385	281	504	335	905	682	633	1468	914	787
Nb	25	34	38	44	60	63	47	84	46	76	108	94	266	125	111
Y	17	17	24	20	32	36	29	40	24	36	139	119	105	61	50
La	24	33	38	32	51	63	41	54	44	65	279	227	45	115	49
Ce	68	70	85	73	112	143	93	109	90	145	486	178	165	189	127
V	183	162	196	170	110	43	204	32	7	0	0	0	0	0	0
Cr	77	85	0	146	0	0	0	5	0	0	0	0	0	0	2
Ni	72	89	20	124	1	6	13	27	8	9	7	0	11	4	7
Cu	41	40	19	38	8	9	19	9	7	3	10	0	0	0	0
Zn	317	152	127	151	126	197	139	160	107	136	208	188	353	77	33
Ga	21	20	22	21	22	26	23	26	24	27	31	29	45	32	31

Major element analyses from Abbott (1968), rock numbers prefix 15- are from the Department of Geology (ANU) collection

fractionation. Progressive depletion in the ligand field stabilised transition elements is also compatible with the hypothesis. Zn, Cu and Pb display abundance patterns which are similar to, although not as simple as, those in the Dawson Strait series. Consideration of Zr and Nb as a residual element pair supports Abbott's suggestion of the existence of two series in the Nandewar volcano. On a Nb/Zr plot (Figure 9-13) almost all of the analysed rocks lie along a well correlated (r = .99) regression line indicating a series from basalt through peralkaline trachyte to alkali rhyolite. The two rocks which lie off this line are a trachyte and a comendite which together may represent a distinct series.

Peralkaline differentiates

The more differentiated trachytes as well as the comendites and alkali rhyolites contain only one feldspar, an alkali feldspar. Fractionation of alkali feldspar, with a peralkaline index close to one, from a trachytic liquid which is only slightly peralkaline (peralkaline indices <1.1) will produce more siliceous derivative liquids which are only slightly more peralkaline than the parental composition. This contrasts with a trend toward more strongly peralkaline derivative liquids which would result if plagioclase or alkali feldspar with a significant An component continued as a major fractionating phase to more siliceous compositions as in the Dawson Strait series.

The alkali rhyolites are strongly depleted in total iron, MnO, MgO, CaO and related trace elements compared with the trachytes which suggests that fractionation of mafic phases has played an important role during the late stages of fractionation. This suggestion is supported by the very simple mineralogy (essentially quartz + feldspar) of the alkali rhyolites.

Differences in chemical composition between glassy and closely associated crystalline comendites in the Dawson Strait series indicate that processes operating during the late stages of crystallisation in peralkaline rocks can modify the magmatic composition and in particular can reduce the sodium content of crystalline rocks. The possibility of sodium loss has not previously been considered for the Nandewar series; perhaps because the rocks are only slightly peralkaline the effective sodium loss would be small, however, it can be calculated that an increase of only .45% Na_2O in the alkali rhyolites would have the effect of making them peralkaline.

It is suggested that the main series in the Nandewar Volcano is from basaltic parent through peralkaline trachyte toward slightly

FIGURE 9-13: Nandewar Volcano.
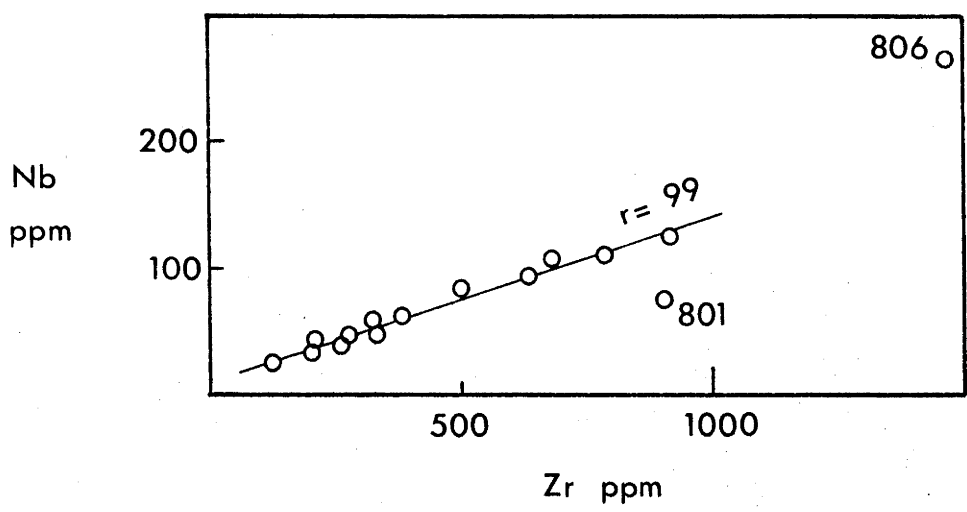
Correlation of Nb with Zr in selected specimens, trachyte 801 and comendite 806 not included.
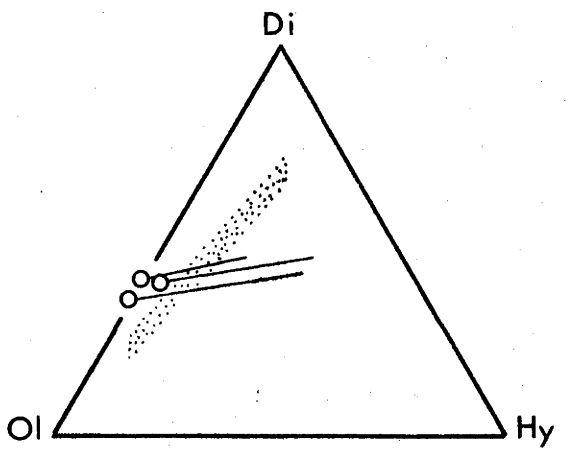
Normative basalt tetrahedron. Open circles are olivine basalts with $Fe_2O_3/FeO=.2$, the end of the line extending to the right marks the position of the samples with the ratio as measured. The low pressure thermal divide is shown stippled.
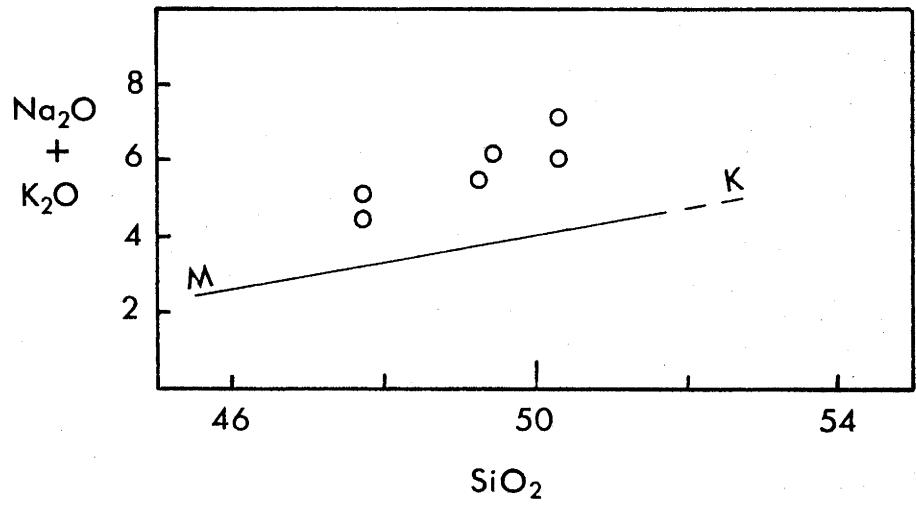
Alkali/silica diagram for basaltic rocks from Nandewar Volcano. M-K divides Hawaiian tholeiitc from alkali rocks. (Macdonald and Katsura, 1964)

peralkaline rhyolites with low Fe content relative to SiO_2. A
second, poorly represented (at least among the analysed specimens)
series includes typical comendites which are generally comparable with
comendites in the Dawson Strait and other series.

A Potassic peralkaline series

The basaltic rocks of Nandewar Volcano are predominantly
fractionated hawaiites and mugearites grading to intermediate benmoreites
but rare olivine basalts are also found. These basalts are mildly alkaline,
hypersthene normative olivine basalts and are transitional in the sense of
Coombs (1963) and Bass (1972) but are distinctly potassic relative to
typical transitional basalts (Figure 9-13). The potassic nature of the
parental basalts is inherited by the silicic differentiates; although
derivative compositions in the Nandewar Suite do become continuously more
sodic during fractionation they approach the low temperature trough in the
system SiO_2-Al_2O_3-Na_2O-K_2O from the potassic side (Figure 9-14). Alkali
ratios in the final Nandewar differentiates are comparable to those in
suites which have entered the low temperature trough from the sodic side
of the system indicating that it is possible for series leading from both
sodic and potassic transitional basalts to end in comparable rock types.
This situation was recognised by Thompson and Mackenzie (1967) but has not
been documented in a naturally occurring suite of rocks.

Tectonic setting

Nandewar Volcano overlies mainly late Palaeozoic sediments which
are part of the New England fold belt forming the central eastern margin
of the Australian Continental block. Tertiary volcanism is considered to
have been located along major fractures formed during upper Mesozoic
compressive movements (Voisey, 1969) and presumably reactivated during
the Tertiary. Opening of the Tasman Sea basin during lower Tertiary
times must certainly have had a major effect on the tectonics of the east
Australian continental margin and the eruption of transitional basalts
and associated rocks is more logically considered in the context of a
rifted continental margin than as part of a volcanic cycle in a stabilizing
continental fold belt.

Although Nandewar Volcano can be related to a tensional environment
this cannot really be compared with the continental or oceanic rift
environment in which comendites are typically located. It may be that this
difference in tectonic setting is the explanation for the potassic nature

FIGURE 9-14: Comendite series.
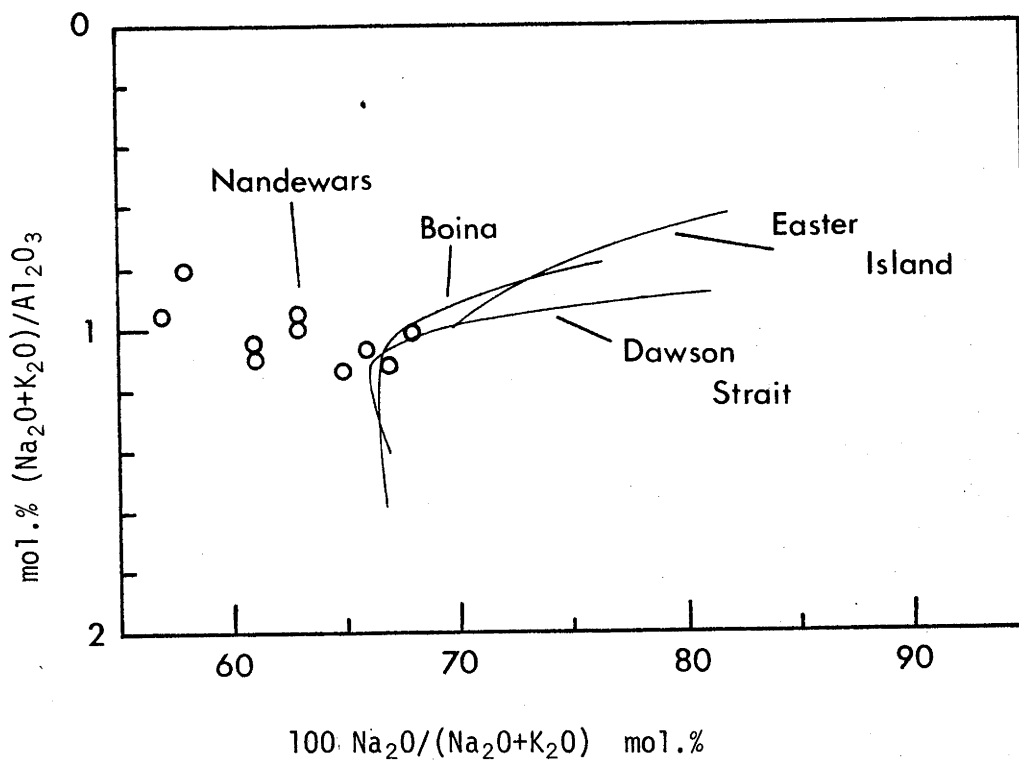
Variation in alkali ratio with respect to peralkalinity in several peralkaline series.
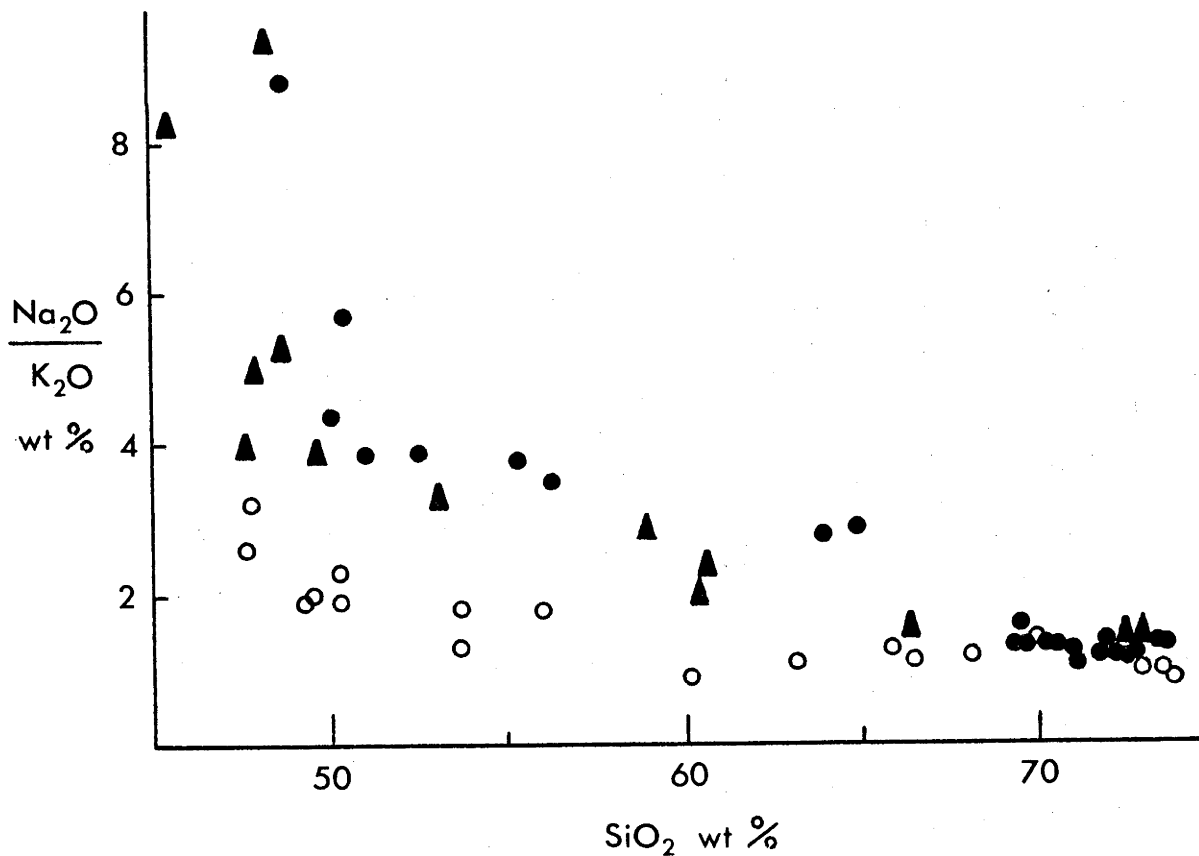
Variation in alkali ratio with respect to SiO_2 in rock suites from Dawson Strait (solid circles), Easter Island (triangles), and Nandewar Volcano (open circles).

of the Nandewar suite.

9- 7   The Peralkaline Rhyolite Association

The association of peralkaline rhyolites with mildly alkaline hy
normative olivine basalt (transitional basalt) was first emphasised by
Coombs (1963). Subsequent work in a number of areas has demonstrated
the operation of fractional crystallisation processes linking the
peralkaline rhyolites with their associated basalts (e.g. Gass and
Mallick, 1968; Cox and others, 1970; Gibson, 1972; Barberi and others,
1975). Even in volcanic provinces where basic and intermediate rocks
are poorly represented it has been argued that the distinctive chemistry
of peralkaline rhyolites points to a process of fractional crystallisation
from a basaltic parent and the transitional basalt-peralkaline rhyolite
association can be inferred (e.g. Ewart and others, 1968).

Peralkaline rhyolites are generally either comendites (less
peralkaline and iron rich, more aluminous) or pantellerites (more peralkaline
and iron rich, less aluminous); only rarely are comendites seen to grade
into pantellerites (e.g. Boina center, Ethiopia; Barberi and others, 1975).
Comendites are the characteristic siliceous products of volcanic islands
located near the crest of active ocean ridges (Ascension, Bouvet, Easter
and Pitcairn Islands, Iceland) and are also found on the continets assoc-
iated with major rifts (Kenya, Ethiopia) or block faulting (Australia,
western United States). As discussed in Chapter 10 the Dawson Strait
comendites are related to an active spreading center. Basalts associated
with the comendites are transitional and poorly alkaline. Pantellerites
are typically found in the continental rift zones but are also known from
oceanic islands rising from extensive submarine plateaux (e.g. Gran Canaria,
Kerguelen, the Azores) or from fracture zones (e.g. Socorro Island) (Baker,
1975). The basalts associated with pantellerites are typically more alkalic
than those associated with comendites and the trend toward
silicic peralkaline rocks may also be paralleled by a trend toward under-
saturated phonolitic members (e.g. Gran Canaria, Kerguelen; Baker, 1975).

It appears that the difference between comendites and pantellerites
is inherited from the basaltic parent. Experimental work (Green, 1971)
indicates that basalts of transitional character can be expected to form
by about 20% melting of mantle material at depths of about 40-60 km;
more alkaline basalts such as those associated with pantellerites probably
originate by a smaller degree of partial melting at slightly greater
depths. Both comendites and pantellerites typically occur in extensional

areas of the earths crust characterised by high heat flow, however, subtle variations in the tectonic regime in these areas of the upper mantle will probably determine the nature of the basalt and hence of the silicic differentiates in the overlying zone.

The most important feature of peralkaline suites is the marked depletion in Al_2O_3. Barberi and others (1971) have suggested that a trend of enrichment in Al_2O_3 could be initiated by early crystallisation of plagioclase relative to clinopyroxene resulting in removal of 'Ca-Tschermack molecule' from the liquid. Experiments (Nesbitt and Hamilton, 1970) demonstrate that the relative order of appearance of plagioclase and clinopyroxene can be reversed by changing the P_{H_2O} which controls the fo_2 conditions in a cooling magma (Hamilton and Henderson, 1968). The composition of the clinopyroxene of undersaturated basaltic magmas has been found to be sensitive to the relative order of appearance of clino-pyroxene and plagioclase if crystallisation takes place at relatively low pressures (Barberi and others, 1971). Early crystallisation of pyroxene results in a Ti-rich clinopyroxene of typical alkaline affinity and subsequent differentiation will yield high alumina trachytes and phonolites. On the other hand the composition of the pyroxene following plagioclase under conditions of low P_{H_2O} will be low in TiO_2 and subsequent removal of the two phases could produce a trend toward Al_2O_3 poor peralkaline differentiates.

This model assumes that the development of peralkaline rhyolites stems from fractionation of basaltic magmas. In fact, although a basalt-comendite series can be modelled in the case of the Dawson Strait rocks there are features which in detail show that they are not a comagmatic series. Geochemical data clearly indicates that fractionation of feldspar has been important in the petrogenetic process which led to the generation of comendite magma but the parental composition could equally have been trachytic in composition. It is suggested that a general petrogenetic model for peralkaline rhyolites could involve the generation of an intermediate parent (trachytic?) by partial melting of pre-existing basalt or of an already fractionated upper mantle source (cf. Green and others, 1974) followed by feldspar fractionation. Although Bailey and Macdonald (1975) have suggested that a volatile phase may be important in the petrogenesis of some African peralkaline rocks, variations in the chemical compositions of the Dawson Strait comendites show no evidence of the operation of such a process.

In comenditic suites peralkalinity is generally reached at about 68% SiO_2; typical Al_2O_3 contents of such comendites are 12-14%. In contrast, pantellerites are commonly associated with peralkaline trachytes (SiO_2 about 65%) and the Al_2O_3 content of pantellerites with 68% SiO_2 is generally less than 10%. The more peralkaline trend observed in pantelleritic suites is presumably related to the differences in parental composition favouring the early crystallisation and removal of plagioclase. The data from the Dawson Strait comendites shows that although plagioclase has been the most important fractionating phase, clinopyroxene fractionation has also taken place.

Crystallisation of quartz as differentiating liquids reach the liquidus minimum the system SiO_2-albite-orthoclase will impose a natural limit on the extent of fractionation of both comenditic and pantelleritic liquids. Experimental work (Carmichael and Mackenzie. 1963; Thompson and Mackenzie, 1967) has shown that the position of the minimum is sensitive to and increases with the ac + ns content of the system (a measure of peralkalinity). Thus mildly peralkaline comenditic liquids are unable to evolve into more peralkaline highly siliceous pantelleritic liquids. The extent of differentiation in peralkaline rhyolites is controlled jointly by the silica content and peralkalinity of the differentiating liquid.

Comenditic associations

The only documented examples of basalt-comendite series in the literature are from Jebel Khariz and Little Aden (Gass and Mallick, 1968; Cox and others, 1970), Easter Island (Baker and others, 1974) and the Nandewars (Abbott 1969); to these can be added the Dawson Strait suite. Differentiation in these suites generally leads to enrichment in K_2O/Na_2O until fractionating liquids enter the low temperature zone in the system SiO_2-Al_2O_3-Na_2O-K_2O at which there is a reversal in trend toward more sodic liquids. An exception to this trend is provided by the rocks from the Nandewars which become progressively more sodic throughout fractionation. This type of behaviour was anticipated by Thompson and Mackenzie (1967) who on the basis of experimental work, predicted that fractionation curves in the system could run into the low temperature zone from both sodic and potassic parental liquids.

An explanation for the behaviour of the Nandewar silicic rocks lies in the relatively potassium rich character of the whole series. The

tectonic setting of the Nandewar suite is not typical of that of other comendite suites and this may explain the differences in parental basalt composition. The importance of the Nandewar result is that it shows the existance of a potash rich transitional basalt to peralkaline rhyolite lineage.

Oceanic and Continental obsidians

Bailey and Macdonald (1970) have used the rather limited chemical data available in the literature to divide glassy comendites (obsidians) into two groups - oceanic and continental. Using their data, the continental comendites form a relatively tight group which shows regular chemical trends whereas the oceanic comendites are widely scattered. For example in the ternary projection SiO_2-Al_2O_3-Na_2O+K_2O the continental comendites plot in a group within and along a quartz feldspar cotectic zone defined by the field boundaries or Or-silica and Ab-silica taken from the systems (K_2O-Al_2O_3-SiO_2 and Na_2O-Al_2O_3-SiO_2 at one atmosphere pressure (Shairer and Bowen, 1955; 1956). The oceanic comendites on the other hand plot as a scattered group trending from the feldspar point toward the quartz-feldspar cotectic zone. Bailey and Macdonald (1970) suggested that this difference is genetically significant, and that because of the close correlation with experimentally determined quartz-feldspar minima the continental comendites may have originated by partial melting within the continental crust possibly in the presence of an alkali bearing vapour. In contrast, the trend of the oceanic comendites from a simple trachytic composition (represented by the alkali feldspar point) toward the quartz-feldspar cotectic zone is consistent with derivation from a trachytic parent.

The scattered spread of Bailey and Macdonald's oceanic comendites field is defined largely by two analyses from Kerguelen Island and by two previously published analyses from the Dawson Strait area (Morgan, 1966). Apart from these the 'oceanic' comendites fall within a field which lies close to the Ab cotectic and overlaps the field of 'continental' comendites (Figure 9-15). The comendites from the Dawson Strait area show a much greater variation in chemical composition than any of the comendite suites used by Bailey and Macdonald (1970) in defining their two types and they appear to represent a more complete series than any previously described comendite suite. The trend shown by the Dawson Strait comendites on Figure 9-15 is that to be expected of a series fractionating
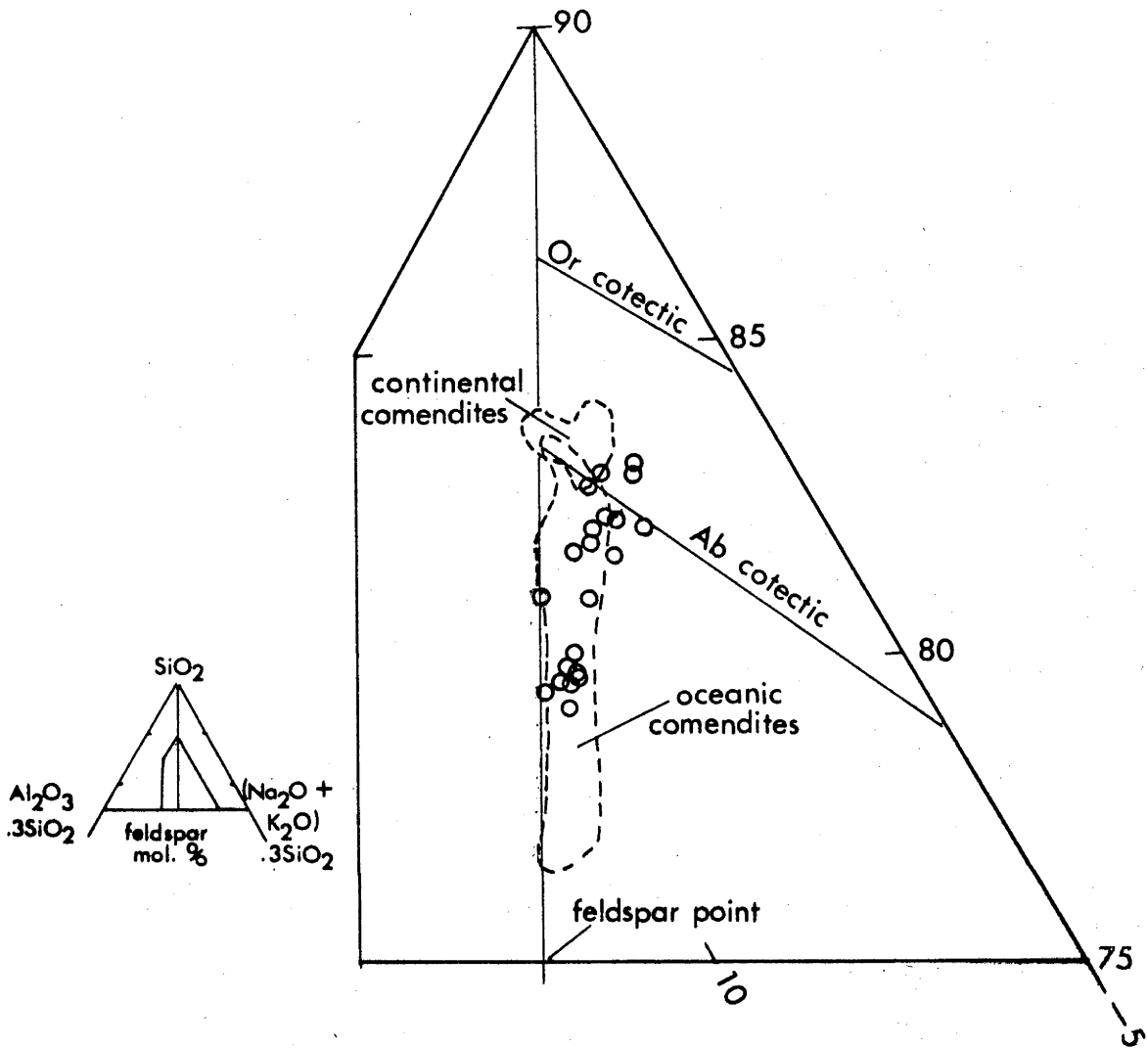
FIGURE 9-15: Part of the ternary system SiO_2-Al_2O_3-Na_2O+K_2O
(molecular percentages) showing the fields of
oceanic and continental comendites (enclosed
by dashed lines) from Bailey and Macdonald
(1970) in relation to the Dawson Strait
comendites (open circles).

feldspar (represented by the alkali feldspar point) and evolving toward
a cotectic composition. On reaching the cotectic further fractionation
will be controlled by both feldspar and quartz and the compositions of
derivative liquids would lie along the cotectic zone. Although this
argument does not preclude the possibility of quartz-feldspar equilibrium
reactions between fractionated comenditic magma and sialic crust, the
possibility that the difference between continental and oceanic comendites
is nothing more than a difference in degree of fractionation seems equally
acceptable.

CHAPTER 10

VOLCANIC EVOLUTION IN SOUTHEASTERN PAPUA

The geological development of southeastern Papua has progressed
in a number of distinct episodes each characterised by a particular
volcanic rock association. Separate volcanic episodes are linked to major
tectonic events which mark stages in the evolution of the boundary
between the Indo-Australian and Solomon Sea plates in Papua.

10-1   Tectonic History

Eastern Papua straddles a plate boundary which has been the focus
of complex changes in relative plate motion during the Cenozoic. The
available evidence points to several clearly defined events which include
both convergence and divergence; some of these are relatively well
documented but others are of necessity speculations based on comparison
with comparable geological settings in other parts of the world.

The present plate boundary

Present day seismicity in eastern Papua is confined to a diffuse
zone extending along the northeast Papuan coast, through the D'Entrecasteaux
Islands and eastward across the Solomon Sea (Denham, 1969; Johnson and
Molnar, 1972; Curtis, 1973). This seismicity defines the southern boundary
of the Solomon Sea plate.

To the east of the D'Entrecasteaux Islands the plate boundary
traverses the Woodlark Basin which has been identified as a Recent
spreading center (Milsom, 1970). The history of spreading in the Woodlark
Basin has been described by Luyendyk and others (1973) on the basis of
marine geophysical data. These workers suggest that the Woodlark Basin
began opening about a pole lying near the tip of eastern Papua approximately
20 m.y. before present but the amount of opening at this stage was no more
than a few degrees. The cause of spreading in the basin was regional left
lateral shear arising from a change in the relative motion between the
Indo-Australian and Pacific plates (Chase, 1971). Renewed spreading in
the Woodlark Basin was initiated approximately 3 m.y. ago and about 1 m.y.
ago spreading in the western part of the basin shifted to the Woodlark
Rise; the pole of present spreading has been located in the Dawson Strait
area of the D'Entrecasteaux Islands.

The interpretation of the Woodlark Basin as a Recent spreading
center is consistent with evidence for block faulting associated with

minor rifting and major late Cenozoic uplift in eastern Papua and the
D'Entrecasteaux Islands (Davies and Ives, 1965; Smith, 1970; Smith
and Davies, 1976). The divergent plate boundary in the Woodlark Basin
marks the southern margin of the Solomon Sea plate which is bounded by
subduction zones to the north and east (New Britain and northern
Solomon Island trenches respectively). Relative plate motion west of
the spreading pole in the Dawson Strait area indicates that movement
on the plate boundary is left lateral transform shear (Johnson and Molnar,
1972) but there is probably also a component of convergence complementary
to spreading in the Woodlark Basin.

Rifting in the Coral Sea Basin

Oceanographic work in the Coral Sea (Falvey and Talwani, 1969;
Ewing and others, 1970; Gardner, 1970) has provided evidence that the
Coral Sea Basin which lies to the south of the Papuan Peninsula opened
by sea floor spreading during the Eocene. DSDP hole 210 drilled in the
basin gave the age of formation of oceanic crust as early Eocene (Burns
and others, 1973). On the basis of this and other data (Mutter, 1975)
it appears likely that this spreading was largely completed by middle
Eocene times (45-50 m.y. ago).

Although opening of the Coral Sea Basin is not strictly a part
of the history of the Papuan plate boundary, current paleo-tectonic
models suggest that spreading in the Coral Sea was complementary to
northward dipping subduction along the Papuan plate boundary which lay
immediately to the north. This subduction ceased with the event which
led to the emplacement of the Papuan ultramafic belt.

Subduction in eastern Papua

The petrogenetic model for andesitic magmas which was developed
in chapter 7 requires the existence of an upper mantle source which has
been modified by interaction with a Si-rich, incompatible element-rich
melt originating as a monor partial melt of basaltic crustal material
(oceanic crust) at relatively high pressures. Although other models
are possible (e.g. catastrophic sinking of basaltic crust transformed
to eclogite at the base of the crust (T. Green and Ringwood, 1968),
the typical association of andesitic volcanoes with Benioff zones and
by implication with subduction suggestes that the most general process
by which the upper mantle is modified involves subduction of oceanic
crust beneath the arc. In eastern Papua the arguement is to some

extent circular; andesites imply subduction and because there has been subduction there are now andesites. Nevertheless by analogy with active andesitic arcs the hypothesis that andesitic volcanoes in eastern Papua are related to a subduction event is considered the most reasonable model on which to base a paleo-tectonic history.

The only volcanic rocks which can be described as subduction related in eastern Papua are the Miocene to Recent rocks forming the northern (chapter 5) and southern (chapter 4) volcanic belts. The chemical compositions of these rocks and especially the variation in K_2O at particular SiO_2 contents suggest that, by analogy with modern andesitic arcs a southward dipping subduction zone has existed beneath the volcanoes until very recent times. Following Dickinson's (1968, 1975) observations a southward dipping subduction zone would underlie the volcanoes at a depth of about 150 km and assuming a dip of 55°, would reach the surface to the north of the Woodlark Rise in the Kiriwina trough. In essence this is Karigs (1972) interpretation of the area but in detail the model encounters important difficulties.

In thermal models for active subduction (Oxburgh and Turcotte, 1970) isotherms are depressed by the underthrusting of relatively cold oceanic crust. This feature is important to some petrogenetic hypotheses because it allows subsolidus dehydration of the slab but it also predicts that the area adjacent to the trench in an arc will be relatively cold. If a southward dipping subduction existed under southeast Papua during the upper Tertiary it is inconceivable that volcanism requiring relatively high heat flow could have developed in the Lusancay Islands (chapter 8) adjacent to the Kiriwina Trough. Thus if currently active volcanoes in eastern Papua (Mount Lamington, Waiowa Volcano, Mount Victory) represent volcanism directly related to subduction there has been a significant time lag (millions of years) between cessation of subduction and eruption of associated magmas.

The sequence of volcanic rocks in southeast Papua - K-rich rocks of the southern volcanic belt followed by more typically andesitic rocks of the northern volcanic belt - differs from that observed in arcs associated with well defined Benioff zones and is the reverse of that predicted by some petrogenetic models (e.g. Jakes and White, 1969). Further, if late Cenozoic volcanism in eastern Papua is modelled on a typical arc situation the arc-tholeiitic rocks which should accompany the early stages of subduction (Jakes and Gill, 1970; Jakes and White, 1972; Nicholls, 1974) are conspicuously absent.

A plate tectonic model for the east Papuan plate boundary suggests that it is in part a diverging boundary and in part a strike slip boundary with a minor component of convergence. Geological evidence indicates that the tectonic regime in eastern Papua has been essentially unchanged at least through the late Cenozoic. Clearly the hypothesis that andesitic volcanism in eastern Papua is directly related to a subduction event is untenable.

Lower Tertiary subduction

The Papuan ultramafic belt has been interpreted as a slice of upper mantle and oceanic crust which formed the hanging wall of a northward dipping subduction zone (Davies, 1968; 1970; Davies and Smith, 1971). Emplacement of the belt is thought to have taken place when sialic material (the Owen Stanley Metamorphics) entered the zone and because of its relatively low density prevented further subduction. Despite some criticism (Rod, 1974) of geophysical models(Milsom, 1973a) which support the overthrusting concept the geological data (Davies, 1968; 1971; Smith and Davies, 1976) supporting the concept appear incontrovertible.

Two lines of evidence have been cited to support a lower Eocene age of emplacement for the Papuan ultramafic belt (Davies and Smith, 1971). Firstly 'tonalite' intrusions in the basaltic component of the belt have been dated at 50 to 55 m.y. The interpretation of the nature of these 'tonalite' intrusions is of critical importance in the timing of events leading to the emplacement of the ultramafic belt because they are the only well dated rocks closely associated with the belt. Davies and Smith (1971) have suggested that the 'tonalites' represent island arc type magmas which developed in response to a northward dipping subduction zone prior to emplacement of the ultramafic belt. However, a reassessment of chemical data from the intrusives (chapter 3) shows that they are quite unlike island arc type rocks but are closely comparable to differentiated rocks characteristic of oceanic crust. They are in fact an integral part of the basaltic component of the ultramafic belt and as such provide no direct evidence as to the time of emplacement of the belt.

A second line of evidence on the age of emplacement of the Papuan ultramafic belt is a date of 52 m.y. determined on a hornblende granulite in the thrust zone underlying the belt. Metamorphism during emplacement of the ultramafic belt produced rocks of greenschist, transitional to

lawsonite-glaucophane schist facies (Pieters, 1974) not rocks as high
as granulite facies. Clearly if the 52 m.y. age of the hornblende
granulite is significant in terms of the time of emplacement of the
ultramafic belt then it must be a reset age produced by retrogressive
metamorphism superimposed on earlier high grade metamorphism. In view
of arguements presented below for emplacement of the ultramafic belt
during late Eocene times this interpretation must be doubted and the
52 m.y. date stands as an unexplained anomaly.

If the 'tonalite' intrusions are an integral part of the Papuan
ultramafic belt they presumably formed by processes related to the
formation of the basaltic component of the belt and the tectonic
emplacement of the belt cannot have taken place earlier than 50-55 m.y.
(early Eocene). If Davies' overthrust model is correct and the ultra-
mafic belt was emplaced when sialic material entered a subduction zone
which was complementary to sea floor spreading in the Coral Sea Basin,
then the most likely time for the event was late Eocene (about 40 m.y.
ago). The late Eocene to early Oligocene was a period of major tectonic
upheaval and metamorphism in northern New Guinea (Dow, 1973a) and it is
reasonable to expect that similar events in eastern Papua correlate with
this. Further evidence for a major tectonic event during this period
comes from a DSDP hole in the Coral Sea Basin (Burns and others, 1973)
where there is evidence for deformation of middle Eocene sediments.

The overthrust model for emplacement of the Papuan ultramafic
belt carries the implication for a northward dipping subduction zone.
By analogy with the geometry of modern volcanic arcs,volcanoes associated
with this zone,100 to 150 km from the surface expression of the zone (the
Papuan ultramafic belt),would be located in the present Solomon Sea
Basin. Pieters (1974) has suggested that Eocene volcanic rocks in New
Britain may have developed in response to subduction in Papua and could
have been removed to their present position by sea floor spreading in
the Solomon Sea Basin. In terms of the spreading rate required (0.7 to
1.0 cm/yr over 40×10^6 years) the hypothesis is feasible but in the absence
of definate information on the age and thickness of sediments in the
Solomon Sea Basin it must remain unresolved. The alternative that
emplacement of the ultramafic belt involved only very limited under-
thrusting is a less dramatic explanation for the absence of associated
volcanics but perhaps for this reason it is more acceptable.

An earlier episode of subduction?

Andesitic volcanoes in eastern Papua are closely associated with, or lie to the south of, a discontinuous belt of ultramafic rocks extending east from the Papuan ultramafic belt. If the ultramafic rocks represent the outcrop of a lower Tertiary subduction/overthrust zone the position of the volcanoes cannot be reconciled with the notion of a subducted slab dipping northward from this zone.

Tertiary geo-tectonics in eastern Papua involve late Eocene subduction or overthrusting complementary to sea floor spreading in the Coral Sea Basin followed by late Tertiary extension and uplift. None of these events are able to account for the modified mantle which it is thought gave rise to andesitic magmas. It is therefore suggested that a subduction event prior to the opening of the Coral Sea Basin may have produced the source of the andesitic rocks in Papua.

In this model southward underthrusting from a relative position equivalent to the present position of the Kiriwina Trough may, by analogy with modern arcs, have produced a zoned source which could explain the present variation in K_2O content of rocks across Papua. This subduction would have taken place beneath the continental margin of north eastern Australia in response to relative westward movement of the Pacific Plate. In general supporting evidence for the hypothesis is lacking although it would explain the evidence for an early (late Mesozoic?) episode of regional metamorphism in the Owen Stanley metamorphics (Pieters, 1974) and in the D'Entrecasteaux Islands. The presence of Cretaceous volcanic rocks in the eastern Highlands of New Guinea provides some evidence for late Mesozoic southward dipping subduction (D.E. Mackenzie, pers. comm.) to the northwest of the Papuan peninsula and it is possible that this correlates with the proposed event in eastern Papua.

From the point of view of andesite petrogenesis this tectonic model has two major implications. Firstly it implies that although andesitic volcanism is a result of subduction it is not consequent upon it. In other words the importance of subduction to andesite petrogenesis is the production of a source material, the tectonic setting of subduction is less important and in eastern Papua because of the complex geotectonic history has ceased to have any direct relevance. Secondly if the andesite source formed as a result of late Mesozoic subduction beneath the Australian continental margin subsequent spreading in the Coral Sea moved the source northward to its present position.

FIGURE 10-1: Generalised tectonic evolution of southeast Papua.

Geological sections - not to scale.

LATE MESOZOIC - southward dipping subduction beneath the
Australian continental margin.
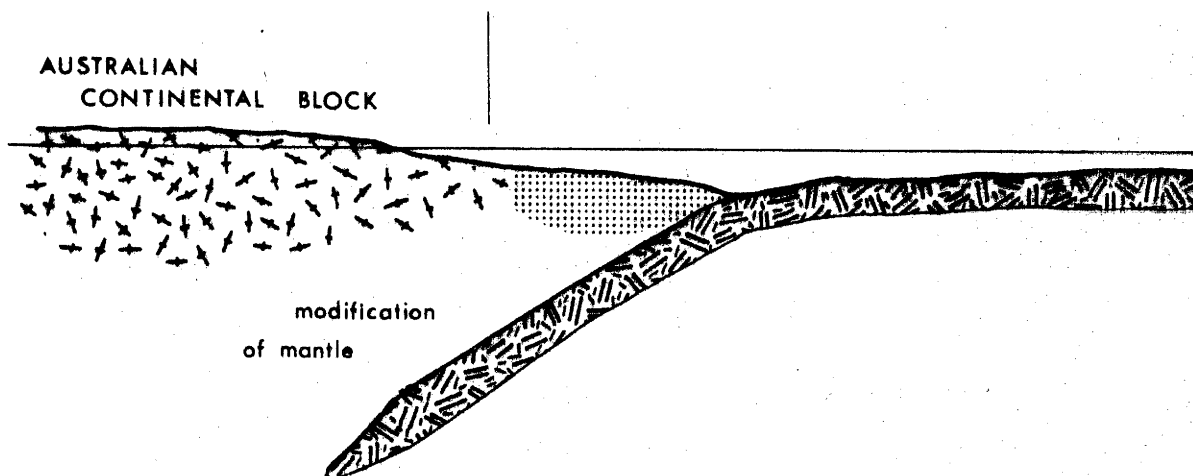
EOCENE - Sea floor spreading and northward dipping subduction.
(formation of the Coral Sea Basin)
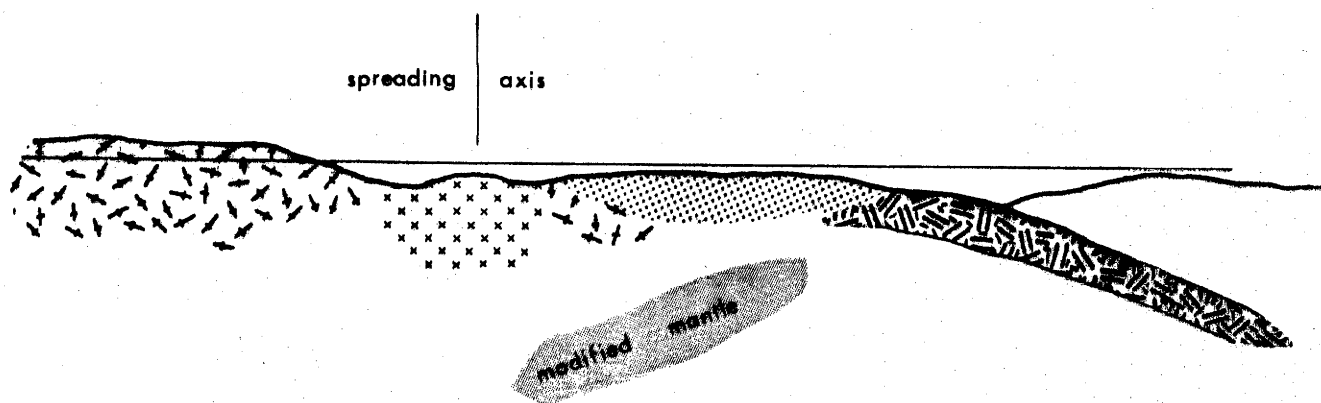
Late Cenozoic magma source

New oceanic crust

Old oceanic crust

Sediments/metamorphics

Continental crust

FIGURE 10-1: (continued)

LATE EOCENE - EARLY OLIGOCENE
Subduction zone immobilised by the entry of relatively light
material into the zone. Emplacement of the Papuan ultramafic belt.

WEST

partial overthrusting of sediments/metamorphics

EAST

complete overthrusting of sediments/metamorphics
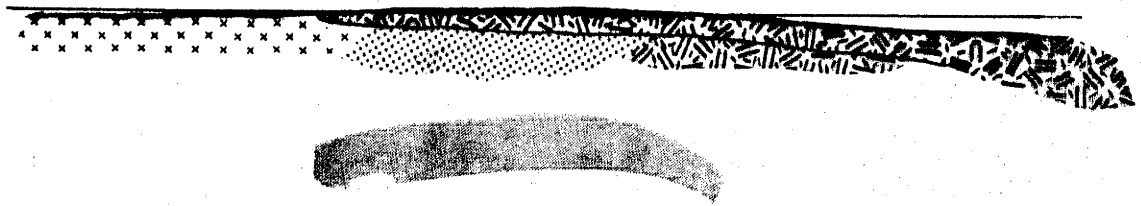
LATE CENOZOIC - Uplift and volcanism.

southeast Papua   D'Entrecasteaux   Lusancay
                            Islands   Islands
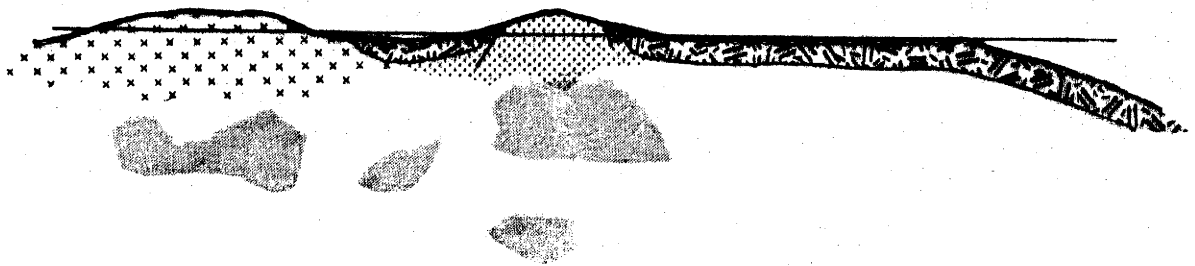
modified mantle source

Tectonic synthesis

The proposed tectonic history outlined in this section is extremely complex especially when compared with plate boundaries such as the Pacific - South America boundary where there is evidence of constant polarity over long periods. The complexity of the Papuan boundary is related to the fact that it has evolved as a result of interaction between a major (the Indo-Australian plate) and a minor (the Solomon Sea plate) plate forming part of a highly active zone between the Indo-Australian and Pacific plates. The model proposed for the east Papuan boundary involves late Mesozoic convergence and subduction, early Tertiary divergence with sea floor spreading, late Eocene convergence with overthrusting and possibly some subduction and late Cenozoic divergence associated with block faulting and uplift of the Papuan peninsula. Of these events only the late Mesozoic subduction is without direct substantive evidence but it is argued that the presence and geometry of the late Cenozoic volcanics require such an event. The tectonic evolution of the east Papuan plate boundary is illustrated in Figure 10-1.

10-2   Volcanic Evolution in Southeastern Papua.

This thesis has attempted to trace the evolution of volcanism on a plate boundary. It can be argued that in fact the volcanic rocks which now make up southeastern Papua have developed not on one boundary but on several boundaries; namely the Coral Sea spreading center, the Woodlark Basin spreading center and the Papuan plate boundary. In the proposed tectonic model andesitic volcanoes which represent the major magmatic event on the boundary are a legacy of an earlier tectonic event distant from the present plate boundary. Nevertheless it is suggested that the sequence of volcanic rocks observed in eastern Papua are representative of the variety of magmas which can develop in a single complex zone of interaction between major crustal plates.

The basement volcanic rocks in southeast Papua are tholeiitic submarine basalts comparable to those of the ocean basins. It is logical to link eruption of these rocks with sea floor spreading in the Coral Sea Basin. The Upper Cretaceous basalts (Goropu Metabasalt) apparently represent former sea floor formed either during an early stage in the formation of the Coral Sea Basin or possibly in an earlier event associated with spreading in the Tasman Sea (Hayes and Ringis, 1973). The metamorphic

grade and distribution of these basalts is consistent with relatively
high P/T metamorphism associated with emplacement of the Papuan ultramafic
belt. Eocene basalts (Kutu volcanics) are thought to have been erupted
as part of the spreading event which formed the Coral Sea Basin but
possibly as a later magmatic phase after the main spreading event.
These basement tholeiites are allochthonous to the east Papuan plate
boundary and were moved into spatial association with a lower Tertiary
subduction zone by spreading in the Coral Sea Basin (chapter 3).

Volcanism on the Papuan plate boundary commenced in the middle
Miocene with eruption of high-K rocks which at present form the eastern
end of the southern volcanic belt. Typically andesitic volcanism started
at the eastern end of the northern volcanic belt in late Miocene times.
Both types of volcanism have continued in spatially distinct belts
through late Cenozoic times and in both belts there has been migration
of centers of activity from east to west. The differences in the lava
types of the two belts are due to differences in the source composition
(chapter 7) and the systematic age relationships may be related to west-
ward migration of the pole of spreading in the Woodlark Basin. It is
argued that the tectonic event which formed the source region of these
rocks was much earlier (possibly late Mesozoic) than the tectonic event
which triggered the formation and eruption of magmas.

The chemical composition of high-K trachytes in the Lusancay
Islands indicates that they have originated by partial melting of a
relatively evolved source material with an eclogite mineral assemblage.
The source may have been comparable to that which gave rise to the
andesitic rocks but clearly the depth of magma segregation was greater.
The Lusancay trachytes are very young (about 1×10^6 m.y.) and it is
likely that the tectonic setting in which the magmas were generated is
comparable to that prevailing at the present time. It is something of
a puzzle therefore that the eruption of the Lusancay trachytes can not
be clearly related to any major Quaternary tectonic event. The Woodlark
rise is a structural entity which has escaped the dramatic uplift of the
mainland to the south; there is evidence only of a small amount of
regional uplift during the Quaternary. It is suggested that volcanism
in the Lusancay Islands may have been triggered by re-equilibration of
the geotherms after the collision event which resulted in emplacement of
the Papuan ultramafic belt. Melting of material at the depths implied
by an eclogite source mineralogy (about 75 km) suggests that there was a

comparatively high heat flux in the area and this suggestion is supported
by the limited heat flow measurements (Macdonald and others, 1973) which
have been taken in region.

The eruption of peralkaline rhyolites in the Dawson Strait area
is apparently anomalous in the circum-Pacific setting. Peralkaline
rhyolites and associated rocks are closely linked with rifting environ-
ments and with spreading at mid-ocean ridges, but are only rarely found
in association with the andesitic arcs characteristic of converging plate
boundaries. The importance of peralkaline volcanism in the Dawson Strait
area is that it so closely follows the pattern of sea floor spreading in
the Woodlark basin immediately to the east. Quaternary volcanic activity
in the D'Entrecasteaux Islands provides an example of overlapping volcanic
associations caused by a change in the tectonic style of a plate boundary.
To the west of the spreading pole in a tectonic environment which is partly
strike-slip shear and partly converging, andesitic magmas have been erupted;
to the east in a setting which can be characterised as an early rift
environment the style of magmatism changes to that typically associated
with rifting. Anomalous and possibly transitional basaltic rocks on
Kukuia Peninsula west of the Dawson Strait area suggest that the volcanic
activity linked with spreading may also be migrating westward.

10-3   Conclusion

One of the most interesting aspects of volcanic evolution in
southeastern Papua is the way in which it mirrors the evolutionary sequence
of voclanic rocks described from Fiji (Gill, 1970; 1972) and predicted
in some models of island arc evolution (e.g. Jakes and White, 1969; 1972).
In Fiji the earliest volcanic rocks are tholeiitic and these are followed
in turn by andesites, shoshonites and alkaline basalts. This has been
interpreted as a subduction related sequence followed by extension linked
to spreading in the Lau Basin. The main difference in the comparison with
southeast Papua is in the nature of the early tholeiites; in Fiji the
early tholeiites mark the beginning of island arc type volcanism, in
Papua they are allochthonous. In both areas eruption of typically
andesitic rocks (including shoshonites) was preceeded by the development
of thickened crust. Both southeastern Papua and Fiji represent variations
in the process by which primary mantle is differentiated toward a
continental crustal composition.

Relative plate motion in southeastern Papua is probably unique in

the sense that the sequence and type of events associated with the plate boundary have not been exactly reproduced elsewhere. The chemical compositions of volcanic rocks have been used to identify and characterise the sequence of tectonic events in the area by analogy with rocks of similar composition in better defined tectonic situations. The interpretation of the significance of andesitic volcanoes in eastern Papua is at variance with more commonly held ideas of magma genesis in andesitic arcs. In these, magma genesis is closely linked to the tectonic event (subduction) which according to current models (chapter 7) is responsible for production of a source material with the potential to produce andesite magma. If the tectonic model presented for eastern Papua is approximately correct then it implies that once a source is formed it can exist as an entity for a significant period of time until magma generation is triggered by some later tectonic event. This is not simply a delay between cause and effect which might be expected in a continuously active arc, it is a delay which may result in andesitic magmas being erupted in response to a quite different tectonic regime. In southeastern Papua andesitic magmas have been erupted into a tectonic setting which is manifestly different from that of typical andesitic volcanic arcs and this must add another dimension to the interpretation of paleo-volcanic tectonic environments.

Study of the volcanic rocks in southeastern Papua has led to a volcano-tectonic model which is consistent with the known geology of the area and with current petrogenetic models for volcanic rocks. This has been possible because of the wide ranging nature of the study encompassing volcanic rocks within an area of about 10×10^3 km^2 and ranging from Upper Cretaceous to Recent. Nevertheless because of the broad scope of the study it must be regarded as a reconnaissance upon which future work in eastern Papua can be based.

BIBILOGRAPHY.

ABBOTT, M.J. 1965. A petrological study of the Nandewar Volcano.
        Ph.D. thesis, Aust. Nat. Univ. (unpublished).

ABBOTT, M.J. 1969. Petrology of the Nandewar Volcano, N.S.W., Australia.
        Contrib. Mineral. Petrol. 20, 115-134.

AOKI, K.I. 1964. Clinopyroxenes from alkaline rocks of Japan. Am.
        Mineral., 49, 1199-1223.

ARTH, J.G., HANSON, G.N. 1972. Quartz diorites derived by partial melting
        of eclogite or amphibolite at mantle depths. Contrib. Mineral.
        Petrol., 37, 161-174.

BAILEY, D.K., MACDONALD, R. 1969. Alkali-feldspar fractionation trends
        and the derivation of peralkaline liquids. Am. J. Sci., 267, 242-
        248.

BAILEY, D.K., MACDONALD, R. 1970. Petrochemical variations among mildly
        peralkaline (comendite) obsidians from the oceans and continents.
        Contrib. Mineral. Petrol., 28, 340-351.

BAILEY, D.K., MACDONALD, R. 1975. Fluroine and clorine in peralkaline
        liquids and the need for magma generation in an open system.
        Min. Mag., 40, 405-414.

BAILEY, D.K., SCHAIRER, J.F. 1964. Feldspar-liquid equilibria in
        peralkaline liquids - the orthoclase effect. Am. J. Sci., 262,
        1198-1206.

BAILEY, D.K., SCHAIRER, J.F. 1966. The system $Na_2O-Al_2O_3-Fe_2O_3-SiO_2$ at
        1 atmosphere and the petrogenesis of alkaline rocks. J. Petrol.,
        7, 114-170.

BAKER, G. 1946. Preliminary note on volcanic eruptions in the Goropu
        Mountains southeastern Papua during the period December 1943 to
        August 1944. J. Geol., 54, 19-31.

BAKER, P.E. 1968. Comparative volcanology and petrology of the Atlantic
        island arcs. Bull. Volcanol., 32, 189-206.

BAKER, P.E. 1975. Peralkaline acid volcanic rocks of oceanic islands.
        Bull. Volcanol., 38, 737-754.

BAKER, P.E., BUCKLEY, F., HOLLAND, J.G. 1974. Petrology and geochemistry
        of Easter Island. Contrib. Mineral. Petrol., 44, 85-100.

BAKER, P.E., GASS, I.G., HARRIS, P.G., LE MAITRE, R.W. 1964. The
        volcanological report of the Royal Society Expedition to Tristan
        de Cunha, 1962. Phil. Trans. Roy. Soc. Lond., Ser. A, 256, 439-
        578.

BARBERI, F., BIZOUARD, H., VARET, J. 1971. Nature of the clinopyroxene
        and iron enrichment in alkalic and transitional basaltic magmas.
        Contrib. Mineral. Petrol., 33, 93-107.

BARBERI, F., FERRARA, G., SANTACROCE, R., TREUIL, M., VARET, J.,1975.
A transitional basalt-pantellerite sequence of fractional
crystallisation, the Boina Centre (Afar Rift, Ethiopia).
J. Petrol., 16, 22-56.

BARTH, T.F.W. 1966. Aspects of the crystallisation of quartzo-feldspathic
plutonic rocks. Tschermaks Mineral. Petrog. Mitt., 11, 209-222.

BASS, M.N. 1972. Occurrence of transitional abyssal basalt. Lithos, 5,
57-67.

BICKELL, R.S. 1974. Reconnaissance geology of Cape Vogel Basin, Papua
New Guinea. Amer. Assoc. Petrol. Geol. Bull., 58, 2477-2489.

BLAKE, D.H. 1976. Madilogo, a late Quaternary volcano near Port Moresby,
Papua New Guinea. In. Volcanism in Australasia, R.W. Johnson (ed).
Elsevier, (in press).

BOETTCHER, A.L. 1973. Volcanism and orogenic belts - the origin of
andesites. Tectonophysics, 17, 223-240.

BOWEN, N.L. 1928. The evolution of the igneous rocks. Princeton
University Press, Princeton, N.J.

BOWEN, N.L., 1945. Phase equilibria bearing on the origin and differen-
tiation of the alkaline rocks. Am. J. Sci., 243 A, 75-89.

BUDDINGTON, A.F., LINDSLEY, D.H. 1964. Iron-titanium oxide minerals
and synthetic equivalents. J. Petrol., 5, 310-357.

BROOKS, C.K. 1968. On the interpretation of trends in element ratios in
differentiated igneous rocks, with particular reference to
strontium and calcium. Chem. Geol., 3, 15-20.

BURNHAM, C.W. 1975. Water and magmas: a mixing model. Geochim. Cosmochim.
Acta, 39, 1077-1084.

BURNS, R.E., ANDREWS, J.E. and others 1973. Initial reports of the deep
sea drilling project, volume 21. Washington (U.S. Government
printing office).

BURNS, R.G. 1970. Mineralogical applications of crystal field theory.
Cambridge university press.

CANN, J.R. 1970. Rb, Sr, Y, Zr and Nb in some ocean floor basaltic rocks.
Earth Planet. Sci. Lett., 10, 7-11.

CANN, J.R. 1971. Major element variations in ocean-floor basalts. Phil.
Trans. Roy. Soc. Lond., Ser. A, 268, 495-505.

CARMICHAEL, I.S.E., 1962. Pantelleritic liquids and their phenocrysts.
Min. Mag., 33, 86-113.

CARMICHAEL, I.S.E. 1967. The iron-titanium oxides of salic volcanic
        rocks and their associated ferromagnesian silicates. Contrib.
        Mineral. Petrol., 13, 36-64.

CARMICHAEL, I.S.E., MACKENZIE, W.S. 1963. Feldspar-liquid equilibria
        in pantellerites: an experimental study. Am. J. Sci., 261,
        382-396.

CARMICHAEL, I.S.E., NICHOLLS, J. 1967. Iron-titanium oxides and oxygen
        fugacities in volcanic rocks. J. Geophys. Res., 72, 4665-4686.

CARTER, J.L. 1970. Mineralogy and chemistry of the earths upper mantle
        based on the partial fusion-partial crystallisation model.
        Geol. Soc. Amer. Bull., 81, 2021-2034.

C.G.G. 1973. Compagnie Generale de Geophysique, aeromagnetic survey,
        eastern Papua, June - July 1970, March - May, 1971. Bur. Miner.
        Resour. Aust. Rec. 1973/60.

CHAO, E.C.T., FLEISCHER, M., 1960. Abundance of zirconium in igneous
        rocks. Rep. XXI Int. Geol. Congr., 1. 106-131.

CHAPPELL, B.W. 1966. Petrogenesis of the granites at Moonbi, N.S.W.
        Ph.D. thesis, Aust. Nat. Univ., (unpubl.).

CHASE, C.G. 1971. Tectonic history of the Fiji plateau. Geol. Soc. Amer.
        Bull., 82, 3087-3110.

CLARK, R.H. 1960. Andesite lavas of the North Island, New Zealand. Rept.
        XXI. Int. Geol. Cong., 13, 123-131.

COLEMAN, R.G., PETERMAN, Z.E. 1975. Oceanic Plagiogranite. J. Geophys.
        Res., 80, 1099-1108.

COOMBS, D.S. 1963. Trends and affinities of basaltic magmas and pyroxenes
        as illustrated on the diopside-olivine-silica diagram. Min. Soc.
        Am. Spec. Pap., 1. 227-50.

COX, K.G., GASS, I.G., MALLICK, D.I.J. 1970. The peralkaline volcanic suite
        of Aden and Little Aden, South Arabia. J. Petrol., 3, 433-462.

CURTIS, J.W. 1973. Plate tectonics and the Papua - New Guinea - Solomon
        Islands region. J. Geol. Soc. Aust., 20, 21-36.

DALLWITZ, W.B. 1968. Chemical composition and genesis of clinoenstatite-
        bearing volcanic rocks from Cape Vogel, Papua: a discussion.
        Rept. XXIII Int. Geol. Cong., 2., 229-242.

DALLWITZ, W.B., GREEN, D.H., THOMPSON, J.E. 1966. Clinoenstatite in a
        volcanic rock from the Cape Vogel area, Papua. J. Petrol. 7,
        375-403.

DAVIES, H.L. 1968. Papuan ultramafic belt. Rept. XXIII Int. Geol. Cong., 1. 209-220.

DAVIES, H.L. 1969. Normanby Island reconnaissance petrography. Bur. Miner. Resour. Aust. Rec., 1969/46 (unpubl.).

DAVIES, H.L. 1971. Peridotite-gabbro-basalt complex in eastern Papua: an overthrust plate of oceanic mantle and crust. Bur. Miner. Resour. Aust. Bull., 128.

DAVIES, H.L. 1973. Fergusson Island, Papua New Guinea - 1:250,000 Geological Series. Bur. Miner. Resour. Aust. explan. Notes, SC/56-5.

DAVIES, H.L., IVES, D.J. 1965. The geology of Fergusson and Goodenough Islands, Papua. Bur. Miner. Resour. Aust. Rept., 82.

DAVIES, H.L., SMITH, I.E. 1971. Geology of eastern Papua. Geol. Soc. Amer. Bull., 82, 3299-3312.

DAVIES, H.L., SMITH, I.E., 1974. Tufi-Cape Nelson, Papua New Guinea - 1:250,000 Geological Series. Bur. Miner. Resour. Aust. explan. Notes, SC/55-8,4.

DE KEYSER, F. 1961. Misima Island, geology and gold mineralisation. Bur. Miner. Resour. Aust. Rep.,57.

DENHAM, D. 1969. Distribution of earthquakes in the New Guinea - Solomon Islands region. J. Geophys. Res., 74, 4290-4299.

DICKINSON, D.R., DODSON, M.R., GASS, I.G. 1969. Correlation of initial $^{87}Sr/^{86}Sr$ with Rb/Sr in some late Tertiary volcanic rocks of south Arabia. Earth Planet. Sci. Lett., 6, 84-90.

DICKINSON, D.R., GIBSON, I.L. 1972. Feldspar fractionation and anomalous Sr^{87}/Sr^{86} ratios in a suite of peralkaline silicic rocks. Geol. Soc. Amer. Bull., 83, 231-240.

DICKINSON, W.R. 1968. Circum-Pacific andesite types. J. Geophys. Res., 73, 2261-2269.

DICKINSON, W.R. 1975. Potash-depth (K-h) relations in continental margin and intra ocean magmatic arcs. Geology, 3 , 53-56.

DICKINSON, W.R., HATHERTON, 1967. Andesitic volcanism and seismicity around the Pacific. Science, 157, 801-803.

DIETRICH, R.V. 1968. Behavior of zirconium in certain artificial magmas under diverse P-T conditions. Lithos, 1, 20-29.

DOW, D.B. 1973a. Structural evolution of Papua New Guinea. Aust. N.Z. Assoc. Adv. Sci., 45th Cong. sect. 3 Abs., 154-158.

DOW, D.B. 1973b. Geology of Papua New Guinea. Bur. Miner. Resour. Aust. Rec., 1973/117 (unpubl.).

ENGEL, A.E.J., ENGEL, C.G., HAVENS, R.G. 1965. Chemical characteristics of oceanic basalts and the upper mantle. Geol. Soc. Amer. Bull., 76, 719-734.

ESSENE, E.J., HENSEN, B.J., GREEN, D.H. 1970. Experimental study of amphibolite and eclogite stability. Phys. Earth Planet. Int., 3, 378-384.

EWART, A., TAYLOR, S.R., CAPP, A.C. 1968. Geochemistry of the pantellerites of Mayor Island, New Zealand. Contrib. Mineral. Petrol., 17, 116-140.

EWING, J.I., HOUTZ, R.E., LUPWIG, W.J. 1970. Sediment distribution in the Coral sea. J. Geophys. Res., 15, 1963-1972.

FALVEY, D.A., TALWANI, M. 1969. Gravity map and tectonic fabric of the Coral Sea (abs). Geol. Soc. Am. abs., 7, 62.

FAURE, G., POWELL, J.L. 1972. Strontium isotope geology. Springer Verlag, 188 pp.

FERRARA, G., TREUIL, M. 1975. Petrological implications of trace element and Sr isotope distributions in basalt-pantellerite series. Bull. Volcanol., 38, 548-574.

FISHER, A.G., HEEZEN, B.C., BOYCE, R.E., and others 1970. Geological history of the western North Pacific. Science, 168, 1210-1214.

FITTON, J.G. 1971. The generation of magmas in island arcs. Earth Planet. Sci. Lett., 11. 63-67.

FREY, F.A., HASKIN, M.A., POETZ, J.A., HASKIN, L.A. 1968. Rare earth abundances in some basic rocks. J. Geophys. Res., 73, 6085-6098.

FYFE, W.S., TURNER, F.J., VERHOOGEN, J. 1958. Metamorphic reactions and metamorphic facies. Geol. Soc. Am. Mem., 73, 1-259.

GARNDER, J.V. 1970. Submarine geology of the western Coral Sea. Geol. Soc. Amer. Bull., 81, 2599-2614.

GASS, I.G., MALLICK, D.I.J. 1968. Jebel Khariz: an upper-Miocene strato-volcano of comenditic affinity on the south Arabia coast. Bull. Volcanol., 32, 33-88.

GAST, P.W. 1967. Isotopic geochemistry of volcanic rocks, In Hess, H.H. and Poldervaart, A. (eds), Basalts, 1, 325-358. Interscience, New York.

GIBSON, I.L., 1972. The chemistry and petrogenesis of a suite of pantellerites from the Ethiopian Rift. J. Petrol., 13, 31-44.

GILL, J.B., 1970. Geochemistry of Viti Levu Fiji and its evolution as an island arc. Contrib. Mineral. Petrol., 27, 179-203.

GILL, J.B., 1972. The geochemical evolution of Fiji Ph.D. thesis, Aust. Nat. Uni., (unpubl).

GILL, J.B. 1974. Role of underthrust oceanic crust in the genesis of a Fijian calc-alkaline suite. Contrib. Mineral. Petrol., 43, 29-45.

GILL, J.B. COMPSTON, W. 1973. Strontium Isotopes in island arc volcanic rocks. In, The western Pacific: Island arcs, marginal seas, geochemistry. P.J. Coleman (ed.), 483-496, Univ. W. Aust Press.

GOODMAN, R.J., 1972. The distribution of Ga and Rb in coexisting groundmass and phenocryst phases of some basic volcanic rocks. Geochim. Cosmochim. Acta, 36, 303-317.

GREEN, D.H. 1970. The origin of basaltic and nephelinitic magmas. Trans. Leicester Lit. Phil. Soc., 44, 26-54.

GREEN, D.H. 1971. Compositions of basaltic magmas as indicators of conditions of origin: application to oceanic volcanism. Phil. Trans. Roy. Soc. Lond., Ser. A, 268, 707-725.

GREEN, D.H. 1972. Contrasted melting relations in a pyrolite upper mantle under mid-oceanic ridge, stable crust and island arc environments. Tectonophysics, 17, 285-297.

GREEN, D.H., EDGAR, A.D., BEASLEY, P., KISS, E., WARE, N.G. 1974. Upper mantle source for some hawaiites, Mugearites and Benmoreites. Contrib. Mineral. Petrol., 48, 33-43.

GREEN, D.H., RINGWOOD, A.E. 1972. A comparison of recent experimental data on the gabbro-garnet granulite-eclogite transition. J. Geol., 80, 277-288.

GREEN, T.H. 1972. Crystallisation of calc-alkaline andesite under controlled high pressure hydrous conditions. Contr. Mineral. Petrol., 34, 150-166.

GREEN, T.H., RINGWOOD, A.E. 1968. Genesis of the calc-alkaline igneous rock suite. Contrib. Mineral. Petrol., 18, 105-162.

GREEN, T.H., RINGWOOD, A.E. 1972. Crystallisation of garnet bearing rhyodacite under high pressure hydrous conditions. J. Geol. Soc. Aust., 19, 203-212.

HAMILTON, D.L., ANDERSON, G.M., 1967. Effects of water and oxygen pressure on the crystallisation of basaltic magmas. In. Basalts, H.H. Hess and A. Poldervaart, (eds), vol. 1, 445-482. New York: Interscience Publishers.

HARRIS, P.G., 1957. Zone refining and the origin of potassic basalts. Geochim. Cosmochim. Acta, 12, 195-208.

HARRIS, P.G., 1967. Segretation processes in the upper mantle. In mantles of the earth and terrestrial planets (ed. S.K. Runcorn). London: Interscience.

HART, S.R. 1971. K, Rb, Cs, Sr and Ba contents and Sr isotope ratios of ocean floor basalts. Phil. Trans. Roy. Soc. Lond., Ser A, 268, 573-587.

HART, S.R., NALWALK, A.J. 1970, K, Rb, Cs and Sr relationships in submarine basalts from the Puerto Rico trench. Geochim. Cosmochim. Acta., 34, 145-155.

HASKIN, L.A., FREY, F.A., SCHMIDT, R.A., SMITH, R.H. 1966. Meteoric, solar and terrestrial rare earth distributions. Phys. Chem. Earth, 7, 167-321.

HAUGHTON, D.R., ROEDER, P.L., SKINNER, B.J. 1974. Solubility of Sulfur in mafic magmas. Econ. Geol., 69, 451-467.

HAYS, D.E., RINGIS, J. 1973. Sea floor spreading in the Tasman Sea. Nature, 243, 454-458.

HEDGE, C.E., LEWIS, J.F. 1971. Isotopic composition of strontium in three basalt-andesite centers along the Lesser Antilles Arc. Contr. Mineral. Petrol., 32, 39-47.

HEDGE, C.E., PETERMAN, Z.E. 1970. The strontium isotopic composition of basalts from the Gordon and Juan de Fuca Rises, northeastern Pacific ocean. Contr. Mineral. and Petrol., 27, 114-120.

HEKINIAN, R., 1971. Chemical and mineralogical differences between abyssal hill basalts and ridge tholeiites in the eastern Pacific Ocean. Marine Geology, 11, 77-91.

HILL, R.E.T., BOETTCHER, A.L. 1970. Water in the earths mantle: melting curves of basalt-water and basalt-water-carbon dioxide. Science, 167, 980-982.

IDDINGS, J.P., 1895. Absarokite - shoshonite - banakite series. J. Geol., 3, 935-959.

IRVINE, T.N., BARAGAR, W.R.A., 1971. A guide to the chemical classification of the common volcanic rocks. Can. J. Earth Sci., 8, 523-548.

IRVING, A.J. 1971. Geochemical and high pressure experimental studies of xenoliths, megacrysts and basalts from southeastern Australia. Ph.D. thesis, Aust. Nat. Uni. (unpubl.)

JAKES, P., GILL, J.B., 1970. Rare earth elements and the island arc tholeiitic series. Earth. Planet. Sci. Lett., 9, 17-28.

JAKES, P., SMITH, I.E., 1970. High potassium calc-alkaline rocks from Cape Nelson, eastern Papua. Contrib. Mineral. Petrol., 28, 259-271.

JAKES, P., WHITE, A.J.R., 1969. Structure of the Melanesian arcs and correlation with distribution of magma types. Tectonophysics, 8, 223-236.

JAKES, P., WHITE, A.J.R., 1970. K/Rb ratios of rocks from island arcs. Geochim. Cosmochim. Acta, 34, 849-356.

JAKES, P., WHITE, A.J.R., 1972. Major and trace element abundances in volcanic rocks of orogenic areas. Geol. Soc. Amer. Bull., 83, 29-40.

JAQUES, A.L., (in press) High potash Island arc volcanics from the Finisterre and Adelbert Ranges, northern New Guinea. Geol. Soc. Amer. Bull.

JOHNSON, R.W., 1975. Plate model for late Cainozoic volcanism at the southern margin of the Bismarck Sea, Papua New Guinea. Bull. Aust. Soc. Explor. Geophys., 6, 71-72.

JOHNSON, R.W., 1976. Potassium variation across the New Britain arc. Earth. Planet. Sci. Lett., in press.

JOHNSON, R.W., MACKENZIE, D.E., SMITH, I.E. (in prep.) Volcanic rock associations at convergent plate boundaries in Papua New Guinea.

JOHNSON, R.W., MACKENZIE, D.E., SMITH, I.E., TAYLOR, G.A.M., 1973. Distribution and petrology of late Cenozoic volcanoes in Papua New Guinea. In, The Western Pacific: Island arcs, marginal seas, geochemistry. P.J. Coleman (ed), 523-533. Uni. W. Aust. Press, Perth.

JOHNSON, R.W. WALLACE, D.A., ELLIS, D.J., 1976. Feldspathoid-bearing potassic rocks and associated types from volcanic islands off the coast of New Ireland, Papua New Guinea: A preliminary account of geology and petrology. In, Volcanism in Australasia, R.W. Johnson (ed) Elsevier (in press).

JOHNSON, T., MOLNAR, P. 1972. Focal mechanisms and plate tectonics of the southwest Pacific. J. Geophys. Res., 77, 5000-5032.

JOPLIN, G.A., 1968. The shoshonite association: A review. J. Geol. Soc. Aust., 15, 275-294.

JOPLIN, G.A., KISS, E., WARE, N.G., WIDDOWSON, J.R., 1972. Some chemical data on members of the shoshonite association. Min. Mag., 38, 936-945.

KARIG, D. 1972. Remnant Arcs. Geol. Soc. Amer. Bull., 83, 1057-1068.

KAY, R., HUBBARD, N.J., GAST, P.W., 1970. Chemical characteristics and origin of oceanic ridge volcanic rocks. J. Geophys. Res., 75, 1585-1613.

KESSON, S.E., 1973. The primary geochemistry of the Monaro alkaline volcanics, southeastern Australia - evidence for upper mantle heterogeneity. Contrib. Mineral. Petrol., 42, 93-108.

KESSON, S.E., PRICE, R.C., 1972. The major and trace element chemistry of kaersutite and its bearing on the petrogenesis of alkaline rocks. Contrib. Mineral. Petrol., 35, 119-124.

KESSON, S.E., SMITH, I.E., 1972. TiO_2 content and the shoshonite and alkaline associations. Nature Phys. Sci., 236, 110-111.

KLEEMAN, A.W., 1965. The origin of granite magmas. J. Geol. Soc. Aust., 12, 35-52.

KORRINGA, M.K., NOBLE, D.C., 1971. Distribution of Sr and Ba between natural feldspar and igneous melt. Earth. Planet. Sci. Lett., 11, 147-151.

KUSHIRO, I., 1973. Origin of some magmas in oceanic and circum-oceanic regions. Tectonophysics, 17, 211-222.

LAMBERT, I.B., WYLLIE, P.J. 1970. Melting in the deep crust and upper mantle and the nature of the low-velocity layer. Phys. Earth. Planet. Inter., 3, 316.

LINDSLEY, D.H., 1971. Synthesis and preliminary results on the stability of aenigmatite ($Na_2Fe_5TiSi_6O_{20}$). An. Rept. Geophys. Lab., 1969-70, 188-190. Carnegie Institute yearbook 1969-1970 p.188.

LIPMAN, P.W., 1965. Chemical comparison of Glassy and crystalline volcanic rocks. U.S. Geol. Surv. Bull. 1201-D.

LUTH, W.C., JAHNS, R.H., TUTTLE, D.F. 1964. The granite system at pressures of 4 to 10 kb. J. Geophys. Res., 69, 759-773.

LUYENDYK, B.P., MACDONALD, K.C., BRYAN, W.B., 1973. Rifting history of the Woodlark Basin in the southwest Pacific. Geol. Soc. Amer. Bull., 84, 1125-1134.

MACDONALD, G.A., 1960. Dissimilarity of continental and oceanic rock types. J. Petrol., 1, 172-177.

MACDONALD, G.A., KATSURA, T., 1964. Chemical composition of Hawaiian lavas. J. Petrol., 5, 82-133.

MACDONALD, K.C., LUYENDYK, B.P., VON HERZEN, R.P. 1973. Heat flow and plate boundaries in Melanesia. J. Geophys. Res., 78, 2537-2546.

MACDONALD, R., BAILEY, D.K., SUTHERLAND, D.S., 1970. Oversaturated
        peralkaline glassy trachytes from Kenya. J. Petrol., 11,
        507-517.

MACKENZIE, D.E., CHAPPELL, B.W. 1972. Shoshonitic and calc-alkaline
        lavas from the highlands of Papua New Guinea. Contrib.
        Mineral. Petrol., 35, 50-62.

MARSH, B.D., CARMICHAEL, I.S.E. 1974. Benioff zone magmatism.
        J. Geophys. Res., 79, 1196-1206.

McBIRNEY, A.R. 1969. Compositional variations in Cenozoic calc-
        -alkaline suites. Proc. Adnesite Confr. Oregon Dept. Geol.
        Mineral. Ind. Bull., 65, 185-189.

MERRILL, J.K., ROBERTSON, J.K., WYLLIE, P.J., 1970. Melting reactions
        in the system $NaAlSi_3O_8$ - $KAlSi_3O_8$ - SiO_2 - H_2O to 20 kilobars
        compared with results for other feldspar-quartz-H_2O and rock-
        H_2O systems. J. Geol., 78, 558-569.

MILSOM, J. 1970. Woodlark Basin, a minor center of sea-floor spreading
        in Melanesia. J. Geophys. Res. 75, 7335-7339.

MILSOM, J. 1973a. Papuan ultramafic belt: gravity anomalies and the
        emplacement of ophiolites. Geol. Soc. Amer. Bull., 84,
        2243-2258.

MILSOM, J., 1973b. The gravity field of the Papuan Peninsula.
        Geologie en mijnbouw, 52, 13-20.

MILSOM, J., SMITH, I.E. 1975. Southeastern Papua: Generation of
        thick crust in a tensional environment. Geology, 3, 117-120.

MINEAR, J.W., TOKSÖZ, M.N., 1970. Thermal regime of a down going
        slab, and the new global tectonics. J. Geophys. Res., 75,
        1397-1419.

MIYASHIRO, A., 1973. The Troodos ophiolitic complex was probably
        formed in an island arc. Earth Planet. Sci. Lett., 19,
        218-224.

MIYASHIRO, A., 1974. Volcanic rock series in island arcs and active
        continental margins. Am. J. Sci., 274, 321-355.

MIYASHIRO, A., SHIDO, F., EWING, M. 1970. Crystallisation and
        differentiation in abyssal tholeiites and gabbros from mid-
        -ocean ridges. Earth Planet. Sci. Lett., 7, 361-365.

MOORE, J.G. 1970. Water content of basalt erupted on the ocean floor.
        Contrib. Mineral. Petrol., 28, 272-279.

MORGAN, W.R., 1966. A note on the petrology of some lava types from
        east New Guinea. J. Geol. Soc. Aust., 13, 583-591.

MURATA, K.J., RICHTER, D.H. 1961. Magmatic differentiation in the Uwekahuna Laccolith, Kilauea Caldera, Hawaii. J. Petrol., 2, 424-437.

MUTTER, J.C., 1975. A structural analysis of the gulf of Papua and northwest Coral Sea region. Bur. Miner. Resour. Aust. Rep., 179.

MYSEN, B.O. 1973. Melting in a hydrous mantle: phase relations of mantle peridotite with controlled water and oxygen fugacities. Carnegie Inst. Wash., Year Book, 72, 467-478.

MYSEN, B.O., 1975. Partitioning of ion and magnesium between crystals and partial melts in peridotite upper mantle. Contrib. Mineral. Petrol., 52, 69-76.

MYSEN, B.O. BOETTCHER, A.L. 1975. Melting of a hydrous mantle II. Geochemistry of liquids and crystals formed by anatexis of mantle peridotite at high pressures and high temperatures as a function of controlled activities of water, hydrogen and carbon dioxide. J. Petrol., in press.

NAGASAWA, H. 1970. Rare earth concentrations in zircons and apatites and their host dacites and granites. Earth. Planet. Sci. Lett., 9, 359-364.

NAGASAWA, H., SCHNETZLER, C.C., 1971. Partitioning of rare earth, alkali and alkaline earth elements between phenocrysts and acidic igneous magma. Geochim. Cosmochim. Acta, 35, 953-968.

NESBITT, R.W., HAMILTON, D.L. 1970. Crystallisation of an alkali olivine basalt under controlled P_{O_2}, P_{H_2O} conditions. Phys. Earth Planet. Int., 3, 309-315.

NICHOLLS, I.A. 1974. Liquids in equilibrium with peridotitic mineral assemblages at high water pressures. Contr. Mineral. Petrol., 45, 289-316.

NICHOLLS, I.A., RINGWOOD, A.E., 1972. Production of silica saturated tholeiitic magmas in island arcs. Earth. Planet. Sci. Lett., 17, 243-246.

NICHOLLS, I.A., RINGWOOD, A.E., 1973. Effect of water on olivine stability in tholeiites and the production of silica saturated magmas in the island arc environment. J. Geol., 81, 285-300.

NICHOLLS, J., CARMICHAEL, I.S.E., 1969a. A commentary on the absarokite-shoshonite-banakite series of Wyoming, USA. Schweitz Mineral. Petrog. Mitt., 49, 47-64.

NICHOLLS, J., CARMICHAEL, I.S.E., 1969b. Peralkaline acid liquids: a petrological study. Contrib. Mineral. Petrol., 20, 268-294.

NOBLE, D.C., 1965. Gold Flat Member of the Thirsty Canyon Tuff - a pantellerite ash-flow sheet in southern Nevada. U.S. Geol. Surv. Prof. Pap., 525-B, 85-90.

NOBLE, D.C., 1968. Systematic variation of major elements in comendite and pantellerite glasses. Earth Planet. Sci. Lett., 4, 167-172.

NOBLE, D.C., HEDGE, C.E. 1969. $^{87}Sr/^{86}Sr$ variations within individual ash-flow sheets. U.S. Geol. Surv. Prof. Pap., 650C, C133-C139.

NOBLE, D.C., SMITH, V.C., PECK, L.C., 1967. Loss of halogens from crystallised and glassy silicic volcanic rocks. Geochim. Cosmoch·m. Acta, 31, 215-223.

OSBORN, E.F. 1959. Role of oxygen pressure in the crystallisation and differentiation of basaltic magma. Am. J. Sci., 257, 609-647.

OXBURGH, E.R., TURCOTTE, D.L. 1970. Thermal structure of island arcs. Geol. Soc. Amer. Bull., 81, 1665-1688.

PAGE, R.W., JOHNSON, R.W., 1974. Strontium isotope ratios of Quarternary volcanic rocks from Papua New Guinea. Lithos, 7, 91-100.

PAUL, A., DOUGLAS, R.W. 1965. Ferrous-ferric equilibrium in binary alkali silicate glasses. Phys. Chem. Glasses, 6, 207-211.

PEARCE, J.A., CANN, J.R., 1971. Ophiolite origin investigated by discriminant analysis using Ti, Zr and Y. Earth Planet. Sci. Lett., 12, 339-349.

PEARCE, J.A., CANN, J.R., 1973. Tectonic setting of basic volcanic rocks determined using trace element analyses. Earth Planet. Sci. Lett., 19, 290-300.

PHILPOTTS, J.A., SCHNETZLER, C.C., 1968. Europium anomalies and the genesis of basalt. Chem. Geol., 3, 5-13.

PHILPOTTS, J.A., SCHNETZLER, C.C., 1970. Phenocrysts-matrix partition coefficients for K, Rb, Sr and Ba, with applications to anorthosite and basalt genesis. Geochim. Cosmochim. Acta, 34, 307-322.

PIETERS, P.E. 1974. Explanatory notes on the Port Moresby-Kalo-Aroa geological map. Geol. Surv. Papua New Guinea Rept. 74/28 (unpubl.)

POWELL, J.L. 1969. Isotopic composition of strontium in volcanic rocks (abs). Symposium on volcano and their roots, Oxford, England. Inter. Assoc. Volc., Chem. Earth's Interior, Vol of Abstracts, 144.

PRICE, R.C., TAYLOR, S.R., 1973. The geochemistry of the Dunedin
        volcano, East Otago, New Zealand: Rare earth elements.
        Contrib. Mineral. and Petrol., 40, 195-205.

PROSTKA, H.J. 1973. Hydrid origin of the absarokite-shoshonite
        banakite series, Absaroka volcanic field, Wyoming.
        Geol. Soc. Amer. Bull., 84, 697-702.

PUSHKAR, P. 1968. Strontium isotope ratios in volcanic rocks of
        three island arc areas. J. Geophys. Res., 73, 2702-2713.

RINGWOOD, A.E., 1966. The chemical composition and origin of the
        earth. In. Advances in Earth Sciences, P.M. Hurley (ed),
        287-356. MIT Press, Boston.

ROD, E., 1974. Geology of eastern Papua: Discussion. Geol. Soc.
        Amer. Bull., 85, 653-658.

ROEDER, P.L., EMSLIE, R.F. 1970. Olivine-liquid equilibrium.
        Contrib. Mineral. Petrol., 29, 275-289.

ROUX, J., VARET, J., 1975. Alkali feldspar liquid equilibrium relation-
        ships in peralkaline oversaturated systems and volcanic rocks.
        Contrib. Mineral. Petrol., 49, 67-81.

RUXTON, B.P. 1966. A late Pleistocene to Recent rhyodacite-trachybasalt-
        basaltic latite volcanic association in northeast Papua.
        Bull. volcanol., 29, 347-374.

SCHNETZLER, C.C. PHILPOTTS, J.A., 1970. Partition coefficients of
        rare-earth elements between igneous matrix material and
        rock-forming mineral phenocrysts. II. Geochim. Cosmochim.
        Acta. 34, 331-340.

SHAIRER, J.F., BOWEN, N.L., 1955. The system $K_2O-Al_2O_3-SiO_2$.
        Am. J. Sci., 253, 681-746.

SHAIRER, J.F., BOWEN, N.L., 1956. The system $Na_2O-Al_2O_3-SiO_2$.
        Am. J. Sci., 254, 129-195.

SHAW, D.M. 1970. Trace element fractionation during anatexis.
        Geochim. Cosmochim. Acta., 34, 237-243.

SHIDO, F., MIYASHIRO, A., EWING, M., 1971. Crystallisation of abyssal
        tholeiites. Contr. Mineral. Petrol., 31, 251-266.

SMITH, I.E. 1969. Notes on the volcanoes Mount Bagana
        and Mount Victory,T.P.N.G. Bur. Miner. Resour. Aust. Rec.
        1969/12 (unpubl.)

SMITH, I.E., 1970. Late Cainozoic uplift and geomorphology in
        southeastern Papua. Search, 1, 222-225.

SMITH, I.E., 1971. Late Cainozoic volcanism in eastern Papua. In, Johnson and others, Short papers on Quarternary volcanic areas in Papua New Guinea. Bur. Miner. Resour. Aust. Rec., 1970/72 (unpubl).

SMITH, I.E., 1972. High-potassium intrusives from southeastern Papua. Contrib. Mineral. and Petrol., 34, 167-176.

SMITH, I.E., 1973a. Late Cainozoic volcanism in the southeast Papuan Islands. Bur. Miner. Resour. Aust. Rec., 1973/67. (unpubl).

SMITH, I.E., 1973b. The geology of the Calvados Chain, southeastern Papua. Geological Papers 1970-71. Bur. Miner. Resour. Aust. Bull. 139, 59-66.

SMITH, I.E., DAVIES, H.L., 1973a. Samarai, Papua New Guniea--1:250,000 geological series. Bur. Miner. Resour. Aust. explan Notes, SC/56-9.

SMITH, I.E., DAVIES, H.L., 1973b. Abau, Papua New Guinea--1:250,000 geological series. Bur. Miner. Resour. Aust. explan Notes, SC/55-12.

SMITH,I.E., DAVIES, H.L., 1976. The geology of the southeast Papuan mainland. Aust. Bur. Miner. Resour. Bull. 165 (in press).

SMITH, I.E., PIETERS, P.E. 1969. The geology of the Louisiade Archipelago, TPNG., excluding Misima Island. Bur. Miner. Resour. Aust. Rec.1969/93 (unpubl.)

STERN, C.R., HAUNG, W.L., WYLLIE, P.J., 1975. Basalt-andesite-rhyolite-H_2O: crystallisation intervals with excess H_2O and H_2O-undersaturated liquidus surfaces to 35 kilobars with implications for magma genesis. Earth Planet. Sci. Lett., 28, 189-196.

STERN, C.R., WYLLIE, P.J., 1973. Water-saturated and undersaturated melting relations of a granite to 35 kilobars. Earth Planet. Sci. Lett., 18, 163-167.

STOEN, J.O., & GARSIDE, I.E., 1973. Nubiam No. 1 well completion report. Amoco Australia Exploration Co. Rept.

SUGIMURA, A., 1961. Regional variation of the K_2O/Na_2O ratios of volcanic rocks in Japan and environs. J. Geol. Soc. Japan, 67, 292-300 (English abstract on p.292).

SUGIMURA, A., 1968. Spatial relations of basaltic magmas in island arcs. In. Basalts, 2. (Eds H.H. Hess and A. Poldervaart). Interscience, New York - London, 537-571.

SUN, S.S., HANSON, G.N., 1975. Origin of Ross Island basanitoids and limitations upon the heterogeneity of mantle sources for alkali basalts and nephelinites. Contr. Mineral. Petrol., 52, 77-106.

SUTHERLAND, D.S., 1971. The Eburru volcano, Kenya. J. Geol. Soc.
    Proc., 127, 417.

TAYLOR, G.A.M., 1958. The 1951 eruption of Mount Lamington, Papua.
    Bur. Miner. Resour. Aust. Bull, 38.

TAYLOR, S.R., 1969. Trace element chemistry of andesites and
    associated calc-alkaline rocks. Proc. Andesite Conference
    (A.R. McBirney ed.) Oregon. Dept. Geol. Min. Resour. Bull.,
    65, 43-63.

TAYLOR, S.R., KAYE, M., WHITE, A.J.R., DUNCAN, A.R., EWART, A., 1969.
    Genetic significance of Co, Cr, Ni, Sc and V content of
    andesites. Geochim. Cosmochim. Acta., 33, 275-286.

THOMPSON, G., SHIDO, F., MIYASHIRO, A., 1972. Trace element distrib-
    utions in fractionated oceanic basalts. Chemical Geology, 9,
    89-97.

THOMPSON, R.N., MACKENZIE, W.S., 1967. Feldspar-liquid equilibria in
    peralkaline acid liquids: an experimental study. Am. J. Sci.,
    265, 714-734.

TILLEY, C.E., MUIR, I.D., 1964. Intermediate members of the oceanic
    basalt-trachyte association. Geol. Foren. För., 85, 434-443.

TRAIL, D.S., 1967. Geology of Woodlark Island, Papua. Bur. Miner.
    Resour. Aust. Rept. 115.

TREUIL, M., VARET, J., BILLHOT, M., 1971. Distribution of nickel,
    copper and zinc in the volcanic series of Erta'Ale, Ethiopia.
    Contrib. Mineral. Petrol., 30, 84-94.

TURNER, F.J., 1968. Metamorphic Petrology. McGraw-Hill, New York.

TUTTLE, O.F., BOWEN, N.L. 1958. Origin of granite in the light of
    experimental studies. Geol. Soc. Amer. Mem., 74.

VERHOOGEN, J. 1962. Oxidation of iron-titanium oxides in igneous rocks.
    J. Geol., 70, 168-181.

VILLARI,L. 1968. On the geovolcanological and morphological evolution
    of an endogenous dome (Pantellerra, Mt Gelkahamar). Geol. Rd.,
    B.57, H.3, 784-794.

VOISEY, A.H., 1969. Geological History (of the New England region).
    In the geology of New South Wales, G.H. Packham (ed.). J. Geol.
    Soc. Aust., 16, 307-310.

WAGER, L.R. 1960. The major element variation of the layered series
    of the Skaergaard Intrusion. J. Petrol., 1, 364-398.

WEAVER, S.D., SCEAL, J.S.C., GIBSON, I.L., 1972. Trace-element data relevant to the origin of trachytic and pantelleritic lavas in the east African rift system. Contrib. Mineral. Petrol., 36, 181-194.

WEISSEL, J.K., HAYS, D.E., 1971. Contrasting zones of sea-floor spreading south of Australia [abs.]. Am. Geophys. Union Trans., 52, 237.

WHITFORD, D.J. 1975. Strontium isotopic studies of the volcanic rocks of the Sunda Arc, Indonesia, and their petrogenetic implications. Geochim. Cosmochim. Acta., 39, 1287-1302.

WONES, D.R., GILBERT, M.C., 1967. The stability of fayalite. Ann. Rept. Geophys. Lab. Yearbook 66, 402-403.

WRIGHT, T.L., 1968. X-ray and optical study of alkali feldspar: II An X-ray method for determining the composition and structural state from measurement of 20 values for three reflections. Am. Mineral., 53, 88-104.

WRIGHT, T.L., DOHERTY, P.C., 1970. A linear programming and least squares computer method for solving petrologic mixing problems. Bull. Geol. Soc. Am., 81, 1995-2008.

WRIGHT, J.B., 1965. Petrographic sub provinces in the Tertiary to Recent volcanoes of Kenya. Geol. Mag., 102, 541-57.

YAGI, K., 1953. Petrochemical studies of the alkalic rocks of the Morotu District, Sakhalin. Geol. Soc. Am. Bull., 64, 769-810.

YAGI, K., 1966. The system acmite-diopside and the bearing on the stability relations of natural pyroxenes of the acmite-hedenbergite-diopside series. Am. Mineral., 51, 976-1000.

YODER, H.S., TILLEY, C.E. 1962. Origin of basalt magmas: an experimental study of natural and synthetic rock systems. J. Petrol., 3, 342-532.

APPENDIX I

ANALYTICAL TECHNIQUES

The bulk of the analytical results presented in this thesis
are X-ray fluorescence determinations carried out in the Department of
Geology, A.N.U. over the period 1971 to 1974. The work was carried out
in two main batches and consistency between separate analytical runs
was checked by means of duplicate analyses.

Sample Preparation

Between 1 and 2kg of rock from which weathered and contaminated
surfaces had been removed were split in a hydraulic splitter to 1cm
(approximately) cubes. This material was then reduced to sand size in
a tungsten carbide siebtechnik swing mill; final crushing of a
representative 100g aliquot in the same mill reduced the grainsize to
less than 20 mesh. Between samples the mill was cleaned with acid,
washed quartz sand and an initial sample crush which was then rejected.
Since crushing in tungsten carbide introduces cobalt and tungsten as
contaminants, these two elements were excluded from analysis.

X-ray Fluorescence Spectrometry

Major and trace element abundances were determined using an
automated Philips PW1220 spectrometer. Operating conditions are
summarised in Table I-1. The accuracy of the method used for major
element analysis has been discussed in detail by Norrish and Hutton
(1969). Accuracy in trace element analysis was estimated by comparison
of the measured trace element abundances in known natural standards
with preferred values obtained by a variety of analytical methods
(Table I-2). Precision and detection limits were determined from
counting statistics (Norrish and Chappell, 1967).

Major Element Analysis

The major elements Si, Ti, Al, Fe, Mn, Mg, Ca, K, P were
determined as oxides (Fe as Fe_2O_3) in glass discs prepared by the
fusion method of Norrish and Hutton (1969). All analyses were carried
out in duplicate. Background interference in the analysis of Mg is
largely due to crystal fluorescence so this was minimised by setting

TABLE 1-1 Summary of analytical conditions for X-ray spectrometry.

element	analytical line	X-ray tube	analysing crystal	collimator	detector	absorption coefficient	background position relative to peak (2θ)
oxide %							
SiO$_2$	K$_\alpha$	Cr	PE	C	F.C.		
TiO$_2$	K$_\alpha$	Cr	LiF(200)	C	F.C.		
Al$_2$O$_3$	K$_\alpha$	Cr	PE	C	F.C.		
Fe$_2$O$_3$	K$_\alpha$	W	LiF(200)	C	F.C		
MnO	K$_\alpha$	W	LiF(200)	C	F.C		
MgO	K$_\alpha$	Cr	ADP	C	F.C		
CaO	K$_\alpha$	Cr	LiF(200)	C	F.C		
K$_2$O	K$_\alpha$	Cr	LiF(200)	C	F.C		
P$_2$O$_5$	K$_\alpha$	Cr	Ge	C	F.C		
S	K$_\alpha$	Cr	Ge	C	F.C		
ppm.							
Ba	L$_\beta$	W	LiF(220)	C	F.C	Fe	±1.20
Rb	K$_\beta$	Mo	LiF(200)	F	S.C	Rb	± .26
Sr	K$_\alpha$	Mo	LiF(200)	C	S.C	Sr	± .35
Pb	L$_\beta$	Mo	LiF(200)	F	S.C	Rb	± .23
Th	L$_\beta$	Mo	LiF(200)	F	S.C	Rb	± .23
U	L$_\alpha$	Mo	LiF(220)	F	S.C	Rb	± .25
Zr	K$_\alpha$	W	LiF(200)	C	S.C	Sr	± .40
Nb	K$_\alpha$	W	LiF(200)	F	S.C	Sr	± .35
Y	K$_\alpha$	Mo	LiF(200)	C	S.C	Sr	± .40
La	L$_\alpha$	W	LiF(220)	C	F.C.	Fe	±1.25
Ce	L$_\beta$	W	LiF(200)	F	F.C	Fe	±1.20
Sc	K$_\alpha$	Cr	LiF(200)	F	F.C	Fe	.50
V	K$_\alpha$	W	LiF(220)	F	F.C	Fe	±1.75
Cr	K$_\alpha$	W	LiF(200)	F	F.C.	Fe	± .90
Ni	K$_\alpha$	Au	LiF(200)	C	S.C	Zn	± .40
Cu	K$_\alpha$	Au	LiF(200)	C	S.C.	Zn	± .40
Zn	K$_\alpha$	Au	LiF(200)	C	S.C.	Zn	± .40
Ga	K$_\alpha$	Mo	LiF(200)	C	S.C	Zn	± .60
Cl	K$_\alpha$	Cr	Ge	C			+1.0

C - coarse collimator = 480μ   F.C - flow counter
F - fine collimator = 160μ   S.C - scintillation counter

TABLE I-2: Comparison of measured trace element abundances
in natural standards with preferred values.

Ba	BCR-1		W-1	
	A.N.U.	preferred	A.N.U.	preferred
Ba	697	700	160	165
Rb	46.6	47.5	21.1	21.6
Sr	330	335	189	185
Pb	19	15	10	8
Th	6	6	3	2.3
Zr	188	180	92	94
Nb	11	13	6	9
Y	33	40	20	26
La	27	24	10	10
Ce	52	52	19	23
V	362	360	234	245
Cr	12	14	91	115
Ni	5	10	66	75
Cu	11	16	102	115
Zn	126	120	90	83
Ga	21	21	17	17

Abundacces in ppm. Preferred values taken from compilations
of superior analytical data.

the pluse height selector window symmetrically below the Mg   peak and also by applying an empirical correction (Norrish and Hutton, 1969).

Na was determined by means of a modified Baird-Atomic double beam photometer with a propane-air flame, using Li as an internal standard; the method is similar to that described by Cooper (1963) for K. All analyses were duplicated.

Determination of FeO in the initial batch of samples involved dissolution of the sample in HF in the presence of an excess of ammonium metavanadate. The excess vanadic ion was then titrated against a ferrous ammonium sulphate solution which had been standardised against BDH standard ceric sulphate. A second technique which was used for determination of FeO in about half of the samples involved dissolution of the sample in HF over a flame followed by titration against a 0.05 N solution of potassium dichromate (Peck, 1964). Consistency between analytical methods was checked by means of replicate analyses and all determinations were carried out in duplicate. Ferric iron was calculated by difference from the total iron content measured by X-ray fluorescence.

H_2O- is the percentage weight loss of a sample after heating for at least 90 minutes at $110^{\circ}C$. H_2O+ and CO_2 were measured by heating a sample for 30 minutes in a tube furnace at 1000 to $1050^{\circ}C$ in a stream of dry, CO_2-free nitrogen. H_2O and CO_2 given off from the sample were collected and weighed in microabsorption tubes containing a mixture of P_2O_5 and pumice, and "carbosorb" soda asbestos respectively.

Trace Elements

Trace element abundances were measured in duplicate on discs of pelletised rock powder with boric acid sides and base. X-ray counts were automatically corrected for detector dead time, and instrument drift was monitored against an internal standard. The analytical line and operating conditions were selected so as to maximise the count rate and minimise inter-element interferences. Background counts measured on either side of the peak position were selected so that interference was minimal and for all elements were

symmetric about the peak position. Following Norrish and Chappell (1967) a further empirical correction for inter-element interferences was applied to the measured intensities; the background profile was also corrected for non-linearity including the effects of tube contamination measured on one or more of the following: Spec pure Al_2O_3, spec pure SiO_2 and "Herasil" (silica glass supplied by Heraeus GmbH., Hanau, W. Germany). Ni blanks are measured on NBS 165 (glass sand).

The concentration (p) of a trace element is related to the intensity of emitted characteristic radiation (c) by the formula

$$p = \frac{A \times c}{K}$$

where A is the mass absorption of the sample for the radiation being analysed and K is a constant for a particular analytical run which is calculated by analysing standards (in most cases synthetic) whose A and p are known, under the same analytical conditions as the samples.

Mass absorption coefficients for samples were measured for shorter wavelengths ($Sr_{K\alpha}$ and $Rb_{K\alpha}$) on undiluted rock powder pressed into a perspex holder of known diameter. The attenuation (Io/I) of the measured wavelength was measured and the mass absorption calculated from the relationship

$$A = \frac{1}{px} \ln (Io/I) \text{ where } px = \text{mass cm}^{-2}$$

For measurements at longer wavelengths ($Zn_{K\alpha}$ and $Fe_{K\alpha}$) the samples were first diluted with an approximately equal amount of cellulose to prevent extreme attenuation.

Electron Microprobe Analysis

Analysis of phenocryst phases in selected specimens was carried out on polished slab mounts or polished thin sections. The electron microprobe, located in the School of Earth Sciences, A.N.U., was a TNO-TH electron microprobe with a 45° electron incidence fitted with an Ortec Si (Li) detector with a 45° take-off angle incorporating an Ortec 716A amplifier. During analysis the emitted X-ray spectrum

was accumulated for 100 seconds at a count rate of about 4000 counts/
second by a Northern Scientific NS710 multichannel analyser. Details
of data reduction and correction procedures have been described by
Reed and Ware (1973; 1975). Analytical conditions were: accelerating
voltage 15kV, beam current 3nA, beam diameter typically 2-3um;
accuracy is about ± 2%.

Spark Source Mass Spectrometry

An AEI MS7 spark source mass spectrograph located in the
School of Earth Sciences, A.N.U., was used to measure the abundance of
the rare earth elements and a limited number of other trace elements
in selected specimens. The method used is that described by Taylor
(1965; 1971) with some recent modifications by Nance (1975). The
main difference between this method and that used by Jakes and Gill
(1970) in the measurement of three tholeiitic basalts from southeastern
Papua is the use of a computer to process the raw data.

Quantitative element abundance data were obtained for La,
Ce, Pr, Nd, Sm, Eu, Gd, Tb, Dy, Ho, Er, Yb and Y in all samples and
data were also obtained for Pb, Th, U, Cs and Sn. Because the method
uses the rare earth element Lu as an internal standard, its abundance
cannot be directly determined and because of interference from a
carbon multiple molecule, the abundance of the rare earth Tm is also
not directly determinable. The abundance of both of these elements
can however, be estimated from the rare earth pattern.

Sample preparation involved mixing about 100mg of powdered
sample with an identical amount of powdered graphite mix (mix F)
containing 50ppm Lu as Lu_2O_3. Electrodes pressed from this material
were then subjected to a high voltage spark under high vacuum in the
source of the mass spectrometer and the ion beam produced collected
on an Ilford Q-2 photographic plate. The densities of mass lines
were determined on a microphotodensitometer and the photoplates
calibrated by plotting the densities of lines for isotope pairs against
their known abundance ratios. The slope of a line drawn through these
points was used to measure the plate response to incident ions thereby

relating line density to beam intensity. The ratio of the intensity of a mass line to the intensity of the internal standard line on the same exposure relates directly to the abundance of that nuclide. Natural standards provide calibration of this ratio to elemental abundance. The computer program also applied corrections for natural Lu, interferences on ^{176}Lu by ^{176}Hf and ^{176}Yb, and for light REE and Ba oxide and carbide interferences on the heavy REE. This last correction was particularly important in view of the high light REE and Ba contents of some of the samples.

Accuracy and precision of the method are dependent upon the total number of exposures used to calculate the abundance of each element as well as on other factors. Two photoplates were exposed for each sample and each contained up to 14 graded exposures; determinations for many elements were based on more than one isotope. In general this resulted in the measured abundance of each element being based on 8-20 determinations but in many of the samples run, the abundances of La and Ce were unusually high and the number of photoplate readings correspondingly small. In these cases element abundances determined by mass spectrometry were significantly lower (up to 50%) than those determined by X-ray fluorescence and the latter were used in preference. The discrepancy between determinations by these two methods underlines the limitations imposed on spark source spectrometry by a photographic detector and is explicable in terms of the range of response of the photoplate to incident ions.

In general the precision of the method for all elements is about 3-5% expressed as standard error. Table I-3 lists recent data on the standard rock BCR-1 which indicate an accuracy for the method of about 10%.

The rare earth element abundances are typically presented diagramatically as rare earth patterns in which the abundance of individual elements is divided by the abundance in chondrites. The chondritic abundances which have been used for normalisation in this thesis are presented in Table I-4.

TABLE I-3:   TRACE ELEMENT DATA FOR BCR-1

element	MS-7 (1)	MS-7 (2)	XRF (ANU)	range
Ba	670	710	697	580 - 713
Pb	15.7	12.4	19	
Th	5.5	4.7	6	4.98 - 6.02
U	1.6	1.5		1.68 - 1.8
Zr	175	188	188	232 - 229
Hf	5.0	4.0		4.57 - 5.23
Nb	13	14	11	
Sn	2.3	2.3		
Y	36	36	33	
La	25.2	23.7	27	23.7 - 26.2
Ce	52.6	52.9	52	51.3 - 54.9
Pr	6.54	6.60	7	
Nd	27.2	31.2	24	28.5 - 32.1
Sm	6.00	6.42		6.52 - 7.44
Eu	1.88	1.96		1.87 - 1.98
Gd	6.45	6.66		6.45 - 8.02
Tb	.99	1.03		.96 - 1.15
Dy	6.20	6.74		5.65 - 6.55
Ho	1.29	1.33		1.15 - 1.46
Er	3.70	3.54		3.51 - 4.5
Yb	3.66	3.60		3.21 - 3.74

MS-7 data from Whitford (1975);   range in abundances from Arth and Hanson (1975), Brunfelt and Heier (1971), Frey and others (1974), Gast and others (1970), Philpotts and Schnetzler (1970).

TABLE I-4: REE IN CHONDRITES

element	ppm	element	ppm
La	.30	Gd	.26
Ce	.84	Dy	.049
Pr	.12	Ho	.31
Nd	.58	Er	.073
Sm	.21	Yb	.20
Eu	.074		

Data from Haskin and others (1966), Haskin and others (1968) and Hubbard and Gast (1971).

References

ARTH, J.G., HANSON, G.N., 1975. Geochemistry and origin of the early Precambrian crust of northeastern Minnesota. Geochim. Cosmochim. Acta, 39, 325-362.

BRUNFELT, A.E., HEIER, K.S., 1971. Determination of 40 elements in Apollo 12 samples by neutron activation analysis. Proc. second Lunar Sci. Conf., 2, 1281-1290.

COOPER, J.A., 1963. The flame photometric determination of potassium in geological materials used for potassium-argon dating. Geochim. Cosmochim. Acta, 27, 525-546.

FREY, F.A., BRYAN, W.B., THOMPSON, G., 1974. Atlantic Ocean floor: Geochemistry and petrology of basalts from legs 2 and 3 of the deep sea drilling project. J. Geophys. Res., 79, 5507-5527.

GAST, P.W., HUBBARD, N.J., WIESMANN, H., 1970. Chemical composition and petrogenesis of basalts from Tranquillity Base. Proc. Apollo 11 Lunar Sci. Conf., 2, 1143-1163.

HASKIN, L.A., FREY, F.A., SCHMITT, R.A., SMITH, R.H., 1966. Meteoritic solar and terrestrial rare-earth distributions. Phys. Chem. Earth, 7, 169-321. Pergamon Press.

HASKIN, L.A., HASKIN, M.A., FREY, F.A., WILDEMAN, T.R., 1968. Relative and absolute terrestrial abundances of the rare earths. In: Origin and Distribution of the Elements (L.H. Ahrens, ed.), 889-912. Pergamon Press.

HUBBARD, N.J., GAST, P.W., 1971. Chemical composition and origin of non-mare lunar basalts. Proc. Second Lunar Sci. Conf., Geochim. Cosmochim. Acta Suppl., 2, 999-1020. M.I.T. Press.

JAKES, P., GILL, J.B., 1970. Rare earth elements and the island arc tholeiitic series. Earth. Planet. Sci. Lett., 9, 17-28.

NANCE, W.B., 1975. Rare earth elements in Australian sediments. M.Sc. Thesis, Aust. Nat. Uni., (unpubl.).

NORRISH, K., CHAPPELL, B.W., 1967. X-ray fluorescence spectrography. In: Physical Methods in Determinative Mineralogy (J. Zussman, ed.), 161-214. Academic Press.

NORRISH, K., HUTTON, J.T., 1969. An accurate X-ray spectrographic method for the analysis of a wide range of geological samples. Geochim. Cosmochim. Acta, 33, 431-454.

PECK, L.C., 1964. Systematic analysis of silicates. U.S. Geol. Surv. Bull., 1170.

PHILPOTTS, J.A., SCHNETZLER, C.C., 1970. Apollo 11 lunar samples: K, Rb, Sr, Ba and rare earth concentrations in some rocks and separated phases. Proc. Apollo 11 Lunar Sci. Conf. 2, 1471-1486.

REED, S.J.B., WARE, N.G., 1973. Quantitative electron microprobe analysis using a lithium drifted silicon detector. X-ray Spectrometry, 2, 69-74.

REED, S.J.B., WARE, N.G., 1975. Quantitative electron microprobe
        analysis of silicates using energy dispersive X-ray
        spectrometry. J. Petrol., 16, 499-519.

TAYLOR, S.R., 1965. Geochemical analysis by spark source mass
        spectrography. Geochim. Cosmochim. Acta, 29, 1243-1261.

TAYLOR, S.R., 1971. Geochemical application of spark source mass
        spectrography - II. Photoplate data processing. Geochim.
        Cosmochim. Acta, 35, 1187-1196.

WHITFORD, D.J., 1975. Geochemistry and petrology of volcanic rocks
        from the Sunda Arc, Indonesia. Ph.D Thesis, Aust. Nat.
        Uni., (unpubl.).

APPENDIX II

LOCALITIES AND BRIEF DESCRIPTION OF ANALYSED SAMPLES

Sample numbers refer to material housed in the collection of the Department of Geology, A.N.U. Samples collected by other people during the course of regional mapping in Papua and samples donated during the course of the study are acknowledged; all others were collected personally. Latitude and longtitude (expressed in degrees and minutes) are from 1:250,000 scale geological maps where they are available or from the 1:1,000,000 scale geological map of Papua New Guinea. Place names are from the same sources.

The following terms are used: boulder - fresh but not <u>in</u> <u>situ</u> samples from a stream bed; float - fresh but not <u>in situ</u> sample in the bush. Mineral abbreviations used are: Plag - plagioclase; Biot - biotite; Cpx - clinopyroxene; Hblde - hornblende; Kfs - alkali feldspar; Ol - olivine; Opq - iron-titanium oxides; Opx - orthopyroxene. Field numbers are given in brackets after the A.N.U. number.

Tholeiitic basalts (Table 3-1).

Prefix 33

557 (4095).   Basalt, boulder, Sige Lele River, ($10^{o}34$'S, $150^{o}38$'E). Plag. (labradorite), cpx, opq, ol (pseudomorphs), interstitial material. Collected G Cifali.

558 (3177).   Coarse basalt, boulder, Kiramara River, ($10^{o}54$'S, $149^{o}41$'E). Plag. (labradorite), cpx, opq.

559 (2041).   Pillow basalt, Touiawaira Creek, ($10^{o}15$'S, $150^{o}25$'E). Plag. (labradorite), cpx, opq, interstitial material. Collected H.L. Davies.

560 (3112).   Basalt, Wamira River, ($10^{o}11$'S, $150^{o}01$'E). Plag. (labradorite), cpx, opq, interstitial material.

561 (3011).   Basalt, Dawa Dawa River, ($10^\circ34'$S, $150^\circ23'$E). Plag. (labradorite), cpx, opq, ol (pseudomorphs), interstitial material.

562 (3116).   Coarse basalt, Nigo Nigo River, ($10^\circ15'$S, $149^\circ56'$E). Plag. (labradorite), cpx, opq, ol (pseudomorphs).

563 (5171).   Microgabbro, Bonua River, ($10^\circ1'$S, $149^\circ7'$E). Labradorite, cpx, opq; minor alteration. Collected C.D. Ollier.

564 (2606).   Pillow basalt, Bonua River, ($9^\circ59'$S, $149^\circ6'$E). Labradorite, cpx, opq, interstitial material. Collected H.L. Davies.

565 (3045).   Basalt, Wamira River, ($10^\circ15'$S, $150^\circ04'$E). Labradorite, cpx, opq, interstitial material.

566 (5533).   Slightly porphyritic basalt, Ulumanu River, ($10^\circ3'$S, $149^\circ27'$E). Rare phenocrysts - labradorite. Groundmass - labradorite, cpx, opq, interstitial material; rare calcite. Collected P.E. Pieters.

567 (2207).   Basalt, boulder, Lavora Bay ($10^\circ08'$S, $150^\circ12'$E). Labradorite, cpx, ol (pseudomorphs), interstitial material. Collected H.L. Davies.

568 (2643).   Coarse basalt, Tavanei River, ($9^\circ58'$S, $149^\circ22'$E). Labradorite, cpx, opq; minor alteration. Collected H.L. Davies.

569 (5180).   Ferrogabbro, Ulumanu River, ($10^\circ6'$S, $149^\circ24'$E). Andesine, cpx, opq; secondary amphibole. Collected C.D. Ollier.

570 (4333B).   Ferrogabbro, East Cape, ($10^{o}14$'S, $150^{o}52$'E). Andesine, cpx, opq; minor quartz. Iron staining and secondary amphibole.

571 (4330A).   Ferrogabbro, East Cape, ($10^{o}14$'S, $150^{o}52$'E). Feldspar (sodic plag), cpx, opq, quartz. Graphic quartz-feldspar intergrowths.

572 (3127).   Glassy basalt, boulder, Origuina River, ($10^{o}13$'S, $149^{o}41$'E). Small labradorite and cpx phenocrysts in glass matrix.

573 (2250).   Glassy basalt, boulder, Kutu River, ($10^{o}06$'S, $149^{o}41$'E). Small labradorite and cpx phenocrysts in glass matrix. Collected H.L. Davies.

574 (3137).   Basalt, Bindi Creek, ($10^{o}59$'S, $149^{o}32$'E). Labradorite, cpx, opq; moderate alteration.

575 (4020).   Basalt, boulder, Dawa Dawa River, ($10^{o}28$'S, $150^{o}29$'E). Labradorite (altered), cpx, opq. Collected G. Cifali.

576 (3238).   Coarse basalt, Tavanei River, ($10^{o}6$'S, $149^{o}18$'E). Labradorite, cpx, opq.

577 (2614).   Coarse basalt, Ulumanu River, ($10^{o}5$'S, $149^{o}24$'E). Labradorite (partly altered), cpx, opq. Collected H.L. Davies.

578 (3091).   Altered basalt, Wamira River, ($10^{o}11$'S, $150^{o}01$'E). Fine grained actinolite, opq, feldspar.

579 (300).   Basalt, Suloga Point, Woodlark Island, ($9^{o}14$'S, $152^{o}44$'E). Labradorite, cpx, opq. Donated P. Ashley.

580 (501).   Slightly porphyritic basalt, Woodlark Island, ($9^{o}13'$S, $152^{o}43'$E). Phenocrysts - labradorite. Groundmass - labradorite, cpx, opq; minor alteration. Donated, J.D. Stoen.

581 (301).   Basalt, Suloga Point, Woodlark Island, ($9^{o}14'$S, $152^{o}44'$E). Labradorite, cpx, opq; minor alteration. Donated, P. Ashley.

582 (516).   Basalt, Suloga Point, Woodlark Island, ($9^{o}14'$S, $152^{o}44'$E). Labradorite, cpx, opq; minor alteration. Donated J.D. Stoen.

583 (3191).   Altered basalt, Ruaba River, ($9^{o}55'$S, $149^{o}30'$E). Labradorite, cpx, opq; moderate alteration.

584 (2525).   Metabasalt, Dayman Dome, ($9^{o}47'$S, $149^{o}19'$E). Epidote, chlorite, albite, relic cpx. Collected H.L. Davies.

585 (2540).   Metabasalt, Dayman Dome, ($9^{o}51'$S, $149^{o}20'$E). Epidote, chlorite, albite, relic cpx. Collected H.L. Davies.

586 (2591).   Basic schist, Mau River, ($9^{o}40'$S, $149^{o}13'$E). Albite, epidote, actinolite; well developed schistosity. Collected H.L. Davies.

587 (2589).   Basic schist, Mau River, ($9^{o}41'$S, $149^{o}13'$E). Albite, eipdote, actinolite; moderate schistosity.

Middle Miocene Volcanic Rocks (Table 4-2)

Prefix 27

465 (3401).   Trachybasalt, agglomerate clast, Aivaguina River, ($10^{o}08'$S, $148^{o}48'$E). Phenocrysts - cpx, ol. Groundmass - plag (An_{54-62}), cpx, opq, ol; minor Kfs. Some zeolites.

466 (4296).   Trachybasalt, boulder, Watuti River, $(10^{o}31'S, 150^{o}16'E)$. Phenocrysts - cpx, ol, opq. Groundmass - plag, cpx, opq. Collected G. Cifali.

469 (4258).   Trachybasalt, agglomerate clast, Modewa River, $(10^{o}38'S, 150^{o}16'E)$. Phenocrysts - cpx, ol, opq. Groundmass - plag, cpx, opq. Collected G. Cifali.

470 (2133).   Trachybasalt, agglomerate clast, Modewa River $(10^{o}36'S, 150^{o}16'E)$. Phenocrysts - plag (An_{55-60}), cpx, opq. Very fine groundmass. Collected H.L. Davies.

471 (4276).   Trachybasalt, Watuti River, $(10^{o}31'S, 150^{o}16'E)$. Phenocrysts - cpx. Groundmass - plag, cpx, opq, interstitial material. Collected G. Cifali.

472 (3403A).   Trachybasalt, agglomerate clast, Aivaguina River, $(10^{o}10'S, 148^{o}44'E)$. Slightly porphyritic, cpx, plag (An_{54-64}), opq, minor glass.

473 (4323).   Trachybasalt, Watuti River, $(10^{o}31'S, 150^{o}16'E)$. Phenocrysts - plag, hblde, cpx. Very fine groundmass. Collected G. Cifali.

Prefix 33
588 (4268).   Trachybasalt, Watuti River, $(10^{o}31'S, 150^{o}16'E)$. Phenocrysts - cpx, ol, opq. Groundmass - plag, cpx, opq. Collected G. Cifali.

589 (6057).   Trachybasalt, Gara River, $(10^{o}36'S, 150^{o}22'E)$. Phenocrysts - cpx, opq. Fine grained groundmass, minor calcite. Collected P.D. Hohnen.

590 (3300).   Trachybasalt, Mullins Harbour, $(10^{o}32'S, 149^{o}48'E)$. Phenocrysts - Plag (An_{60}), ol, cpx. Groundmass - plag, cpx, opq, glass.

591 (3443).   Trachybasalt, Cloudy Bay Area, (10^o9'S, 148^o40'E).
               Phenocrysts - cpx, plag (An_{55}). Groundmass - plag,
               cpx, opq.

592 (3298).   Trachybasalt, Mullins Harbour, (10^o31'S, 149^o57'E).
               Phenocrysts - cpx, ol, labradorite, opq. Groundmass -
               plag, cpx, ol, opq.

593 (3402B).   Trachybasalt, agglomerate clast, Aivaguina River,
               (10^o8'S, 148^o47'E). Phenocrysts - ol, cpx. Ground-
               mass - plag (An_{59}), ol, cpx, opq, analcime.

594 (3402A).   Trachybasalt, agglomerate clast, Aivaguina River,
               (10^o8'S, 148^o47'E). Phenocrysts - ol (altered), cpx.
               Small equant analcime. Very fine groundmass.

595 (3402C).   Trachybasalt, agglomerate clast, Aivaguina River,
               (10^o8'S, 148^o47'E). Phenocrysts - cpx, ol (altered).
               Small equant analcime. Very fine groundmass.

596 (3406A).   Trachybasalt, boulder, Liba River, (10^o3'S, 148^o50'E).
               Phenocryst - plag (An_{68}); cpx, minor ol (altered).
               Groundmass mainly plag with abundant opq.

597 (2083).   Trachybasalt, dyke, Sige Lele River (10^o34'S,
               150^o38'E). Phenocrysts - cpx, opq. Feldspathic
               groundmass. Collected H.L. Davies.

598 (3406B).   Trachybasalt, boulder, Liba River, (10^o3'S, 148^o50'E).
               Phenocrysts - labradorite, cpx, opq. Groundmass -
               plag, cpx, opq, biot.

599 (3335).   High-k basaltic andesite, agglomerate clast, Suwen
               River, (10^o37'S, 150^o12'E). Phenocrysts - plag, cpx,
               hblde, biot, opq. Very fine groundmass.

600 (3444).   High-k andesite, Cloudy Bay Area, ($10°9'S$, $148°40'E$).
Phenocrysts - plag, cpx, opq. Very fine groundmass.

601 (3403C).   High-k andesite, Aivaguina River ($10°10'S$, $148°44'E$).
Phenocrysts - plag (An_{42}), opq. Very fine groundmass.

602 (3403D).   High-k andesite, Aivaguina River ($10°10'S$, $148°44'E$).
Phenocrysts - plag (An_{42}), cpx, opq, rare hblde.
Fine groundmass.

Calvados Islands and Egum Atoll (Table 5-1)
Prefix 33

603 (3689E).   Andesite, agglomerate clast, Panaroa Island ($11°7'S$,
$152°30'E$). Plag (An_{40}), cpx; minor opx, opq; rare
hblde, ol (pseudomorphs).

604 (3689C).   Porphyritic andesite, agglomerate clast, Panaroa
Island, ($11°7'S$, $152°30'E$). Phenocrysts - hblde, cpx;
groundmass Plag (An_{54}), hblde, cpx, opx, biot, opq.

605 (3689A).   Dacite, agglomerate clast, Panaroa Island, ($11°7'S$,
$152°30'E$). Plag (An_{40}), cpx; minor opx, opq.

606 (3681A).   Porphyritic dacite, dyke, Moturina Island, ($11°5'S$,
$152°34'E$). Phenocrysts - hblde, plag (altered);
groundmass - cpx, hblde, plag.

607 (223).   Porphyritic andesite, Egum Islands, ($9°22'S$, $151°57'E$).
Phenocrysts - plag (An_{45-50}), cpx, hblde (opq pseudo-
morphs); minor ol (pseudomorphs).

608 (217).   Porphyritic andesite, Egum Islands, ($9°22'S$, $151°57'E$).
Phenocrysts - plag (An_{45-50}), opq (after hblde and
biot); minor cpx.

609 (218).   Porphyritic andesite, Egum Islands, ($9^{o}22$'S, $151^{o}57$'E).
Phenocrysts - plag (An_{45-50}), opq (after hblde and
biot); minor cpx, biot (fresh).

610 (213).   Porphyritic andesite, Nasakori Island, ($9^{o}23$'S,
$151^{o}58$'E). Phenocrysts - plag (An_{45-50}), cpx, opq
(after hblde and biot); minor opx.

Normanby Island (Table 5-2)

Prefix 33

611 (3731).   Porphyritic basalt, ($9^{o}53$'S, $150^{o}52$'E). Phenocrysts -
ol, cpx; groundmass - plag, cpx, opq.

612 (3793A).   Basalt, float, ($9^{o}50$'S, $150^{o}55$'E). Phenocrysts - plag,
cpx. Groundmass - plag, cpx, opq.

613 (3733B).   Basalt, agglomerate clast, ($9^{o}55$'S, $150^{o}53$'E). Plag
(An_{50-55}), opx, ol.

614 (275).   Porphyritic basalt, float, ($9^{o}58$'S, $150^{o}53$'E). Pheno-
crysts - plag (An_{45-55}), ol, cpx; groundmass - plag,
cpx, opq.

615 (3736).   Basaltic andesite, float, ($9^{o}57$'S, $150^{o}55$'E). Pheno-
crysts - plag (An_{50-55}), cpx. Groundmass - plag, cpx,
opq.

616 (3793B).   Basaltic andesite, float, ($9^{o}50$'S, $150^{o}55$'E). Pheno-
crysts - ol, cpx, plag (An_{50-55}). Groundmass - plag,
fine interstitial material.

617 (272).   Basaltic andesite, ($9^{o}53$'S, $150^{o}52$'E). Phenocrysts -
plag (An_{55-60}), ol, cpx. Some clusters. Groundmass -
plag, opq.

618 (276).   Basaltic andesite, agglomerate clast, ($9^{o}58$'S, $150^{o}53$'E).
Ol, cpx, plag (An_{35-40}), opq.

619 (3771A).   Porphyritic andesite, agglomerate clast ($10^{\circ}2'S$, $150^{\circ}58'E$). Phenocrysts - plag (An_{50-55}), ol (altered), cpx, opx; groundmass - plag, cpx, opq.

620 (3727B).   Andesite, ($9^{\circ}52'S$, $150^{\circ}52'E$). Sparse phenocrysts - plag (An_{50-55}), cpx; fine feldspathic groundmass.

621 (283).   Andesite, ($10^{\circ}1'S$, $150^{\circ}59'E$). Phenocrysts - plag (An_{50-55}), cpx, opx. Groundmass - plag, glass.

622 (274).   Andesite, ($9^{\circ}55'S$, $150^{\circ}53'E$). Phenocrysts - plag (An_{50-55}), cpx, ol, hblde (opq rims). Groundmass - plag, glass.

623 (3730).   Porphyritic andesite, ($9^{\circ}51'S$, $150^{\circ}51'E$). Phenocrysts - plag (An_{30-35}), ol, cpx; minor hblde, biot. Crystal clusters.

624 (3726B).   Andesite, ($9^{\circ}50'S$, $150^{\circ}51'E$). Phenocrysts - plag (An_{45-50}), cpx, hblde (opq rims), opq (after hblde). Fine feldspathic groundmass.

625 (270).   Dacite, ($9^{\circ}51'S$, $150^{\circ}52'E$). Phenocrysts - plag (An_{35-40}), opx, cpx, biot. Fine feldspathic groundmass.

626 (282).   Dacite, ($10^{\circ}1'S$, $150^{\circ}56'E$). Phenocrysts - plag (An_{30-35}), biot. Fine feldspathic groundmass.

627 (3726A).   Rhyolite, float, ($9^{\circ}50'S$, $150^{\circ}51'E$). Phenocrysts of oligoclase in a fine feldspathic groundmass containing quartz.

Amphlett Islands (Table 5-3)

Prefix 33

628 (127).   Basaltic andesite, agglomerate clast, Wamea Island, ($9^{\circ}15'S$, $150^{\circ}54'E$). Small phenocrysts of ol in fine feldspathic groundmass.

629 (91).   Basaltic andesite, Wawiwa Island ($9^{\circ}17'$S, $150^{\circ}44'$E). Phenocrysts of ol in a feldspathic groundmass.

630 (104).   Basaltic andesite, agglomerate clast, Wawasi Island, ($9^{\circ}20'$S, $150^{\circ}53'$E). Sparse phenocrysts of ol in a glassy groundmass.

631 (103).   Basaltic andesite, float, Wawasi Island ($9^{\circ}20'$S, $150^{\circ}53'$E). Phenocrysts of ol in a feldspathic groundmass.

632 (225).   Andesite, agglomerate clast, Tewara Island ($9^{\circ}28'$S, $150^{\circ}58'$E). Phenocrysts - plag (An_{50-55}), cpx, ol, opx, hblde (opq rims). Fine glassy groundmass.

633 (224).   Andesite, Tewara Island ($9^{\circ}28'$S, $150^{\circ}58'$E). Phenocrysts - plag (An_{50-55}), cpx, opx, ol. Groundmass - plag, opq, glass.

634 (231).   Andesite, float, Uama Island ($9^{\circ}28'$S, $150^{\circ}57'$E). Ol, plag, cpx.

635 (229).   Andesite, float, Uama Island ($9^{\circ}28'$S, $150^{\circ}57'$E). Phenocrysts - cpx, opx, ol. Groundmass - plag, cpx, opq.

636 (122).   Andesite, Tuboa Island ($9^{\circ}13'$S, $150^{\circ}49'$E). Phenocrysts - plag (An_{45-50}), cpx, opx, hblde, biot. Fine grained groundmass.

637 (90).   Andesite, Wawiwa Island ($9^{\circ}17'$S, $150^{\circ}44'$E). Plag (An_{30-35}), cpx, opq; rare ol.

638 (87).   Andesite, Watota Island, ($9^{\circ}18'$S, $150^{\circ}42'$E). Phenocrysts - ol, opx, cox. Fine feldspathic groundmass.

639 (120).   Porphyritic andesite, Noupoi Island, ($9^{\circ}15'$S, $150^{\circ}47'$E). Phenocrysts - plag (An_{40}), cpx, ol; rare opx with reaction rims.

640 (105).   Andesite, Wata Island, $(9^{\circ}19\text{'S}, 150^{\circ}52\text{'E})$. Phenocrysts - ol. Groundmass - cpx, plag; very fine.

641 (95).   Dacite, Yabwaia Island, $(9^{\circ}17\text{'S}, 150^{\circ}47\text{'E})$. Phenocrysts - plag (An_{40-45}), cpx, opx, hblde, biot. Fine feldspathic groundmass.

642 (86).   Dacite, Watota Island, $(9^{\circ}18\text{'S}, 150^{\circ}42\text{'E})$. Phenocrysts - plag (An_{40-45}), cpx, opx, hblde. Feldspathic groundmass.

643 (79).   Dacite, Wagabu Island, $(9^{\circ}20\text{'S}, 150^{\circ}41\text{'E})$. Phenocrysts - plag (An_{40-45}), opq (after hblde), cpx, opx, rare biot. Cpx clusters. Fine groundmass.

644 (133).   Dacite, Urasi Island, $(9^{\circ}13\text{'S}, 150^{\circ}52\text{'E})$. Phenocrysts - plag (An_{40-45}), opx, cpx, hblde. Fine feldspathic groundmass.

Moresby Strait Area (Table 5-4)

Prefix 33

645 (155).   Basalt, boulder, Kukuia Peninsula, $(9^{\circ}37\text{'S}, 150^{\circ}28\text{'E})$. Phenocrysts - ol, plag (An_{50-55}), opq. Groundmass - plag, cpx, ol, opq.

646 (154).   Basalt, boulder, Kukuia Peninsula, $(9^{\circ}37\text{'S}, 150^{\circ}28\text{'E})$. Slightly porphyritic. Phenocrysts - plag (An_{55}), ol, cpx. Groundmass - abundant opq, plag, cpx.

647 (203).   Basalt, boulder, Goodenough Island, $(9^{\circ}22\text{'S}, 150^{\circ}21\text{'E})$. Phenocrysts - ol, cpx, plag (An_{55-60}). Fine feldspathic groundmass.

648 (68).   Basalt, recent cones, Bwaido Peninsula, $(9^{\circ}28\text{'S}, 150^{\circ}24\text{'E})$. Phenocrysts - ol, minor cpx. Fine feldspathic groundmass.

649 (49).   Basalt, Bwaido Peninsula, ($9^{o}28'S$, $150^{o}22'E$). Pheno-
            crysts - plag (An_{55-60}), ol, cpx. Groundmass - plag,
            cpx, ol, opq.

650 (199). Basaltic andesite, float, Iamalele Area, ($9^{o}30'S$,
            $150^{o}31'E$). Phenocrysts - plag (An_{55-60}), cpx, ol.
            Groundmass - plag, opq, cpx.

651 (191). Basaltic andesite, boulder, Iamalele Area, ($9^{o}30'S$,
            $150^{o}32'E$). Vesicular. Phenocrysts - ol, cpx, plag
            (An_{55-60}). Groundmass - plag, cpx, glass.

652 (198). Basaltic andesite, Iamalele Area, ($9^{o}29'S$, $150^{o}31'E$).
            Phenocrysts - ol, cpx. Groundmass - plag, cpx, opq,
            glass.

653 (62).   Basaltic andesite, Wagipa Island, ($9^{o}30'S$, $150^{o}23'E$).
            Phenocrysts - plag (An_{55-60}), ol, cpx; some clusters.
            Groundmass - plag, cpx, opq, glass.

654 (64).   Basaltic andesite, Wagipa Island, ($9^{o}30'S$, $150^{o}23'E$).
            Phenocrysts - plag (An_{50-55}), ol, cpx. Very fine
            groundmass.

655 (76).   Basaltic andesite, recent flow, Mud Bay, ($9^{o}24'S$,
            $150^{o}21'E$). Vesicular. Phenocrysts - plag (An_{60-65}),
            ol, cpx. Groundmass - plag, cpx, glass.

656 (55).   Basaltic andesite, Wagipa Island, ($9^{o}30'S$, $150^{o}23'E$).
            Phenocrysts - plag (An_{60-65}), ol, cpx. Groundmass -
            plag, cpx, opq, interstitial material.

657 (57).   Basaltic andesite, float, Wagipa Island, ($9^{o}30'S$,
            $150^{o}23'E$). Phenocrysts - plag (An_{55-60}), cpx, ol.
            Groundmass - plag, cpx, opq. Some phenocryst clusters.

658 (72).   Basaltic andesite, recent cones, Bwaido Peninsula, $(9^o28'S, 150^o24'E)$. Sparsely porphyritic. Phenocrysts - plag (An_{55-60}); minor cpx, ol, opq. Groundmass - plag, cpx, opq.

659 (166).   Basaltic andesite, boulder, Kukuia Peninsula, $(9^o37'S, 150^o31'E)$. Phenocrysts - plag (An_{55-60}), cpx, ol. Groundmass - plag, cpx, ol (altered), opq, interstitial material.

660 (178).   Basaltic andesite, Kukuia Peninsula, $(9^o35'S, 150^o29'E)$. Phenocrysts - plag (An_{55-60}), cpx, ol. Groundmass - plag, cpx, interstitial material.

661 (173).   Basaltic andesite, float, Kukuia Peninsula, $(9^o36'S, 150^o31'E)$. Phenocrysts - plag (An_{55-60}), cpx, ol. Groundmass - plag, cpx, ol, opx, opq, interstitial material.

662 (196).   Andesite, float, Iamalele Area, $(9^o29'S, 150^o31'E)$. Phenocrysts - ol, cpx, rare plag (An_{55-60}). Groundmass - plag, cpx, opq, ol (altered). Ol - cpx clusters common.

663 (165).   Andesite, boulder, Kukuia Peninsula, $(9^o37'S, 150^o31'E)$. Phenocrysts - plag (An_{55-60}), cpx, ol. Groundmass - plag, cpx, opq. Some phenocryst clusters.

664 (172).   Andesite, Kukuia Peninsula, $(9^o36'S, 150^o31'E)$. Phenocrysts - plag (An_{55-60}), cpx, ol. Groundmass - plag, cpx, opq.

665 (174).   Andesite, float, Kukuia Peninsula, $(9^o36'S, 150^o31'E)$. Phenocrysts - plag (An_{55-60}), cpx, ol. Groundmass - plag, cpx, opq.

666 (197).   Andesite, float, Iamalele Area ($9^\circ 29$'S, $150^\circ 31$'E).
              Sparsely porphyritic. Phenocrysts - ol, cpx. Ground-
              mass - plag, opq, cpx.

667 (175).   Andesite, float, Kukuia Peninsula, ($9^\circ 36$'S, $150^\circ 31$'E).
              Phenocrysts - plag (An_{60-65}), cpx, ol. Groundmass -
              plag, cpx, ol (altered), opq.

668 (195).   Andesite, Iamalele Area, ($9^\circ 29$'S, $150^\circ 31$'E). Pheno-
              crysts - ol, cpx, opq. Groundmass - plag, opq, glass.

669 (59).   Andesite, Wagipa Island ($9^\circ 30$'S, $150^\circ 23$'E). Small
              phenocrysts, cpx, ol. Groundmass - plag, cpx, opq.

670 (77).   Andesite, northern Goodenough Island, ($9^\circ 15$'S, $150^\circ 17$'E).
              Phenocrysts - ol, cpx. Fine feldspathic groundmass.

671 (52).   Porphyritic andesite, Bwaido Peninsula, ($9^\circ 28$'S,
              $150^\circ 20$'E). Phenocrysts - plag (An_{50-55}), ol, hblde,
              biot, opq; rare cpx. Groundmass - plag, cpx, opq,
              devitrified glass.

672 (180).   Andesite, float, Kukuia Peninsula, ($9^\circ 34$'S, $150^\circ 29$'E).
              Phenocrysts - plag (An_{45-50}), cpx, hblde (with opq rims),
              biot (altered to opq). Groundmass - plag, cpx, opq.

673 (156).   Dacite, float, Kukuia Peninsula ($9^\circ 37$'S, $150^\circ 28$'E).
              Phenocrysts - opx, biot, plag (An_{35-40}), opq (after
              hblde). Fine feldspathic groundmass.

674 (67).   Dacite, Bwaido Peninsula, ($9^\circ 29$'S, $150^\circ 21$'E). Pheno-
              crysts - plag (An_{40-45}), hblde, biot, opq. Very fine
              feldspathic groundmass.

Rhyolites in the Moresby Strait Area (Table 6-1)

Prefix 33

675 (184). Porphyritic rhyolite, float, Kukuia Peninsula, (9°35'S, 150°29'E). Phenocrysts - andesine, cpx, opx, hblde (opq rims), opq.

676 (181). Porphyritic rhyolite, float, Kukuia Peninsula, (9°35'S, 150°29'E). Phenocrysts - oligoclase, hblde, opq.

677 (183). Porphyritic rhyolite, float, Kukuia Peninsula, (9°35'S, 150°29'E). Phenocrysts - oligoclase, hblde, cpx, opq. Rare plag - opx clusters.

678 (167). Porphyritic rhyolite, boulder, Kukuia Peninsula, (9°37'S, 150°31'E). Phenocrysts - oligoclase (typically in clusters), biot, opq.

679 (161). Porphyritic rhyolite, Kukuia Peninsula (9°38'S, 150°30'E). Phenocrysts - oligoclase, biot, opq; rare hblde. Zircon microlites.

680 (162). Obsidian, Kukuia Peninsula, (9°38'S, 150°30'E). Microlites - oligoclase, biot, cpx, zircon.

681 (189). Rhyolite, Fagululu Area, (9°31'S, 150°32'E). Plag, hblde.

682 (177). Obsidian, float, Kukuia Peninsula, (9°35'S, 150°29'E). Microlites - plag, biot.

683 (182). Obsidian, float, Kukuia Peninsula, (9°35'S, 150°29'E). Microlites - plag, biot; rare zircon.

684 (186). Rhyolite, Fagululu Area, (9°31'S, 150°32'E). Oligoclase, hblde.

685 (158).   Obsidian, Kukuia Peninsula, (9°38'S, 150°30'E). Small
phenocrysts - oligoclase, biot. Rare zircon microlites.

686 (159).   Obsidian, Kukuia Peninsula, (9°38'S, 150°30'E). Small
phenocrysts - oligoclase, biot.

687 (164).   Rhyolite, Kukuia Peninsula, (9°38'S, 150°30'E). Small
rare phenocrysts - oligoclase, quartz.

688 (171).   Porphyritic obsidian, Kukuia Peninsula, (9°37'S,
150°31'E). Sparse phenocrysts - oligoclase, biot.
Microlites - hblde.

Lusancay Islands (Table 8-1)

Prefix 33

689 (143).   Trachyte, Simsim Island, (8°24'S, 150°40'E). Pheno-
cryst - cpx. Groundmass mainly feldspar with minor
quartz.

690 (144).   Trachyte, Simsim Island, (8°24'S, 150°40'E). Cpx
phenocrysts in feldspathic groundmass containing minor
quartz.

691 (142).   Trachyte, Simsim Island, (8°24'S, 150°40'E). Cpx
phenocrysts in fine feldspathic groundmass.

692 (140).   Trachyte, Simsim Island, (8°24'S, 150°40'E). Cpx
phenocrysts in fine feldspathic groundmass containing
minor quartz.

693 (141).   Trachyte, Simsim Island, (8°24'S, 150°40'E). Cpx
phenocrysts in fine feldspathic groundmass containing
minor quartz.

694 (139).   Trachyte, float, Kawa Island, (8°33'S, 150°20'E).
Cpx and biot phenocrysts in feldspathic groundmass.

695 (148).   Trachyte, Wagalasa Island, ($8^o24'S$, $150^o40'E$). Cpx
               and biot in fine feldspathic groundmass.

696 (150).   Trachyte, Wagalasa Island, ($8^o24'S$, $150^o40'E$). Cpx
               and biot in very fine feldspathic groundmass.

697 (151).   Trachyte, Wagalasa Island, ($8^o24'S$, $150^o40'E$). Cpx
               and biot in fine feldspathic groundmass containing
               minor quartz.

698 (152).   Trachyte, Wagalasa Island, ($8^o24'S$, $150^o40'E$). Cpx
               and biot phenocrysts in fine feldspathic groundmass
               containing minor quartz.

699 (137).   Trachyte, Nauria Island, ($8^o33'S$, $150^o20'E$). Cpx
               phenocrysts in fine feldspathic groundmass. Rare opq.

700 (147B).   Basaltic inclusion in trachyte, Wagalasa Island, ($8^o24'S$,
               $150^o40'E$). Cpx, labradorite, opq. Some alteration.

701 (147A).   Basaltic inclusion in trachyte, Wagalasa Island, ($8^o24'S$,
               $150^o40'E$). Cpx, labradorite, opq. Moderate alteration.

702 (145B).   Basaltic inclusion in trachyte, Wagalasa Island, ($8^o24'S$,
               $150^o40'E$). Cpx, labradorite, opq.

744 (145A).   Basaltic inclusion in trachyte, Wagalasa Island, ($8^o24'S$,
               $150^o40'E$). Cpx, labradorite, opq.

Basaltic and Intermediate Rocks in the Dawson Strait Area (Table 9-6)

Prefix 33

703 (32).   Basalt inclusion in comendite, eastern Dobu Island,
               ($9^o46'S$, $150^o53'E$). Phenocrysts - plag (An_{60}), ol.

704 (28).   Basalt inclusion in comendite, eastern Dobu Island,
               ($9^o46'S$, $150^o53'E$). Phenocrysts - plag (An_{60}), cpx, ol.

705 (248).   Hawaiite, float, Sanaroa Island, ($9^o37'S$, $150^o59'E$).

706 (13).   Hawaiite inclusion in comendite, eastern Dobu Island, ($9^o46'S$, $150^o53'E$). Phenocrysts - plag (An_{45-50}), pyx, ol.

707 (34).   Hawaiite inclusion in comendite, eastern Dobu Island, ($9^o46'S$, $150^o53'E$). Phenocrysts - plag (An_{40-45}), pyx.

708 (29).   High-Si hawaiite, inclusion in comendite, eastern Dobu Island, ($9^o46'S$, $150^o53'E$). Phenocrysts - plag (An_{40-50}), pyx, ol.

709 (2).   High-Si mugearite, block in ash deposit, northern Dobu Island, ($9^o44'S$, $150^o52'E$). Phenocrysts - plag (An_{40}), pyx, opq.

710 (259).   Trachyte, float, north of Numanuma Bay, ($9^o39'S$, $150^o55'E$). Phenocrysts - plag (oligoclase), pyx, ol, opq.

711 (101).   Trachyte, southeast of Lamonai, ($9^o38'S$, $150^o55'E$). Phenocrysts - plag (oligoclase), pyx, ol, opq.

Comendites in the Dawson Strait Area (Table 9-4)

Prefix 33

712 (12).   Crystalline comendite, eastern Dobu Island, ($9^o46'S$, $150^o53'E$). Kfs, cpx, ol.

713 (249).   Crystalline comendite, northern side of Sebutuia Bay, ($9^o34'S$, $150^o51'E$). Kfs, opx, ol, opq.

714 (253).   Crystalline comendite, northeast flank of Lamonai, ($9^o36'S$, $150^o54'E$). Kfs, cpx, opq.

715 (8).   Crystalline comendite, block in ash deposit, northern Dobu Island, ($9^o45'S$, $150^o52'E$). Kfs, cpx.

716 (855).   Crystalline comendite, eastern crater, Dobu Island, (9°46'S, 150°53'E). Kfs, cpx.

717 (261).   Crystalline comendite, dyke, north of Numanuma Bay, (9°39'S, 150°55'E). Very fine grained

718 (24).   Crystalline comendite, recent lava dome in central crater, Dobu Island, (9°45'S, 150°52'E). Kfs, cpx, opq.

719 (41).   Glassy comendite, recent flow, Oiau crater, (9°41'S, 150°52'E). Kfs, cpx, opq, ol.

720 (38).   Glassy comendite, recent flow, Oiau crater, (9°41'S, 150°52'E). Kfs, cpx, opq, ol.

721 (254).   Glassy comendite, float, northeastern flank of Lamonai, (9°36'S, 150°54'E). Kfs, cpx, opq.

722 (210).   Glassy comendite, eastern flank of Oiau, (9°41'S, 150°52'E). Kfs, cpx, opq.

723 (211).   Glassy comendite, eastern flank of Oiau, (9°41'S, 150°52'E). Kfs, cpx, opq.

724 (26).   Glassy comendite, eastern end of Dobu Island, (9°46'S, 150°53'E). Kfs, cpx, opq.

725 (11).   Glassy comendite, eastern end of Dobu Island, (9°46'S, 150°53'E). Kfs, cpx, opq, ol.

726 (42).   Glassy comendite, recent flow, Oiau crater, (9°41'S, 150°52'E). Kfs, cpx, opq, ol.

727 (30).   Glassy comendite, eastern end of Dobu Island, (9°46'S, 150°53'E). Kfs, cpx, opq.

728 (16).   Glassy comendite, recent flow on northern side of main crater, Dobu Island, (9°45'S, 150°52'E). Kfs, cpx, opq, ol.

729 (99).   Glassy comendite, northern flank, Lamonai, (9°35'S, 150°54'E). Kfs, cpx, opq, ol.

730 (240).   Crystalline comendite, western Sanaroa Island, (9°36'S, 150°59'E). Kfs, opq, aenigmatite.

731 (244).   Glassy comendite, western Sanaroa Island, (9°36'S, 150°59'E). Kfs, cpx, opq.

732 (245).   Glassy comendite, western Sanaroa Island, (9°36'S, 150°59'E). Kfs, cpx, opq.

733 (206A). Crystalline comendite, Numanuma Bay, (9°40'S, 150°53'E). Kfs, cpx, opq.

734 (206).   Crystalline comendite, Numanuma Bay, (9°40'S, 150°53'E). Kfs, cpx, opq.

735 (854).   Crystalline comendite, Deidei thermal area, (9°40'S, 150°52'E). Kfs, cpx, opq.

736 (6).   Crystalline comendite, block in ash deposit, northern Dobu Island, (9°44'S, 150°52'E). Kfs, cpx, opq, amphibole.

737 (237).   Crystalline comendite, northwest side of Numanuma Bay, (9°40'S, 150°53'E). Kfs, cpx, opq, amphibole, aenigmatite.

738 (5).   Glassy comendite, block in ash deposit, northern Dobu Island, (9°44'S, 150°52'E). Kfs, cpx, opq, ol.

739 (209).   Glassy comendite, Numanuma Bay, $(9^{o}40'S, 150^{o}53'E)$.
Kfs, cpx, opq, amphibole.

740 (235).   Glassy comendite, northwest of Numanuma Bay, $(9^{o}40'S, 150^{o}53'E)$. Kfs, cpx, opq.

741 (257).   Glassy comendite, north of Numanuma Bay, $(9^{o}39'S, 150^{o}55'E)$. Kfs, cpx, opq.

742 (260).   Glassy comendite, north of Numanuma Bay, $(9^{o}39'S, 150^{o}55'E)$. Kfs, cpx, opq, ol.

743 (258).   Glassy comendite, north of Numanuma Bay, $(9^{o}39'S, 150^{o}55'E)$. Kfs, cpx, opq, ol.

APPENDIX III: C.I.P.W. NORMS

        C.I.P.W. Norms for all of the analysed samples are
presented in the following pages.   The Norms are organised into
tables which correspond to tables of analyses in the text of
the thesis.

        The Norms have been calculated following the method
of Kelsey (1965) with the ratio Fe_2O_3/FeO wt. % standardised
to a value of 0.2.

Reference

KELSEY, C.H., 1965. Calculation of the C.I.P.W. Norm.
                Min. Mag., 34, 276-282.

THOLEIITIC BASALTS AND ASSOCIATED ROCKS (Table 3-1)

No.	557	558	559	560	561	562	563	564	565	566	567	568	569	570	571	572
Q	-	-	-	-	-	-	-	-	-	-	-	.49	-	1.05	5.66	17.54
or	.77	.41	.41	1.42	.83	.47	1.42	.30	.89	.53	.41	.77	.95	.53	.71	3.07
ab	21.58	17.77	23.27	18.62	17.77	29.62	21.83	18.79	19.46	20.82	19.04	20.90	25.30	21.15	26.65	16.33
an	28.55	28.84	27.01	25.43	29.72	19.52	23.97	26.70	27.16	26.16	26.26	28.99	20.95	22.35	16.61	15.64
di	2.14	6.86	25.13	25.93	20.37	9.95	25.47	26.51	25.08	25.39	24.75	16.01	18.87	18.50	13.08	-
hy	29.83	32.94	5.19	16.05	20.71	16.29	8.69	13.72	14.41	11.20	19.21	18.60	21.30	24.54	23.22	30.32
ol	9.05	5.94	10.77	4.81	1.16	14.04	9.75	5.49	2.33	6.93	1.50	-	1.05	-	-	-
mt	2.57	2.71	2.45	2.71	2.57	3.23	2.91	2.84	2.61	2.86	2.97	3.38	3.73	4.18	4.76	2.67
il	2.73	2.2	2.45	2.24	2.45	2.64	2.79	2.45	2.98	2.54	2.68	7.24	3.74	4.94	5.51	1.44
ap	.31	.24	.26	.14	.17	.31	.24	.26	.31	.28	.26	.24	.45	.19	.71	.19
pr	-	-	-	-	-	-	.30	.04	-	.11	-	-	-	-	-	C 3.43

No.	573	574	575	576	577	578	579	580	581	582	583	584	585	586	587
Q	15.97	-	-	-	-	-	-	.34	-	.15	2.55	-	-	-	-
or	.89	5.32	8.10	2.48	1.89	2.30	.41	.83	.35	.30	.65	.53	.83	5.32	4.55
ab	13.71	19.06	24.96	20.82	29.79	27.08	20.65	22.93	21.32	22.34	14.05	30.81	30.21	20.73	24.29
an	28.85	25.64	20.37	27.45	19.65	21.59	29.33	26.25	29.85	28.96	33.07	10.90	21.75	24.82	22.52
ne	-	4.80	-	-	-	-	-	-	-	-	-	.22	1.10	-	-
di	8.30	9.42	10.61	19.67	20.27	21.23	27.35	23.87	27.52	26.77	22.22	24.22	21.16	22.36	21.93
hy	19.97	-	12.15	19.80	9.55	12.86	13.93	16.76	11.21	14.25	21.09	-	-	1.43	6.65
ol	-	24.69	14.95	.47	8.72	7.76	.72	-	2.84	-	-	13.72	14.62	13.90	9.56
mt	2.60	2.41	2.89	2.65	3.26	2.80	2.55	2.57	2.60	2.61	2.07	2.74	2.75	2.86	2.83
il	1.48	1.88	2.83	3.42	3.40	2.43	2.54	2.54	2.60	2.6	1.01	3.38	3.32	3.70	3.38
ap	.17	.36	.36	.50	.45	.14	.28	.33	.28	.33	.12	.45	.45	.47	.47
pr	-	-	-	.22	-	-	.04	.07	.02	.19	.34	.02	-	.41	.47

MIDDLE MIOCENE VOLCANICS (Table 4-2)

No.	588	471	469	589	590	466	465	591	592	473	593	594	595	596	597	598
C	-	-	4.09	-	-	-	-	-	-	-	-	-	-	-	-	-
or	14.77	18.02	15.36	13.30	15.36	23.93	22.75	22.16	17.73	18.61	7.98	7.62	10.05	22.16	21.16	23.64
ab	11.00	23.45	20.73	10.59	14.75	7.17	7.71	8.51	11.87	26.75	28.73	27.11	27.90	24.12	9.47	26.81
an	23.34	20.69	17.11	14.90	22.96	12.14	15.22	18.76	23.73	16.17	16.56	15.59	16.87	28.25	21.08	23.63
ne	-	1.28	-	.68	1.41	2.99	5.45	2.27	3.20	4.07	1.63	4.79	.70	-	5.87	4.73
di	16.63	7.22	-	35.95	24.48	19.63	24.28	20.67	23.33	14.56	22.38	22.16	22.33	3.17	19.83	3.82
hy	7.02	-	26.00	-	-	-	-	-	-	-	-	-	-	3.92	-	-
ol	21.04	20.43	5.82	16.07	14.85	26.35	14.22	15.79	13.22	12.81	11.37	11.22	11.15	9.08	12.85	8.35
mt	2.15	1.75	2.03	2.41	2.00	3.02	2.16	2.20	2.22	2.02	2.26	2.25	2.28	1.62	2.39	1.42
il	1.14	1.03	1.42	1.18	1.16	1.48	1.92	1.84	1.52	1.23	1.96	2.01	2.05	1.84	1.39	1.84
ap	.92	.95	1.16	1.09	.95	1.61	1.94	2.08	1.09	1.23	2.06	2.25	2.06	1.63	1.33	1.30

No.	472	599	470	600	601	602
Q	-	3.71	-	5.69	10.27	4.48
C	-	-	-	-	4.95	.48
or	15.96	18.32	15.07	24.23	18.32	20.09
ab	27.92	24.12	21.87	35.12	34.27	35.12
an	24.21	25.26	26.26	17.83	12.63	23.24
ne	1.60	-	2.13	-	-	-
di	11.59	6.57	15.40	1.21	-	10.45
hy	-	13.71	-	9.89	11.74	10.45
ol	10.20	-	10.26	-	-	-
mt	2.09	1.77	2.29	1.15	1.35	1.30
il	2.22	1.37	1.67	1.04	1.52	1.44
ap	1.42	1.33	.76	.90	1.10	1.09

CALVADOS ISLANDS AND EGUM ATOLL (Table5-1)

No.	603	604	605	606	607	608	609	610	611	612	613	614	615	616	617	618
Q	9.58	11.07	17.43	20.46	1.94	7.23	3.06	8.98	-	-	-	-	4.27	1.90	.93	.49
C	-	-	.34	1.77	-	-	-	-	-	-	-	-	-	-	-	-
or	12.70	15.66	18.32	13.59	12.11	11.58	14.36	13.41	13.30	4.43	9.51	9.28	9.34	9.34	12.53	13.00
ab	25.39	27.08	29.62	34.27	31.82	37.57	35.54	35.37	21.15	32.01	34.27	30.38	31.31	25.81	29.62	35.71
an	20.02	18.74	19.79	15.21	15.70	17.34	17.19	16.58	19.51	27.98	22.09	21.62	24.84	21.75	19.97	20.21
di	7.63	6.48	-	-	13.49	8.92	10.97	11.18	12.43	14.88	10.61	13.03	7.10	11.88	10.43	11.59
hy	19.28	14.32	11.01	9.91	19.40	11.51	14.11	10.72	9.48	-	12.76	14.41	13.82	22.74	19.46	11.66
ol	-	-	-	-	-	-	-	-	13.81	12.41	.65	2.67	-	-	-	-
mt	1.38	1.29	.88	.81	1.25	1.23	1.17	.99	2.26	2.07	1.99	2.20	1.83	1.74	1.65	1.55
il	1.35	1.56	.91	.91	1.14	1.23	1.16	1.06	3.19	3.32	3.80	3.67	2.83	2.13	2.28	2.58
ap	.52	.76	.59	.43	.66	.78	.69	.71	1.99	.85	1.75	1.47	1.16	.73	.85	1.16
pr	-	-	-	-	-	-	.04	-	-	-	-	-	-	-	.04	-
ne										.31						

NORMANBY ISLAND (Table 5-2)

No.	619	620	621	622	623	624	625	626	627
Q	4.76	7.73	8.18	6.24	9.18	10.07	11.04	15.31	15.22
C	-	-	-	-	-	-	-	.58	-
or	12.41	12.70	16.61	15.48	16.55	17.73	24.70	24.64	25.11
ab	30.04	34.69	27.75	32.92	30.89	35.54	47.22	40.53	50.35
an	19.34	23.49	17.88	17.89	17.64	14.85	6.18	10.47	2.67
di	8.05	3.71	7.00	7.24	4.60	3.56	2.20	-	.64
hy	18.06	11.85	16.63	15.45	15.23	11.63	4.95	4.59	3.06
mt	1.48	1.41	1.30	1.29	1.23	1.12	.80	.58	.55
il	2.11	2.28	1.75	1.75	1.73	1.65	1.16	1.48	.74
ap	.97	.78	.88	.78	.66	.64	.43	.66	.19
pr	-	-	-	.04	-	-	.02	-	-

AMPHLETT ISLANDS (Table 5-3)

No.	628	629	630	631	632	633	634	635	636	637	638	639	640	641	642
Q	-	-	-	-	4.06	5.98	5.84	6.76	6.25	8.08	6.17	7.04	8.71	9.92	15.18
or	15.72	10.58	13.77	15.19	18.14	16.66	13.18	14.83	19.38	11.40	12.11	17.67	15.19	23.76	14.30
ab	30.12	28.01	33.17	33.93	31.05	33.17	30.80	34.10	34.52	36.72	35.54	33.68	32.92	35.45	38.59
an	16.19	19.50	17.00	16.08	17.33	19.07	16.91	16.98	14.95	19.79	14.88	12.79	15.33	11.04	16.59
di	15.30	12.47	13.96	9.83	8.46	5.75	8.07	7.18	6.19	7.54	6.90	7.69	6.85	5.30	1.37
hy	1.95	19.59	11.11	15.55	14.36	12.85	20.27	13.90	12.24	11.52	19.65	15.67	16.84	10.71	10.04
ol	13.57	3.38	5.03	2.74	-	-	-	-	-	-	-	-	-	-	-
mt	1.71	1.84	1.54	1.59	1.38	1.39	1.46	1.41	1.19	1.86	1.30	1.26	1.23	.87	.90
il	2.18	2.34	1.79	2.47	1.92	2.07	1.54	2.09	1.80	1.90	1.42	1.90	1.50	1.31	1.18
ap	1.23	.88	.95	1.07	1.09	.97	.47	.92	.92	.50	.47	.76	.69	.66	.47
pr	.04	-	.04	.04	-	-	-	-	-	-	-	-	.02	-	-

No.	643	644
Q	14.31	13.42
or	14.71	20.62
ab	38.42	37.06
an	16.14	11.53
di	2.69	4.37
hy	10.61	9.52
mt	.90	.84
il	1.14	1.22
ap	.52	.62

ANDESITIC ROCKS FROM THE MORESBY STRAIT AREA (Table 5-4)

No.	645	646	647	648	649	650	651	652	653	654	655	656	657	658	659	660
Q	-	-	-	-	-	-	-	1.15	2.15	1.35	-	3.64	4.39	1.56	3.13	3.35
or	3.07	2.84	5.79	7.33	9.34	7.50	10.52	13.77	9.81	9.04	9.87	7.39	7.86	13.53	10.87	9.87
ab	23.95	26.71	26.74	28.30	31.82	32.15	33.25	24.29	29.02	33.59	29.95	24.71	26.15	36.89	34.52	33.85
an	24.13	27.86	25.30	23.52	30.87	28.31	22.31	18.90	30.21	24.46	22.34	28.25	30.28	21.85	24.82	25.79
ne	2.61	3.36	-	.44	-	-	-	-	-	-	-	-	-	-	-	-
di	16.20	15.91	13.02	15.44	8.46	12.18	11.06	20.38	7.64	12.14	12.35	13.99	10.62	7.73	9.42	8.84
hy	-	-	6.31	-	3.38	12.22	13.44	13.65	15.27	12.09	17.82	16.58	15.18	11.50	10.84	12.28
ol	22.45	15.16	14.92	19.03	7.66	1.30	1.31	-	-	-	2.00	-	-	-	-	-
mt	2.10	2.19	1.93	1.80	1.58	1.62	1.65	1.48	1.84	1.84	1.73	1.87	1.84	1.71	1.44	1.49
il	3.11	3.80	2.72	2.11	3.11	2.39	2.24	2.72	2.05	3.17	2.18	1.82	1.94	2.77	2.22	2.24
ap	.88	.88	1.87	1.23	1.21	.92	.97	1.47	.73	.81	.81	.69	.71	1.33	.73	.71
pr	-	.07	-	-	-	.02	.02	-	-	-	-	-	-	-	.04	.04

No.	661	662	663	664	665	666	667	668	669	670	671	672	673	674
Q	3.68	3.78	2.63	3.87	4.36	5.89	5.55	5.81	5.40	6.71	5.33	10.71	15.77	11.22
or	10.52	12.59	9.99	10.52	10.16	15.78	9.81	15.54	15.31	9.93	18.56	15.72	16.31	24.46
ab	34.52	26.15	35.71	36.05	36.89	31.22	35.29	30.29	28.35	26.57	43.92	36.89	38.92	47.05
an	25.24	19.95	23.98	23.78	24.05	23.60	24.43	21.46	16.93	20.92	12.56	17.46	14.91	8.44
di	7.52	15.28	9.56	6.78	6.25	4.78	7.01	8.30	14.86	10.80	3.93	4.66	2.99	.28
hy	12.52	16.97	11.36	12.98	12.19	12.50	12.21	12.70	13.19	20.68	9.82	9.85	6.83	5.43
mt	1.46	1.48	1.41	1.49	1.42	1.44	1.39	1.39	1.26	1.55	1.19	1.09	1.01	.72
il	2.24	1.82	2.18	2.20	2.18	2.18	2.15	1.98	1.90	1.31	2.18	1.50	1.65	1.35
ap	.73	1.02	.66	.76	.73	1.14	.66	1.04	1.04	.47	1.09	.62	.64	.59
pr	.04	-	-	.02	.02	.02	-	.02	-	-	-	.02	-	-

RHYOLITES FROM WEST FERGUSSON ISLAND (Table 6-1).

No.	675	676	677	678	679	680	681	682	683	684	685	686	687	688
Q	19.05	23.17	26.41	21.91	22.87	22.81	27.74	24.00	25.11	28.28	32.05	32.22	32.72	32.69
C	-	1.76	.32	.56	.03	-	1.25	-	-	.04	.11	.09	.61	.33
or	20.51	22.22	25.65	22.99	21.63	26.30	23.58	26.24	26,65	24.05	27.01	27.48	27.71	27.60
ab	40.36	37.15	30.29	39.69	41.46	43.92	39.35	42.73	42.39	41.12	35.29	34.95	34.35	34.52
an	10.73	8.72	9.52	8.60	7.22	2.31	4.00	2.94	2.53	3.87	2.76	3.22	2.42	2.78
di	1.22	-	-	-	-	1.04	-	.43	.53	-	-	-	-	-
hy	5.38	2.69	3.63	3.91	3.30	1.52	1.59	1.87	1.63	1.35	1.20	.54	1.09	1.30
mt	.77	.58	.57	.49	.46	.32	.26	.32	.30	.26	.20	.07	.20	.22
il	1.18	1.10	.76	.91	.65	.49	.47	.49	.46	.44	.30	.30	.32	.32
ap	.40	.28	.21	.43	.21	.09	.07	.09	.07	.09	.19	.02	.19	.48
pr	-	.04	-	-	-	-	-	-	-	-	-	-	-	-

TRACHYTES AND INCLUSIONS FROM THE LUSANCAY ISLANDS.

No.	689	690	691	692	693	694	695	696	697	698	699	700	701	702	744
Q	13.78	15.94	16.18	17.81	18.58	16.09	12.47	12.67	12.50	13.25	14.30	-	-	-	-
or	31.20	33.09	32.38	31.26	32.30	35.40	40.48	41.84	43.85	43.31	47.16	.77	.77	1.36	2.13
ab	25.13	24.54	25.89	26.32	24.45	25.98	20.48	19.04	18.87	21.15	22.25	10.24	14.38	12.69	11.93
an	12.30	10.64	10.03	10.88	11.85	7.79	7.03	6.67	5.51	5.25	5.34	40.57	44.57	39.90	23.99
di	9.84	9.39	10.58	6.45	5.64	8.42	9.00	9.85	9.86	8.14	2.10	12.68	12.43	9.42	28.55
hy	1.97	1.66	.88	2.26	2.39	2.51	4.67	4.06	4.16	4.23	3.73	19.46	11.83	28.73	21.43
ol	-	-	-	-	-	-	-	-	-	-	-	7.88	9.26	.24	5.42
mt	.68	.67	.62	.67	.68	.64	.87	.83	.80	.80	.74	3.76	2.77	2.42	2.29
il	1.82	1.77	1.67	1.65	1.71	1.46	1.92	1.98	1.94	1.92	1.88	1.92	1.69	1.23	1.58
ap	1.02	.99	.90	.92	.92	.73	1.07	1.04	.99	.99	1.07	.07	.09	.19	.40
pr	.02	.04	-	.04	.04	-	.04	.04	-	-	-	.04	.04	.04	.04

COMENDITES FROM THE DAWSON STRAIT AREA (Table 9-4)

No.	712	713	714	715	716	717	718	719	720	721	722	723	724	725	726
Q	12.92	13.24	13.00	14.19	14.37	15.31	15.85	15.91	15.80	15.13	15.80	15.76	16.18	15.40	15.84
or	27.42	23.99	28.60	28.31	28.96	22.63	28.66	28.01	28.36	28.48	28.48	28.90	28.66	28.90	28.96
ab	48.18	53.88	48.36	46.99	45.76	52.49	46.50	45.67	45.44	46.72	45.64	45.51	45.42	45.71	45.30
ac	1.65	.91	1.53	1.59	1.56	1.48	1.42	1.56	1.56	1.48	1.50	1.45	1.42	1.50	1.53
ns	.56	—	1.06	1.01	1.25	.59	1.13	1.58	1.63	1.32	1.55	1.49	1.50	1.49	1.70
di	3.58	2.29	1.60	2.47	2.90	1.42	1.53	1.41	1.68	1.46	1.40	1.45	1.44	1.78	1.44
hy	4.22	3.09	4.51	3.81	4.05	4.26	3.91	4.06	3.92	4.07	4.16	4.02	3.72	4.22	4.39
mt	—	.30	—	—	—	—	—	—	—	—	—	—	—	—	—
il	.70	.89	.63	.61	.72	.55	.57	.80	.55	.55	.55	.55	.57	.55	.57
ap	.09	.09	.09	.12	.12	.12	.05	.07	.07	.05	.07	.05	.07	.07	.07

No	727	728	729	730	731	732	733	734	735	736	737	738	739	740	741
Q	15.85	15.72	17.14	18.76	20.02	25.25	20.57	23.00	24.22	23.22	25.73	23.39	25.36	25.37	28.90
or	28.66	29.07	29.19	28.66	29.25	27.89	27.12	27.95	27.77	28.54	27.66	28.13	27.36	27.42	25.71
ab	46.50	46.42	44.97	43.49	39.16	34.26	38.84	35.08	32.99	36.27	31.45	35.43	31.16	33.53	29.79
ac	1.42	1.42	1.36	—	1.68	1.91	2.17	2.20	2.46	1.82	2.37	1.91	2.40	1.97	2.14
ns	1.13	1.29	1.31	—	2.00	2.83	1.14	2.07	1.82	2.10	2.43	3.20	4.56	3.30	4.14
di	1.53	1.40	1.36	.47	1.54	1.21	1.71	1.58	1.37	.90	1.27	1.07	.89	.82	.75
hy	3.91	4.04	3.64	4.68	4.79	5.53	6.10	6.07	7.27	5.35	7.09	5.61	7.26	5.94	6.31
mt	—	—	—	.91	—	—	—	—	—	—	—	—	—	—	—
il	.55	.53	.53	.51	.49	.51	.55	.57	.66	.57	.87	.55	.63	.51	.47
ap	.05	.05	.05	.05	.05	.02	.07	.07	.05	.02	—	.05	.05	.02	.02
an				.23											

277.

COMENDITES (Table 9-4)

No.	742	743
Q	28.33	29.29
or	26.30	26.41
ab	30.11	30.10
ac	2.11	2.17
ns	4.11	4.20
di	.81	.75
hy	6.55	6.39
il	.47	.47
ap	.05	.02

ASSOCIATED ROCKS (Table 9-6)

No.	703	704	705	706	707	708	709	710	711
Q	-	-	-	-	-	1.20	2.23	1.64	6.34
or	1.95	4.37	6.09	4.67	7.03	6.74	8.80	16.49	14.71
ab	23.19	27.42	33.59	34.70	38.44	36.47	44.09	65.92	61.01
an	42.20	39.94	25.71	21.37	21.13	19.99	13.96	1.35	5.28
ne	.78	-	-	1.83	.40	-	-	-	-
di	13.52	10.92	12.19	18.37	15.91	14.22	9.30	8.00	2.90
hy	-	.85	4.13	-	-	13.69	11.12	2.83	5.44
ol	11.98	9.71	9.06	9.93	9.17	-	-	-	-
mt	1.45	1.44	2.32	2.44	2.07	1.83	2.04	1.04	1.06
il	2.13	2.22	3.82	4.90	3.76	3.08	4.37	1.69	1.54
ap	.47	.57	.97	1.07	.90	.64	1.71	.59	.71

APPENDIX IV: STRONTIUM ISOTOPES IN VOLCANIC ROCKS FROM SOUTHEAST PAPUA.

INTRODUCTION.

The strontium isotopic data presented in this appendix extends a reconnaissance of $^{87}Sr/^{86}Sr$ ratios in young volcanic of Papua New Guinea by Page and Johnson (1974) and in addition provides further in-- formation on the age of andesitic volcanoes in the D'Entrecasteaux Islands. The results presented here form the basis of a joint project with Dr W. Compston (Research School of Earth Sciences, A.N.U.).

In addition to its use in dating, the radioactive decay of ^{87}Rb to ^{87}Sr provides a constraint to petrogenetic models of igneous rocks. There are two assumptions commonly made in strontium isotope studies of volcanic rocks.

1)   That the observed range of initial $^{87}Sr/^{86}Sr$ ratios in rocks from the ocean basins represents the range of values which can be generated independently of evolved crustal material. Because of the fractionation of Rb and Sr between crust and mantle (Hedge and Walthall, 1973) $^{87}Sr/^{86}Sr$ ratios in crustal rocks are typically significantly higher than those in rocks assumed to be of mantle origin.

2)   That comagmatic lavas have the same $^{87}Sr/^{86}Sr$ ratio at the time of crystallisation regardless of variation in the content of Rb relative to Sr; this is one of the basic assumptions of the isochron method of dating (e.g. Faure and Powell, 1972).

In effect the value of the initial $^{87}Sr/^{86}Sr$ ratio in a rock provides information about the amount of fractionation in the source region. If modern fresh ocean ridge tholeiites ($^{87}Sr/^{86}Sr$ .7020 to .7030, Hedge and Peterman, 1970; Hart, 1971) represent the range of values which can be derived from the primative upper mantle at the present time then values which are higher than this require that the source material is fractionated with respect to Rb and Sr and that the Rb/Sr ratio and hence the rate of evolution of $^{87}Sr/^{86}Sr$ is higher than that of unfractionated mantle. In practice this implies that the source material of alkaline rocks, continental tholeiites and island arc type rocks is relatively enriched in Rb over primative mantle. This is consistent with evidence for a fractionation event which preceeded the magma generative event in Antarctic basinitoids (Sun and Hanson, 1975) and with some current models of island arc petrogenesis which involve an incompatible element enriched source.

The only strontium isotope data available on volcanic rocks from southeast Papua prior to the present study were three $^{87}Sr/^{86}Sr$ ratios measured on andesitic rocks from the Cape Nelson volcanic complex and the D'Entrecasteaux Islands. The data presented here include measurements of the $^{87}Sr/^{86}Sr$ ratio in whole rock specimens which are representative of four distinct Cenozoic volcanic episodes in southeast Papua; namely, eruption of submarine tholeiitic basalts in the Eocene, Miocene to Recent andesitic volcanism, eruption of Pleistocene high-K trachytes in the Luscancay Islands and Recent peralkaline volcanism in the Dawson Strait area.

ANALYTICAL METHODS.

Most of the samples were made up as unspiked preparations using a representative 2g aliquot of rock powder digested in hydrofluoric and perchloric acids and the Sr separated by cation exchange methods. The two tholeiites (563,564) were made up as spiked preparations using 0.1g of lunar $^{84}/85$ spike to .02 g of sample and the comendites (718,725,278) were made up with 0.1g of a mica spike to .2g of sample. Isotopic ratios were measured on a single focusing 9 in, 60° sector mass spectrometer (Clement and Compston, 1972) using a triple Re filament source, automatic magnetic field switching and digital output. Results were normalised to a value of 8.3752 for $^{88}Sr/^{86}Sr$. All of the mass spectrometric results were carried out by Dr W. Compston or by technical staff at the Research School of Earth Sciences. Most of the whole rock Rb and Sr abundances were measured by X-ray fluorescence in the Department of Geology using techniques described in appendix I.

DISCUSSION OF RESULTS.

Total rock $^{87}Sr/^{86}Sr$ and related data for twenty eight selected specimens are presented in table IV-I and are discussed below in their geographic context.

Eocene Tholeiites

Tholeiitic submarine basalts form the main ranges of southeastern Papua. Foraminifera in associated limestone lenses (Belford *in* Smith and Davies, 1976) date the basalts as middle Eocene (about 45 my. old). Because the chemical compositions of these tholeiitic basalts are closely comparable to those of basalts erupted at the mid-ocean ridge

TABLE IV-1: STRONTIUM ISOTOPE DATA ON VOLCANIC ROCKS FROM SOUTHEAST PAPUA.

	Rb(ppm)	Sr(ppm)	Rb/Sr	^{87}Rb/^{86}Sr	^{87}Sr/^{86}Sr	initial ratio
EOCENE THOLEIITES (≈45 my.)						
563 basalt, Kutu Volcanics.	5.0*	116.7*	.043	.124	.70379 ±5	.70371
564 basalt, Kutu Volcanics.	1.2*	120.0*	.010	.0295	.70367 ±4	.70365
SOUTHERN VOLCANIC BELT (≈12 my.)						
590 trachybasalt, Fife Bay Volcanics.	99	540	.183	.530	.70406 ±2	.70405
592 trachybasalt, Fife Bay Volcanics.	127	606	.210	.606	.70437 ±2	.70436
597 trachybasalt, Fife Bay Volcanics.	81	846	.096	.277	.70491 ±2	.70490
602 high-K andesite,Cloudy Bay Volcanics.	83	1648	.050	.146	.70364 ±4	.70364
NORTHERN VOLCANIC BELT (Pliocene-Recent)						
608 andesite,Egum Atoll.	51	1216	.042	.121	.70414 ±2	
614 basalt,Normanby Island.	30	669	.045	.130	.70399 ±4	
626 dacite,Normanby Island.	113	478	.236	.683	.70436 ±7	
628 basaltic andesite,Amphlett Islands.	61	1063	.057	.165	.70431 ±3	
638 andesite,Amphlett Islands.	47	667	.071	.203	.70425 ±3	
641 dacite,Amphlett Islands.	104.0*	905.5*	.115	.331	.70443 ±4	
646 basalt,Moresby Strait.	5	463	.011	.0312	.70321 ±3	
655 basaltic andesite,Moresby Strait.	40	608	.066	.190	.70398 ±4	
658 basaltic andesite,Moresby Strait.	41	996	.041		.70381 ±2	
674 dacite,Moresby Strait.	110.8*	305.2*	.363	1.048	.70409 ±5	
676 rhyolite,Moresby Strait.	120	269	.446	1.289	.70409 ±6	
678 rhyolite,Moresby Strait.	98	326	.301	.868	.70406 ±2	
679 rhyolite,Moresby Strait.	104.2*	253.1*	.412	1.188	.70399 ±8	
LUSANCAY ISLANDS (1.0 my.)						
694 high-K trachyte.	85	1923	.044	.128	.70457 ±2	
695 high-K trachyte.	145	1566	.093	.267	.70432 ±3	
744 'accidental' inclusion.	2	197	.010	.293	.70437 ±2	
DAWSON STRAIT AREA (Recent)						
706 transitional basalt,Dobu Island.	10	391	.026	.074	.70312 ±2	
708 hawaiite,Dobu Island.	39	372	.105	.303	.70309 ±2	
710 trachyte,Numanuma Bay.	56	156	.359	1.037	.70378 ±3	
718 crystalline comendite,Dobu Island.	107.3*	2.021*	53.093	153.2	.7104 ±4	
725 glassy comendite,Dobu Island.	114.2*	3.084*	37.030	106.9	.7042 ±3	
728 glassy comendite,Dobu Island.	114.5*	3.250*	35.138	101.6	.70513 ±2	

* Rb and Sr determined by mass spectrometry, remainder by X-ray fluorescence.

systems and because they are demonstrably submarine in character their origin is linked to sea floor spreading in the Coral Sea Basin which lies to the south of the Papuan Peninsula.

Fresh ocean-ridge tholeiites from the Atlantic, Pacific and Indian oceans have, with the exception of one low value (.7012), a mean $^{87}Sr/^{86}Sr$ ratio of .7020 to .7030 (Hedge and Peterman, 1970; Hart, 1971). Tholeiitic and alkaline basalts of the oceanic islands have ratios in the range .703 to .706 (eg. Gast 1967). The two ratios measured on tholeiitic basalts from southeast Papua give initial ratios, when corrected for an assumed 45 my. age, of .7037. This value, higher than the ocean ridge basalt range but close to the lower end of the ocean island basalt range, is difficult to reconcile with the very close geochemical comparison between the Papuan tholeiites and typical ocean ridge tholeiites.

Although apparently fresh in thin section one explanation for these comparatively high ratios is that there has been some modification to the initial $^{87}Sr/^{86}Sr$ ratio in these basalts possibly as a result of inter-action with sea water. Some indication of this is given by the $^{87}Rb/^{86}Sr$ ratios (.124 and .0295) which are higher than the typical value of .008 in ridge tholeiites. An alternative explanation, that the mantle source of these tholeiites contains evolved strontium cannot be evaluated in view of the limited data available.

The northern and southern volcanic belts.

Two sub-parallel belts of late Cenozoic volcanoes extending south-eastward from the Owen Stanley Range are referred to respectively as the northern and southern volcanic belts. Rock types in the southern belt are predominantly under saturated (ne <5%), high-K basaltic rocks; those in the northern belt range from slightly undersaturated basalts to rhyolites but are dominated by andesites. Because the compositional fields of rocks from the two belts overlap and because they are comparable in age it is thought that they are linked in a common tectono-volcanic event.

Four representative specimens from the southern volcanic belt show a range in initial $^{87}Sr/^{86}Sr$ ratio (assuming an age of 12 my. based on. K-Ar dating) of .7036 to .7049 which is within the range of values reported in Quaternary volcanic rocks from Papua New Guinea by Page and Johnson (1974). There is no clear relationship between the initial $^{87}Sr/^{86}Sr$ ratio and either Rb, Sr or SiO_2 content although the lowest ratio is

found in specimen 602 which has the highest Ba and SiO_2 content and is

apparently fractionated. Powell (1969) has suggested that a negative

initial ratio/SiO_2 correlation could, in some circumstances, be taken

as an indication of crustal contamination. One explanation of this is

that the initial $^{87}Sr/^{86}Sr$ ratios in rocks with lower Sr contents are

more easily changed by contamination (Faure and Powell, 1972) but this

is unlikely to be an explanation in this case because Sr content is

comparatively high in all specimens.

The observed range in initial $^{87}Sr/^{86}Sr$ ratios is high for a group

of rocks which are assumed to be closely related. As there is no evidence

for contamination or even for the underlying presence of crustal material

which could include evolved strontium, this range of values is assumed

to be a primary feature of the magmas and by implication of the source

material which gave rise to the rocks of the southern volcanic belt.

$^{87}Sr/^{86}Sr$ ratios for thirteen samples from the eastern part of the

northern volcanic belt are presented in Table IV-I; all of these samples

were collected from volcanoes in the islands north and east of the mainland.

A further three ratios from the northern volcanic belt have been published

(Page and Johnson, 1974), one of these is from Goodenough Island in the

D'Entrecasteaux Group and two are from the Cape Nelson Volcanic complex

on the Papuan Peninsula. Because the available data indicates that these

volcanoes are all very young (<10my.) no correction has been applies to

the measured $^{87}Sr/^{86}Sr$ ratios. Excluding an anomalously high value for

a basalt from the Cape Nelson complex (.7054) and an anomalously low

value for a basalt from the Moresby Strait area (.70321 in specimen 646)

the $^{87}Sr/^{86}Sr$ ratios in specimens from the northern volcanic ranging

from basaltic to rhyolitic compositions show a range of .7038 to .7047

with a mean of .7042 (standard deviation = .0003). the ratio values do

not appear to be correlated with either geographic location or whole rock

chemical composition. They are typical of $^{87}Sr/^{86}Sr$ ratios for many

island arc type rocks (eg. Pushkar, 1968; Gill and Compston, 1973;

Whitford, 1975), are higher than the mean value (.7036 ± .0001) reported

by Page and Johnson (1974) for the volcanoes in northern New Guinea

and are within the range reported for oceanic island basalts (Gast, 1967).

The uniformity of $^{87}Sr/^{86}Sr$ ratios in andesitic rocks in the offshore

implies a source material which is isotopically homogeneous and is in

marked contrast to the range in values measured in rocks of the southern

r,

volcanic belt. The petrogenesis of volcanic rocks in the northern
and southern volcanic belts is modelled on southward dipping subduction
and modification of overlying mantle by interaction with partial melts
from subducted oceanic crust (chapters 7 and 10). If this model is
correct then it appears that in the early part of the modification process,
when temperatures in the subducted slab first rise above the solidus,
the slab melt is more homogeneous and the extent of mixing to form an
andesite source more complete than it is at deeper levels in the
subduction zone.

The initial $^{87}Sr/^{86}Sr$ ratio in specimen 646 from the Moresby Strait
area is markedly lower than that of any other andesitic rock in eastern
Papua. Several other features of the chemical composition of this rock
are unusual when compared with other basalts in the northern volcanic
belt. Rb, Ba, Sr, and $^{87}Rb/^{86}Sr$ are low and TiO_2 and K/Rb are high.
This specimen is comparable in composition to transitional basalts
associated with Recent peralkaline rhyolites in the Dawson Strait
area and possibly indicates an extension to the west of this type of
volcanism.

The relatively high $^{87}Sr/^{86}Sr$ ratio in a basalt from the Cape
Nelson complex reported by Page and Johnson (1974) is difficult to
interpret because of the lack of data from the other mainland volcanoes.
Further work could be directed at determining whether the mainland
volcanoes are isotopically different from those in the offshore islands.

The Lusancay Islands.

Isolated outcrops of a high-k trachyte in the Lusancay Islands
represent an episode of Quaternary (dated at about 1 my.) volcanism
quite distinct from that in the northern and southern volcanic belts.
$^{87}Sr/^{86}Sr$ ratios of two high-k trachytes (table IV-I) are .70457 and
.70432, slightly higher than those of the northern volcanic belt but
within the range of both island arc and ocean island rocks.

The high-K trachytes contain gabbroic inclusions which on the basis
of chemical composition are interpreted as accidental. In this inter-
pretation an $^{87}Sr/^{86}Sr$ ratio of .70437 measured on one of the inclusions
(744) and which is closely comparable to values measured in the trachytes
is anomalous. It is possible that there has been equilibration of Sr
between host and inclusion but this appears unlikely in view of the lack

of recrystallisation in the inclusion. Further, $^{87}Sr/^{86}Sr$ ratios measured on basaltic inclusions in comendite flows in the Dawson Strait area do not show any evidence of equilibration on this scale. If the $^{87}Sr/^{86}Sr$ ratio of inclusion 774 is not an artefact of equilibration of the host trachyte then it implies that the Woodlark Rise which underlies the Lusancay Islands includes isotopically evolved Crelative to oceanic crust basaltic material.

Peralkaline Volcanism in the Dawson Strait area.

The occurrence of peralkaline rhyolites (comendites) in the Dawson Strait area of the D'Entrecasteaux Islands is anomalous in the tectonic context of circum-Pacific andesitic volcanism. The comendites are associated with minor trachyte and contain inclusions of basaltic rock types; together these rocks are interpreted as a transitional basalt-comendite association which can on geochemical grounds be modelled as a comagmatic series and from a tectonic point of view are related to rifting associated with sea floor spreading to the east.

$^{87}Sr/^{86}Sr$ ratios of three comendites and three of the associated rocks are presented in Table IV-I. In view of the strong geochemical evidence for a close genetic relationship the spread in ratios shown by these samples is surprising. Two basaltic specimens (706,708) show ratios which are identical to within experimental error. These ratios are close to the lower end of the range for basaltic rocks in the ocean islands reported by Gast (1967). Strontium in trachyte 710 is significantly more radiogenic than that in the basaltic rocks. Model age calculations based on an initial $^{87}Sr/^{86}Sr$ ratio of .7031 (the ratio in the basaltic rocks) give an unacceptably high age (74 my.) for this trachyte which shows clearly that it is not comagmatic with the basaltic rocks. Comparable differences in the $^{87}Sr/^{86}Sr$ ratios of basaltic rocks and closely associated more 'evolved' rocks are common in Gast's (1967) documentation of ocean island values; these are clearly not due to differences in age and suggest that the source region for ocean island lavas has undergone an early fractionation event and is isotopically heterogeneous. This conclusion is supported by the work of Sun and Hanson (1975) who present evidence for a fractionation event which preceeded the magma generative event by 1000 to 3000 my.

The spread in $^{87}Sr/^{86}Sr$ ratios in the three comendites is surprising because all were collected from topographic features which appear to be related to the most recent activity from Dobu Island and all have chemical

compositions which are closely comparable. The calculated model age
of comendite 718 (2.9 my. assuming an initial ratio of .7042) is quite
distinct from that of the other two, although all three are assumed on
geomorphic grounds to have been erupted within the last 0.1 my. Even
the differences in the $^{87}Sr/^{86}Sr$ ratios of comendites 725 and 728 are
difficult to reconcile with the hypothesis of a comagmatic series
suggested by their chemical compositions and with geomorphic evidence
of their relative ages.

Variable $^{87}Sr/^{86}Sr$ ratios in suites of apparently comagmatic
rocks are apparently a feature of peralkaline rhyolite associations
(eg. Dickinson and Others, 1969; Dickinson and Gibson, 1972; Ferrara
and Treuil, 1975). Explanations for this feature involve contamination
by equilibrium with crustal rocks or ground water (e.g. Noble and Hedge
1969) or fractionation of strontium isotopes during a late stage in
fractionation of the magma (Dickinson and Gibson, 1972; Ferrara and Treuil,
1975). Dickinson and Gibson (1972) suggested that the variation they
observed in $^{87}Sr/^{86}Sr$ ratios of pantellerites from Fantae Volcano could
be explained by enrichment in Rb relative to Sr and hence in ^{87}Sr
relative to ^{86}Sr during fractionation and that this enrichment could
become measurable in peralkaline rhyolites because of their characteristic
extreme Sr depletion. This model which requires that members of a
comagmatic series linked by feldspar fractionation lie along an isochron
cannot be applied to the three comendites from Dobu Island.

Comendite 718 with an apparently anomalously high $^{87}Sr/^{86}Sr$ ratio
(.7104) is crystalline, the other two are obsidians. Although comendite
718 is apparently fresh there is ample evidence (chapter 9) to suggest
that mobile components are lost from comendite magma during crystallis-
ation. The high $^{87}Sr/^{86}Sr$ ratio cannot be explained by differences in
age because of topographic evidence which indicates that the comendite
was erupted in very recent times and it is suggested that late magmatic
processes associated with crystallisation of the comendite have modified
the initial ratio.

The hypothesis that Sr isotopes can be fractionated as a result of
petrogenetic processes which give rise to high Rb/ Sr ratios and very low
Sr contents which characterise these rocks. Although Dickinson and Gibson's
(1972) simple feldspar fractionation model does not appear relevant to
the Dawson Strait comendites the difference in $^{87}Sr/^{86}Sr$ ratio between
the two glassy comendites may be due to fractionation in the source
region. The Sr isotope data available to this study are not sufficient

to allow discussion of this possibility but the alternative that the two glassy comendites of closely comparable chemical composition collected from demonstrably youthful topographic features forming part of a small Recent Volcano are not closely related is unacceptable.

DATING OF ROCKS IN THE NORTHERN VOLCANIC BELT.

K-Ar dates on volcanic rocks from the northern volcanic belt (Smith, 1973) range from 11.0 to 0.4 my. The oldest rocks are found in the Calvados Islands at the eastern end of the belt and, based on preservation of volcanic landforms it has been suggested that volcanic activity has migrated westward through the late Cenozoic. Rb-Sr dates on five rocks from the central part of the belt presented in table IV-2 do not conflict with this general concept but they extend the period of activity in the Moresby Strait area back to at least 6 my. A more acceptable interpretation of the age data is that volcanism was initiated along the northern volcanic belt during the late Miocene (6-12 my. ago) but was relatively short lived in the eastern part of the belt because of the change in tectonic environment associated with sea floor spreading in the Woodlark Basin.

TABLE IV-2: STRONTIUM ISOTOPE DATA ON WHOLE ROCKS AND MINERAL SEPARATES FROM SELECTED ANDESITIC ROCKS.

Rock No.	Rock type and locality	Rb(ppm)	Sr(ppm)	$^{87}Rb/^{86}Sr$	$^{87}Sr/^{86}Sr$	calculated age
626	dacite, Normanby Island					
	total rock	113[+]	478[+]	.683	.70436 ±7	3.2 ±0.2 my.
	biotite	268.3	40.85	18.95	.70521 ±5	
	biotite	267.8	40.23	19.21	.70520 ±6	
	plagioclase	1.31	733.6	.00515	.70437 ±14	
641	dacite, Amphlett Islands					
	total rock	104.0	905.5	.331	.70433 ±4	4.4 ±1.0 my.
	biotite	274.9	135.4	5.857	.70469 ±5	
	plagioclase	3.44	3965	.00251	.70452 ±3	
	plagioclase	.35	3891	.00026	.70459 ±4	
674	dacite, Moresby Strait					
	total rock.	110.8	305.2	1.048	.70409 ±5	0.8 ±0.9 my.
	biotite			2.651	.70406 ±3.6	
	plagioclase				.70400 ±3	
678	rhyolite, Moresby Strait					
	total rock	98[+]	326[+]	.868	.70406 ±2	6.27 ±0.12 my.
	biotite	248.4	24.58	29.16	.70659 ±5	
	plagioclase	.27	1271	.0006	.70408 ±3	
679	rhyolite, Moresby Strait					
	total rock	104.2	253.1	1.188	.70399 ±8	3.6 ±0.1 my.
	biotite	240.3	30.4	22.81	.70499 ±3	
	plagioclase	4.24	940.1	.013	.70373 ±4	

[+] Rb and Sr determined by X-ray fluorescence, remainder by mass spectrometry.

REFERENCES

Clement, S.W.J., Compston, W., 1972. The application of beam
          transport theory to mass spectrometer design.
          Int. J. Mass Spectrom. Ion Phys., 10, 323-342.

Dickinson, D.R., Dodson, M.R., Gass, I.G., 1969. Correlation of initial
          $^{87}Sr/^{86}Sr$ with Rb/ Sr in some late Tertiary volcanic rocks
          of South Arabia. Earth. Planet. Sci. Lett., 6, 84-90.

Dickinson, D. R., Gibson, I.L., 1972. Feldspar fractionation and anomalous
          $^{87}Sr/^{86}Sr$ ratios in a suite of peralkaline silicic rocks.
          Geol. Soc. Amer. Bull.,83, 231-240

Faure, G., Powell, J.L., 1972. Strontium isotope geology Springer-
          Verlag, 188pp.

Ferrara, G., Treuil, M., 1975. Petrological implications of trace
          element and Sr isotope distributions in basalt-pantellerite
          Series. Bull. Volcanol., 38, 548-574.

Gast, P.W., 1967. Isotope geochemistry of volcanic rocks.
          In Basalts, 1, Hess, H.H., Poldervaart, A., (eds), 325-358.
          Interscience, New York.

Gill, J., Compston, W., 1973. Strontium isotopes in island arc
          volcanic rocks. In the Western Pacific: Island arcs,
          marginal seas, geochemistry, Coleman, P.J. (ed), 483-496,
          Univ. W. Aust. Press, Perth.

Hart, S.R., 1971. K, Rb, Cs, Sr and Ba contents and Sr isotopes of
          ocean floor basalts.
          Phil. Trans. R. Soc. Lond. (A), 268, 575-587.

Hedge, C.E., Peterman, Z.E., 1970. The strontium isotopic composition
          of basalts from the Gordon and Juan de Fuca Rises, northeast
          Pacific Ocean. Contr. Mineral. Petrol., 27, 114-120.

Hedge, C.E., Walthall, F., 1963. Radiogenic Sr^{87} as an index of geologic
          processes. Science, 140, 1214-1217.

Noble, D. C., Hedge, C.E., 1969. $^{87}Sr/^{86}Sr$ variations within individual
          ash-flow sheets. U.S. Geol. Surv. Prof. Pap.,650C, C133-C139.

REFERENCES   (..cont'd.)

Page, R.W., Johnson, R.W., 1974.   Strontium isotope ratios of Quaternary
        volcanic rocks from Papua New Guinea.   Lithos, 7, 91-100.

Pushkar, P., 1968.   Strontium isotope ratios in volcanic rocks of three
        island arc areas.   J. Geophys. Res., 73, 2701-2713.

Powell, J.L., 1969.   Isotopic composition of strontium in volcanic
        rocks (abs).   Symposium on volcanoes and their roots,
        Oxford, England.   Inter. Assoc. Volc., Chem. Earth. Int.,
        vol of abstracts, 144.

Smith, I.E., 1973.   Late Cainozoic volcanism in the southeast Papuan
        Islands.
        Bur Miner. Resour. Aust. Rec, 1973/67. (unpubl.)

Smith, I.E., Davies, H.L., 1976.   The geology of the southeast Papuan
        mainland.
        Bur. Miner. Resour. Aust. Bull., 165 (in press)

Sun, S.S., Hanson, G.N., 1975.   Origin of Ross Island basanitoids and
        limitations upon the heterogeneity of mantle sources for
        alkali basalts and nephelinites.
        Contr. Mineral. Petrol., 52, 77-106.

Whitford, D.J., 1975.   Strontium isotopic studies of the volcanic
        rocks of the Sunda Arc, Indonesia, and their petrogenetic
        implications.
        Geochim. Cosinochim. Acta. 39. 1287-1302.